Antimicrobial Chelators and their Mechanism of Action

BEECROFT, MARIKKA,SHANNON

Antimicrobial Chelators and their Mechanism of Action

Thesis submitted for the degree of Doctor of Philosophy

Marikka S Beecroft

School of Biological and Biomedical Sciences

Durham University

2018

Contents

List of Figures

List of Tables

Abbreviations

ATP	Adenosine triphosphate
BCS	Bathocuproinedisulfonic acid
Ca	Calcium
CHA	Octanohydroxamic acid
Co	Cobalt
Cu	Copper
DMSO	Dimethylsulfoxide
DMSA	Dimer captosuccinic acid
DNA	Deoxyribonucleic acid
DTPA	Diethylenetriaminepentaacetic acid
DTPMP	Diethylenetriamine pentamethylene phosphonic acid
EDTA	Ethylenediaminetetraacetic acid
Fe	Iron
Fe-MOCO	Iron-molybdenum cofactor
Fe-S	Iron-sulphur cluster
FIC	Fractional Inhibitory Concentration
GLDA	Tetrasodium Glutamate Diacetate / L-Glutamic acid, N,N-bis(carboxymethyl)-, sodium salt
HBED	N,N'-Bis(2-hydroxybenzyl)ethylenediamine-N,N'-diacetic acid
ICP-MS	Inductively coupled Plasma Mass spectrometry
LB	Luria-Bertani
LPS	Lipopolysaccharide
Mb	Molybdenum
Mg	Magnesium
MGDA	Methyl glycine diacetic acid trisodium salt
MIC	Minimum Inhibitory Concentration
Mn	Manganese
MOCO	Molybdenum cofactor
mRNA	Messenger Ribonucleic acid
Na	Sodium
Ni	Nickel
P	Phosphorous
PET imaging	Positron-emission tomography imaging
RNA	Ribonucleic acid
RNA-SEQ	RNA Sequencing
SDS	Sodium dodecyl sulphate
SOD	Superoxide dismutase
WT	Wild type
Zn	Zinc

Acknowledgements

I would like to openly say thank you to the many people who have helped me along this long process and guided me through my studies.

My principle supervisor Dr. Gary Sharples for his boundless enthusiasm, patience and kindness he has afforded me throughout my PhD. Without his expertise and supervision this work would not have been possible. My second supervisor Dr. Nigel Robinson whose knowledge and drive gave me great direction throughout my study. Dr. Deenah Osman for running samples through the ICP-MS on my behalf and her support and guidance which have aided me immensely. Dr. Robek Pal who has run samples on his microscope for me and provided some interesting conversation. Dr. Raminder Mulla for allowing me to use his data and was a constant collaborator during my PhD.

Finally, a huge thank you to my family for their love, care and reassurance throughout my studies. This includes my inspirational partner Dr. Christopher William Thoroughgood who I couldn't have done this without. Thank you.

Declaration

This thesis is submitted to Durham University in support of my application for the degree of Doctor of Philosophy. This document has been composed by the author and has not been submitted in any previous application for any degree.

The work detailed herein was generated by the author unless otherwise explicitly specified.

The research detailed within was funded by the EPSRC and Procter and Gamble Co.

- Marikka Beecroft

Abstract

Limiting the availability of metals in an environment is known to restrict bacterial growth and proliferation. For example, humans sequester metals to help prevent infection by pathogens, a system termed nutritional immunity. Chelators are small molecules that bind tightly to metals and thus have antibacterial properties that mimic these innate immune processes. This activity of chelators has not been studied extensively, although experiments with EDTA suggest that it disrupts bacterial membrane permeability by stripping lipopolysaccharide from the bacterial outer surface, possibly due to the stabilising Mg^{2+} and Ca^{2+}. The work described here examines in detail the antibacterial effect of 11 chelators on *Escherichia coli* and how this relates to cellular starvation. Four distinct effects on cellular metal content were found with these chelators i) no change, ii) reduction to manganese, iii) reduction in zinc, and iv) reduction in iron combined with an increase in manganese. There was limited correlation between chelant metal affinities in solution with effects seen in cells. The chelants also exhibited variation in antibacterial efficacy, which was enhanced when used in combination, most yielding synergistic or additive effects. These chelants therefore offer significant potential as tools to probe metal homeostasis systems and as antibacterials.

EDTA, DTPMP and Octopirox were studied further; screening their effects on growth using a selection of *E. coli* mutants. DTPMP and Octopirox have similar effects on cellular metal content, depriving cells of iron and inducing uptake of manganese; mutant data suggests that DTPMP primarily affects Fe3+ uptake, while Octopirox Fe2+. All three chelators also seem t have effects on oxidative damage and tolerance, especially EDTA which deprives cells of manganese. The *E. coli* transcriptional response to EDTA was also investigated by RNA-SEQ showing wide-ranging effects on cellular metabolism, upregulating genes involved in carbon utilisation, energy production, translation and transcriptional regulators, including some iron-sulphur cluster proteins. Overall, the results offer the first detailed insight into the antibacterial effect of a structurally diverse group of chelants and the first step in understanding the relationship between metal affinity and their antibacterial mechanisms of action.

Chapter 1. Introduction

1.1. The importance of metals to biological systems

Metals have been an important aspect of life on earth since its conception and perform integral functions both cellularly and subcellularly (Anastassopoulou and Theophanides, 1995). Indeed in humans the misplacement, regulation and accumulation of metals such as zinc, copper and iron is linked to several neurodegenerative conditions and low iron levels a feature of cancerous cells (Anastassopoulou and Theophanides, 1995; Kozlowski *et al.*, 2009). In bacteria, the demand for metals is evident and it is estimated that a third of bacterial proteins require metals (Andreini, Bertini and Rosato, 2004; Bertini and Cavallaro, 2007) with the prevalence or quota of such metals changing according to geochemistry (Dupont *et al.*, 2006). Bioinformatic analysis of known protein structures, however, contests this estimation and argues that almost half of the bacterial proteome need metals, forty percent being proteins containing a metal cofactor (Andreini *et al.*, 2008; Waldron *et al.*, 2009). The ability of proteins to catalyse diverse chemical reactions is partly due to this capacity to incorporate organic and inorganic clusters of metal atoms as a catalytic centre or structural element (Finkelstein, 2009). This requirement for metals is fuelled by their intrinsic properties making them versatile and unique, filling a niche needed by biological systems. Their ability to increase acidity, encourage heterolysis, accept and donate electrons and participate as both nucleophilic or electrophilic species make them integral to numerous cellular chemical reactions (Waldron *et al.*, 2009). The catalytic utility of metals is caused by their speciation and spin states. Most of the metals adopted by cells can exist at multiple valences or charged states, which during reactions can act as an intermediary. The spin state of metals can also change between high and low, thus dictating the pairing and distribution of electrons in the various energy orbitals (Maret, 2016). Despite the necessity of metals for cellular functionality and viability, their presence is also somewhat paradoxical as all metals under certain conditions or environmental stressors can become toxic and lethal to a cell. Therefore, the regulation and concentration of metals is strictly controlled by complex homeostasis systems

(Waldron and Robinson, 2009). This introduction will focus, in turn, on each of the key metals used by bacteria and how their levels are maintained at the appropriate concentrations to avoid harmful deprivations or excesses.

1.2. Metal homeostasis systems

The metal homeostasis systems discussed in this and subsequent chapters mainly refers to K-12 non-pathogenic *E. coli*. Much of this information therefore does not apply to other bacteria such as gram-positives or other microbes, for example fungi.

1.2.1. Iron

Elemental iron is an essential factor in many integral cellular processes, including the tricarboxylic acid (TCA) cycle, nitrogen fixation, respiration, gene regulation and DNA synthesis (Andrews, Robinson and Rodríguez-Quiñones, 2003). The need for iron as a prosthetic moiety is due to a number of factors: it is abundant in the Earth's crust, it has versatile spin states and can readily interchange between charged states (Beinert, Holm and Münck, 1997). Iron is commonly found in ferric (Fe^{3+}) or ferrous (Fe^{2+}) states. The ferrous form is dominant in anoxic conditions, whereas the ferric state predominates in the presence of oxygen. Since ferric iron is less soluble, specific acquisition systems are needed for its uptake by bacteria living in aerobic environments.

Import of ferric iron is controlled by the Fur protein - the Ferric Uptake Regulator (Hantke, 1981). The assigned nomenclature is misleading as Fur actually controls genes for the ferrous uptake system (Kammler, Schon and Hantke, 1993), iron storage (Nandal *et al.*, 2010), manganese uptake and oxidative stress responses (Touati, 2000). Hence, some workers refer to Fur as the global iron response protein. Fur regulates the transcription and translation of a substantial array of genes (Bagg and Neilands, 1987; Patzer and Hantke, 2001). The Fur protein associates with Fe^{2+} inside *E. coli* cells when the element is plentiful, and this increases its affinity for DNA (**Figure 1-1**). The Fur-Fe(II) complex recognises and binds specific DNA sequences, known as Fur boxes, located in the promoter regions of the genes it regulates (Bagg and Neilands, 1987; Escolar, Pérez-Martín and de Lorenzo, 1999). Binding of Fur typically

inhibits transcription of the target gene by blocking access of RNA polymerase to the promoter. During iron starvation, the Fur-Fe(II) complex does not form and the genes formerly repressed are now induced (Bindereif and Neilands, 1985; Andrews, Robinson and Rodríguez-Quiñones, 2003). The small antisense RNA (*ryhB*) is an important component of the Fur regulation system and its expression is inhibited by the Fur-iron complex. In the absence of iron, *ryhB* is transcribed and targets specific gene transcripts for degradation, including *sodB*, *ftn* and *dps* (Massé and Gottesman, 2002).

Acquisition of ferric iron by *E. coli* occurs by two mechanisms, 1) the production and transport of iron siderophores and 2) the reduction of ferric iron into the ferrous form (Andrews, Robinson and Rodríguez-Quiñones, 2003). The most common route of iron uptake amongst bacteria involves chelation by high affinity binding molecules, known as siderophores (Neilands, 1995). *E. coli* produces only one siderophore, called enterobactin, but has transport systems for siderophores produced by fungi and other bacteria (Braun and Braun, 2002). Production of enterobactin is facilitated by the *entE, entF* and *entB/G* genes whose products supply key steps in the biosynthetic pathway (Hantash and Earhart, 2000). The iron-siderophore complex is imported into the cell *via* an outer membrane transporter, which in *E. coli* is FepA. The complexed iron is released from the complex by reduction. Reduction of ferric iron externally in the surrounding environment has been observed, however, the precise mechanism of reduction has yet to be characterised (Cowart, 2002). Ferrous uptake has also been detected and is mainly facilitated by the Feo protein, an outer membrane transporter composed of FeoA and FeoB (Lau, Krewulak and Vogel, 2016).

Iron storage is also used by bacteria to survive periods when the metal is scarce. These iron stores consist of spherical cages composed of Dps or bacterioferritin proteins (Andrews, 1998). These proteins are only expressed when iron is abundant to take advantage of the conditions present, storing 2000-3000 atoms of iron. The ferrous form of iron is the preferred, stable form inside bacterial cells, however, in these stores ferrous is reduced to ferric iron. The

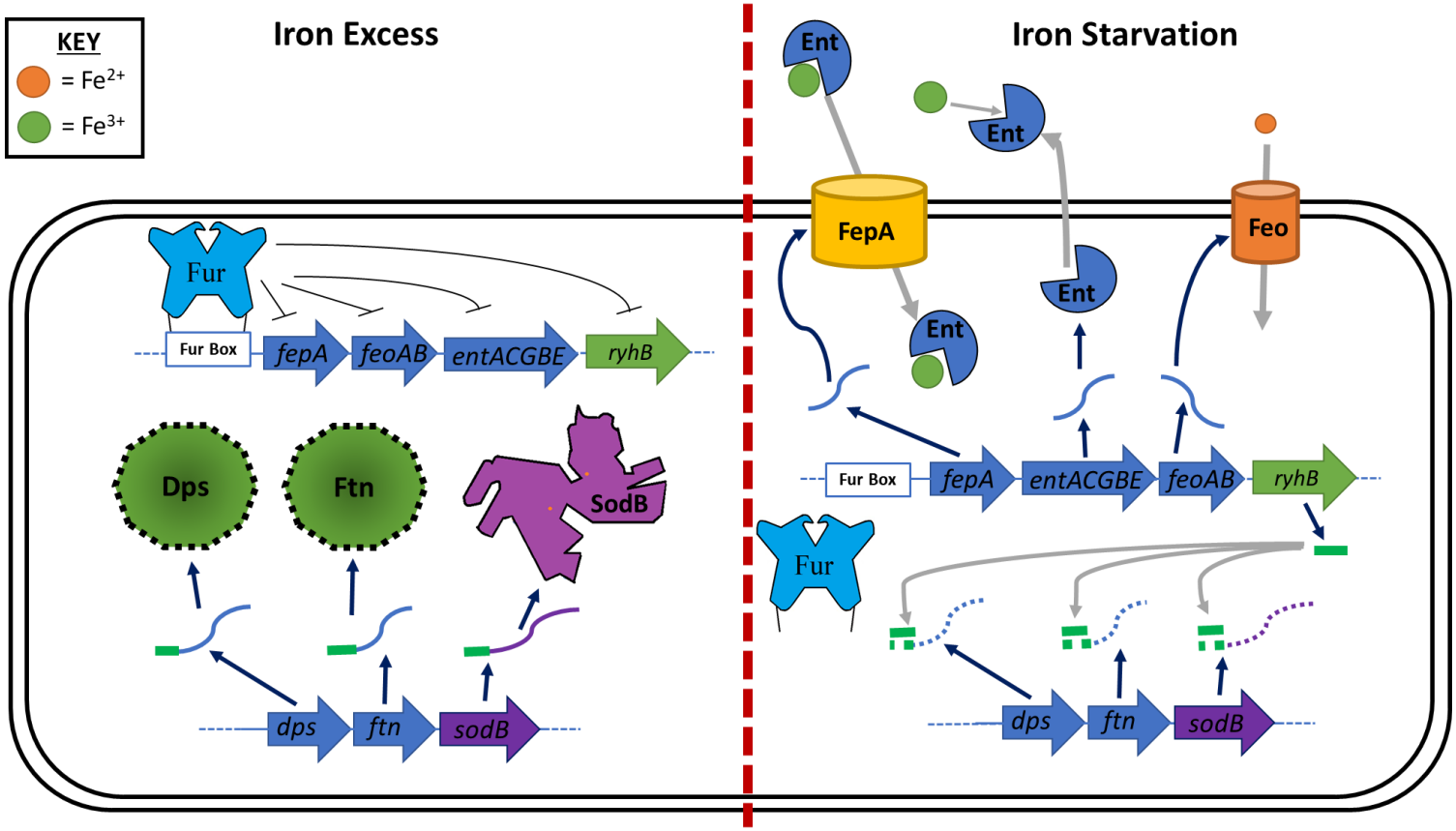

Figure 1-1. The iron homeostasis system of *E. coli*. Repressed genes are indicated with a thin truncated (⊥) line. Transcription and translation are indicated with thick dark blue arrows; transport of proteins, transcripts, ions or macromolecules with grey arrows. RNA transcripts and anti-sense RNA are indicated by green lines. Dashed blue or purple lines indicate RNA degradation

large, amorphous, ferric phosphate core can be oxidised to the ferrous form when required (Chiancone *et al.*, 2000; Andrews, Robinson and Rodríguez-Quiñones, 2003).

These mechanisms for acquisition and storage of iron ensure that bacteria are well equipped for conditions of scarcity and also to fulfil cellular quotas for normal function. Export of iron during high levels has yet to be defined in bacteria, however, its cellular toxicity is well known. Oxygen and iron together can be a lethal combination as iron has the propensity to enhance oxygen toxicity through Fenton reactions. These reactions cause the relatively inert hydrogen peroxide to convert into hydroxyl radicals and the ferryl iron (Fe^{4+}). Oxygen itself, via superoxides, can also interact with iron-containing molecules, releasing the metal and increasing the intracellular concentration of iron. This, in turn, can cause further Fenton reactions, however, the strict uptake and storage of iron as well as the Fur protein controlling the production of superoxide dismutases usually helps prevent this deleterious cycle from occurring (Dubrac and Touati, 2000; Touati, 2000).

1.2.2. Manganese

The role of manganese in *E. coli* is as important and integral as other metals such as iron, despite the fact that under laboratory conditions the cellular manganese concentration is approximately five times less than iron (Posey and Gherardini, 2000). Manganese has a unique redox profile, structurally stabilises many macromolecules and is an essential catalyst for many cellular processes (Waters, Sandoval and Storz, 2011). Due to similarity in its dimensions, manganese can interchange with other metals in proteins, for example Fe^{2+} has a radius of 0.76Å, while Mn^{2+} is 0.80Å (Yocum and Pecoraro, 1999). This versatility of manganese is important in oxidative stress, central carbon metabolism, for the regulator cyclic-di-GMP, among other functions (Kehres and Maguire, 2003; Papp-Wallace and Maguire, 2006). The similarity to iron means that under iron-limiting conditions that the manganese can be substituted instead which shows as manganese uptake increases via uptake through the MntH importer (Martin and Imlay, 2011). These two homeostasis systems are

therefore connected and respond to each other and shouldn't be thought of as distinctly separate.

Manganese homeostasis is controlled by MntR, which fulfils serves several roles as an initial sensor of manganese, a transcriptional regulator and as a quantifying element of intracellular manganese concentrations (Guedon and Helmann, 2003; Kehres and Maguire, 2003). Its primary role is as a transcriptional regulator and binds directly to the promoter regions of its target genes when complexed with manganese. This can either induce or repress the transcript ion of the MntR regulon (Waters, Sandoval and Storz, 2011). In *E. coli*, the MntR protein controls the transcription of three genes: *mntH*, *mntS* and *mntP* (Martin *et al.*, 2015). The *mntH* gene encodes importer that imports Mn^{2+} and to a lesser extent cadmium, cobalt, nickel, zinc and copper (Kehres *et al.*, 2000; Makui *et al.*, 2000; Patzer and Hantke, 2001). Whilst the *mntP* gene encodes an efflux pump involved in export when manganese levels are considered sufficiently high to be toxic. MntS is required by MntR to help suppress transcription of MntH and is hypothesised to be a manganese chaperone during limiting conditions at specific cellular locations (Waters, Sandoval and Storz, 2011; Martin *et al.*, 2015) (**See Figure 1-2**).

Manganese plays an essential role in *E. coli* against oxidative stress; mutants lacking the manganese importer MntH cannot survive when hydrogen peroxide is present through substitution of iron in enzymes to avoid fenton-reactions (Anjem, Varghese and Imlay, 2009). Superoxide dismutases (SOD) which are also needed for growth have three isozyme forms (Hassan *et al.*, 1977); one is co-factored with copper and zinc (Benovs and Fridovichg, 1994), one with iron (Cozi, Yost and Fridovich, 1973) and another with manganese (Keele, Mccord and Fridovich, 1970). The manganese superoxide dismutase is needed for the detoxification of oxygen radicals within the cytoplasm of the cell during aerobic growth (Touati, 1988) and is the only SOD to be regulated by SoxRS the oxidative stress response regulator specific for superoxide and nitric oxide (Storz and Imlay, 1999; Krapp, Humbert and Carrillo, 2011). The MntH importer is also regulated by OxyR, an inducer of genes needed for protection against hydrogen peroxide (Christman, Storz and Ames, 1989). The presence of manganese inside

cells in low molecular weight molecules can detoxify oxygen reactive species and can also induce Dps (an iron storage protein) to protect DNA against damage and convert $Fe^{2+}$to Fe^{3+}; this reaction uses H_2O_2 to produce water and oxygen (Juttukonda and Skaar, 2015).

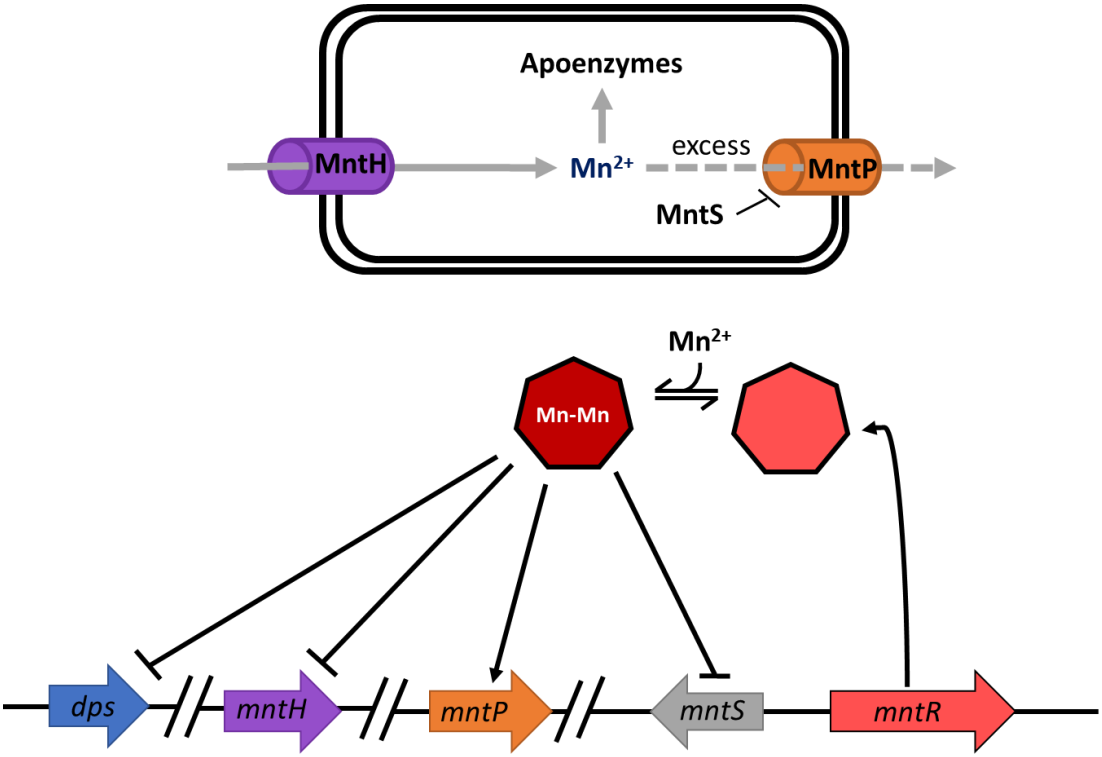

Figure 1-2. The manganese homeostasis system in *E. coli*. Activated genes are shown with a black arrow, repressed genes with a truncated (⊥) line. Transport of ions is indicated by grey arrows; solid arrows indicate import under Mn^{2+} limited conditions while dashed lines indicates export when Mn^{2+} is in excess. The diagram was adapted from Martin et al. (2015).

1.2.3. Copper

The existence of copper cofactors within cells is due in part to the advent of oxygen in the atmosphere, changing the chemistry of copper into a more reactive and advantageous species. Copper in biological systems exists in either Cu(II) or Cu(I) states and is bound to different ligands to induce a stable or reactive effect in proteins. The use of copper proteins is prevalent in organisms that require oxygen for life and fulfils a role in iron transport, oxidative stress protection and respiration. Despite its importance, copper can also be extremely toxic, due in part to copper's redox-active capacity. In the presence of oxygen, copper can induce production of reactive oxygen species and superoxides, which damage DNA, proteins and

other macromolecules. Anoxic conditions cause copper to shift from Cu(II) to Cu(I), where the latter can diffuse through the cytoplasmic membrane which causes gross disruption of the cell through Fenton reactions, unregulated binding to molecules and displacement reactions. Hence, copper levels are tightly regulated to avoid the damaging consequences of reactive oxygen species, particularly with Cu(I).

In *E. coli*, copper sensing is undertaken by two distinct systems, CueR and CusRS, monitoring cytoplasmic and periplasmic levels (Rensing and Grass, 2003), respectively (**Figure 1-3**). The CueR cytoplasmic sensor regulates transcription of the *copA* and *cueO* genes (Stoyanov, Hobman and Brown, 2001). CopA is a P-type ATPase that exports cytoplasmic copper into the periplasm (Outten *et al.*, 2000). It can also be induced by CpxR, a cell envelope stress responder (E. H. Kim *et al.*, 2011). CueO is an oxidase that prevents the toxic reactions of copper from occurring in the periplasm (**Figure 1-3**) (Grass and Rensing, 2001). The CusRS system is a two component system that regulates transcription of the *cusCFBA* operon (Munson *et al.*, 2000). This operon encodes an exporter that transports copper out of the periplasm and into the external environment (Outten *et al.*, 2001).

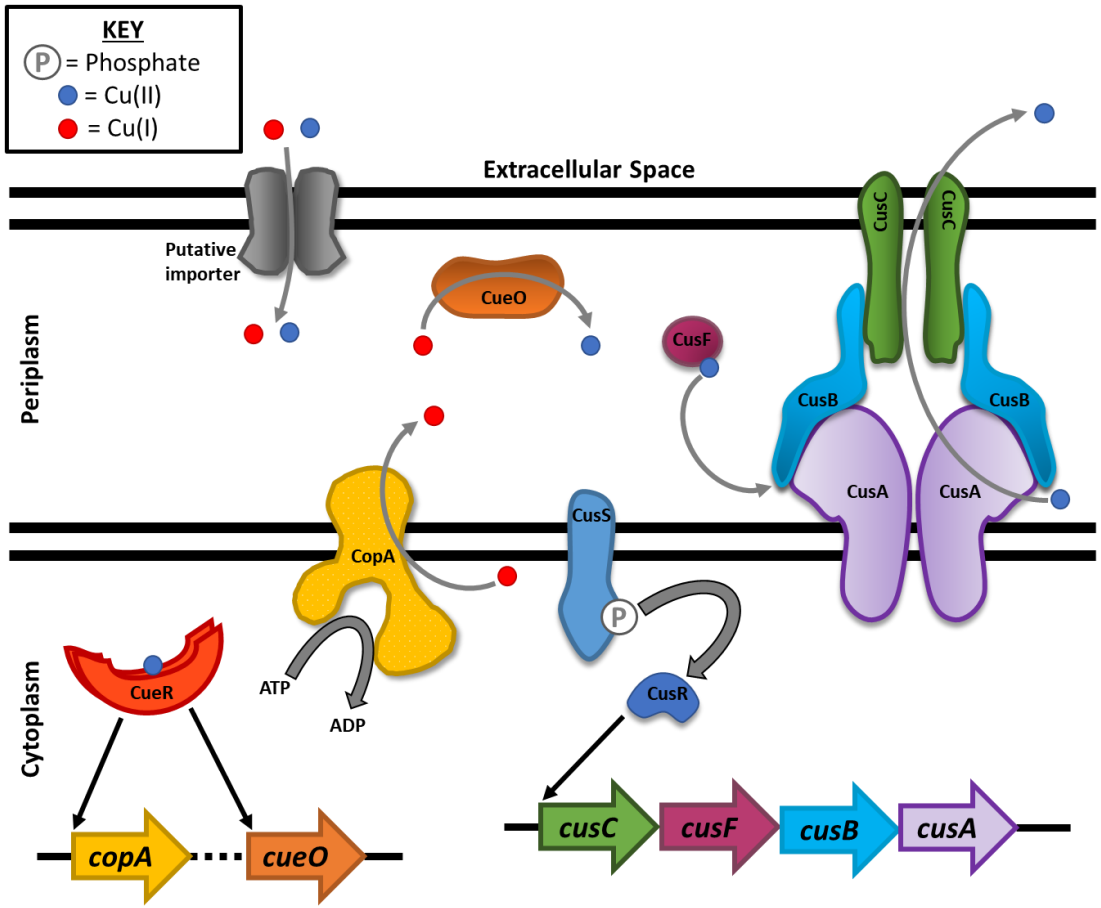

Figure 1-3. Copper homeostasis in *E. coli*. Transport of ions and molecules are indicated by grey arrows. Activation of transcription is indicated by black arrows. The **Figure** was adapted from Kim et al. 2001.

1.2.4. Zinc

Homeostasis of zinc in *E. coli* relies on two import systems and three export systems. The import systems specifically mediate the influx of zinc into the cytoplasm and consist of ZupT and ZnuABC, low and high affinity transporters, respectively (Patzer and Hantke, 1998; Grass, Franke, *et al.*, 2005). Transcriptional activation of the high affinity transporter, ZnuABC, is controlled by Zur a homolog of the Ferric Uptake Regulator (Patzer and Hantke, 2000). Deletion of both importers, however, causes little phenotypic change suggesting that there are undiscovered importers or that other systems can substitute in their absence (Outten and O'Halloran, 2001). Three zinc exporters have been identified in *E. coli*: two low affinity efflux pumps, ZitB and YiiP, and a high affinity pump, ZntA (Wang, Hosteen and Fierke, 2012). All three proteins function as efflux pumps to ensure that toxic levels of zinc do not accumulate. ZntA and ZitB are transcriptionally activated when ZntR binds zinc, while the mechanism for YiiP activation is not known (Grass, Otto, *et al.*, 2005; Takahashi *et al.*, 2015; Choi *et al.*, 2017) (**Figure 1-4**).

The zinc quota in *E. coli* is approximately 2×10^5 atoms per cell, the second most abundant metal after iron (Outten and O'Halloran, 2001; Hensley, 2012). Zinc, unlike other metals discussed so far, exists in a single redox state, Zn^{2+}, and unlike copper and iron does not form reactive oxygen species. Despite the lack of charged states, zinc is still biologically valuable and can be harnessed as a catalyst by acting as a Lewis acid. This feature can lower the activation energy of a reaction when one substrate is an anionic intermediate (Maret, 2016). The metal can also act as a strong nucleophile at pH7 by polarising O-H bonds (Vallee and Auld, 1993).

The toxicity of zinc is linked to the Irving-Williams series, which predicts the relative stabilities of protein-metal complexes. The order, Mn < Fe < Co < Ni < Cu > Zn, holds true for stability in all complexes (Irving and Williams, 1953). Zinc is the second strongest of the transition metals in this series and therefore the mechanism of toxicity is linked to this; it is

able to out-compete other metals inducing mis-metallation and inactivation of enzymes (Wang and Fierke, 2013), which can be disastrous for cells.

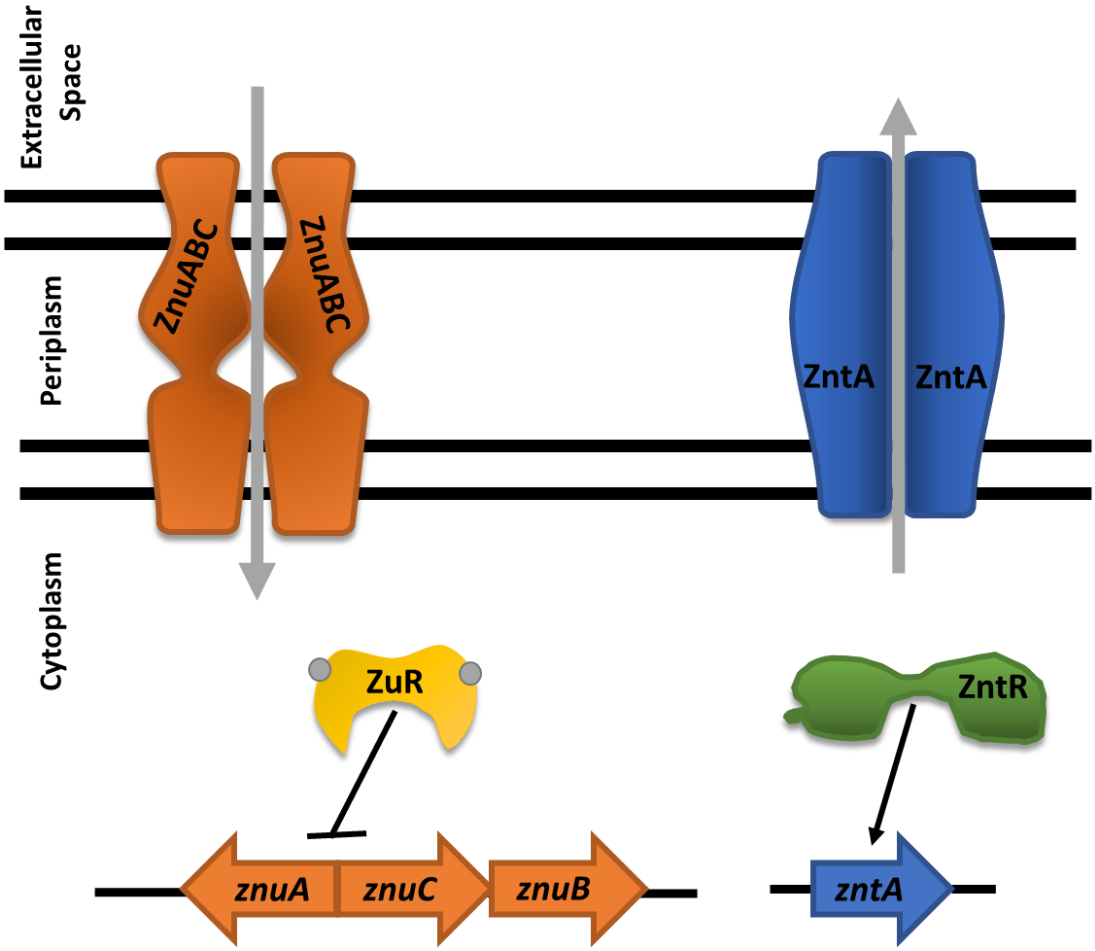

Figure 1-4. Zinc homeostasis in *E. coli*. Zinc(II) atoms are represented by grey circles. Grey arrows indicate the the direction of zinc ion transport. The black arrow represents transcriptional activation whereas the truncated (⊥) line indicates transcriptional repression. Adapted from Takahashi et al. (2015).

1.2.5. Nickel

The role of nickel in *E. coli* is mostly connected to Ni-Fe hydrogenases, which are upregulated during growth in anoxic environments. The nickel homeostasis system in *E. coli* is controlled by NikR and RcnR, transcriptional regulators of the *nikABCDE* and *rcnA* operons, respectively (Iwig, Rowe and Chivers, 2006). The products of the *nikABCDE* operon are directly linked to hydrogenase activity and encode a nickel transporter (Rowe, Starnes and

Chivers, 2005). NikR negatively regulates this operon when nickel is plentiful in the cytoplasm (Schreiter *et al.*, 2006). The RcnA protein functions as an efflux pump for both cobalt and nickel and transcription of the *rcnA* gene is downregulated when RcnR binds to its promoter. Binding of the regulator is inhibited when nickel or cobalt levels in the cell become excessive (**Figure 1-5**; (Huang *et al.*, 2018). RcnA is another example of cross-talk between two different metal homeostasis systems in *E. coli*.

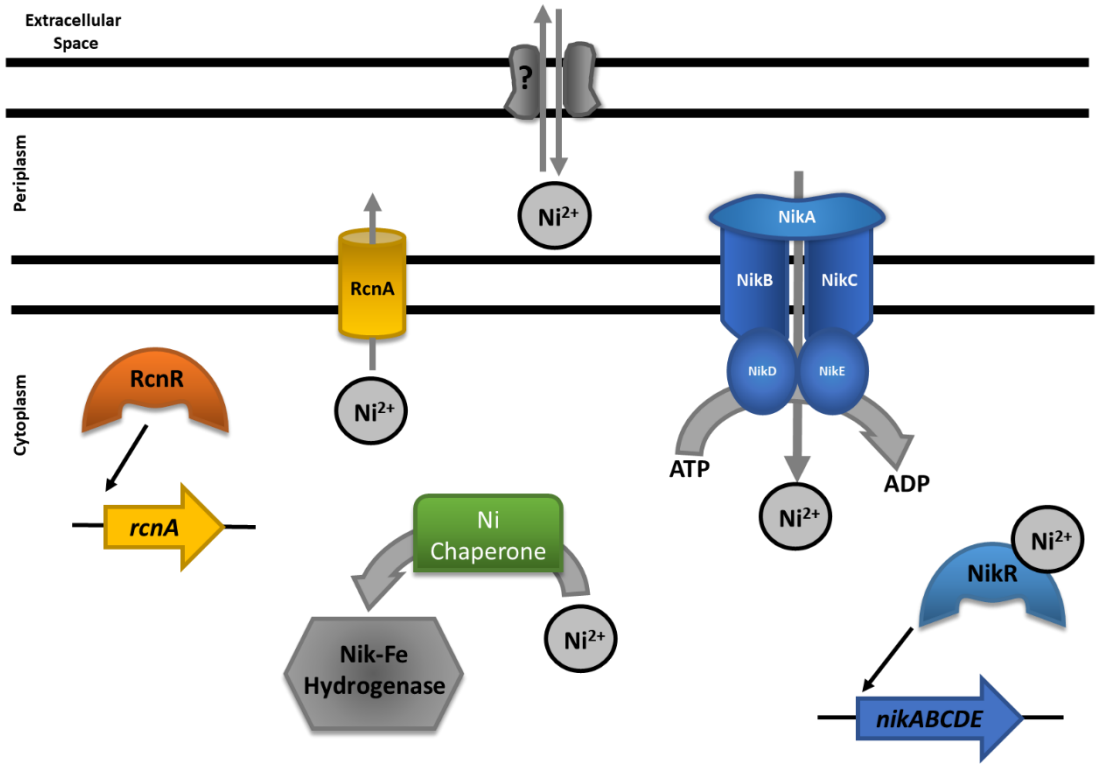

Figure 1-5. Nickel homeostasis in *E. coli*. Grey arrows indicate transport of ions and molecules whilse black arrows indicate transcription of genes. Adapted from Iwig and Chivers (2010).

1.2.6. Magnesium

Magnesium is a useful biological cation due to its unique solute chemistry and charge density. It is a key component of many enzymes and also mediates stability of the cell membrane. Uptake of Mg^{2+} is initiated by CorA, the primary influx pump, which can switch from open to closed states depending on the cytoplasmic abundance of magnesium (Smith and Maguire, 1998). The subcellular location of the influx pump is in the inner membrane and its constituents include a periplasmic domain and three helices integrated into the lipid bilayer

(Park, Wong and Lusk, 1976). A similar influx pump, MgtA, is also present in *E. coli* and is a P-type ATPase which is produced in low intracellular magnesium conditions (Tao *et al.*, 1995). Expression of MgtA is controlled by the PhoQP two component system (Kato, Tanabe and Utsumi, 1999) and MgtL. The latter protein destabilises the ribosome during low levels of magnesium and affects transcription of MgtA through destabilisation of the ribosome (Chadani *et al.*, 2017). The final protein in this homeostasis system is MgtS which is an inner membrane protein that promotes the accumulation of MgtA in the membrane and also stabilises the pump so that it is not degraded (Wang *et al.*, 2017).

1.2.7. Calcium

While the previously discussed homeostasis systems in *E. coli* have been partly or fully characterised, very little information is currently known concerning calcium homeostasis (Arif, Howard and Tisa, 2014). Four possible genes involved in calcium regulation were identified in *E. coli* by Brey and Rosen (1979), however, little subsequent analysis has occurred since then.

1.3. Exploitation of metals

1.3.1. Human nutritional immunity and defence

As previously discussed, the importance of metals in biological systems cannot be understated. Hence, it is not surprising that restricting metal availability has been adopted by higher organisms as a means to defend against invading microorganisms. In humans, a range of different approaches are harnessed to combat infection, one of which is nutritional immunity, a component of the innate immune response. The human body sequesters metals, such as iron, manganese and zinc, to prevent bacterial growth (Kehl-Fie and Skaar, 2010; Hood and Skaar, 2012).

Iron in human bodies is the most abundant element, mirroring environmental levels. Due to its integral role in bacterial growth and its inherent toxicity, the majority of iron is sequestered into haem that is further used in red blood cells for the transport of oxygen around the body (Cassat and Skaar, 2013). Iron is also stored bound to ferritin within human cells that can only

be released by bacteria if they can mediate host cell lysis. Free iron that is not being utilised or stored is bound to lactoferrin found in many bodily secretions and the transport of iron requires the metal to be bound to transferrin to ensure it is inaccessible to pathogens (Cassat and Skaar, 2013; Parrow, Fleming and Minnick, 2013). Exploitation of iron limitation is also common in macrophages. For instance, NRAMP1 is an integral membrane transporter that actively exports iron and manganese from the phagosomal compartment to starve bacteria of these metals (Juttukonda and Skaar, 2015).

Limiting the availability of manganese and zinc in the human body also helps prevent bacterial growth by creating inhospitable conditions. Vertebrates employ a family of S100 proteins to bind calcium, however, a few of these proteins can also effectively bind zinc (Donato, 1999; Kehl-Fie and Skaar, 2010). For example both calgranulin and psoriasin both sequester Zn^{2+} (Gläser *et al.*, 2005; Perera, McNeil and Geczy, 2010) while another major protein, calprotectin, chelates Mn^{2+} and Zn^{2+}. Calprotectin exhibits considerable antimicrobial activity and is found predominantly in neutrophils (Clark *et al.*, 2016). Its antimicrobial activity has been linked to its ability to chelate metals via three binding sites on the molecule, two high-affinity zinc sites and one manganese affinity site (Kehl-Fie *et al.*, 2011; Damo *et al.*, 2013).

In addition to killing organisms through iron, zinc and manganese starvation, metals in excess are also used to induce toxicity and mediate killing. After engulfing *E. coli*, macrophages release large quantities of zinc into the phagosome to promote killing (Stafford *et al.*, 2013; Haase and Rink, 2014). Copper is also harnessed in a similar fashion as an antibacterial. Cu(I) is delivered to the phagolysosomal compartment in macrophages alongside proteases and reactive oxygen species (White *et al.*, 2009; Stafford *et al.*, 2013). When *Salmonella enterica* sv. *typhimurium* is engulfed by macrophages it has been shown that the bacteria upregulates two copper exporters; deletion of these exporters leads to lower survival rates (Osman *et al.*, 2013). It has been shown that the increase in copper into the phagosome is controlled by the copper pump ATP7A a P-type ATPase (Ladomersky *et al.*, 2017). Elevated copper levels in tissues surrounding sites of infection are also recognised as a means of generating hostility

towards the tuberculosis bacillus, *Mycobacterium tuberculosis* (Darwin, 2015; Sepehri *et al.*, 2017).

1.3.2. Uses of chelants and ionophores – manipulating metal regulation

The various sections of this introduction have mentioned a number of naturally synthesised metal chelating molecules, such as siderophores and haem. Chelation is defined simply as a ligand that can form two or more bonds with a metal atom and the so-called chelators can be employed in many situations in industry and health. In medicine, chelation has long been used to help bind radiometals during imaging. One such example is the gadolinium-based contrasting agent and the chelator, DOTA, which when complexed together pass through the body's system harmlessly (Dai *et al.*, 2018). Another example is the hydroxypyridione chelators in combination with gallium that are needed for PET (Positron-emission tomography) imaging (Cusnir *et al.*, 2017). One hydrocypyridone, deferiprone, is used in the treatment of iron overload in patients and is administered orally due to its lack of toxicity (Chaves *et al.*, 2010). Treatment of patients who have suffered lead poisoning also involves chelators, specifically dimer captosuccinic acid (DMSA) but is only used for severe cases (van Eijkeren *et al.*, 2017). Chelation therapy has a long established history and has been extensively studied with both long and short term effects of the treatment being evaluated (Barry *et al.*, 1974; Rogan *et al.*, 2001; Leitch *et al.*, 2017).

Metal homeostasis has also been considered as a target for development of antibacterial agents and recent studies have focussed attention on ionophores. These compounds can complex with ions (usually metals) and increase their transport across the cell membrane (Freedman, 2012). One example of this approach is bi(thiosemicarbazones) complexed with Cu(II) which can inhibit the growth of *Neisseria gonorrhoeae* (Djoko *et al.*, 2014). This particular ionophore increases the intracellular concentration of copper which can impede the respiratory chain in bacteria by inhibiting NADH dehydrogenases (Djoko, Donnelly and McEwan, 2014). This mechanism of action is specific for *N. gonorrhoeae*, however, and depends on the peculiar physiology of this species (Djoko *et al.*, 2015).

Manipulation of metals offers considerable scope and potential for preventing bacterial proliferation in a healthcare setting. However, chelators and their antibacterial effects have not been actively studied to date. The first investigation of the specific effect of a chelator on bacteria was conducted by Loretta Leive in 1965 when she observed increased cell membrane permeability in *E. coli* treated with EDTA (Leive, 1965). Further work showed that this increased permeability was caused by release of lipopolysaccharide (LPS) from the outer membrane, thought to result from membrane instability due to chelation of magnesium or calcium (Leive, Shovlin and Mergenhagen, 1968). Membrane sites sensitive to EDTA chelation were also hypothesised to lie in the proximity of porin proteins (Lugtenberg and Van Alphen, 1983). Release of membrane components as a consequence of chelant exposure has been observed in other organisms, such as *Trypanosoma cruzi, Bacillus subtilus* (note these organisms lacks LPS), *S. enterica typhimurium, Klebsiella pneumoniae* and *Pseudomonas aeruginosa* (Goldberg *et al.*, 1983; Marvin, Ter Beest and Witholt, 1989; Pelletier, Bourlioux and Van Heijenoort, 1994; Folorunso, Amisu and Ogungbe, 2015). The antimicrobial effect of EDTA, however, cannot be solely attributed to LPS disruption. In *Salmonella enterica,* the outer membrane was affected more during early exponential phase of growth than in any other growth state. However, this LPS release did not differ significantly from other time points, suggesting that other factors contribute to the effect of EDTA on cell growth and viability (Alakomi, Saarela and Helander, 2003).

Microarray experiments have been conducted with TPEN, a well-known zinc and copper chelator (Hyun *et al.*, 2001). Transcription of all of the Zur regulated genes increased when TPEN was present, in addition to a large proportion of the Fur regulon. Overall 32 genes related to metal homeostasis were differentially expressed, 4 belonging to the Zur regulated genes and 28 regulated by Fur. Anabolic processes were also affected, along with SoxRS and other stress related genes which all showed enhanced transcription. Downregulated genes included those involved in flagellar biosynthesis, sugar metabolism, iron and copper metabolism, metabolic proteins and selected stress proteins (Sigdel, Easton and Crowder,

2006). The results suggest that TPEN does affect metal homeostasis but also alters expression of a range of other cellular processes involved in stress or damage tolerance that may be directly or indirectly related to metal depletion.

1.3.3. Aims of the study

As discussed, the known impact of chelation on bacteria is limited to LPS release and outer membrane damage with EDTA. The gene expression analysis with TPEN confirms a link with cellular metal homeostasis, however, a range of other genes are also affected that are unrelated to metal regulation. The lack of knowledge concerning the mode of action of chelators, especially with respect to antimicrobial activity, means that their potential for other applications may not yet be fully realised. For example, chelators could be deployed in combination with certain antibiotics to enhance efficacy. Resistance to β-lactam type antibiotics, such as carbapenems and cephalosporin, is provided in some bacteria by the protein IMP-1, a metallo-β-lactamase (Senda, Arakawa, Ichiyama, *et al.*, 1996; Mendes *et al.*, 2006). The gene encoding IMP-1 is found in *Pseudomonas aeruginosa* (Senda, Arakawa, Nakashima, *et al.*, 1996), *Serratia marcescens* (Osano *et al.*, 1994), *Klebsiella pneumoniae* and *Chryseobacterium meningosepticum* (García-Sáez *et al.*, 2003). The problems associated with β-lactam antibiotic resistance could potentially be reversed by the application of a suitable chelator that deprives resistance factors of the metal they need to function. However, a clearer understanding of the effect of these chelators on bacterial metal content and metal homeostasis is needed.

This thesis endeavours to characterise a collection of 11 chelants with diverse structures and metal affinities to evaluate their effect on bacterial growth and how this correlates with metal sequestration. In addition, combinations of these chelants have been studied to identify chelant pairings with synergistic antibacterial activity that may have industrial and therapeutic applications. The mechanism of action of EDTA has been explored in the most detail, using transcriptome analysis to investigate the cross-talk between metal regulatory systems and other biological processes. The results yield insight into the function of these chelators and

how *E. coli* responds to metal chelation using chelants that mimic the iron, manganese and zinc deprivations encountered by pathogens experiencing nutritional immunity. Hence the work provides insight helpful for researchers studying metal homeostasis in bacteria, in addition to future applications of chelators in biotechnology, industry and medicine.

Chelants chosen in this study had known metal affinity data or known chelation effects on biological systems for example TPEN and BCS have been used in previous studies on human cells such as thymocytes, keratinocytes, fibroblasts and gut epithelial cells with known effects on zinc and copper cellular concentrations (McCabe, Jiang and Orrenius, 1993; Parat *et al.*, 1997; Chimienti *et al.*, 2001; Nose *et al.*, 2010). Octopirox/piroctone olamine has known antimycotic effects and whilst the full mechanism of action on fungi has not been elucidated it has been observed that the effect of the chelant can be slightly negated by the addition of iron atoms into media (Sigle *et al.*, 2006).

Chapter 2. Materials and Methods

2.1. Bacterial Strains and Growth Conditions

All *Escherichia coli* strains used in the study are described in Table 1. *E. coli* cultures were grown in Luria Bertani broth (Sigma Aldrich, L3022, 10g/L Tryptone, 5g/L Yeast Extract, 5g/L NaCl) at 37˚C with orbital shaking at 180 rpm (Stuart Orbital Incubator SI500) in 5 ml overnight starting cultures. *E. coli* cultures for short-term storage were streaked from frozen stocks on Luria Bertani agar (Sigma Aldrich, L7533, 15g/L Agar, 10g/L Tryptone, 5g/L Yeast Extract, 5g/L NaCl) and incubated at 37˚C overnight (16-18 h) to allow formation of colonies. For long-term storage, sterile 80% glycerol and overnight culture were mixed at a 1:1.6 ratio and frozen at -80˚C (Datsenko and Wanner, 2000; Baba *et al.*, 2006) see **table 2-1**.

Table 2-1. *E. coli* strains used in this study. These were obtained from the Keio Collection at Durham University.

JW GENE ID	NAME	GENOTYPE
BW25113	*wt*	F$^-$ Δ(*araD-araB*)*567* Δ*lacZ4787* (::*rrnB-3*) *rph-1* Δ(*rhaD-rhaB*)*568 hsdR514*
JW0598	*ΔahpC*	As BW25113 but Δ*ahpC744*::*kan*
JW0473	*ΔcopA*	As BW25113 but Δ*copA767*::*kan*
JW3789	*ΔcorA*	As BW25113 but Δ*corA767*::*kan*
JW3882	*ΔcpxA*	As BW25113 but Δ*cpxA767*::*kan*
JW5558	*ΔcpxP*	As BW25113 but Δ*cpxP767*::*kan*
JW3883	*ΔcpxR*	As BW25113 but Δ*cpxR767*::*kan*
JW0119	*ΔcueO*	As BW25113 but Δ*cueO767*::*kan*
JW0476	*ΔcueR*	As BW25113 but Δ*cueR767*::*kan*
JW0560	*ΔcusR*	As BW25113 but Δ*cusR767*::*kan*
JW3832	*ΔdsbA*	As BW25113 but Δ*dsbA767*::*kan*
JW3372	*ΔfeoB*	As BW25113 but Δ*feoB767*::*kan*
JW5086	*ΔfepA*	As BW25113 but Δ*fepA767*::*kan*
JW1893	*Δftn*	As BW25113 but Δ*ftn767*::*kan*
JW0669	*Δfur*	As BW25113 but Δ*fur767*::*kan*
JW2663	*ΔgshA*	As BW25113 but Δ*gshA767*::*kan*
JW0957	*ΔhyaD*	As BW25113 but Δ*hyaD767*::*kan*

JW2961	*ΔhybD*	As BW25113 but Δ*hybD767*::*kan*
JW5493	*ΔhybF*	As BW25113 but Δ*hybF767*::*kan*
JW2687	*ΔhycI*	As BW25113 but Δ*hycI767*::*kan*
JW3914	*ΔkatG*	As BW25113 but Δ*katG767*::*kan*
JW1100	*Δmfd*	As BW25113 but Δ*mfd767*::*kan*
JW2388	*ΔmntH*	As BW25113 but Δ*mntH767*::*kan*
JW3610	*ΔmutM*	As BW25113 but Δ*mutM767*::*kan*
JW0097	*ΔmutT*	As BW25113 but Δ*mutT767*::*kan*
JW2928	*ΔmutY*	As BW25113 but Δ*mutY767*::*kan*
JW3441	*ΔnikA*	As BW25113 but Δ*nikA767*::*kan*
JW3446	*ΔnikR*	As BW25113 but Δ*nikR767*::*kan*
JW1625	*Δnth*	As BW25113 but Δ*nth767*::*kan*
JW5346	*ΔrcnB*	As BW25113 but Δ*rcnB767*::*kan*
JW2669	*ΔrecA*	As BW25113 but Δ*recA767*::*kan*
JW2788	*ΔrecB*	As BW25113 but Δ*recB767*::*kan*
JW3677	*ΔrecF*	As BW25113 but Δ*recF767*::*kan*
JW2860	*ΔrecJ*	As BW25113 but Δ*recJ767*::*kan*
JW5416	*ΔrecN*	As BW25113 but Δ*recN767*::*kan*
JW5855	*ΔrecQ*	As BW25113 but Δ*recQ767*::*kan*
JW1850	*ΔruvA*	As BW25113 but Δ*ruvA767*::*kan*
JW1849	*ΔruvB*	As BW25113 but Δ*ruvB767*::*kan*
JW1852	*ΔruvC*	As BW25113 but Δ*ruvC767*::*kan*
JW1993	*ΔsbcB*	As BW25113 but Δ*sbcB767*::*kan*
JW3311	*ΔslyD*	As BW25113 but Δ*slyD767*::*kan*
JW3879	*ΔsodA*	As BW25113 but Δ*sodA767*::*kan*
JW1648	*ΔsodB*	As BW25113 but Δ*sodB767*::*kan*
JW1638	*ΔsodC*	As BW25113 but Δ*sodC767*::*kan*
JW4019	*ΔuvrA*	As BW25113 but Δ*uvrA767*::*kan*
JW1898	*ΔuvrC*	As BW25113 but Δ*uvrC767*::*kan*
JW3254	*ΔzntR*	As BW25113 but Δ*zntR767*::*kan*

2.2. Chemicals, Reagents and Kits

Unless stated otherwise, all analytical chemicals were obtained from VWR International, Sigma Aldrich or Melford Laboratories Ltd. Media was obtained from Sigma Aldrich and sterilised at 121˚C for 15 min at 15 psi in a Dixons Vario 1528 autoclave. Solutions were

sterilised using the same autoclave conditions or were filter-sterilised by passing through a 0.2 µM Sarstedt Filtropur unit. Media and reagents were made up using mQ H_2O from water purification system Milli-Q® Integral 15, Merck Millipore. Acid-washed glassware was used for experiments that required metal content analysis or RNA extraction. Glassware was soaked in 4% HNO_3 for a minimum of 16 h and rinsed with mQ H_2O. Chelating agents used in this study are listed in **Table 2-2**.

Table 2-2. Chelating agents used in this study.

Chelator Synonym / Formal Name	Chemical Formula	Company, Item Number
BCS / Bathocuprionedisulphonate acid disodium salt	$C_{26}H_{18}N_2Na_2O_6S_2$	Sigma Aldrich, B1125
Catechol / 1,2-dihydroxybenzene	$C_6H_4(OH)_2$	Sigma Aldrich, 135011
CHA / Octanohydroxamic acid	$C_8H_{17}NO_2$	Fluorochem, 227638
DTPA / Diethylenetriaminepentaacetic acid	$C_{14}H_{23}N_3O_{10}$	Sigma Aldrich, D1133
DTPMP / Diethylenetriaminepentamethylene phosphonic acid	$C_9H_{28}N_3O_{15}P_5$	Sigma Aldrich, D2565
EDTA / Ethylenediaminetetraacetic acid	$C_{10}H_{16}N_2O_8$	Melford, E5810
GLDA / N,N-bis(carboxymethyl)-L-glutamic acid tetrasodium salt	$C_9H_9NNa_4O_8$	Carbosynth, FC36385
HBED / N,N'-Di(2-hydroxybenzyl)ethylenediamine-N,N'-diacetic acid monohydrochloride hydrate	$C_{20}H_{24}N_2O_6$	StremChemicals, 07-0422
MGDA / N-(1-Carboxylatoethyl)iminodiacetate Hydrate	$C_7H_8NNa_3O_6.xH_2O$	TSI, T2202
Octopirox / Piroctone olamine / 1-Hydroxy-4-methyl-6-(2,4,4-trimethylpentyl)-2(1H)-pyridone ethanolammonium salt	$C_{14}H_{23}NO_2.C_2H_7NO$	Combi-Blocks, QA-6124
TPEN - N,N,N',N'-tetrakis(2-pyridinylmethyl)-1,2-ethanediamine	$C_{26}H_{28}N_6$	Cayman Chemical, 13340

2.3. *E. coli* growth experiments

2.3.1. Monitoring bacterial growth in 96 well microtitre plates

Overnight cultures were diluted 1 in 10 in LB Lennox broth and dispensed in aliquots (90 µl) into a Microtest 96 well plate with round wells (82.1583.001, Sarstedt). The plate was incubated at 37˚C at 300 rpm in a plate reader (Spectrostar Nano, BMG Labtech) for 16 hours. Optical density readings (OD_{650nm}) were recorded at 10 min intervals. Chelants were added (10 µl) to each well during the early exponential phase of growth of each strain. Experimental replicates were repeated 6 times.

2.3.2. Doubling time analysis

Doubling time was determined from the turbidity of cultures measured at OD_{650} nm. Initial OD and times were chosen after the early exponential phase exposure to chelants (≥0.2) but before stationary phase of growth (≤1.0). The OD used for determination of growth rate was approximately double the initial or OD^1 value used. The growth rate was used to determine doubling times of *E. coli* WT and mutants as described (Widdel, 2010).

$$Growth\ rate = \ln\left(\frac{OD^1}{OD^2}\right) / \frac{T^1}{T^2}$$

$$Doubling\ Time = \frac{ln2}{Growth\ rate}$$

2.4. Minimum and Fractional Inhibitory Concentration Assays

All experiments were carried out in triplicate. Some experiments were repeated 6 times to ensure validation of results; these included TPEN & BCS and TPEN &GLDA combinations.

2.4.1. Minimum Inhibitory Concentration (MIC)

E. coli cultures were grown to 0.07 at OD_{650} nm (BOECO Germany, S-30 Spectrophotometer) equivalent to a 0.5 MacFarland standard (240 µM $BaCl_2$ in 0.18 M H_2SO_4 aq.) and diluted 10-fold in LB broth for use as an inoculum (Andrews, J.M. *et al.*, 2001, *J. Antimicrob. Chemother.* 48:5-16). The diluted culture (50 µl) was then transferred into a 96-well microtitre plate. Chelants from stock samples, prepared in water, ethanol or dimethyl sulfoxide, were diluted

in LB broth and 50 µl mixed with the diluted inoculum. Plates were incubated at 37˚C with shaking at 130 rpm (Stuart SI50) for 16 hours and optical density (OD_{650nm}) monitored on a Spectrostar Nano plate reader. Minimum inhibitory concentrations were defined as the minimum concentration of chelant needed to inhibit growth by ≥90% (Hamilton-Miller, 1985)

2.4.2. Fractional Inhibitory Concentration (FIC) determination by a chequerboard assay

Stock solutions of chelators were the maximum concentration of chelants that could dissolve in either water, dimethyl sulfoxide (CHA, HBED and Octopirox) or ethanol (TPEN). These stocks were diluted to yield a 2-fold series in LB broth. One chelator was added in decreasing concentrations horizontally across the microtitre plate with the second chelator added in decreasing concentrations vertically to create a chequerboard. Fractional Inhibitory Concentrations were defined as the minimum concentration of chelant needed to inhibit growth by ≥90% individually and in combination as defined in the equation below (Hamilton-Miller, 1985; Wambaugh *et al.*, 2017). The sum of the FICs is the overall FIC for the experiment.

$$Single\ chelant\ FIC = \frac{MIC\ of\ chelant\ alone}{MIC\ of\ chelant\ in\ combination}$$

$$\sum FIC = FIC_1 + FIC_2$$

2.5. Gene expression analysis by RNA-SEQ and RT-PCR

2.5.1. RNA-SEQ

A chelant concentration inhibiting *E. coli* cells (1 x 10^7) by 10-15% in 50 ml LB broth was grown to mid-log phase (approx. absorbance 0.3-0.4 OD_{650} nM) in a 250 ml conical flask at 37˚C with shaking at 130 rpm. Cells were incubated with 10 ml RNAlater™ (ThermoFisher Scientific, AM7021), pelleted by centrifugation (11000g, 5 min, BOECO Germany U320), flash frozen in liquid N_2 and stored at -80°C.

Following procedures were conducted by Dr. Darren Smith's group from Northumbria University who also performed statistical and bioinformatics as well.

Total RNA was purified from thawed pelleted (10000 g, 5 min, 4˚C, BOECO Germany M-240R) cells using a NucleoSpin® RNA kit (Macherey-Nagel) and prepared for sequencing using the ScriptSeq™ complete kit for bacteria (Illumina). Total RNA was quantified using the Qubit RNA high sensitivity assay kit (Invitrogen) and the RNA integrity number (RIN) determined using the Agilent 2100 Bioanalyzer system with Agilent RNA 6000 Nano kit (Agilent); all samples yielded a RIN of >9. Total RNA concentration for each replicate was adjusted to 1 µg and processed to remove ribosomal RNA using Ribo-Zero rRNA removal solution for bacteria (Illumina). Depleted RNA was fragmented and reverse transcribed to cDNA using random hexamers. The cDNA was then barcoded by PCR amplification for 15 cycles using Failsafe PCR enzyme with FailSafe PCR premix E as per the manufacturer's instructions (Epicentre). Amplified libraries were quantified using the Qubit high sensitivity DNA kit (Invitrogen) and size determined using the Agilent 2100 Bioanalyzer system with the Agilent high sensitivity DNA kit (Agilent). Samples were pooled in triplicates and diluted to 12 pM with an 8 % PhiX spike and sequenced on the MiSeq system (Illumina) using a V3 150 cycle reagent cartridge.

Raw fastq data was quality checked using FastQC (Andrew, 2010). Rockhopper2 (McClure *et al.*, 2013) was used to analyse differential expression of the RNA-seq data between the controls and the test conditions. R studio (RStudio Team, 2015) was used to generate a heatmap showing the mean difference in gene expression. A Principal Component Analysis (PCA) plot of the data were created using the raw counts, using a pipeline for R studio. This required the bacterial genome to be indexed and the fastq reads mapped back to the genome using Hisat2 (Kim, Langmead and Salzberg, 2015). The mapped reads were sorted using Samtools (Li *et al.*, 2009)and used to generate expression counts using HT-Seq count (Love, Huber and Anders, 2014). This data was then piped through DeSeq2 (Love, Huber and Anders, 2014) in R (RStudio Team, 2015) The PCA plots were generated in R using this data.

2.6. Protein analysis

2.6.1. Protein extraction and quantification

Pelleted *E. coli* cells from 50 ml cultures were resuspended in 0.5 ml buffer A (10 mM HEPES pH 7.8, 160 mM KCl, 40 mM NaCl). 5 µl of protease inhibitor cocktail (Sigma Aldrich) was added and cells lysed by sonication on a machine on 35% power for 30 seconds on ice. The lysate was centrifuged at 19000 g, 10 minutes at 4 ˚C (5430/5430R, Eppendorf) and the supernatant retained. Soluble proteins were stored at -20˚C and quantified by the Bradford assay using absorbance at 595 nM using the dye reagent (Thermo Scientific) (Bradford, 1976). Standard used was bavine albumin serum in known quantities (A2153, Sigma-Aldrich).

2.6.*2.* Sodium Dodecyl Sulphate Polyacrylamide Gel Electrophoresis (SDS-PAGE)

The resolving gel layer consisted of 10% (v/v) acrylamide, 375 mM Tris.HCl pH8.8, 0.1% (w/v) SDS, 0.1% (w/v) ammonium persulphate, 3.4 mM TEMED (Bioline). The stacking gel used contained 5% (v/v) acrylamide, 125 mM Tris.HCl pH 6.8, 0.1% (w/v) SDS, 0.1% APS and 3.54 mM TEMED. Lysate samples were standardised to 5 mg/ml and mixed 4:1 with SDS-PAGE loading buffer (250 mM Tris.HCl pH 6.8, 10% (w/v) SDS, 30% (v/v) glycerol, 10 mM DTT, 0.05% (w/v) bromophenol blue) and incubated at 95˚C for 3 minutes prior to loading 15 µl on the prepared SDS gel. 5 µl of PageRuler™ Plus prestained protein ladder (ThermoScientific) was applied to the gel to provide a molecular mass standard. Gels were electrophoresed at 160 V for 40 minutes in 1x SDS-page running buffer (25 mM Tris Base, 192 mM glycine, 3.5 mM SDS).

2.6.3. Non-denaturing gel electrophoresis (Native PAGE)

10% resolving gels and 5% stacking gels were made according to the specifications detailed above in section 2.7.2. but omitting SDS. Lysate samples were standardised to 5 mg/ml and mixed 1:1 with native loading buffer (62.5 mM Tris.HCl pH 6.8, 25% (w/v) glycerol, 1% (w/v) bromophenol blue) and 20 µl of the mixture was loaded and the gel electrophoresed at 100 V, 2-3 h at 4˚C using native page running buffer (25 mM Tris-HCl, 192 mM Glycine, pH 8.3).

2.6.4. Superoxide dismutase activity assay

Native PAGE was washed with mqH_2O to remove traces of running buffer and further steps conducted in the absence of light unless otherwise stated. Gel was soaked in 50 ml riboflavin solution (100 mM phosphate buffer, pH 7.8 (Melford), 28 µM riboflavin (Sigma Aldrich), 28 mM TEMED (Biorad)) for 15 minutes and agitated using a gel rocker at 8-10 rpm **(Unable to find notes on make of equipment)**. Solution was discarded and soaked in 25 ml nitroblue tetrazolium (NBT) solution (100 mM phosphate buffer, pH 7.8 (Melford), 2.5 mM NBT (Sigma Aldrich)) for 15 minutes with rocking. Gels were then left under normal light bulb to develop. Images of gels were taken using BioRad Gel Doc XR+.

2.7. Cell metal content

Chelant was added to *E. coli* (1 x 10^7) cells in 50 ml LB broth to inhibit growth by 10-15% during mid-log phase (Approx. 0.3 - 0.4 OD_{650}nM, 3-4 hours of growth). Cultures were grown in a 250 ml conical flask at 37˚C at 130 rpm. Cells were pelleted by centrifugation (19000 g, 25 min) and the supernatant discarded. The cell pellet was resuspended in 50 ml wash buffer (0.5 M sorbitol, 10 mM HEPES) and centrifuged once again at 19000 g for 25 min. The supernatant was removed, and the pellet stored at -80˚C. The cells were then digested in 5 ml, 65% HNO_3 (Suprapur®, Sigma Aldrich) for a minimum of 16 h. These pellet digests were diluted with 2% HNO_3 and 5.89 x 10^{-4} µM silver standard for ICP (12818, Sigma Aldrich) in a 1:8:1 ratio. Calibration samples were made using known quantities of metals in nitric acid (ICP multi-element standards, CertiPUR®, Sigma Aldrich & Merck) diluted in matrix matched solution. Further dilutions of the digests for analysis used matrix matched solution. Dilutions and a calibration curve were analysed using inductively coupled plasma mass spectrometry (ICP-MS, Thermo XSERIES 2). Instrument control, analysis and quantification was obtained using software interface PlasmaLab (Thermo Scientific) and further analysis was conducted using Microsoft Excell.

Chapter 3. Antibacterial effects of chelating agents and their impact on cellular metal concentration in *E. coli*

3.1. Introduction

Metal chelation is a well known antimicrobial mechanism and in human nutritional immunity, a component of the innate immune system, sequesters essential metals to restrict microbial growth. Free iron levels, for example, are scarce in the body because of rapid chelation by ferritin, transferrin, lactoferrin and haem, the latter often harnessed by red blood cells for trafficking oxygen (Kehl-Fie and Skaar, 2010; Hood and Skaar, 2012; Cassat and Skaar, 2013). This host chelation offers protection against microbes, however, chelation using other natural or synthetic chelators have not been properly investigated. Little is known about the antibacterial effect of chelators, their mode of action and how they could be deployed to mimic nutritional immunity. This study aims to investigate a range of chelators for antibacterial applications and to investigate their effects on bacterial homeostasis using *E. coli* as a model system.

The term minimum inhibitory concentration (MIC) is often used in diagnostic laboratories to determine antimicrobial activity *in vitro* by monitoring antibiotic resistance of bacterial strains and assess efficacy. An MIC is defined as "the lowest concentration of antibiotic that inhibited visible growth" (D'Amato *et al.*, 1975). Currently, broth dilution methods are the most appropriate way to determine MIC values because they can estimate concentrations of antimicrobials effectively. The methodology most frequently applied is micro-dilution which uses small (µl) volumes and microtitration plates has significant advantages over macro-dilution, including reduced space and resource requirements and better reproducibility (Balouiri, Sadiki and Ibnsouda, 2016). It requires a specified number of cells to be grown with compounds diluted (2-fold serial dilution) in media. The protocol was formally standardised by Andrews in 2001 and later updated with further specialised protocols by Wiegand, Hilpert and Hancock in 2008. (Prichard and Shipman, 1990; Andrews, 2001; Wiegand, Hilpert and Hancock, 2008).

In the case of gram negative bacteria, the added protection of an outer membrane allows the cell to counteract the negative effects of antibiotics by acting as a physical barrier. The outer membrane can allow the diffusion of small hydrophilic molecules via porin channels but otherwise remains impermeable to macromolecules and many hydrophobic compounds (Delcour, 2009). Because of this most antibiotics do not readily diffuse through the outer membrane of gram negative bacteria as they tend to be hydrophobic or large hydrophilic compounds (Guo *et al.*, 2013) One method of increasing diffusion of antimicrobials into the cell is through increasing the permeability of the outer membrane (Guo *et al.*, 2013). Chelators are thought to increase the permeability of bacterial membranes by removing stabilising metal cations, such as Mg^{2+} and Ca^{2+}, from LPS binding sites. This action releases LPS from the membrane in large quantities which rupture the outer membrane making the cell susceptible to antibiotics (Leive, 1965; Leive, Shovlin and Mergenhagen, 1968; Vaara, 1992).

Despite published literature on the effect of chelant binding of metal ions and the resultant effect on membranes and antibiotic efficacy, the inhibitory effect of chelators alone on bacteria has not been extensively explored. In addition, the effect chelation has on cellular metal levels is also unclear, with studies restricted to magnesium and calcium binding and only in relation to LPS (Leive, 1965; Leive, Shovlin and Mergenhagen, 1968; Goldberg *et al.*, 1983; Marvin, Ter Beest and Witholt, 1989; Pelletier, Bourlioux and Van Heijenoort, 1994; Alakomi, Saarela and Helander, 2003). In this chapter, a modified version of the MIC methodology has been adopted to study the antibacterial effect of a set of 11 chelators on *E. coli* (**Table 3-1**). The effect of these chelating agents on the metal content of the *E. coli* cell is also described. Hence, the relationship between bacterial growth inhibition and metal chelation can be interrogated to give insight into the mode of action of each of the compounds tested. All experiments were performed with *E. coli* (strain BW25113) during 16 hours of growth at 37˚C. Experiments with ICP-MS on EDTA, DTPA, CHA and Octopirox and MIC data on Octopirox, HBED and CHA were conducted by Dr. Raminder Mulla.

3.2. Selection of chelants

The 11 chelators selected for analysis were chosen based on their predicted metal affinities and features of their chemistry, with the consideration that variation in structure might provide a greater range of cellular effects. Industrial parameters were also considered, including regulatory frameworks and cost. The chemical structures of these chelants is shown in **Table 3-1** and their metal affinities in solution, where known, indicated in **Table 3-2.** The chelants are: (i) EDTA and three closely related aminocarboxylates, DTPA, GLDA, MGDA, expected to bind well to a broad spectrum of metals, (ii) the well-established phosphonate analogue DTPMP, (iii) HBED, also an aminocarboxylate, but additionally incorporating phenolate units that favour binding to Fe^{3+}, together with catechol, known to have considerable selectivity for Fe^{3+}, (iv) CHA and Octopirox, both based on the hydroxamate unit – well-known for binding to Fe^{3+}, (v) TPEN and BCS which can be regarded as somewhat softer ligands that typically favour binding to the late transition metals, particularly Zn^{2+} and Cu^{2+},respectively.

In terms of industrial applications, CHA is of interest due to current use in beauty care. EDTA is the industry standard and is widely used commercially as an additive that improves efficacy of preservatives. GLDA and MGDA were chosen due to their biodegradability and the efficacy of these chelators in more alkaline conditions. Octopirox was included as it has known antimicrobial properties and, as such, is used in products to control fungal growth (Turowski-Wanke and Simsch, 2003).

Table 3-1. Chelators used in this study. Chelants are listed in alphabetical order of synonym with formal name (chemical nomenclature) and a representation of its structure.

Chelator synonym / formal name	***Structure***
BCS / Bathocuprionedisulphonate acid disodium salt	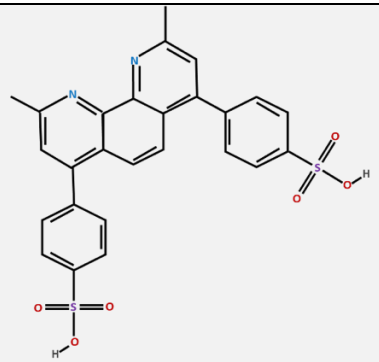
Catechol / 1,2-dihydroxybenzene	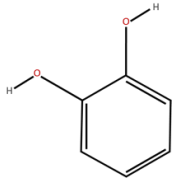
CHA / Octanohydroxamic acid	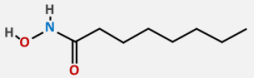

DTPA / Diethylenetriaminepentaacetic acid

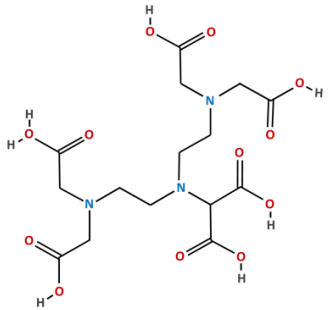

DTPMP / Diethylenetriaminepentamethylene phosphonic acid

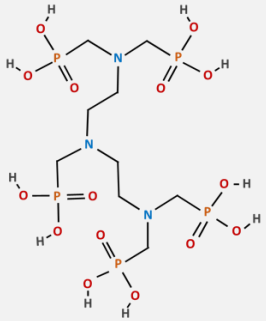

EDTA / Ethylenediaminetetraacetic acid

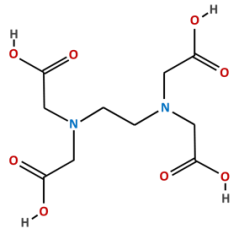

GLDA / N,N-bis(carboxymethyl)-L-glutamic acid tetrasodium salt	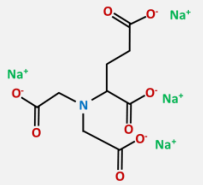
HBED / N,N'-Di(2-hydroxybenzyl)ethylenediamine-N,N'-diacetic acid monohydrochloride hydrate	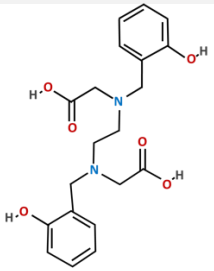
MGDA / N-(1-Carboxylatoethyl)iminodiacetate Hydrate	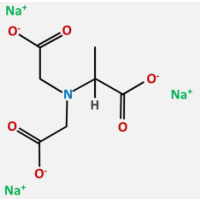
Octopirox / Piroctone olamine / 1-Hydroxy-4-methyl-6-(2,4,4-trimethylpentyl)-2(1H)-pyridone ethanolammonium salt	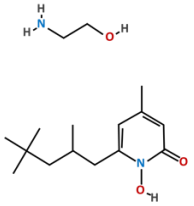

TPEN - N,N,N',N'-tetrakis(2-pyridinylmethyl)-1,2-ethanediamine

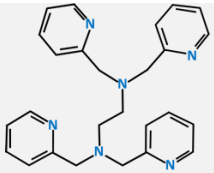

Table 3-2. Metal affinities of chelants selected for study. The stability or equilibrium constant (K), expressed as log K are shown. Values obtained from the IUPAC Stability Constants Database and were determined at 25°C, I = 0.1 M. The first value for BCS with Cu^{2+} and Zn^{2+} refers to ML complex formation (also for BCS with Fe^{2+}), the second refers to ML_2 complex formation; BCS with Ca^{2+} refers to ML_3 complex formation. The second value for BCS with Fe^{2+} corresponds to ML_3 complex formation. Note that ML_2 and ML_3 affinities are not directly comparable with ML_1 values. Octopirox is the ethanolammonium salt of piroctone and is predicted to be a strong iron chelator.

Ligand	**Mg^{2+}**	**Ca^{2+}**	**Mn^{2+}**	**Fe^{2+}**	**Fe^{3+}**	**Cu^{2+}**	**Zn^{2+}**
BCS		18.8		20.3		7.1,10.8	10.1,14.9
CHA					11.24		
Catechol	1.98	1.7	7.52		18.52	8.09	9.50
DTPA	9.3	10.7	14.31	15.97	28.7	21.5	18.61
DTPMP	6.4	7.11	11.15			19.47	16.45
EDTA	8.83	10.61	13.81	14.27	25.0	18.7	16.44
GLDA	5.2	5.9	7.6	–	15.35	13.1	11.5
HBED	10.51	9.29	14.78		39	22.95	18.95
MGDA	5.8	7.0	8.4		16.5	13.9	10.9
TPEN	–		10.27	14.6		20.6	15.58
Octopirox							

3.2. Chelator inhibition profile and influence on metal content

The effect of individual chelators on levels of iron, manganese, copper, zinc, magnesium and calcium in *E. coli* is explored in the following sections. In each case, efforts were made to determine metal profiles at 10-15% growth inhibition to avoid adverse results. For instance, lysed cells could release their metal content for uptake by viable cells; metals originally scarce could thus be acquired skewing the results between treated and untreated cultures. The sensitivity of *E. coli* to chelators was estimated in parallel with MIC values, whereby a growth inhibition of ≥90% was considered effective. The chelant MICs are compared with those determined using antibiotics, as listed in **Table 3-3**, to assess relative efficacy. Possible mechanisms of inhibition by each chelator are discussed. All chelant MIC data can be found in **Table 3-4**.

Table 3-3. Known MICs of antibiotics against *E. coli* wild-type (WT) strain BW25113. MICs are provided in µg/ml and µM concentrations with data taken from Guo *et al.* (Guo *et al.*, 2013).

	***E. coli* BW25113**	
Antibiotic	**MIC (µg/ml)**	**MIC (µM)**
Ampicillin	5.0	14.3
Streptomycin	8.7	15.0
Tetracycline	0.9	2.0
Kanamycin	29.0	59.9

Table 3-4. Average MICs of chelants against *E. coli* wild-type (WT) strain BW25113. MICs are provided in µM concentrations. Standard deviations are given as ± of the average MIC value.

	MIC / µM
CHA	$2.1 \times 10^3 \pm 0.59 \times 10^3$
Catechol	$2.3 \times 10^4 \pm 1.6 \times 10^4$
DTPA	$2.9 \times 10^4 \pm 1.9 \times 10^4$
DTPMP	$3.1 \times 10^4 \pm 1.9 \times 10^4$
EDTA	$4.9 \times 10^4 \pm 1.6 \times 10^4$
GLDA	$1.1 \times 10^5 \pm 3.3 \times 10^4$
HBED	-
MGDA	-
Octopirox	$1.3 \times 10^2 \pm 0.5 \times 10^2$
TPEN	$3.8 \times 10^2 \pm 1.3 \times 10^2$

3.2.1. Bathocuprione disulphonate acid disodium salt (BCS)

BCS is a known copper chelator that preferentially binds Cu(I) over Cu(II) in vitro and under tissue culture conditions is nontoxic (Mohindru, Fisher and Rabinovitz, 1983; Chen et al., 2016). BCS did not fully inhibit *E. coli* growth after 16 hours, with the maximum concentration used (100000 µM) only inhibiting growth by 41% ±10.23. There is no reference in the literature for BCS inhibiting growth of any bacterial species.

The 10-15% growth inhibition target was achieved by BCS at 3000 µM, which yielded 12% ±0.062 inhibition. Treated BCS samples showed no significant difference from the controls with P values above 0.05 using a t-test. The t-test was used as the only experimental data set within the 10-15% fit experimental criteria and anything above or below this inhibition margin could influence experimental bias. Quantification of copper concentrations predicted in the literature as preferred by BCS (Mohindru, Fisher and Rabinovitz, 1983; Chen et al., 2016) was also not significantly different from the untreated control (**Figure 3-1**). Hence, BCS does not seem to affect metal content of *E. coli*, although it is possible that metals are somehow sequestered and unavailable to the proteins that require them for activity.

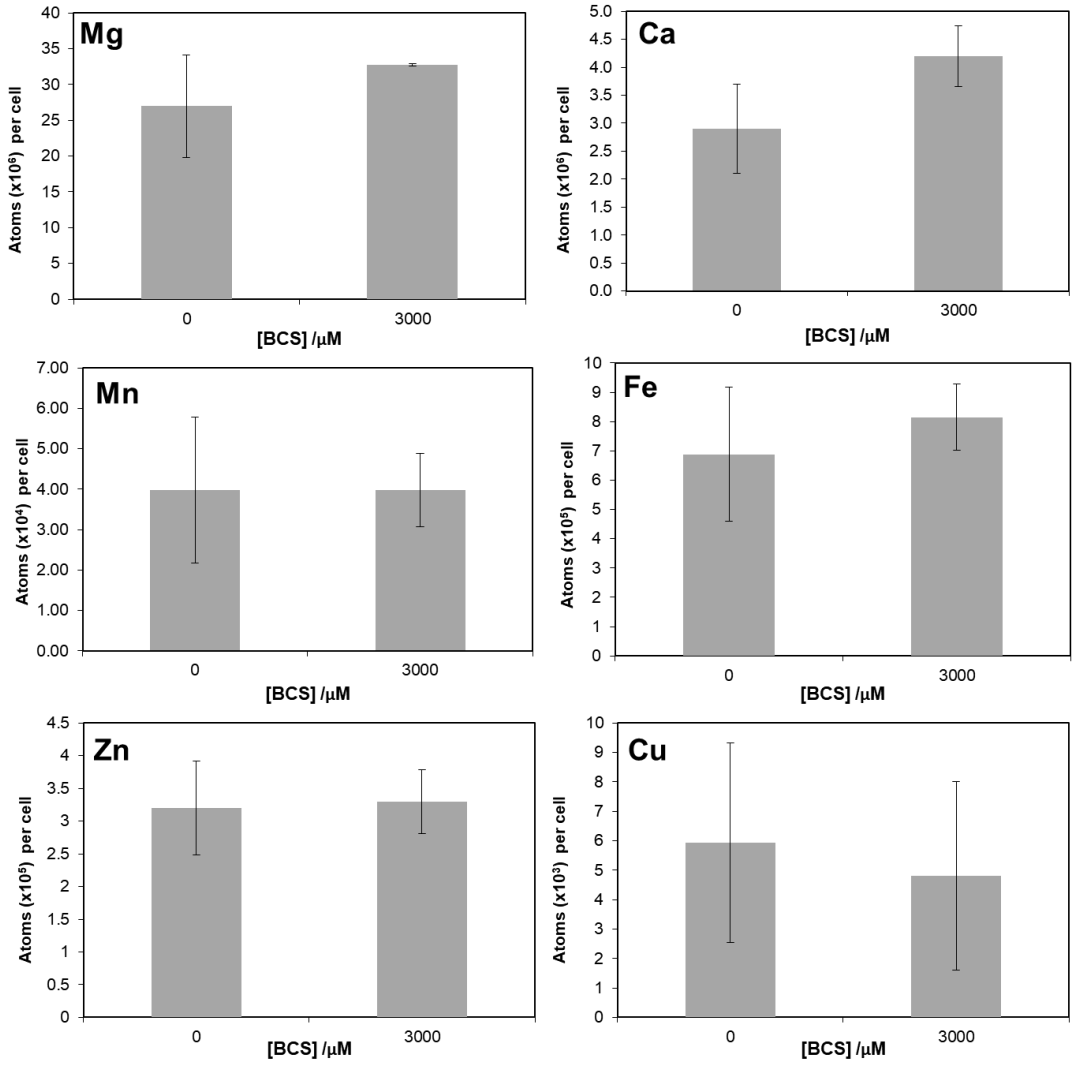

Figure 3-1. ICP-MS metal analysis of *E. coli* cells in mid-log phase of growth at 37˚C in the absence or presence of BCS at 3000 μM. Each graph represents the abundance of biologically relevant metals in number of atoms per cell. Depending on elemental abundance, these have differing 10^X values. Mg = magnesium, Ca = calcium, Fe = iron, Mn = manganese, Zn = zinc and Cu = copper.

3.2.2. Catechol / 1,2-dihydroxybenzene

Catechol is a colourless organic compound found typically in trace amounts in fruits and vegetables (Wishart et al., 2007). It is a phenolic acid commercially used in a range of products, from pesticides to fragrances, and derivatives of this compound are being developed for therapeutic applications (Wishart et al., 2007, 2009, 2012). A known bacterial siderophore made by *E. coli*, called enterobactin, is a triscatechol derivative and binds Fe(III) with a high affinity (K = 1052 M−1) (Carrano and Raymond, 1979; Raymond, Dertz and Kim, 2003;

Miethke and Marahiel, 2007). Catechol groups in these compounds are known to be essential in binding metals.

The MIC of catechol ranged between 62500 µM and 15625 µM; dual values for an MIC can frequently arise due to minor differences in growth conditions, variation in pipetting and occasionally due to changes in compound characteristics over time (Kambli et al., 2015). The high concentration of catechol required to induce inhibition of *E. coli* growth suggests that it is not an effective antimicrobial under the conditions used; the catechol concentration is over 1000 times higher than the antibiotics shown in **table 3-2**.

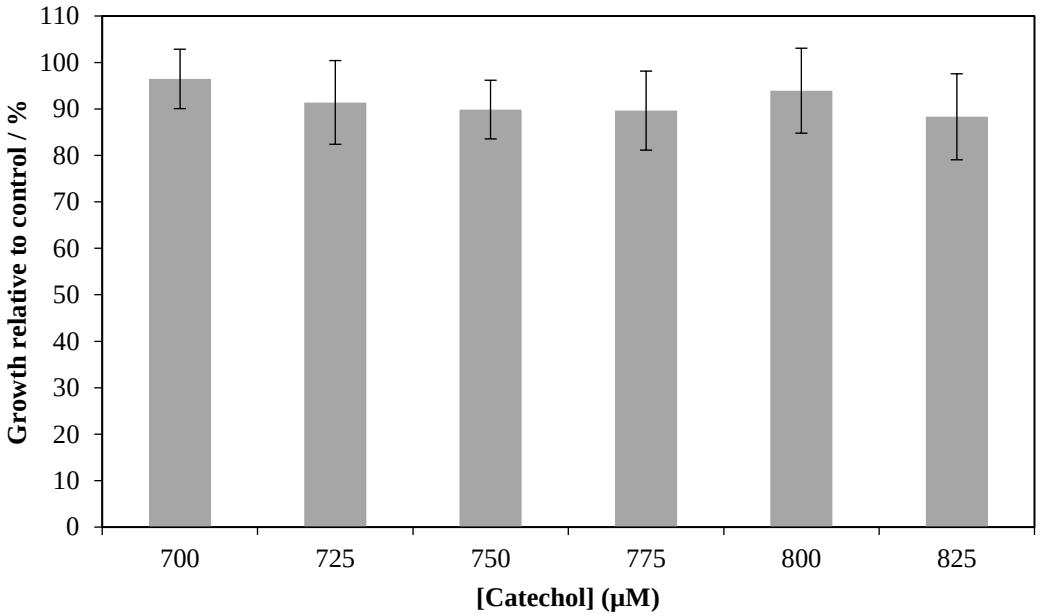

Figure 3-2. Inhibition profile of catechol on *E. coli* grown at 37˚C at 125 rpm until mid-log phase of growth. Catechol concentrations ranged from 700 µM to 825 µM in 25 µM increments. The data presented shows the growth of the sample when compared to an untreated control and is therefore a relative representation; referred to on the Y-axis as growth relative to control / %67.

Metal content analysis of cells treated with catechol using a range of concentrations gave samples with growth inhibition between 3 and 13% (**Figure 3-2**). All the tested conditions were analysed by ICP-MS to determine the impact on cellular metal content. As noted with BCS, catechol failed to show any difference in metal content between treated and untreated *E.*

coli cells (**Figure 3-3**). This is despite evidence supporting a role as an iron chelator (Rogers, 1973).

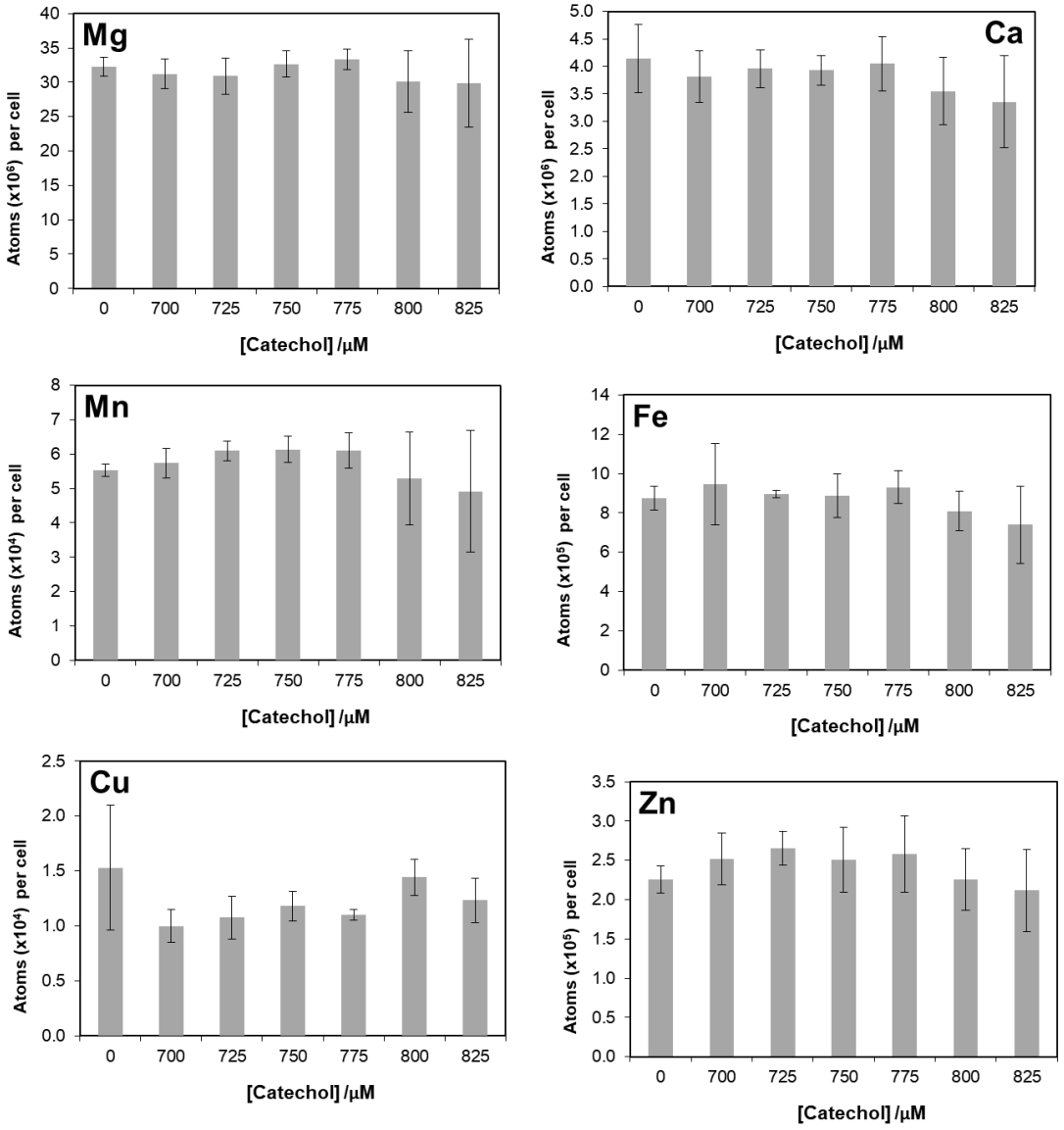

Figure 3-3. ICP-MS metal analysis of *E. coli* cells in mid-log phase of growth at 37˚C in the absence or presence of catechol at 700-825 µM in 25 µM increments. Each graph represents different biologically relevant metals and their abundance shown in atoms per cell. Depending on elemental abundance, these have differing 10^X values. Mg = magnesium, Ca = calcium, Fe = iron, Mn = manganese, Zn = zinc and Cu = copper.

3.2.3. Octanohydroxamic acid (CHA)

Hydroxamic acids, such as CHA, are bacterial and fungal metabolites and are chelates in plants (Nenortiene, Sapragoniene and Stankevicius, 2002). CHA binds both Fe(II) and Fe(III) although only forms a stable Fe(III) complex; this complex can be broken down and the released iron assimilated by mammals (Crumbliss, 1990; Palma, Sapragoniene and Stankevicius, 2003). These qualities make CHA an interesting candidate for analysis of its antibacterial activity and effect on cellular levels of metal.

Complete growth inhibition of *E. coli* cultures occurred at 2500-1250 μM, which is 100-fold higher than the MIC of kanamycin against the same strain. The low efficacy could be due to it being a hydroxamic acid, which is a natural metabolite of bacteria (Nenortiene, Sapragoniene and Stankevicius, 2002). *E. coli* may have enzymatic pathways to degrade or utilise CHA, explaining the requirement for a relatively high concentration to inhibit growth.

Metal content analysis was conducted with 40 and 50 μM CHA which resulted in 8.1 and 13.6% inhibition, respectively (**Figure 3-4**). As with BCS and catechol, no significant difference in metal content was observed between treated samples and chelant-free control *P* values (0/40 μM CHA p = 0.0733 – 0.9451; t-test and 0/50 μM CHA p = 0.1065-0.8147; t-test).

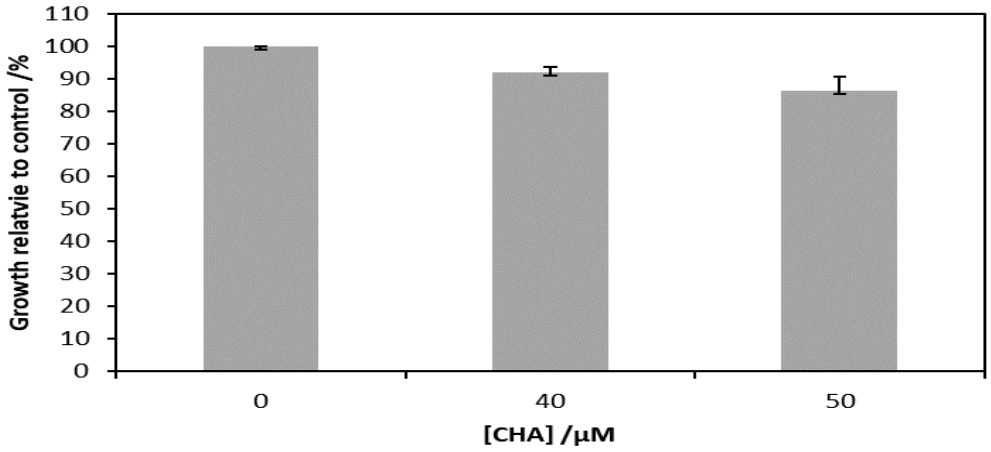

Figure 3-4. Inhibition profile of CHA on *E. coli* grown at 37˚C at 125 rpm until mid-log phase of growth. CHA concentrations used were 40 μM and 50 μM. The data presented shows the growth of the sample when compared to an untreated control and is therefore a relative representation.

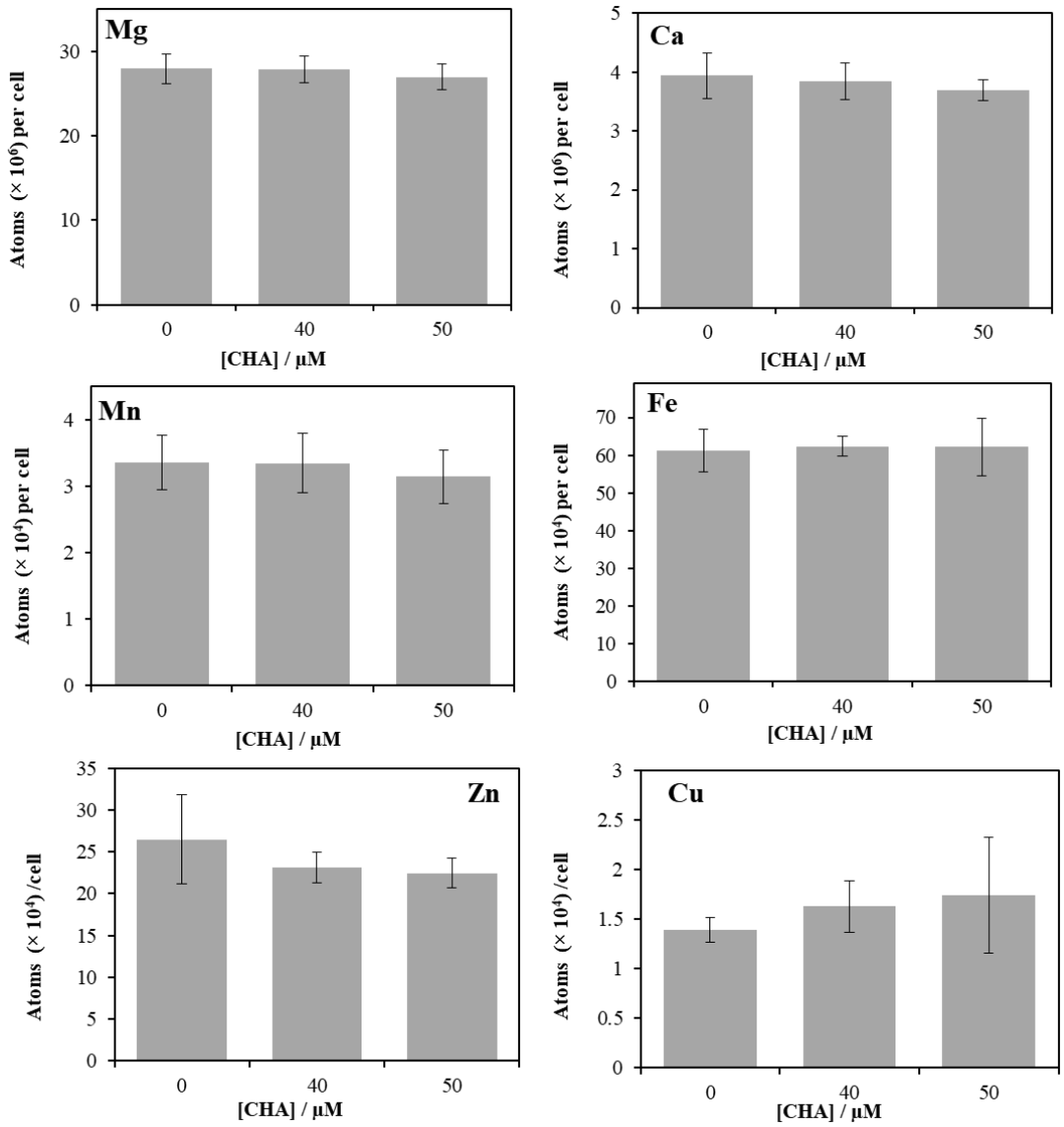

Figure 3-5. ICP-MS metal analysis of *E. coli* cells in mid-log phase of growth at 37˚C in the absence or presence of CHA at 40 and 50 µM. Each graph represents different biologically relevant metals and how abundant they are in the cell sample which is shown in atoms per cell. Depending on elemental abundance, these have differing 10^X values. Mg = magnesium, Ca = calcium, Fe = iron, Mn = manganese, Zn = zinc and Cu = copper.

3.2.4. Diethylenetriaminepentaacetic acid (DTPA)

DTPA is an aminocarboxylic acid with non-specific binding preference and is known to bind lead, iron, copper, magnesium and zinc. It can form eight bonds in a metal complex and because of this strong binding is used in medical treatments for heavy metal poisoning and

iron storage disorders (Powell and Thomas, 1967; Zhou *et al.*, 2010; Kim *et al.*, 2016). Despite the widespread therapeutic applications of DTPA and extensive knowledge of its chelating capabilities, little is known about its impact on bacterial growth and metal homeostasis.

The MIC of DTPA in experimental micro-dilution experiments was between 15625 and 62500 μM. Relatively high concentrations of DTPA were needed to observe antimicrobial activity. Hence, its strong metal binding affinity does not seem to directly correlate with bacterial growth inhibition, which is 1000-fold higher than the MIC with kanamycin in this *E. coli* strain.

The metal binding profile for DTPA in *E. coli* cultures was performed at 0, 16, 18, 20 and 30 μM which provided a large inhibition range of 15%, 16%, 12.1% and 23.1% (see **Figure 3-6**). The 20 μM DTPA treatment gave the least growth inhibition of the concentrations used. Despite this variability, metal analysis was completed and a robust data that fit calibration curve values was achieved for all metals with the exception of copper which did not reach suitable threshold levels. At the DTPA concentrations analysed by ICP-MS, there were distinct differences in the levels of certain metals (see **Figure 3-7**). No difference was detected in magnesium and calcium levels in the cells between control and experimental conditions at all DTPA concentrations. In contrast, manganese levels decreased significantly in the presence of the chelant with the lowest concentration of 16 μM inducing a 2-fold reduction. At 20 and 30 μM manganese levels dropped more severely, exhibiting a 7.7 and 8.4-fold reduction compared to the control. The increase in DTPA concentration correlated with a decrease in manganese levels in the sample. However, this step-like reduction relative to concentration was not observed with the other metals. The control decreased from 23 $x10^4$ atoms per cell with zinc to 14 $x10^4$ atoms per cell in the 16 μM DTPA treated cells. This 1.6-fold reduction was seen in all DTPA treated samples and did not decrease further with increasing DTPA concentration. The final metal analysed, iron, showed no difference between the control and the three lowest concentrations of DTPA. At 30 μM, however, iron levels dropped 3.67-fold and was the only concentration to suggest that iron chelation was occurring.

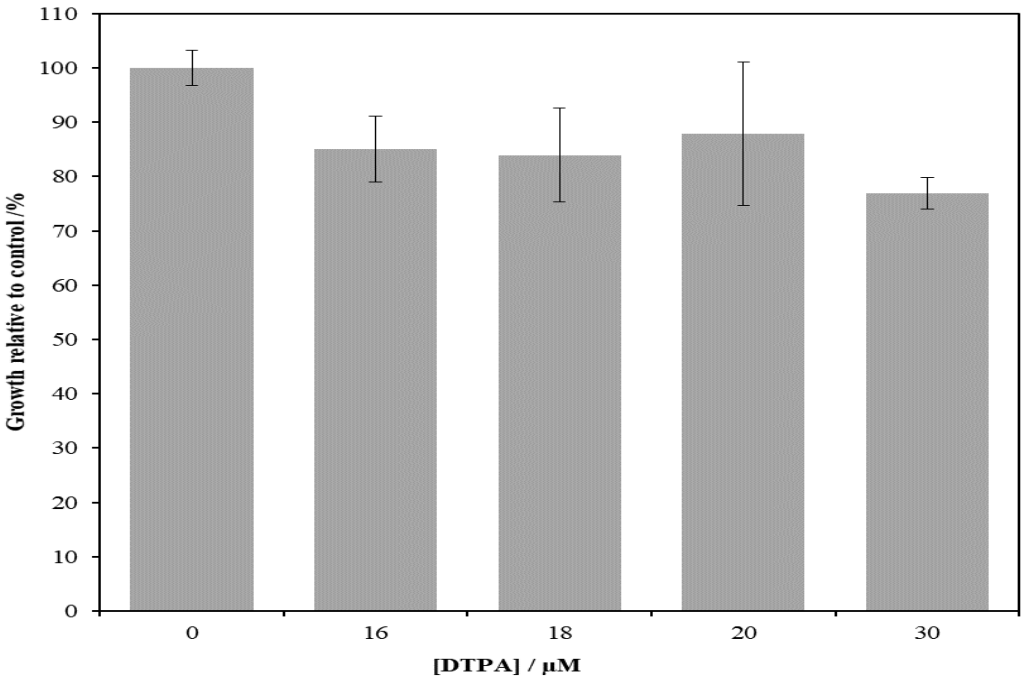

Figure 3-6. Inhibition profile of DTPA on *E. coli* grown at 37˚C at 125 rpm until mid-log phase of growth. Catechol concentrations ranged from 700 µM to 825 µM in 25 µM increments. The data presented shows the growth of the sample when compared to an untreated control and is therefore a relative representation.

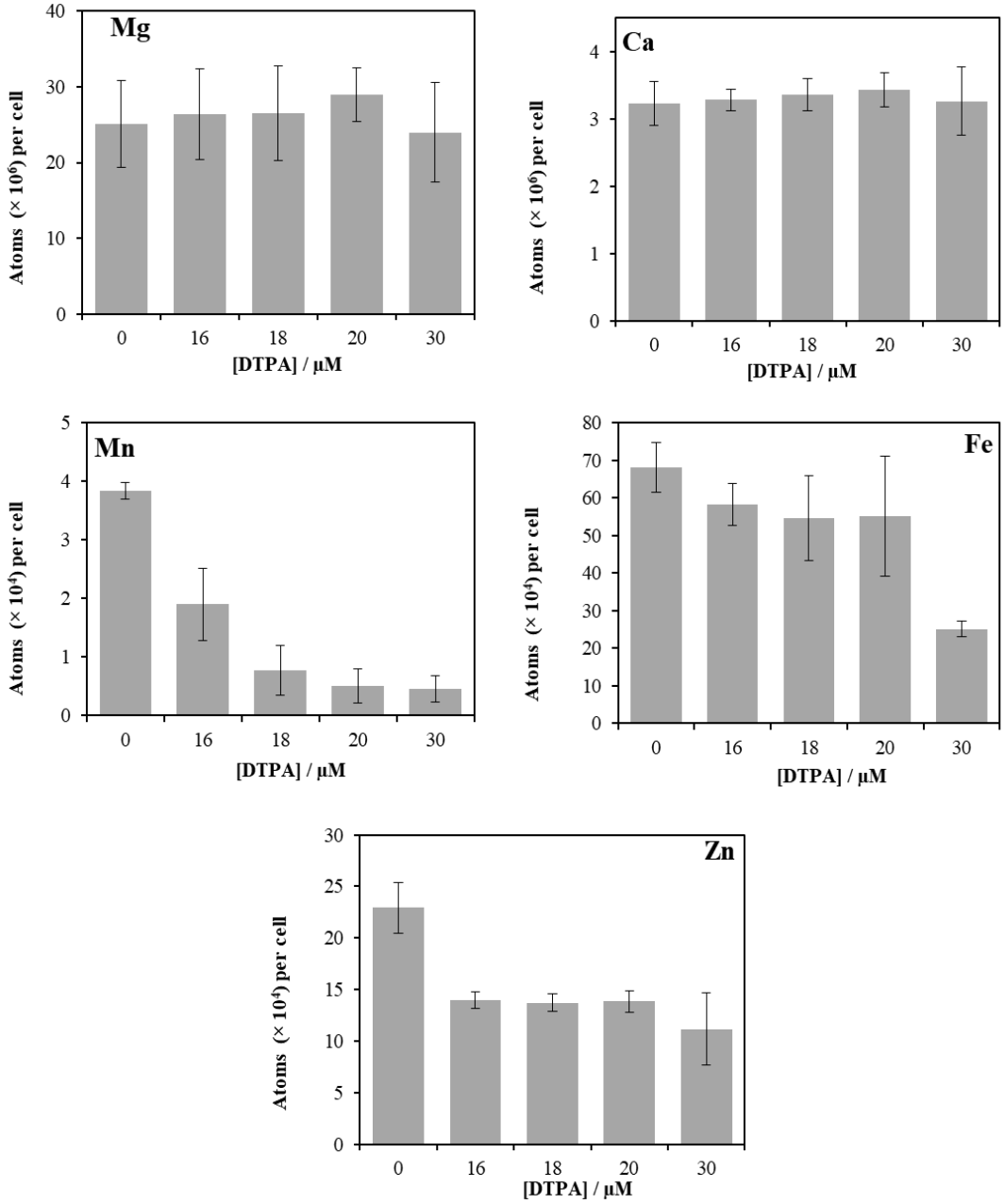

Figure 3-7. ICP-MS metal analysis of *E. coli* cells in mid-log phase of growth at 37˚C in the absence or presence of DTPA at 16, 18, 20 and 30 µM. Each graph represents different biologically relevant metals and how abundant they are in the cell sample which is shown in atoms per cell. Depending on elemental abundance, these have differing 10^X values. Mg = magnesium, Ca = calcium, Fe = iron, Mn = manganese and Zn = zinc.

3.2.5. Diethylenetriaminepentamethylene phosphonic acid / DTPMP

DTPMP is a nitrogenous organic polyphosphonic acid that can chelate and prevent corrosion. It is known to sequester iron, manganese, copper, zinc, magnesium and calcium ions and can also be degraded biologically by a strain of cyanobacterium *Anabaena variabilis* (Drzyzga *et al.*, 2017; Zschimmer & Schwarz, 2018). The effect of DTPMP on bacterial growth has not been explored and, despite availability of defined metal binding affinities in solution, no published information was found for its effect on metal homeostasis.

The MIC with DTPMP ranged from 62500 to 31250 μM in the micro dilution assays, similar to the MIC determined for catechol and DTPA. As with the other chelators examined so far, DTPMP has limited antibacterial efficacy with MIC values over 1000 times higher than the known antibiotics used for comparison (**Table 3-3**). The effect of DTPMP in combination with other chelators with similar MIC profiles is investigated further later in this chapter.

The metal profile of *E. coli* cells exposed to DTPMP was performed at a single concentration of 10 μM DTPMP which produced an 11% ±0.003 growth inhibition. The data on copper failed to fall within the calibrated range and were therefore excluded from the analysis. The results showed that DTPMP had no effect (p values >0.5) on magnesium and zinc levels, however changes in calcium, manganese and iron were observed (**Figure 3-8**). Calcium showed a modest but significant reduction of 0.2 x 10^6 atoms per cell between control and chelant samples (t-test, p-value 0.0037). However, iron levels in treated cells showed a 2.54-fold decrease from 66 x 10^4 to 26 x 10^4 atoms per cell (p-value 0.0001). Conversely, manganese levels increased by 2.60-fold from 5 x 10^4 to 13 x 10^4 atoms per cell (**Figure 3-8**; p-value 0.0001).

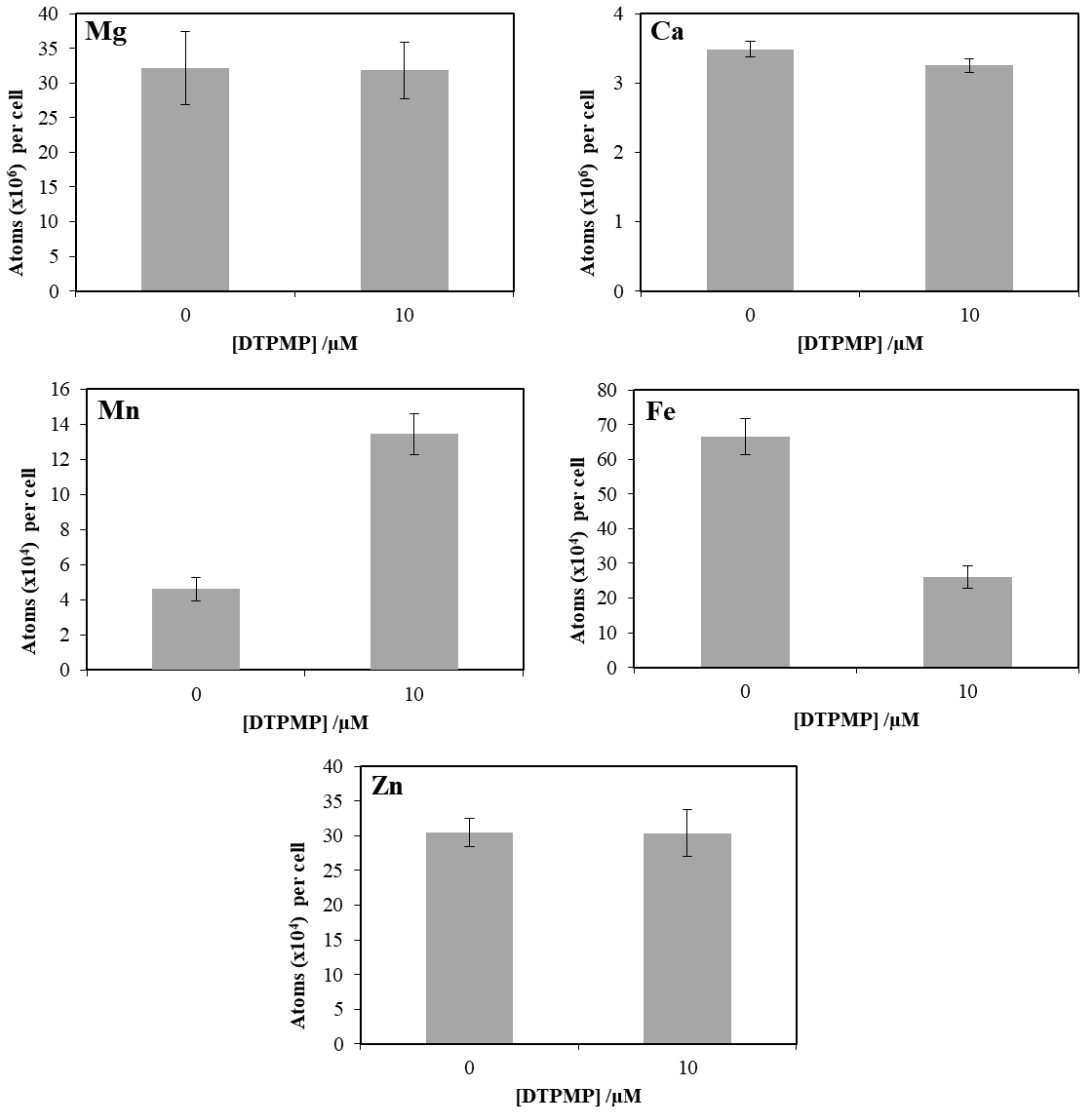

Figure 3-8. ICP-MS metal analysis of *E. coli* cells in mid-log phase of growth at 37˚C in the absence or presence of DTPMP at 0 and 10 µM. Each graph represents different biologically relevant metals and how abundant they are in the cell sample which is shown in atoms per cell. Depending on elemental abundance, these have differing 10^X values. Mg = magnesium, Ca = calcium, Fe = iron, Mn = manganese and Zn = zinc.

3.2.6. Ethylenediaminetetraacetic acid / EDTA

EDTA is a polydentate chelating agent able to form six bonds with a metal ion. It binds a range of different metals and is used widely as a food additive, cleaning products and in manufacture of pharmaceuticals (Darwish, 1963; Fujii, 1979; Kim *et al.*, 2016). EDTA is known to alter bacterial cell membrane permeability, which when used in combination with antibiotics improves efficacy (Wooley, Jones and Shotts, 1984). EDTA forms tight complexes with metals that rarely dissociate, a feature employed to help recover heavy metals from soil and promote metal uptake in plants by adding such complexes to fertilisers (Kolodynska, 2011; Tsang and Hartley, 2014). As with most other chelators, little is known concerning the effect of EDTA on bacterial growth or the metals affected within the cell.

The MIC of EDTA varied from 62500 - 31250 µM which is high for antimicrobials but similar to Catechol, DTPA and DTPMP. The effect of EDTA on cellular metal profiles was examined at 30, 50 and 70 µM, which resulted in growth inhibition from 10-17%. The highest concentration of EDTA at 70 µM produced the smallest inhibition in growth (**Figure 3-9**).

Figure 3-9. Inhibition profile of EDTA on *E. coli* grown at 37˚C at 125 rpm until mid-log phase of

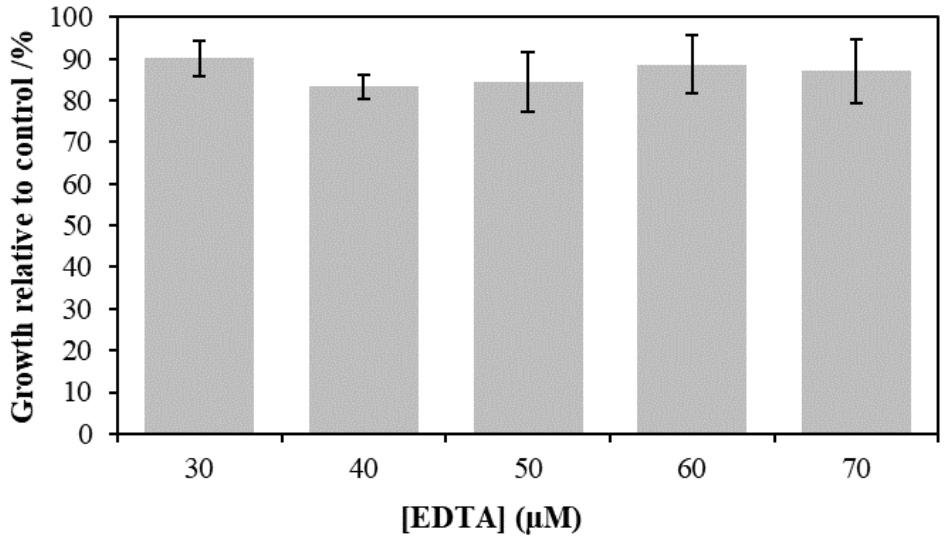

growth. Catechol concentrations ranged from 700 µM to 825 µM in 25 µM increments. The data presented shows the growth of the sample when compared to an untreated control and is therefore a relative representation.

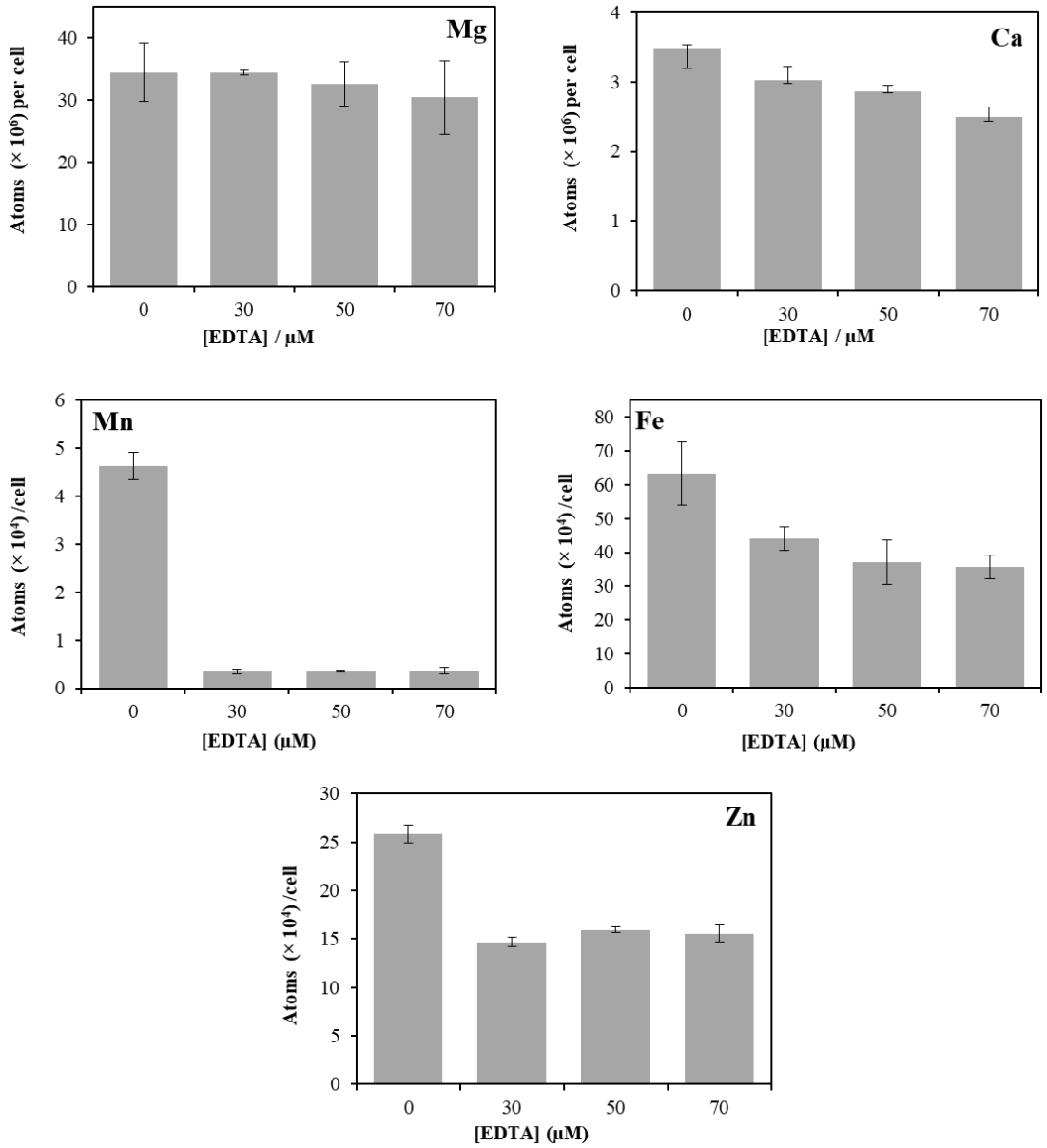

Figure 3-10. ICP-MS metal analysis of *E. coli* cells in mid-log phase of growth at 37˚C in the absence or presence of EDTA at 0, 30, 50 and 70 µM. Each graph represents different biologically relevant metals and how abundant they are in the cell sample which is shown in atoms per cell. Depending on elemental abundance, these have differing 10^X values. Mg = magnesium, Ca = calcium, Fe = iron, Mn = manganese and Zn = zinc.

All analysis was carried out for biological relevant metals apart from copper, as it did not fulfil the criteria set by the calibration standards. No significant change in cellular magnesium was detected in EDTA-treated bacteria remaining at similar levels of 3.0-3.4 x 10^7 atoms per cell (**Figure 3-10**). Calcium decreased with increasing chelant concentration, with the largest effect noted with 70 μM EDTA, although the difference was relatively small (0.98x10^6 atoms per cell). Iron, manganese and zinc atoms followed a comparable downward trend. Of these metals, manganese showed the most significant decline (13.2-fold) from 4.62 to 0.35 x10^4 atoms per cell at 30 and 50 μM EDTA. Iron levels decreased by ~1.7-fold, with zinc reduced by 1.6-fold by EDTA, which showed no additional depletion of these metals with increasing chelant concentration (**Figure 3-10**).

Given the substantial reduction in manganese resulting from EDTA treatment, we assessed whether growth inhibition of *E. coli* with 5 mM EDTA could be reversed by supplementation of the media with manganese chloride (see **Figure 3-11**). Although growth was not fully restored to levels in the absence of EDTA, supplementation of the media with 12.5 mM manganese substantially improved bacterial growth, eventually reached the same optical density after 16 hours of growth. Under the same conditions, 5 mM manganese only slightly improved growth relative to cultures with 5 mM EDTA without manganese. Higher concentrations of manganese (25 and 50 mM) did improve growth but less well than 12.5 mM manganese, probably due to toxicity. Addition of 12.5 mM manganese appears to be close to optimal for restoring *E. coli* growth in the presence of EDTA, with concentrations on either side of this either being insufficient for improvement or subject to toxicity. The results suggest that removal of manganese by EDTA is a possible reason for the growth inhibition observed with this chelant. Alternatively, manganese could be blocking the chelation of EDTA against other metals in the media at the concentrations used. Further experimentation is needed to elucidate the reasons behind this observation.

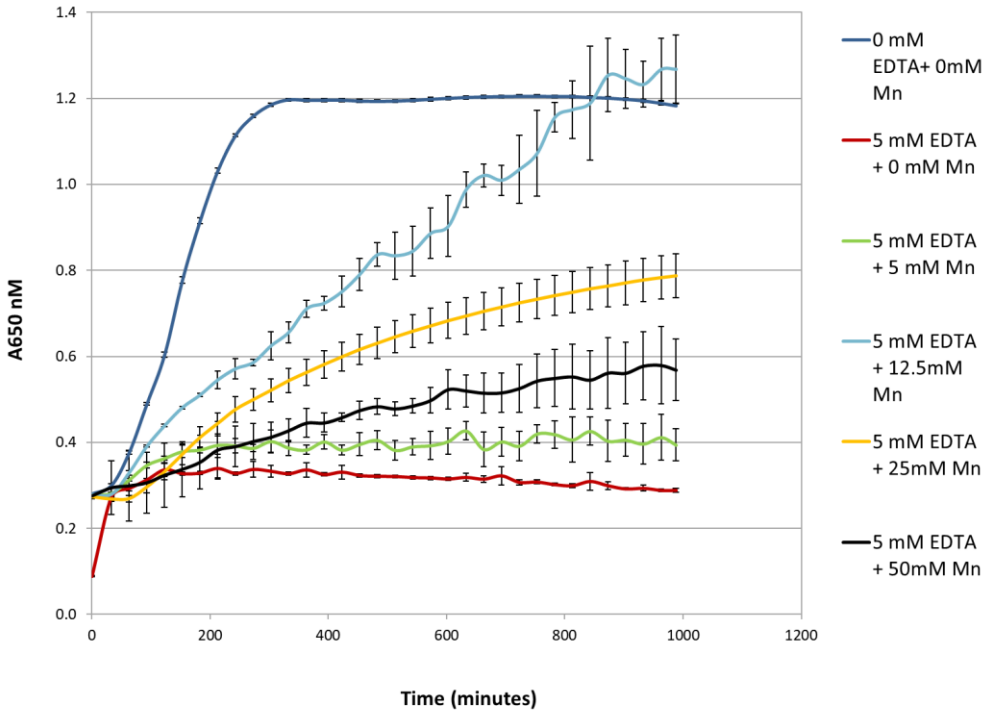

Figure 3-11. Growth of *E. coli* in the presence or absence of 5 mM EDTA supplemented with manganese chloride at the outset. Bacteria were grown in LB media for 16.6 hours with growth monitored at A_{650nm}.

3.2.7. N,N-bis(carboxymethyl)-L-glutamic acid tetrasodium salt / GLDA

GLDA is a glutamic acid diacetic acid chelator agent with affinity for a wide range of metal ions, including iron, manganese, copper, lead, chromium and zinc. It is an attractive alternative to EDTA for soil remediation, waste treatment and in biocides because of its biodegradability (AkzoNobel, 2014; Pinto, Neto and Soares, 2014; Tsang and Hartley, 2014). GLDA represents an ideal subject for further study as it is one of the few chelators with a complete set of metal stability constants available and its suitability for environmental applications.

GLDA exhibited an MIC with *E. coli* of 125000 µM (125 mM), one of the highest measured in this study. It is possible that this high MIC value is due to rapid breakdown under the conditions used. *E. coli* may be able to utilise GLDA as a metabolite, since it was originally designed on naturally occurring raw materials so that microorganisms would be able to use it for metabolism (Mahmoud *et al.*, 2011). Metal content analysis used GLDA concentrations of

1, 5.5, 10, 17.5 and 25 µM which achieved an inhibition profile of 5-13% (**Figure 3-12**). All sample concentrations were analysed by ICP-MS and data for all biologically relevant metals was obtained, with the exception of copper. There was a fair amount of variation in the data, with calcium, iron and zinc gradually reducing in response to increasing GLDA, although these differences are not statistically significant. However, a large and significant decrease in manganese (5.14-fold) was observed at 25 µM GLDA, with cells showing a linear decrease in this metal with increasing concentrations of this chelant (**Figure 3-13**).

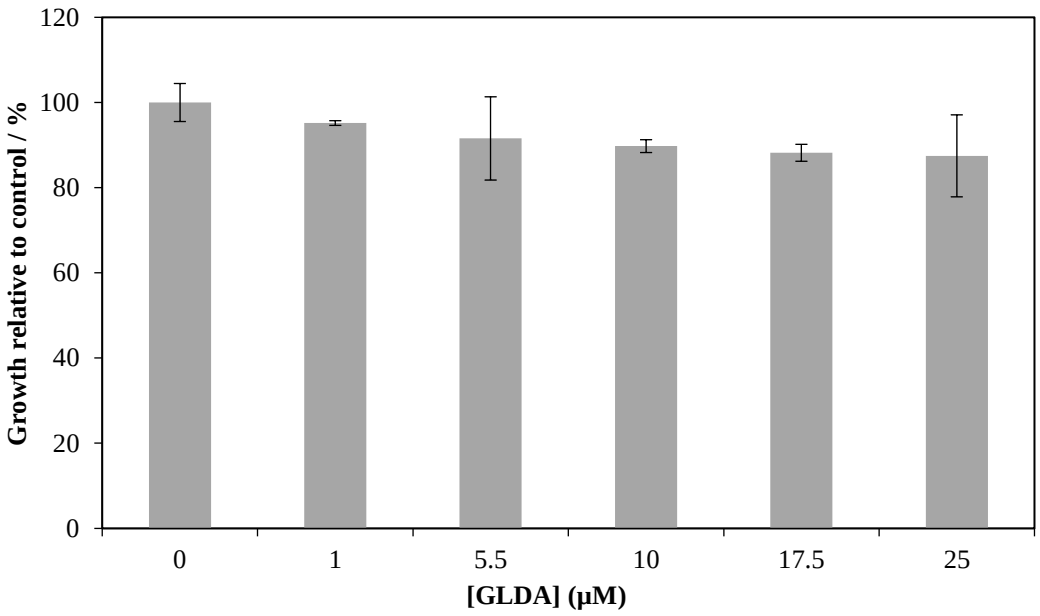

Figure 3-12. Inhibition profile of GLDA on *E. coli* grown at 37˚C at 125 rpm until mid-log phase of growth. GLDA concentrations used were 0, 1, 5.5, 10, 17.5 and 25 µM. The data presented shows the growth of the sample when compared to an untreated control and is therefore a relative representation.

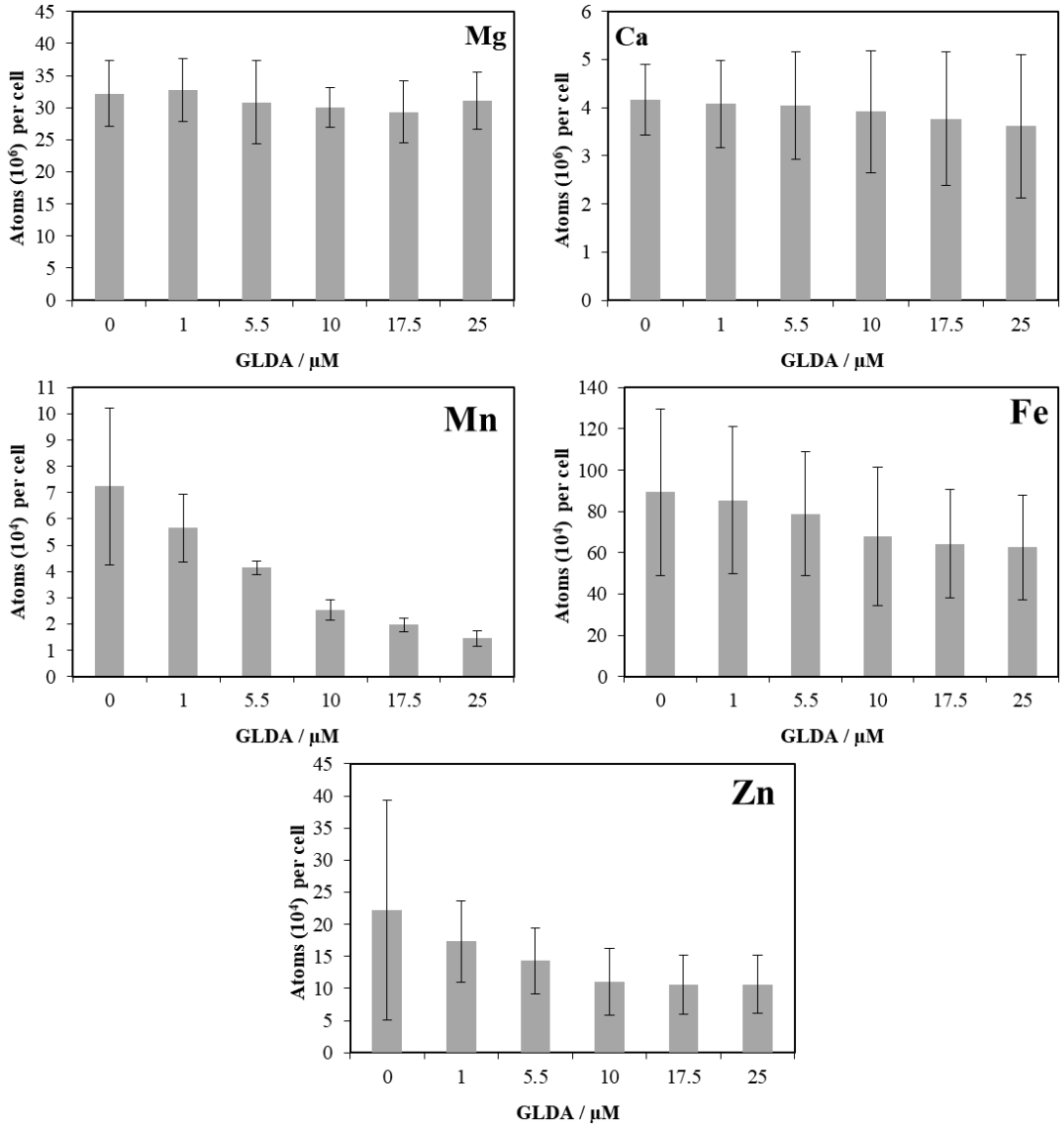

Figure 3-13. ICP-MS metal analysis of *E. coli* cells in mid-log phase of growth at 37˚C in the absence and presence of GLDA at 0, 1, 5.5, 10, 17.5 and 25 µM. Each graph represents different biologically relevant metals and how abundant they are in the cell sample which is shown in atoms per cell. Depending on elemental abundance, these have differing 10^X values. Mg = magnesium, Ca = calcium, Fe = iron, Mn = manganese and Zn = zinc.

3.2.8. N,N'-Di(2-hydroxybenzyl)ethylenediamine-N,N'-diacetic acid monohydrochloride hydrate / HBED

The aminocarboxylate HBED is a synthetic iron chelator, that forms stable complexes with iron that cannot be readily displaced by other more reactive competing cations such as copper or calcium (López-Rayo, Hernández and Lucena, 2009). This chelate provide neuroprotective

effects *in vivo* and is used as a treatment option for transfusional iron overload and in fertilisers (Bergeron, Wiegand and Brittenham, 1998; López-Rayo, Hernández and Lucena, 2009; Stachowski and Schwarcz, 2012; Kim *et al.*, 2016). The applications of HBED and its preference for iron make this a good candidate to help understand how disruption to iron metal homeostasis affects bacterial growth and metal management systems.

In microdilution assays, HBED failed to achieve ≥90% growth inhibition to allow MIC dtermination at the maximal concentration (2500 μM) tested. This concentration of HBED reduced growth to approximately 27% when compared to controls. Other chelators that also failed to fulfil the MIC criteria were BCS and MGDA (section 3.2.1 and 3.2.9) which have no obvious similarities to HBED either structurally or in metal affinity. Solubility issues prevented further testing of HBED at higher concentrations.

The concentrations used in metal profiling experiments with HBED were between 15 and 20 μM in 1 μM increments. This concentration range gave *E. coli* growth inhibition levels from 5-25% relative to the control without chelant. Metal analysis of HBED-exposed gave data for all the transition metals analysed. HBED does not readily dissolve in water so was resuspended in DMSO, meaning that all controls included an appropriate concentration of DMSO to provide the controls without chelant. There was no discernible difference in growth between DMSO and a control without chelant and DMSO at the concentrations assayed. HBED exposure affected levels of both iron and manganese in *E. coli* but had no significant effect on the other metals (**Figure 3-14**). HBED produced a significant drop (2.73-fold) in iron concentration at 15 μM and little significant decrease thereafter with increasing chelant up to 20 μM. The opposite effect was found with manganese, with levels increasing by 2.98-fold following HBED exposure at 20 μM. There was a gradual, significant elevation in manganese concentration from 15-20 μM (**Figure 3-14**).

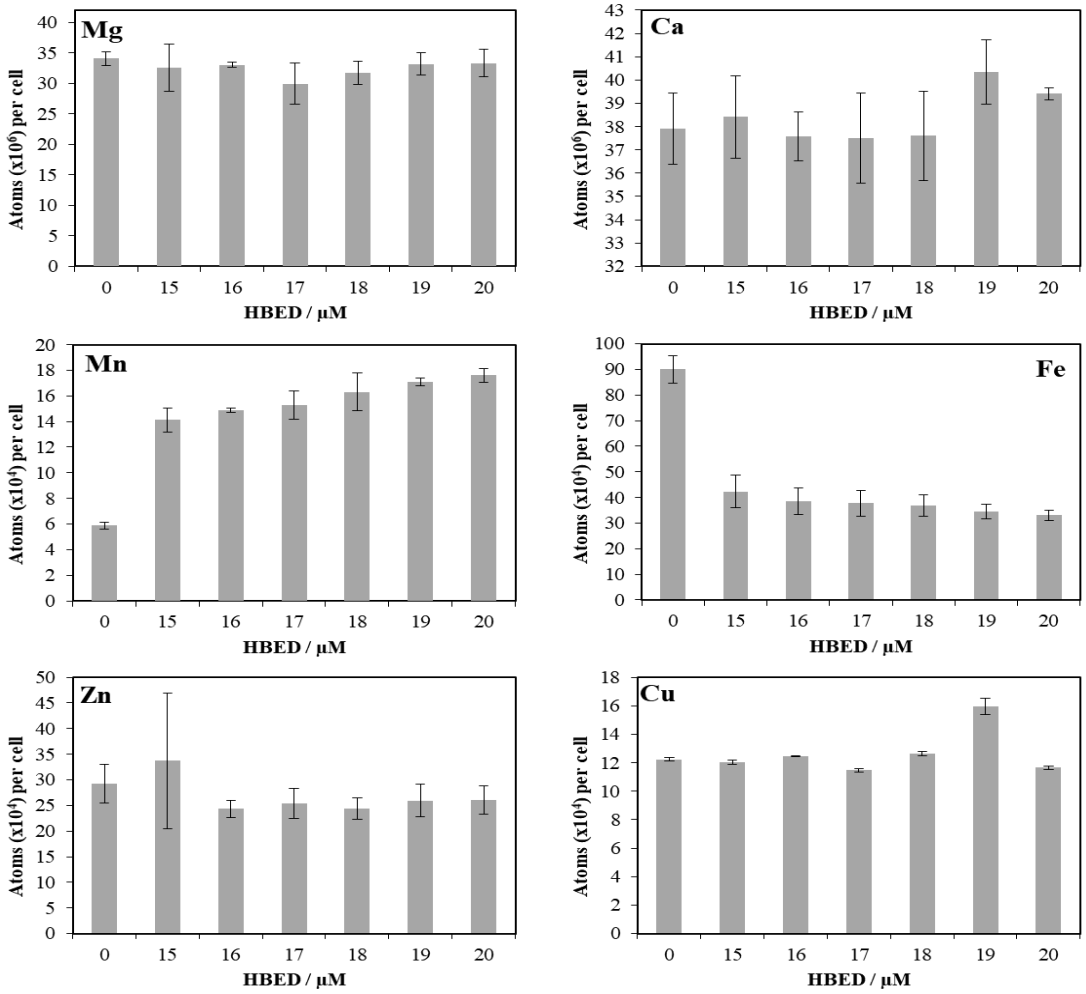

Figure 3-14. ICP-MS metal analysis of *E. coli* cells in mid-log phase of growth at 37˚C in the absence or presence of HBED at 15 – 20 µM in 1 µM increments. Each graph represents different biologically relevant metals and how abundant they are in the cell sample which is shown in atoms per cell. Depending on elemental abundance, these have differing 10^X values. Mg = magnesium, Ca = calcium, Fe = iron, Mn = manganese, Zn = zinc and Cu = copper.

3.2.9. Methylglycindiacetic acid / MGDA

MGDA is an aminocarboxylate chelant with defined metal affinity constants known for copper, zinc and nickel. MGDA is biodegradable with 89-100% being degraded by phytoremediation within 14 days; EDTA is stable under similar conditions even after 30 days (Kolodyńska, Jachula and Hubicki, 2009; Jachula, Kolodyńska and Hubicki, 2011; Pinto, Neto and Soares, 2014). The structural and functional similarities of MGDA and EDTA make it of

interest for study, alongside its potential as an environmentally-friendly alternative to existing chelators.

Metal content analysis was performed at 2-5 µM MGDA in 0.25 µM increments and these concentrations showed a bacterial growth inhibition range from 5-20% (see **Figure 3-15**). Cellular concentrations were determined for five metals, with copper again producing results that were not suitable for interpretation. Elements such as calcium and iron showed only a slight decrease at the highest concentrations of chelant, whereas manganese and zinc showed the largest declines (**Figure 3-16**). Zinc levels reduced by 1.86-fold with MGDA exposure, although there was no substantial further decreases with increasing concentration of MGDA. This effect was mirrored with manganese too, with a -fold reduction at 2 µM MGDA (**Figure 3-15**). MGDA failed to yield a clear MIC value and at the highest concentration used only inhibited *E. coli* growth by 46% at the maximum concentration tested of 125000 µM. There was considerable variation in growth in the presence of MGDA, possibly due its degradability, meaning that it may not function well as an antibacterial, at least on its own.

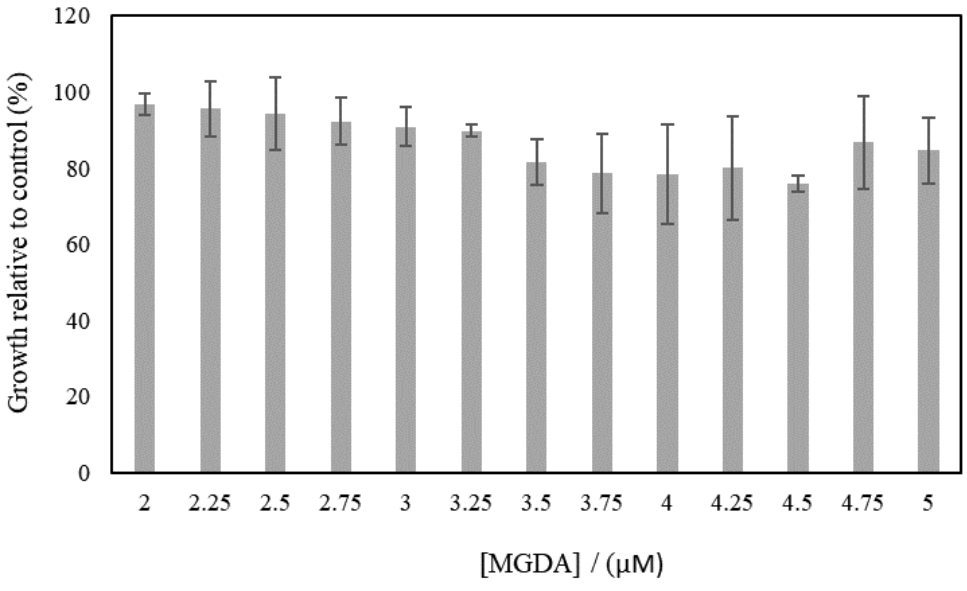

Figure 3-15. Inhibition profile of MGDA on *E. coli* grown at 37˚C at 125 rpm until mid-log phase of growth. MGDA concentrations used were 0, 2-5 µM in 0.25 µM increments. The data presented shows the growth of the sample when compared to an untreated control and is therefore a relative representation.

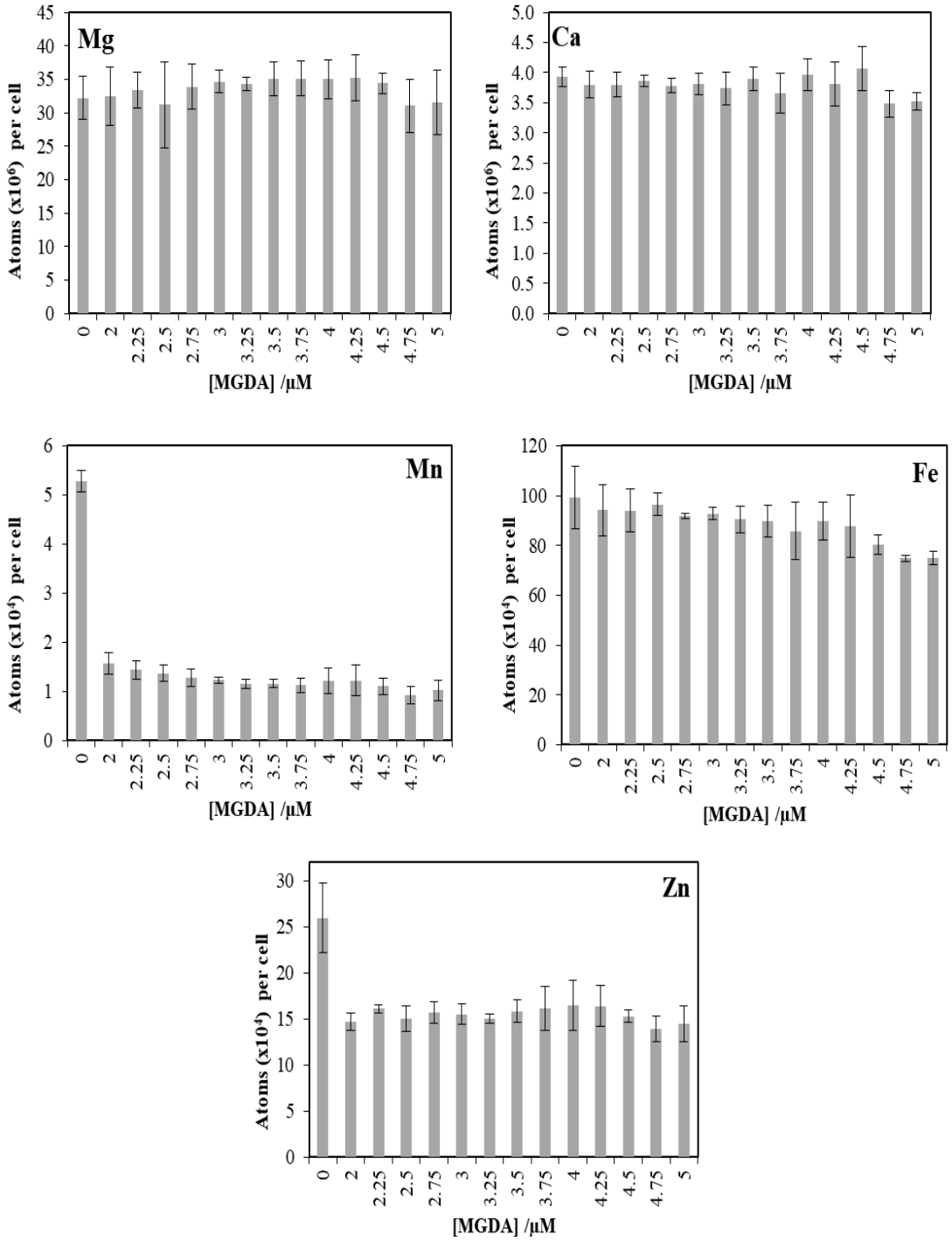

Figure 3-16. ICP-MS metal analysis of *E. coli* cells in mid-log phase of growth at 37˚C in the absence or presence of MGDA at 2-5 µM in 0.25 µM increments. Each graph represents different biologically relevant metals and how abundant they are in the cell sample which is shown in atoms per cell. Depending on elemental abundance, these have differing 10^X values. Mg = magnesium, Ca = calcium, Fe = iron, Mn = manganese and Zn = zinc.

3.2.10. Piroctone olamine / Octopirox

Octopirox is an ethanolamine salt of a hydroxamic derivative of piroctone with many applications in industry, biotechnology and research. The compound is known to have bactericidal effects on both gram negative and positive bacteria as well as fungi (Dubini *et al.*, 2011; Y. Kim *et al.*, 2011; Shakibaie *et al.*, 2014). The wide-ranging applications of Octopirox, including use in research studies, and its distinctly different structure compared to other chelants evaluated in this study, make it an interesting candidate for further investigation.

Out of all chelants tested Octopirox showed the lowest MIC when tested in microdilution at 125-62.5 μM. Its pronounced antimicrobial activity could be due to the ability of the compound to penetrate membranes and sequester metals in the cytosol. An intracellular target could potentially disrupt metal homeostasis more rapidly so that cells have less time to adapt than if the chelant bound metal outside the cell. The MIC for Octopirox is more similar to those of known antibiotics, like kanamycin, which in BW25113 is only 2-4 fold less than Octopirox (**Table 3-3**).

The total metal content of cells exposed to Octopirox during exponential growth was performed with concentrations from 2-20 μM, yielding a broad inhibition profile from 0-60%. Only two of the concentrations gave an inhibition profile of 10-15% which was at 6 and 12 μM with 14 μM inhibiting growth by 16% (**Figure 3-17**). These samples were analysed by ICP-MS to determine the concentration of all six transition metals being examined. Magnesium, calcium and copper ion concentration showed no change with increasing concentration of Octopirox. However, significant differences in manganese and iron were apparent at higher chelant concentration (≥12 μM) resulting in growth inhibition of >15% (**Figure 3-18**). As with DTPMP and HBED, Octopirox treatment induced a decrease in iron levels and a substantial increase in manganese. The reduction in iron was >2-fold at higher concentrations of the chelant. In contrast, manganese levels rose sharply with increasing Octopirox from 12 μM (growth inhibition >10%) where p-values were <0.05. Manganese

levels were 4.72-fold greater at the highest concentration of Octopirox relative to the control without chelant (**Figure 3-18**).

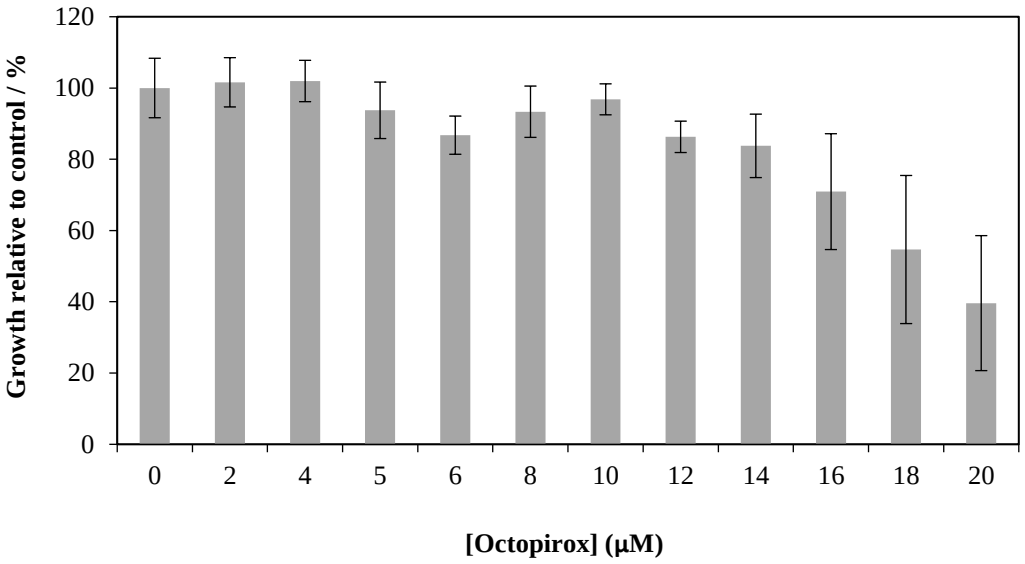

Figure 3-17. Inhibition profile of Octopirox on *E. coli* grown at 37˚C at 125 rpm until mid-log phase of growth. Octopirox concentrations used were 2-20 µM in 2 µM increments. The data presented shows the growth of the sample when compared to an untreated control and is therefore a relative representation.

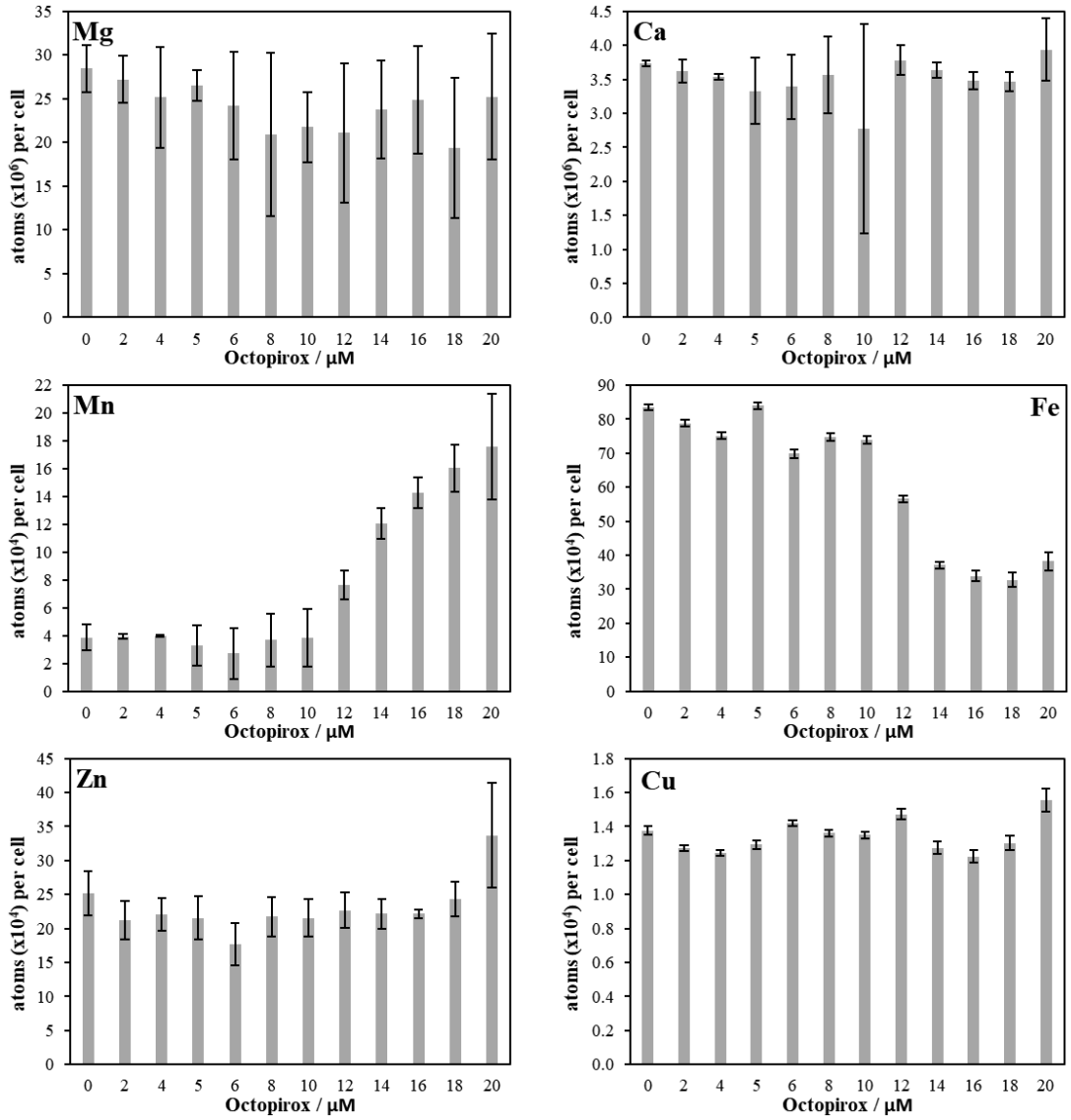

Figure 3-18. ICP-MS metal analysis of *E. coli* cells in mid-log phase of growth at 37˚C in the absence or presence of Octopirox at 2-20 µM in 2 µM increments with an additional concentration at 5 µM. Each graph represents different biologically relevant metals and how abundant they are in the cell sample which is shown in atoms per cell. Depending on elemental abundance, these have differing 10^X values. Mg = magnesium, Ca = calcium, Fe = iron, Mn = manganese, Zn = zinc and Cu = copper.

3.2.11. N,N,N',N'-tetrakis(2-pyridinylmethyl)-1,2-ethanediamine / TPEN

TPEN is a N-substituted ethylenediamine where four amino hydrogens are replaced by 2-pyridylmethyl groups. It is a known zinc chelator that can permeate membranes and induce apoptosis in eukaryotic cells (Cho *et al.*, 2007, 2010; ChEBI, 2016). Unlike other chelators in this study, it is known that it can traverse cell membranes. Understanding if these properties

provide a more robust antimicrobial effect or improved disruption of metal homeostasis would help in the design of future chelators.

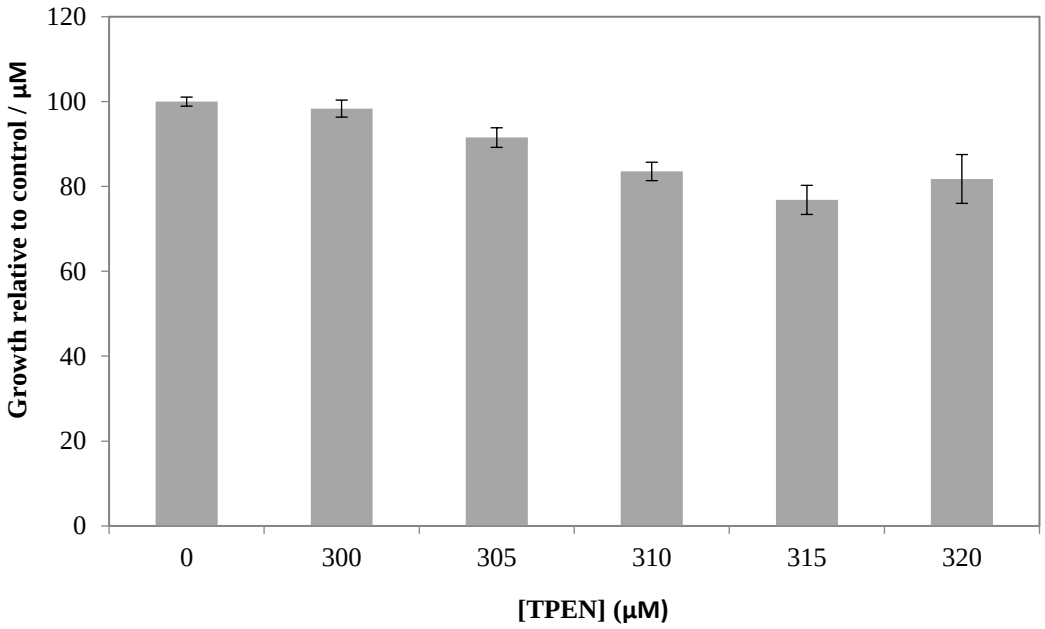

Figure 3-19. Inhibition profile of TPEN on *E. coli* grown at 37˚C at 125 rpm until mid-log phase of growth. TPEN concentrations used were 300, 305, 310, 315 and 320 µM. The data presented shows the growth of the sample when compared to an untreated control and is therefore a relative representation.

The MIC for TPEN ranged between 625 and 312.5 µM. This MIC value is one of the lowest achieved for a chelant in this study, only outperformed by Octopirox. Differences in structure and ability to bypass membranes and target intracellular metals may be a factor in this low concentration. The MIC for TPEN is also only 10 times higher than the MIC for kanamycin with this *E. coli* strain. Metal content analysis of cells exposed to TPEN was carried out at 300, 305, 310, 315 and 320 µM producing a growth inhibition profile of 10, 15, 16, 8 and 11% (**Figure 3-19**). TPEN is only soluble in ethanol so appropriate controls were conducted in parallel but showed no detrimental effects in samples without chelant and ethanol at the concentrations used. The metal content analysis revealed no difference between ethanol treatment and untreated controls with the exception of copper, hence data for this metal were not used.

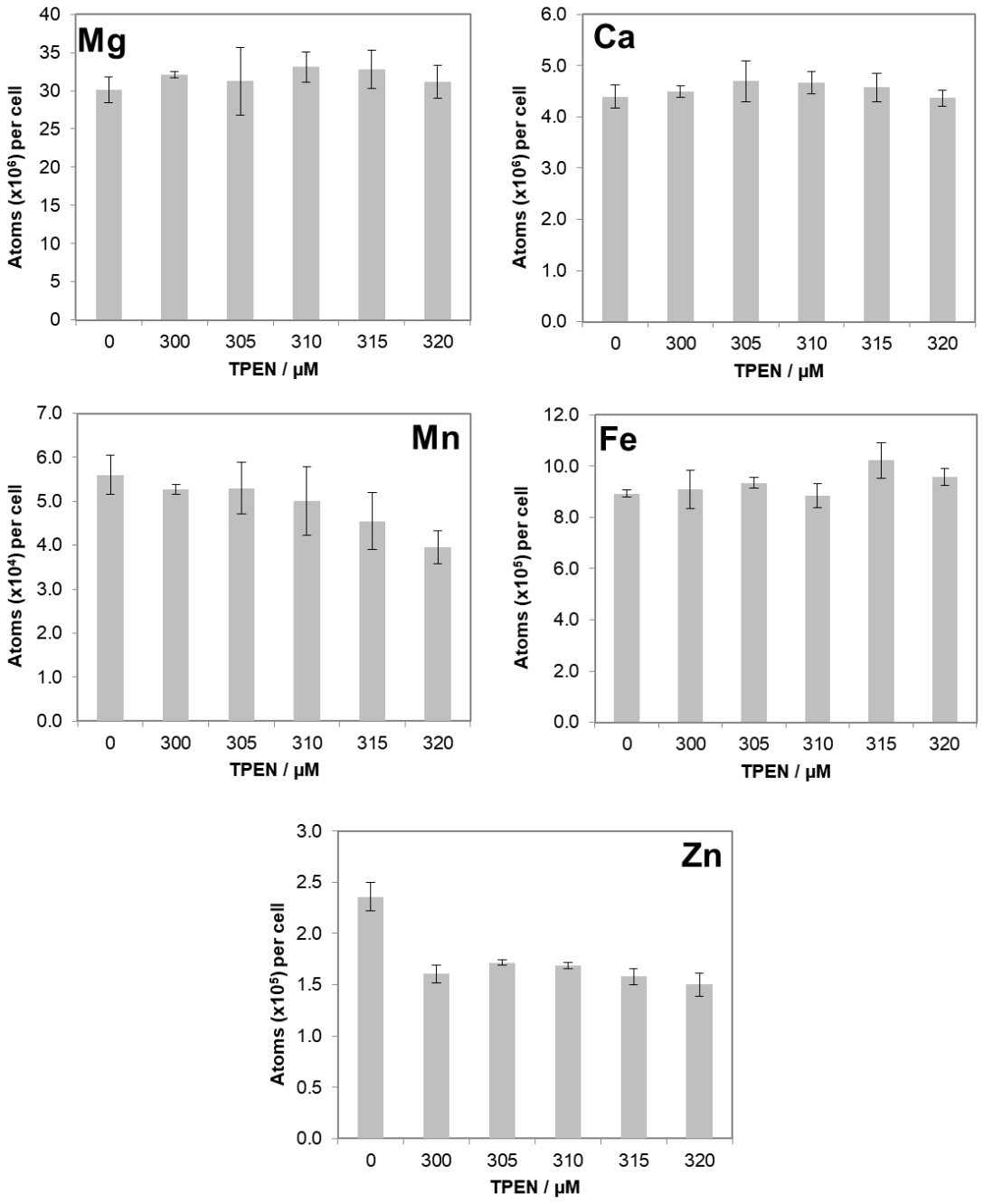

Figure 3-20. The ICP-MS metal analysis of *E. coli* cells in mid-log phase of growth at 37˚C in the absence or presence of TPEN at 300 – 320 µM in 5 µM increments. Each graph represents different biologically relevant metals and how abundant they are in the cell sample which is shown in atoms per cell. Depending on elemental abundance, these have differing 10^X values. Mg = magnesium, Ca = calcium, Fe = iron, Mn = manganese and Zn = zinc.

TPEN-treated cells generally showed little change in magnesium, calcium, manganese and iron in comparison with the control lacking chelant (**Figure 3-20**). A modest decrease in

manganese was observed, although only at the highest concentration (320 μM) was a significant difference of 1.5 x 10^4 atoms per cell noted between TPEN and the control. Zinc was the only metal that declined appreciably in the presence of TPEN with the lowest treatment of the chelant resulting in an 8 x 10^4 atom per cell reduction (1.5-fold). No further decrease in zinc levels was found with higher TPEN concentrations (**Figure 3-19**). The results support published work stating that TPEN is a proficient zinc chelator (Nakatani *et al.*, 2000; Hyun *et al.*, 2001; Sigdel, Easton and Crowder, 2006; Cho *et al.*, 2007) but may also bind manganese at higher concentrations (**Figure 3-20**).

3.3. Discussion of chelant effects on bacterial growth and cellular metal content

The 11 chelants examined in this chapter show a range of effects on metal content and antibacterial activity on *E. coli* cells, which cluster into distinct functionally similar groups. The *a priori* hypothesis that antibacterial efficacy of chelators is linked to metal binding capabilities was not supported by the results, suggesting a more complex relationship influenced by bacterial structural features and responses to metal deprivation. Further work is needed to ascertain metal binding systems of chelants in media or particular cellular compartments in relation to chelant partitioning coefficients and how these factors apply to gram negative bacteria.

3.3.1. Antibacterial activity of chelants by MIC

With respect to MIC, chelants could be differentiated based on efficacy and were grouped based on an MIC of ≤1000 μM, 1001-10,000 μM, MIC 10,001-100,000 μM and MIC >100,000 μM (**Table 3-5**). An additional group incorporated those that reduced *E. coli* growth by <90%. Compared to several known antibiotics and their MIC values, 2.0-59.9 μM seen in **table 3-4** (Guo *et al.*, 2013), the majority of chelants are poor inhibitors of *E. coli* growth. There are several possible reasons for the weak antibacterial activity of chelants, including limited efficacy, poor metal binding affinity or bacterial metabolism, essentially resulting in inactivation of the compound. These features will be discussed further in this section in relation to each of the chelants studied.

Octopirox and TPEN have the lowest MIC values (≤1000 μM) and are therefore two of the most effective chelants. Their MIC values are closest to the MIC of kanamycin at 59.9 μM on the same *E. coli* strain **table 3-4** (Guo *et al.*, 2013).

Table 3-5. Chelant groups based on the values of their MIC range which fit into the five specified categories. The poor growth inhibition group indicates chelants that could not inhibit bacterial growth by a predetermined cut off value of ≥90%. Other categories indicate that the chelant has achieved this inhibition cut off value and thus are separated into groups based on their MIC. The compounds belonging to each group are listed with their MIC ranges shown in brackets in μM.

Categories	Chelants
≤1000 μM	Octopirox (62.5-125 μM), TPEN (312.5-625 μM)
≤10,000 μM	CHA (1250-2500 μM)
≤100,000 μM	Catechol (15625-62500 μM), DTPA (15625-62500 μM), DTPMP (31250-62500 μM), EDTA (31250-62500 μM)
>100,000 μM.	GLDA (125000 μM)
No inhibition	BCS, HBED, MGDA

However, Octopirox and TPEN have radically different metal binding profiles suggesting that depletion of a specific metal is not the reason for their efficacy. Previous studies suggest that both compounds can associate and penetrate eukaryotic cell membranes, including granulocytes, thymocytes and lymphocytes (Arslan *et al.*, 1985; McCabe, Jiang and Orrenius, 1993). TPEN is a lipid soluble metal chelator that is able to enter eukaryotic cells (Arslan *et al.*, 1985; McCabe, Jiang and Orrenius, 1993). Octopirox is also capable of traversing eukaryotic membranes to form Fe(III) complexes, which can decrease mitochondrial metabolism and affect energy production (Y. Kim *et al.*, 2011). Octopirox has biocidal activity when complexed with zinc against a varied group of microorganisms, including bacteria and yeast (Turowski-Wanke and Simsch, 2003). The ability of Octopirox and TPEN to enter the

cytosolic compartment may explain their improved efficacy relative to the other chelants tested. Intracellular metal chelation may have a more rapid and detrimental effect on bacterial growth, presumably by starving essential metalloenzymes of their required cofactors. However, it has not yet been established whether Octopirox and TPEN can bypass both the inner and outer leaflets of the gram negative bacterial envelope.

CHA was the only chelant to fall within the 1001-10,000 µM MIC range, 10-fold less effective than TPEN and Octopirox but more effective than the others tested. CHA is a part of the hydroxamic group whose members vary based on substituent carbon chain length. CHA has a 7-carbon chain length that alters its hydrophobicity to make it more amphiphilic, allowing it to form micelles alone or with other compounds (Crumbliss, 1990). It can bind iron, forming a complex that is more stable with Fe(III) than Fe(II), that can be metabolised by mammals and is a natural metabolite of both bacteria and plants (Palma, Sapragoniene and Stankevicius, 2003). CHA can disrupt bacterial membranes (Hetrick and Schoenfisch, 2006) but, unlike TPEN or Octopirox, it is naturally found inside plant and bacterial cells alike (Nenortiene, Sapragoniene and Stankevicius, 2002). The higher MIC value compared to TPEN and Octopirox suggests that CHA is more readily tolerated, perhaps because it can be metabolised, and its effect is neutralised over time.

Aminocarboxylate chelators DTPA, DTPMP, EDTA and catechol had MIC values between 10,001 and 100,000 µM. These values were in some cases more than 100-fold higher than the MIC for kanamycin (Guo *et al.*, 2013). All four compounds are presumed to be exogenous chelators and unable to enter the cell, with effects predicted to be due to metal chelation in the media (Smith, 2013). Cells have several mechanisms to manage the scarcity of metals in the environment and can compensate by switching to utilise alternative, more abundant metals or activate scavenging pathways (Lemire, Harrison and Turner, 2013). Rapid adaptation would therefore result in a larger quantity of chelator being needed to exert an inhibitory effect on cell growth.

GLDA showed the highest MIC at 125000 μM and the only chelant that is readily biodegradable (AkzoNobel, 2014). It is not known to penetrate or insert into cell membranes and so is likely to chelate extracellular metals like other aminocarboxylates (Smith, 2013). The fact that GLDA is biodegradable (Pinto, Neto and Soares, 2014) is in keeping with the large concentration of GLDA needed to cause an inhibitory effect.

The final group of chelates, BCS, HBED and MGDA, did not produce an MIC according to a growth inhibition cut off ≥90%, although some reduction in *E. coli* growth was detected (HBED approximately 40-60%, MGDA approximately 30-40%). It could be that concentrations of each chelant were insufficient to observe inhibition. The maximal concentrations used were chosen due to solubility, availability of compound in sufficient quantities or the manufacturer's stock concentration of liquid chelants. It is possible that chelators cannot function well as bacterial growth inhibitors because they simply cannot sequester enough of the available metals, alongside the fact that cells are well-adapted to manage situations where metal abundance is low. In the context of bacterial growth, chelators may not form sufficiently robust associations with metal ions leading to metal complexes that can be readily dissociated. MGDA, like GLDA, is biodegradable (Pinto, Neto and Soares, 2014) which would explain why bacterial growth is relatively unaffected by this compound.

3.3.2. Chelant metal profiles

One of the goals in this study was to define any changes in metal composition in *E. coli* in response to chelant exposure to help characterise the mode of action of each compound. The metal composition of cells under chelant stress was performed using ICP-MS to determine quantitatively the number of atoms per cell of metals such as magnesium, calcium, iron, manganese and zinc. Nickel and copper levels are difficult to reliably estimate in *E. coli* due to their very low concentrations, although in several cases copper concentrations could be calculated. A relatively low 10-15% growth inhibition range in mid-log cultures was chosen and the results summarised in **Table 3-5**. Based on these results the chelants can be assigned to discrete groups based on how they affect cellular metal content, notably through their

differential effects on zinc, iron and manganese concentrations. In all cases, magnesium and calcium levels were unaffected by the presence of chelators, potentially because the media contains very large quantities of these two elements (**Table 3-5**).

Chelators can be categorised as follows: a) those which show no change in metal content, b) those which show a decrease in iron coinciding with an increase in manganese, c) those which show a decrease in manganese and d) those that primarily show a decrease in zinc. When reviewing the metal content data, fold change values are used and scrutinised using cut off points of 0.6 for a decrease and >2 for an increase in metal concentration.

Three chelators in **Table 3-5**, BCS, CHA and Catechol, showed no change in cellular metal content of exposed *E. coli* cells at 10-15% inhibition of growth. Copper levels (not shown in the table) also showed no change with p-values above 0.05, which is surprising in the case of BCS, a known copper chelator (Mohindru, Fisher and Rabinovitz, 1983). These three chelants are expected to bind and form complexes with metal ions, however, this is not reflected in the metal composition of treated cells. There is limited metal affinity data available for CHA although the IUPAC metal stability database (Pettit, 2006) states that the compound has an equilibrium constant, expressed as a log K, of 11.24 with Fe^{3+} which indicates a strong likelihood of forming a chelate-metal complex (**Table 3-2**). Similarly, IUPAC database values for catechol support the formation of stable complexes with Fe^{3+}, Mn^{2+}, Cu^{2+} and Zn^{2+} (Pettit, 2006).

Explanations for this unexpected outcome include shortcomings of the analysis itself regarding potential chelator mechanisms. Some chelators, including CHA, associate with cell membranes, by passage or insertion, due to their lipophilicity or amphiphilic properties (Ponka, Grady Ania Wilczynska and Schulman, 1984; Hyun *et al.*, 2001; Smith, 2013). Chelation therefore could occur at the cell surface or intracellularly, not altering overall metal levels but restricting availability. This difference in bioavailability cannot be elucidated by ICP-MS, which only measures overall metal content of cultured cells. Another possibility is that the compounds themselves fail to show chelation effects at the 10-15% growth inhibition

selected because they are weak chelators; higher concentrations would be necessary to observe significant cellular effects. To clarify if these compounds are functional chelators requires further experimentation.

Chelants categorised as iron depleting and manganese increasing are DTPMP, HBED and Octopirox (**Table 3-6**). Studies have shown that iron and manganese metal homeostasis systems are linked *via* the ferric uptake regulator (Fur) and the proton-dependent manganese transporter MntH (Seo *et al.*, 2014). In *E. coli*, Fur downregulates specific genes at Fur promoter regions when complexed with Fe^{2+} (Escolar, Pérez-Martín and de Lorenzo, 1999). When ferric iron levels are low, binding affinity of the Fur protein to DNA is decreased leading to upregulation of these genes. One such gene negatively regulated by Fur-Fe^{2+} is MntH which fits with increased manganese import when iron is scarce (Patzer and Hantke, 2001; Seo *et al.*, 2014). There is also evidence that many iron enzymes have manganese equivalents that can be substituted during iron limitation. For example, *E. coli* possesses iron and manganese isozymic forms of superoxide dismutase that are expressed under different environmental conditions (Dubrac and Touati, 2000). The Fur protein positively regulates the iron superoxide dismutase (SodB) when bound to Fe^{2+}; conversely, the manganese superoxide dismutase (SodA) is negatively regulated (Niederhoffer *et al.*, 1990). When iron levels in the cell decrease, SodB is not expressed whereas SodA is actively transcribed and translated, switching from iron to manganese to perform the same function (Hassan and I Fridovich, 1977; Touati, 1988; Hassan and Sun, 1992; Dubrac and Touati, 2000; Massé, Escorcia and Gottesman, 2003). The decreased levels of iron combined with increased manganese induced by these chelators can be explained by bacterial adaptation to protect against iron starvation.

DTPA, EDTA, GLDA and MGDA are chelators that predominantly decrease cellular levels of manganese to approximately 10-fold less than untreated controls (**Table 3-6**). EDTA, DTPA and MGDA also confer minor reductions in zinc, with EDTA and GLDA also showing reduced iron levels, although these are small compared to the drastic reduction in manganese. As described previously, manganese fulfils an important role during iron starvation but the

metal itself is also inherently important for cell viability. In *E. coli,* manganese contributes to signal transduction modulated by the Mn^{2+}-dependent PrpA and PrpB serine/threonine phosphatases (Missiakas and Raina, 1997). The Prp proteins also regulate the periplasmic stress response protease DegP/HtrA which provides a protective role during elevated temperatures and oxidative stress (Missiakas and Raina, 1997; Skoâ Rko-Glonek *et al.,* 1999). Manganese is also critical for the function of multiple enzymes needed for survival, such as manganic catalase, Mn-dependent ribonucleotide reductase, arginase and the previously discussed SodA (Kehres and Maguire, 2003). The metal itself is also biologically important for detoxifying reactive oxygen species, stabilising peptidoglycan cell walls and for bacterial non-enzymatic products (Jakubovics and Jenkinson, 2001). The importance of manganese during oxidative stress and other generalised cell functions means that the lows levels imposed by DTPA, EDTA, GLDA and MGDA could lead to general stress on cellular functions, instability of cell walls and increased susceptibility to oxidative damage. Manganese starvation contradicts the predicted metal binding affinity data on these chelants; which would be expected to bind Fe^{2+} or Fe^{3+} in preference to Mn^{2+} (Pettit, 2006). It is possible that physiological conditions in the proximity of the cell influence formation of chelant-metal complexes. For example, bacterial siderophores out competing chelants for iron in the media. Interestingly, supplementation of the media with manganese could restore bacterial growth in EDTA-treated cultures, suggesting that this metal is the key factor in growth restriction with this chelant.

The final compound, TPEN, was categorised as a zinc chelator due to its ability to decrease cellular zinc levels. At 10-15% growth inhibition, TPEN also resulted in a slight in decrease manganese which could potentially also contribute to the effect on bacterial growth. In *E. coli* zinc is the most concentrated of the transition metals and the minimal quota for proper function is 2×10^5 atoms per cell, corresponding to ~0.2 mM (Hyun *et al.*, 2001); these estimates are based on growth in minimal media with *E. coli* at a zinc concentration 2000 times lower than that found in bacterial cells (Hensley, 2012).

Table 3-6. The cellular metal content of *E. coli* BW25113 cultures exposed to concentrations of chelant inhibiting growth by 10-15% at mid-log phase (0.3-0.4 OD_{650nm}). Results are shown for calcium, magnesium, iron, manganese and zinc. The data is presented as a atoms per cell of the metal with standard deviation indicated. Light orange boxes indicate a decrease in metal concentration as indicated by a a decrease of 40% - <50% relative to control. Red boxes indicate a decrease of ≥50% relative to the control. Dark green boxes indicate a fold change of greater than double.

	Atoms per cell									
Chelant	**Calcium ($x10^6$)**		**Magnesium ($x10^6$)**		**Iron ($x10^5$)**		**Manganese ($x10^4$)**		**Zinc ($x10^5$)**	
	Control	**Experimental**	**Control**	**Experimental**	**Control**	**Experimental**	**Control**	**Experimental**	**Control**	**Experimental**
BCS	2.9±0.8	4.2±0.5	27±7.2	33±0.2	6.9±2.3	8.2±0.5	4.0±1.8	4.0±0.9	1.8±0.7	2.2±0.5
CHA	3.9±0.4	3.8±0.3	28±1.7	28±1.5	6.1±0.6	6.2±0.3	3.4±0.4	3.4±0.5	2.7±0.6	2.3±0.3
Catechol	4.1±0.6	4.0±0.5	32±1.3	33±1.5	8.7±0.6	9.3±0.8	5.5±0.2	6.1±0.5	2.3±0.2	2.6±0.5
DTPA	3.2±0.3	3.4±0.3	25±5.7	29±3.5	6.8±0.7	5.8±1.6	3.9±0.1	1.9±0.3	2.3±0.3	1.4±0.1
DTPMP	3.5±0.1	3.3±0.1	32±5.3	32±4.1	6.6±0.5	2.6±0.3	4.6±0.7	13.4±1.2	3.0±0.2	3.0±0.3
EDTA	3.5±0.2	2.9±0.1	34±4.9	33±3.5	6.3±1.0	3.7±0.6	4.6±0.3	0.35±0.03	2.6±1.0	1.6±0.5
GLDA	4.2±0.7	3.8±1.4	32±5.1	29±4.9	8.9±4.0	6.4±2.6	7.2±3.0	2.0±0.3	2.2±1.7	1.1±0.5
HBED	3.8±1.5	3.8±1.9	34±1.1	32±1.9	9.0±0.5	3.7±0.4	5.9±0.3	1.6±1.5	2.9±3.7	2.4±0.4
MGDA	3.9±0.2	3.7±0.3	32±3.2	34±1.0	9.9±1.3	9.4±0.5	5.3±0.2	1.2±0.1	2.6±0.4	1.5±0.05
TPEN	4.4±0.2	4.7±0.2	30±1.7	32±2.0	8.9±0.2	8.8±0.5	5.6±0.4	5.0±0.8	2.4±0.1	1.7±0.03
Octopirox	3.7±0.04	3.6±0.1	28±2.7	24±5.6	8.4±0.7	3.7±0.7	3.9±0.9	12.1±1.1	2.5±0.7	2.2±0.2

Accumulation of zinc during starvation conditions highlights its importance for the viability of most organisms (Hensley, 2012). A large proportion of the proteome utilise this metal as a structural motif or catalytic centre, frequently in a zinc finger configuration in *E. coli* (Malgieri *et al.*, 2015). Zinc is needed by both DNA and RNA polymerases and also for normal ribosome function (Patzer and Hantke, 1998; Outten and O'Halloran, 2001; Waldron and Robinson, 2009). Depletion of zinc by TPEN in the cell would therefore be expected to have a major impact by disrupting protein folding and functionality with deleterious effects on DNA metabolism, transcription and translation. It should be noted that DTPA, EDTA, GLDA and MGDA also reduce zinc levels to an equivalent low level (**Table 3-7**), which may exacerbate the effects of manganese depletion with these chelants.

3.3.3. Concluding remarks and further work

Overall, the chelators tested show a relatively weak antimicrobial effect on *E. coli* cells compared to several well-characterised antibiotics. The chelants with the lowest MIC values, Octopirox, TPEN and CHA, are predicted to associate with the bacterial envelope that may be responsible for their increased efficacy, in some cases by 1000-fold, when compared to the predicted exogenous chelators. Metal chelation of these compounds is not necessarily linked to inhibitory capacity; Octopirox and DTPMP share very similar cellular metal content profiles but considerably different MIC values. Metal binding affinity of chelators, bioavailability of metals to the cell, susceptibility of the compound to degradation and distribution of the compound in cellular compartments are all factors likely to contribute to efficacy of growth inhibition.

Significantly, metal stability constants for compounds are not a reliable predictor of the effect of a chelant on bacterial cells; examples of this are CHA, BCS and Catechol where chelation profiles could not be determined, and further investigation is warranted to determine their mode of action. In many cases, metal affinity database information contradicted the results of ICP-MS analysis and further work is needed to understand this discrepancy and what physiological factors affect chelation behaviour. One hypothesis is that the metal chelate

complex may be able to cross the outer membrane into the bacterial cell even if the chelant itself is not. The analysis of metal content of the media before cell growth using ICPMS and also of the media after growth may help understand the chelant-bacteria relationship further.

Chapter 4. Antibacterial and metal binding profiles of chelants in combination

4.1. Introduction

Understanding the relationship between combinations of antimicrobials has been explored extensively in microbiology (Jawetz *et al.*, 1955). For example, the main *in vitro* testing methods adopted for antibiotic pairings are time-kill, E-test and chequerboard assays (White *et al.*, 1996; Sopirala *et al.*, 2010). The time-kill and E-test approaches were discounted here as they are time-consuming and require pre-made strips containing appropriate concentrations of the test compounds. While the chequerboard technique as a gauge of bacterial growth inhibition can yield mixed results, it is relatively simple to perform, uses readily-available, inexpensive materials and yields results that are easily interpretable (Berenbaum, 1984; White *et al.*, 1996).

The chequerboard assay generates a value known as the fractional inhibitory concentration (FIC) index which denotes how a combination of two antibiotics react with one another in terms of growth inhibition of the bacterium being tested. When such testing was established in the 1950s, the methodology and terminology were frequently used interchangeably which proved problematic. However, in 1985 a unifying testing method was introduced which clarified both the terms used and how the data should be interpreted (Hamilton-Miller, 1985).

In this chapter, the chequerboard assay has been used to evaluate the antibacterial efficacy of chelants individually and in combination. Chelant combinations may offer a new approach to restricting bacterial growth, either to reduce the use of preservatives in products or to treat wound infections, potentially enhancing the efficacy of antibiotics. An FIC index was determined for all possible pairings of the 11 selected chelators and an outcome assigned as either synergistic, additive, indifferent or antagonistic based on the criteria defined by Hamilton-Miller (Hamilton-Miller, 1985). Synergistic combinations are those with an FIC index of ≤ 0.5 indicating that the pair of chelants exert inhibitory effects greater than the sum of their effects alone. In general terms, the lower the FIC value the better the antibacterial

A TPEN + DTPA – synergistic

[TPEN]/μM	0	122.1	244.140625	488.3	976.5625	1953.125	3906.25	7812.5	15625	31250	62500	[DTPA] /μM
0	100	81	56	43	24	16	25	8	7	5	-	0
19.53125	105	79	54	33	22	12	18	8	4	0	-	0
39.0625	74	47	23	25	12	10	17	6	2	0	-	0
78.125	54	28	14	12	10	9	8	2	0	-	0	0
156.25	20	10	10	9	8	5	2	1	1	1	1	1
312.5	13	10	8	7	3	2	1	1	1	1	1	1
625	2	1	2	1	1	1	2	2	2	2	2	2
1250	2	2	2	1	1	2	1	1	1	1	2	

$$FIC = \frac{78.12\ \mu M}{625\ \mu M} + \frac{244.14\ \mu M}{7812.5\ \mu M} = 0.124 + 0.031 = 0.155$$

B GLDA + Octopirox – additive

[glda]/μM	0	0.98	1.95	3.91	7.81	15.625	31.25	62.5	125	250	[Octopirox] /μM
0	100	99	99	100	100	102	103	50	0	-2	
1953	103	102	102	103	103	103	102	64	0	0	
3906	102	101	101	103	102	100	102	57	0	0	
7813	102	101	101	102	101	100	104	53	0	0	
15625	98	98	97	97	99	98	106	64	3	3	
31250	80	79	81	78	83	87	87	56	2	2	
62500	43	25	26	30	37	29	8	4	4	5	
125,000	4	4	3	4	3	4	3	3	3	4	

$$FIC = \frac{62500\ \mu M}{125000\ \mu M} + \frac{31.25\ \mu M}{125\ \mu M} = 0.5 + 0.25 = 0.75$$

C EDTA + HBED – indifferent

[EDTA]/μM	0	19.53	39.06	78.13	156.25	312.5	625	1250	2500	[HBED] /μM
0	100	129	127	130	128	126	114	62	23	
1953.13	101	103	107	96	100	100	84	58	21	
3906.25	78	87	83	69	78	69	50	29	16	
7812.50	34	42	45	34	41	29	22	14	13	
15625	23	19	18	21	20	17	14	14	13	
31250	18	16	20	16	15	14	13	11	6	
62500	7	6	6	6	6	5	5	5	5	
125000	4	4	4	4	4	4	4	5	5	

$$FIC = \frac{31250\ \mu M}{62500\ \mu M} + \frac{2500\ \mu M}{2500\ \mu M} = 0.5 + 1 = 1.5$$

D BCS + TPEN – antagonistic

[BCS]/μM	0	19.53	39.06	78.13	156.25	312.5	625	1250	[TPEN] /μM
0	100	113	115	100	80	3	- 0	0	
1562.50	113	113	105	91	65	1	- 0	0	
3125.00	117	115	103	99	76	11	- 0	0	
6250.00	105	116	104	88	81	11	- 0	0	
12500	108	119	89	82	81	43	1	0	
25000	105	104	77	71	49	26	6	1	
50000	83	88	71	68	60	38	14	1	
100000	59	65	72	57	53	42	15	1	

$$FIC = \frac{100000\ \mu M}{100000\ \mu M} + \frac{625\ \mu M}{312.5\ \mu M} = >1 + 2 = >3$$

Figure 4-1. Representative datasets of the four different outcomes of FIC values. A) Synergistic, FIC is between ≤0.5. B) Additive, FIC >0.5-1.0. C) Indifferent, FIC = >1.0-≤4.0. D) Antagonistic, FIC >4.0. The percentage growth is shown from experiments performed in triplicate; the extent of blue correlates with the level of *E. coli* growth (white = no growth). An MIC of <10% growth was selected (where possible) for each chelant alone and in combination to determine the FIC for each pair of chelants (see Chapter 2 for details on calculating FIC).

efficacy of the combination (this aspect is discussed further below). Additive combinations give an FIC index of >0.5-1.0 consistent with inhibition of bacterial growth equivalent to the sum of their individual effects. Indifferent pairings show inhibitory effects similar to their effects alone with FIC values of >1.0-≤4.0 (Hall, Middleton and Westmacott, 1983; Meletiadis

et al., 2010). Antagonistic combinations are defined as those where the inhibitory effect of the pairing is less than the sum of their effects alone and give FIC indices >4. Representative data can be seen below in **Figure 4-1**.

The effect of chelants in combination on growth and cellular metal content of *E. coli* cells has not previously been explored and whether specific metal deprivation correlates with synergistic activity is of interest in unravelling the mode of action of these chelants. I would like to thank Dr Raminder Mulla who conducted the cellular metal content analysis in this chapter using ICP-MS and has given permission for me to present and interpret his data here.

4.2. Antibacterial efficacy of chelator combinations and effects on cellular metal content

E. coli growth of ≤10% was used in all chequerboard assays to define the MIC for individual chelants alone, which is needed to calculate a FIC index. Several of the chelators described previously (Chapter 3.2) allowed bacteria to grow above this 10% cut-off when used individually; in these cases, the maximum concentration of chelant was chosen to provide the MIC. Overall 55 chelant pairings were tested and FIC indices determined, revealing 2 antagonistic, 13 indifferent, 15 additive and 25 synergistic combinations. The efficacy of these combinations is discussed in relation to what is known of their effects on metal content in *E. coli* as defined in Chapter 3.

4.2.1. Chelants with no effect on cellular metal content

In Chapter 3, three chelants (BCS, CHA and Catechol) showed no apparent effect on the cellular metal content of *E. coli*. Catechol exhibited a high MIC range of 15625-62500 µM, whereas CHA gave a much lower MIC of 2500 µM indicating a greater antibacterial effect. BCS alone failed to reduce bacterial growth below 10%, although good antibacterial activity and synergism was observed in combination with GLDA (FIC 0.5) and DTPA (FIC 0.156), both of which result in a decrease in cellular manganese levels (**Table 4-1**). GLDA also reduces iron in the cell at 10-15% growth inhibition. The GLDA/BCS FIC index is higher than that for DTPA/BCS indicating that it is less effective at inhibiting growth. This synergism however, could not be reproduced for other chelators known to lower manganese levels, such

as EDTA or MGDA, which decreased both manganese, and to a lesser extent, iron. These two chelators yielded a FIC index of 0.96 and 2, making the relationship additive and indifferent with BCS, so if a decrease in manganese was an advantage for BCS inhibition we should have also detected this with EDTA. BCS combined with TPEN produced an FIC index of 1.02 but was observed to be antagonistic at certain concentrations above the MIC. Hence, the BCS-TPEN pairing was assigned as antagonistic despite the additive effect seen at concentrations below the MIC (see **Table 4-1**).

Table 4-1. FIC indexes for the chelants BCS, Catechol and CHA in combination with other chelants. Index values are assigned as synergistic (≤0.5), additive (>0.5-1.0), indifferent (>1.0-4.0) or antagonistic (>4.0). Experiments were performed with *E. coli* BW25113 in LB broth at 37°C. Synergistic pairings are highlighted in green. The asterisk indicates a FIC that was antagonistic only at certain concentrations of the two chelants.

Chelant	BCS	Catechol	CHA
BCS	–	0.75	1.02
CHA	1.02	1	–
Catechol	0.75	–	1
DTPA	0.156	0.35	0.035
DTPMP	1.25	0.094	0.063
EDTA	0.96	0.094	0.188
GLDA	0.5	0.5	0.125
HBED	2	1.25	1.02
MGDA	2	0.625	0.625
Octopirox	2	1	1
TPEN	1.02*	0.188	0.156

CHA and catechol produced a similar pattern of effects in combination, showing synergistic pairings with the same chelant partners: DTPA, DTPMP, EDTA, GLDA and TPEN. This suggests that CHA and catechol likely share a similar, if not identical, inhibitory mechanism despite their different structures. The fact that the synergistic pairings are also vary with the specific metals each decrease or increase in cells, means that both CHA and catechol tend to

function beneficially with several chelators (see **Table 4-1**). However, the efficacy of chelants in combination, in terms of FIC values, suggests there are subtle differences between the CHA and Catechol mechanism of action. CHA has lower FIC indexes than catechol for DTPA, DTPMP, GLDA and TPEN suggesting an improved efficacy with these chelators over Catechol. In fact, Catechol only performed better than CHA in combination with EDTA. When BCS, Catechol and CHA are used in combination with each other, they show additive effects consistent with a similar mode of action, although the other combinations do highlight differences between BCS and the other two chelants.

4.2.2. Chelants that deprive cells of manganese

As determined in Chapter 3, this category of chelant incorporates DTPA, EDTA, GLDA and MGDA which were evaluated in combination with the other eight chelators and each other to identify any beneficial antimicrobial pairings that might inform their mode of action. The only chelant that produced synergism with all four manganese-depleting chelants was TPEN (**Table 4-2**). It is possible that this effect is due to a combination of manganese and zinc removal that prevents growth, although it should be noted that DTPA, EDTA, GLDA and MGDA also reduce levels of iron and zinc which could contribute to antibacterial efficacy. At some concentrations of GLDA and TPEN, an antagonistic effect was observed which resulted in an increase in growth rather than inhibition. Out of all chelants in this category, MGDA produced the least number of synergistic pairings, only when combined with GLDA (FIC 0.5) and TPEN (FIC 0.28), with the remainder of pairs yielding additive or indifferent outcomes (**Table 4-2**). Of the other chelators from this category, DTPA and GLDA showed synergistic pairings with seven other chelants while EDTA displayed synergism with only five.

DTPA showed synergistic combinations with BCS, CHA, Catechol, DTPMP, GLDA, TPEN and Octopirox (**Table 4-2**). With the exception of GLDA, these chelators show different metal binding profiles compared to DTPA which results in a 10-fold reduction in manganese (Chapter 3.2). DTPMP and Octopirox both deplete iron while increasing levels of manganese. Addition of DTPA to either of these two chelants could inhibit bacterial growth by starving

cells of essential amounts of both iron and manganese. DTPA has its lowest FIC indexes with these two chelants. Surprisingly, however, another chelator, HBED, which has the same metal profile as DTPMP and Octopirox, has an additive effect when paired with DTPA. Out of all the chelators in this category where iron is decreased, and manganese increased, HBED failed to fulfil the <10% growth cut-off for MIC. Hence the additive relationship (FIC 0.53) with DTPA/HBED may be due to reduced antibacterial efficacy by HBED rather than the combination of metals affected by chelant exposure. DTPA paired with CHA showed the best synergism (FIC 0.035) suggesting that their antibacterial effect arises from a different mechanism of action.

Table 4-2. FIC indexes for the chelants DTPA, EDTA, GLDA and MGDA in combination with other chelants. Index values are assigned as synergistic (≤0.5), additive (>0.5-1.0), indifferent (>1.0-4.0) or antagonistic (>4.0). Experiments were performed with *E. coli* BW25113 in LB broth at 37°C. Synergistic pairings are highlighted in green. The asterisk indicates a FIC that was antagonistic only at certain concentrations of the two chelants.

Chelant	DTPA	EDTA	GLDA	MGDA
BCS	0.156	0.96	0.5	2
Catechol	0.35	0.188	0.125	0.625
CHA	0.035	0.094	0.5	0.625
DTPA	-	1.5	0.2	1
DTPMP	0.06	1.5	2	1.5
EDTA	1.5	-	0.3	0.75
GLDA	0.2	0.3	-	0.5
HBED	0.53	1.5	0.516	1.02
MGDA	1	0.75	0.5	-
Octopirox	0.039	0.063	0.75	0.75
TPEN	0.156	0.141	0.312*	0.28

GLDA exhibited a similar synergistic pattern to that seen with DTPA, although it failed to give synergism with DTPMP (FIC 2) or Octopirox (FIC 0.75). As might be anticipated for chelants that show similar functionality in the metals they target in *E. coli*, most combinations

of DTPA, EDTA, GLDA and MGDA yielded additive or indifferent effects (Table 4-2). However, GLDA in combination with DTPA, EDTA or MGDA produced a synergistic outcome suggesting that factors other than metal depletion also contribute to bacterial growth inhibition. This could mean that certain chelants sequester metals at different cellular locations, thereby making them unavailable to the enzymes that require them for activity. Further work is needed to explain these observations. GLDA worked best with DTPA (FIC 0.2) and its highest with DTPMP (2).

EDTA produced synergistic pairings with Catechol, CHA, GLDA, Octopirox and TPEN with the lowest FIC of 0.063 detected with Octopirox (**Table 4-2**). As suggested before, the synergism observed between EDTA and DTPMP/Octopirox could be due to depletion of both iron and manganese. However, the lack of this synergism between EDTA and DTPMP/HBED suggests that other factors in addition to simple chelation are responsible for these inhibiting bacterial growth.

4.2.3. Chelants that cause reduction in iron but an increase in manganese

As noted in Chapter 3, DTPMP, HBED and Octopirox cause a decrease in iron levels but increase manganese levels in *E. coli* cells at 10-15% growth inhibition. Of these three, DTPMP showed the most synergistic pairings with six, while Octopirox and HBED produced only three and two, respectively (**Table 4-3**). This group of chelators showed little similarity in which chelant combination produced synergism, although all three were similar in their additive or antagonistic effects with BCS, MGDA and GLDA. Synergism was observed within this group between HBED and DTPMP (FIC 0.188) and Octopirox and DTPMP (FIC 0.078), whereas HBED and Octopirox displayed an additive FIC value of 0.516. As with other chelant categories with similar metal profiles, there does not seem to be a simple correlation between metal affinity, effects on cellular metal content and antibacterial activity.

Table 4-3. FIC indexes for the chelants DTPMP, HBED and Octopirox in combination with other chelants. Index values are assigned as synergistic (≤0.5), additive (>0.5-1.0), indifferent (>1.0-4.0) or antagonistic (>4.0). Experiments were performed with *E. coli* BW25113 in LB broth at 37°C. Synergistic pairings are highlighted in green. The asterisk indicates a FIC that was antagonistic only at certain concentrations of the two chelants.

Chelant	DTPMP	HBED	Octopirox
BCS	1.25	2	2
Catechol	0.063	1.02	1
CHA	0.094	1.25	1
DTPA	0.06	0.53	0.039
DTPMP	-	0.188	0.078
EDTA	1.5	1.5	0.063
GLDA	2	0.516	0.75
HBED	0.188	-	0.516^{C}
MGDA	1.5	1.02	0.75
Octopirox	0.078	0.516^{C}	-
TPEN	0.125	0.5	0.562

DTPMP and HBED were both synergistic with TPEN, however with Octopirox the combination was additive. DTPMP is thought to be an external chelant unable to enter cells or have very low permeability (Drzyzga *et al.*, 2017) whilst HBED, TPEN and Octopirox are thought to be able to pass through cell membranes and shown to affect intracellular concentrations of metals (Hyun *et al.*, 2001; Stachowski and Schwarcz, 2012; Shakibaie *et al.*, 2014). Combinations of DTPMP and Octopirox with DTPA produced strong synergistic FIC indexes of 0.06 and 0.039, respectively, which were the most beneficial combination for each of these chelants. The presumed iron and manganese depletion caused by these functionally distinct chelants seems particularly effective at preventing *E. coli* growth as discussed in **section 4.2.2**.

4.2.4. A chelant that causes reduction in zinc

TPEN was the only chelator that showed its primary effect on reducing zinc levels in *E. coli*, although manganese is also reduced slightly. Seven out of ten combinations with TPEN proved synergistic: CHA, Catechol, DTPA, DTPMP, EDTA, HBED and MGDA (Table 4-4). The chelation profiles of these chelants ranges from manganese depletion to iron depletion with some having unknown metal profiles. The successful combinatory effects of TPEN indicates that it acts by a different mechanism from most of the other chelants, presumably via its association with zinc. Alternatively, TPEN may differ in its ability to traverse the bacterial envelope and target intracellular pools of metals (Nakatani *et al.*, 2000; Walkup *et al.*, 2000; Hyun *et al.*, 2001). If this were the case for TPEN, or any of the other chelants, it would not be easy to determine which metals were affected since metal content need not necessarily change; metals could just be sequestered in the cytosol or at inner-outer membranes and unavailable for access.

TPEN achieved its lowest FIC index score of 0.125 when paired with DTPMP, an iron depletion chelator (based on data presented in **Chapter 3**). The highest FIC value, at 1.02, was obtained with BCS, showing an indifferent effect. At 312.5 μM TPEN all *E. coli* growth was inhibited, however, addition of increasing concentrations of BCS restored bacterial growth. This increase in relative growth suggests an adverse interaction between TPEN and BCS at high concentrations of the latter. Certain concentrations of BCS and GLDA also yielded similar antagonistic effects at certain concentration ratios.

A similar antagonistic effect was also observed between TPEN and GLDA. At 312.5 μM TPEN growth of *E. coli* was almost fully inhibited by the chelator, however, addition of GLDA increased growth to 25-38% relative to a positive control. Bacterial growth is then fully inhibited only when ≥31250 μM GLDA was included in the media. The specified FIC index for this chelant pair (0.312; **Table 4-2**) is therefore not fully indicative of the interaction taking place between TPEN and GLDA.

Table 4-4. FIC indexes for the chelant TPEN in combination with other chelants. Index values are assigned as synergistic (≤0.5), additive (>0.5-1.0), indifferent (>1.0-4.0) or antagonistic (>4.0). Experiments were performed with *E. coli* BW25113 in LB broth at 37°C. Synergistic pairings are highlighted in green. The asterisk indicates an FIC that was antagonistic only at certain concentrations of the two chelants.

Chelants	TPEN
BCS	1.02*
Catechol	0.156
CHA	0.188
DTPA	0.156
DTPMP	0.125
EDTA	0.141
GLDA	0.312*
HBED	0.5
MGDA	0.28
Octopirox	0.562

4.2.5. Lowest FIC indexes

The best performing combinations of chelants as judged by a FIC index <0.1, are shown in **Table 4-5**. It should be noted that a considerable reduction in only one of a pair of chelants but not the other when used in combination may produce higher FIC values. This means that some potent combinations may be overlooked when relying solely this approach to assess efficacy. All but one (DTPMP/Octopirox) of the chelant pairings differed in their cellular metal binding profiles, which fits with the expectation that depletion of distinct metal targets should yield synergistic outcomes. However, the strong synergism observed with the DTPMP/Octopirox pair of chelators is at odds with this conclusion as in *E. coli* both behave in a similar fashion, decreasing levels of iron while increasing manganese (see **Chapter 3**). Thus, as hinted at earlier, the situation is more complex than a simple correlation between metals targeted and antibacterial efficacy.

Table 4-5. Chelant combinations that produce an FIC index <0.1. The fold decrease in concentration of each of a pair of chelants is the reduction relative to its MIC.

Chelant combination	FIC index	Fold decrease in concentration in combination relative to MIC
DTPA / CHA	0.035	128 / 32
DTPA / Octopirox	0.039	128 / 32
DTPA / DTPMP	0.060	32 / 32
DTPMP / Catechol	0.063	32 / 32
EDTA / Octopirox	0.063	1024 / 16
DTPMP / Octopirox	0.078	16 / 64
DTPMP / CHA	0.094	32 / 16
EDTA / CHA	0.094	32 / 16

Out of the chelants tested, DTPMP, appears in half of the combinations listed in **Table 4-5**. DTPA, Octopirox and CHA are found in three combinations, whereas EDTA and catechol only seen in two and single combinations, respectively. The frequency of a chelator's occurrence in the table does not correlate with either the FIC index or the fold reduction in concentration when compared to its individual MIC value.

The top three chelator pairs that appear to be most synergistic all contain DTPA in combination either CHA, Octopirox or DTPMP, giving the lowest FIC indexes of 0.035, 0.039 and 0.06, respectively. A 128-fold decrease in the concentration of DTPA was observed with the CHA and DTPA pairings, while in the DTPA / DTPMP combination both chelants were only reduced by 32-fold to give a similar outcome as the chelants acting alone.

EDTA shows the largest fold decrease out of all the chelators listed in Table 4-5, displaying a 1024-fold decrease in concentration when combined with Octopirox. This dramatic decrease in one chelator doesn't produce a substantially lower FIC indexes for this pairing because Octopirox levels are only reduced 16-fold. In the case of Octopirox, greater fold decreases

were noted with other chelators such as DTPA. The greatest fold difference in Octopirox concentration (64-fold) is when it was paired with DTPMP. EDTA when combined with DTPMP or CHA gave an FIC index in both cases of 0.094, showing a 16-fold decrease in CHA when combined with each chelator. Interestingly, CHA together with DTPA appears to function more effectively as an antibacterial than the CHA / EDTA and CHA / DTPMP combinations. This suggests that there is a mechanism of action with DTPA that is not replicated with EDTA or DTPMP; this is somewhat surprising given that EDTA and DTPA both deplete the cells of manganese and share similar chemical structures.

Overall, further experimental analysis is needed to explain the results observed and determine where chelation occurs in the bacterial cell and to identify the chelating capabilities of CHA and catechol. In an effort to address some of these unknowns, two chelant combinations were probed for their effect on the total metal content of *E. coli* cells.

4.3. Metal profiles of chelants in combination

E. coli cells were exposed to a combination of chelants during the exponential phase of growth. One of the chelants tested was used at a fixed concentration to give a 10-15% growth inhibition as described in the previous chapter. The second chelant was added at a concentration that would generate a 20-25% level of inhibition when combined with the first. The reciprocal relationship was also investigated to confirm the effects observed. Cells were harvested, washed several times and resuspended in 65% nitric acid prior to ICP-MS analysis to determine total cellular metal content (see section 2.7).

The inherent difficulties in performing these experiments meant that only two chelant combinations were tested; these were DTPA with Octopirox and DTPMP with Octopirox. There were a number of reasons for selecting and evaluating these two pairings of chelants. Firstly, these two correspond to two of the most effective synergistic pairings, exhibiting low FIC indexes (**Table 4-5**). Secondly, BCS, CHA and Catechol produced no apparent change in metal content and therefore would be unlikely to yield any further insight into their mechanism of action. Thirdly, combinations of synergistic pairings that exhibit the same (DTPMP /

Octopirox) or different (DTPA / Octopirox) *in vivo* metal sequestering profiles, as defined in Chapter 3, would hopefully be useful in explaining their antibacterial efficacy.

4.3.1. Cellular metal content of *E. coli* cells exposed to DTPA and Octopirox

Earlier in this chapter, chequerboard experiments revealed that out of the 25 synergistic chelant pairings, DTPA and Octopirox was the second most effective based on a low FIC index (**Table 4-5**). The results from Chapter 3 indicated that that at 16 μM, DTPA inhibited *E. coli* growth by 10-15% and this concentration was kept constant in this combination experiment. Octopirox was then added at 0.5 μM, reducing growth to 77%, within the inhibitory range established for the experiment (**Figure 4-3A**). Higher concentrations of Octopirox were not tested. The metals quantified by ICP-MS were magnesium, calcium, manganese, iron and zinc; amounts of other metals, such as cobalt, copper and nickel were not determined due to their low levels and difficulties in fulfilling the strict calibration criteria for the instrument.

DTPA by itself depletes the cells of manganese and the ICP-MS data obtained shows with the addition of Octopirox to the culture, this is reduced further (**Figure** 4-3B). An unpaired t-test confirmed that this reduction is statistically significant with a p-value of 0.0001, suggesting that Octopirox further reduces manganese levels in the presence of DTPA. Cellular iron levels with addition DTPA alone show only a small decrease of 12 x 10^4 atoms per cell relative to the control. Addition of Octopirox affects iron content further with a decrease of 27 x 10^4 atoms per cell relative to the control, which is statistically different to DTPA alone (p-value 0.0157). Magnesium, calcium and zinc levels in this experiment did not change significantly between control and test conditions (**Figure 4-3B**).

The reverse combination of chelants was also examined, with increasing DTPA concentration monitored alongside a fixed concentration of Octopirox . Octopirox at 14 μM gave an *E. coli* growth inhibition of approximately 10% in this experiment. The addition of DTPA at different concentrations produced a 14-33% inhibition range on *E. coli* cultures (**Figure 4-4A**), which were subsequently analysed for cellular metal content using ICP-MS (**Figure 4-4B**). It is

interesting that increasing concentrations of DTPA seem to improve overall growth slightly when combined with Octopirox (**Figure 4-4A**).

Manganese levels rose from control levels with the addition of Octopirox to the culture (p-value 0.005) and maintained the same level regardless of the presence of DTPA at the concentrations tested (p-value 0.169). Iron levels however, fell significantly with 14 μM Octopirox (p-value 0.0024) but did not alter further with addition of DTPA, being no different to Octopirox alone (p-value 0.717; **Figure 4-4B**).

Magnesium levels with the addition of DTPA showed significant changes from Octopirox by itself at 8.5, 9.5 and 10 μM DTPA, with Anova one-way statistical analysis suggesting that these differences are significant ($p = 0.028$). This reduction in magnesium was not observed previously with either Octopirox or DTPA alone (Chapter 3), suggesting that this feature only arises when these chelants are combined and may contribute to their antibacterial efficacy.

Levels of calcium slightly increased following addition of DTPA and statistical analysis shows this difference is significant (0.045), however, the fold increase between the conditions is only 1.1 from the controls which seems an insubstantial amount. With zinc, the observed reduction was not significant with a p-value of 0.369.

Overall, the two sets of experiments with DTPA and Octopirox produce slightly different results. DTPA with Octopirox showed reductions in manganese and iron when combined. Whereas, the Octopirox and DTPA experiments showed little change in the reduced iron apparent with Octopirox alone or in the increased manganese levels. Magnesium levels were significantly reduced which could be a factor contributing to synergism in this pairing although the differences were relatively small.

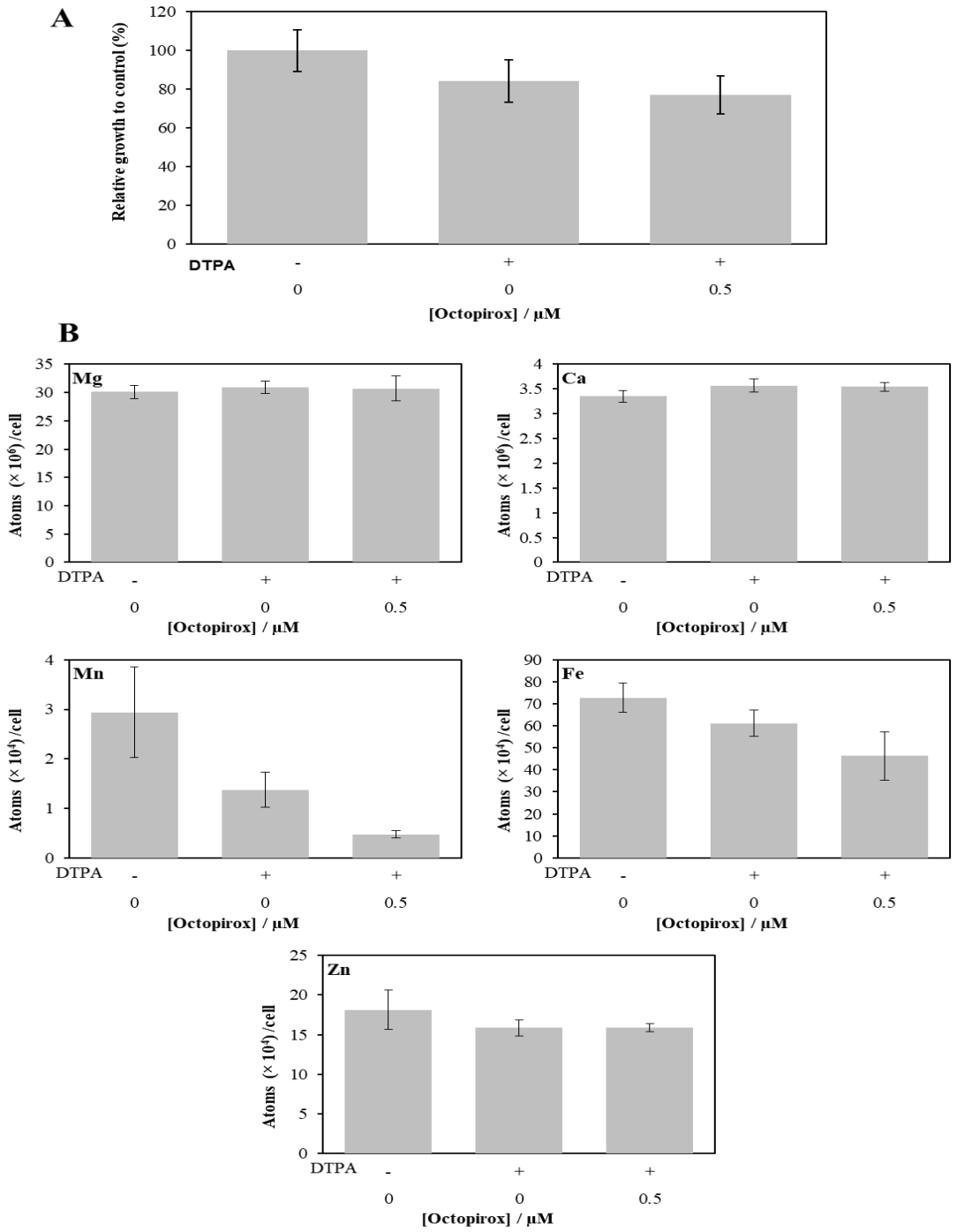

Figure 4-3. Effect of DTPA and Octopirox in combination on bacterial growth and cellular metal content. A) Inhibition profile of *E. coli* cells in the presence (+) or absence (-) of 16 µM DTPA and in the presence or absence of 0.5 µM Octopirox as indicated. B) ICP-MS metal analysis of *E. coli* cells in mid-log phase of growth at 37˚C in the presence or absence of DTPA at 16 µM (indicated by + or – symbol) and with or without 0.5 µM Octopirox. Each graph represents different biologically relevant metals and their abundance shown in atoms per cell. Depending on elemental abundance, the axes differ in scale (10^X values). Mg = magnesium, Ca = calcium, Fe = iron, Mn = manganese and Zn = zinc.

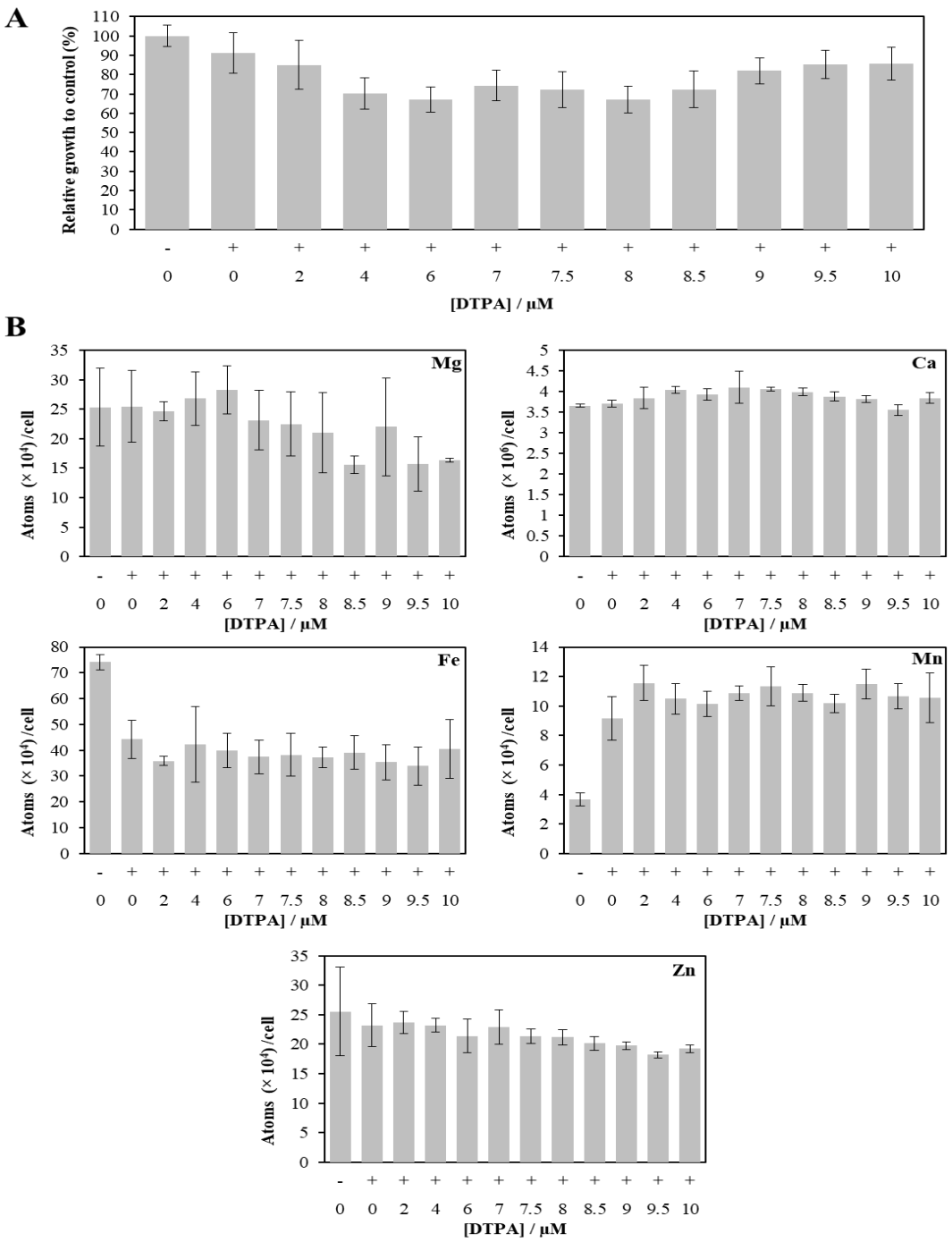

Figure 4-4. Effect of Octopirox and DTPA in combination on bacterial growth and cellular metal content. A) Inhibition profile of *E. coli* cells in the presence (+) or absence (-) of 14 µM Octopirox and in the presence or absence of 2-10 µM DTPA as indicated. B) ICP-MS metal analysis of *E. coli* cells in mid-log phase of growth at 37˚C in the presence or absence of Octopirox at 14 µM (indicated by + or – symbol) and with or without 2-10 µM DTPA. Each graph represents different biologically relevant metals and their abundance shown in atoms per cell. Depending on elemental abundance, the axes differ in scale (10^X values). Mg = magnesium, Ca = calcium, Fe = iron, Mn = manganese and Zn = zinc.

4.3.2. Cellular metal content of *E. coli* cells exposed to DTPMP and Octopirox

DTPMP and Octopirox were selected for further investigation because they proved to be an effective antimicrobial pairing despite having apparently identical effects on *E. coli* cellular levels of iron (down) and manganese (up). Octopirox was employed at a fixed concentration (15 μM) in initial experiments which resulted in a 13% inhibition of bacterial growth. DTPMP was then added at 1.25 μM, with increasing increments of 1.25 μM up to 10 μM, causing a further reduction in growth ranging between 84 and 66%; within the inhibition range set for the experiment (**Figure 4-5A**).

Despite the results for iron showing a downward trend, the large variability within repeats suggests that there is no difference between Octopirox alone and in combination with DTPMP (p-value = 0.192). Hence, no firm can conclusions based on the data available for iron concentrations (**Figure** 4-5B). The manganese data, however, showed that control cultures with no chelator contain 5×10^4 atoms per cell, which with the addition of Octopirox increases to 8×10^4; nearly double the amount (p=0.0113). The overall increase observed between Octopirox and Octopirox / DTPMP is statistically significant with a p value of 0.000119. Thus DTPMP increases cellular manganese more so than Octopirox alone. The initial 1.25 μM DTPMP showed cells have 3×10^4 atoms more than the 15 μM Octopirox and in some cases nearly double that amount (**Figure 4-5B**).

Levels of zinc consistently decreased in response to addition of DTPMP relative to Octopirox levels alone (**Figure** 4-5B). There was no significant difference between control and Octopirox alone (p = 0.225), although addition of DTPMP at any of the tested concentrations resulted in a significant decrease in cellular levels of zinc (p= <0.0001). The initial supplement of 1.25 μM DTPMP showed a 14% reduction compared to control conditions, while that reduction increased with addition of 5 and 10 μM DTPMP giving decreases of 25 and 36%, respectively.

In the presence of DTPMP, Octopirox or both an unpaired t-test showed that magnesium concentration was unaffected (p-value = 0.3) and, similarly, there was no change in calcium at all tested conditions (p = 0.903).

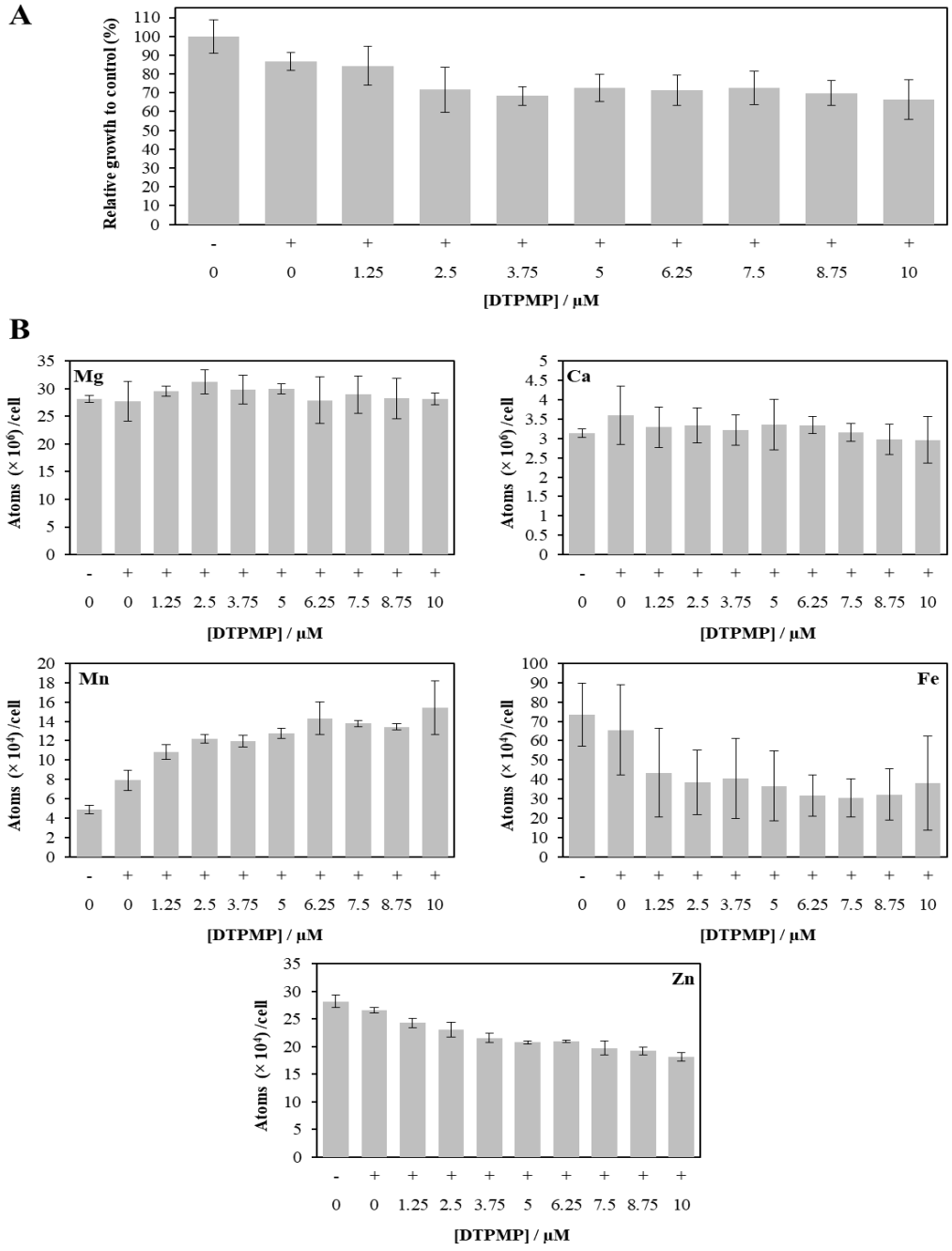

Figure 4-4. Effect of Octopirox and DTPMP in combination on bacterial growth and cellular metal content. A) Inhibition profile of *E. coli* cells in the presence (+) or absence (-) of 15 µM Octopirox and in the presence or absence of 1.25-10 µM DTPMP as indicated. B) ICP-MS metal analysis of *E. coli* cells in mid-log phase of growth at 37˚C in the presence or absence of Octopirox at 15 µM (indicated

by + or – symbol) and with or without 2-10 µM DTPMP. Each graph represents different biologically relevant metals and their abundance shown in atoms per cell. Depending on elemental abundance, the axes differ in scale (10^X values). Mg = magnesium, Ca = calcium, Fe = iron, Mn = manganese and Zn = zinc

A second experiment was conducted which kept DTPMP at a fixed concentration of 10 µM, inhibiting growth of the culture by 7%. Octopirox was then added at 12-16 µM, in 1 µM increments, reducing growth between a range of 93 to 85% (**Figure 4-5A**). As before, levels of magnesium and calcium remained unchanged with addition of chelators (p = 0.990 and 0.871) suggesting that these two chelators do not affect cellular levels of these metal ions. Alternatively, the concentrations of magnesium and calcium in the media may be sufficiently high so that these chelants have no effect at the concentrations tested. Exposure to these chelants did, however, alter the cellular levels of iron, manganese and zinc (**Figure 4-5**).

A sharp decrease in iron, approximately half that of the control without chelant, was detected with *E. coli* exposed to DTPMP alone (p = 0.0268); however, addition of Octopirox at any concentration did not additionally affect iron levels (p = 0.634; **Figure 4-5**). The converse effect was seen with manganese, whereby addition of DTPMP increased manganese significantly, by more than double the control (p = 0.015). Addition of Octopirox alongside DTPMP did not cause any further increase in manganese (p=0.845). Hence, the *in vivo* metal chelation profiles observed in Chapter 3 for these chelants individually does not appear to change when both are mixed together.

Addition of DTPMP on its own caused a decrease in cellular zinc concentration to 6.4×10^4 atoms per cell, approximately 25% less than the control (p = 0.044). As with iron and manganese, there was no difference in levels of zinc (p=0.134) when both chelants are together, suggesting that DTPMP is responsible for zinc reduction but not Octopirox (**Figure 4.4 and 4-5**).

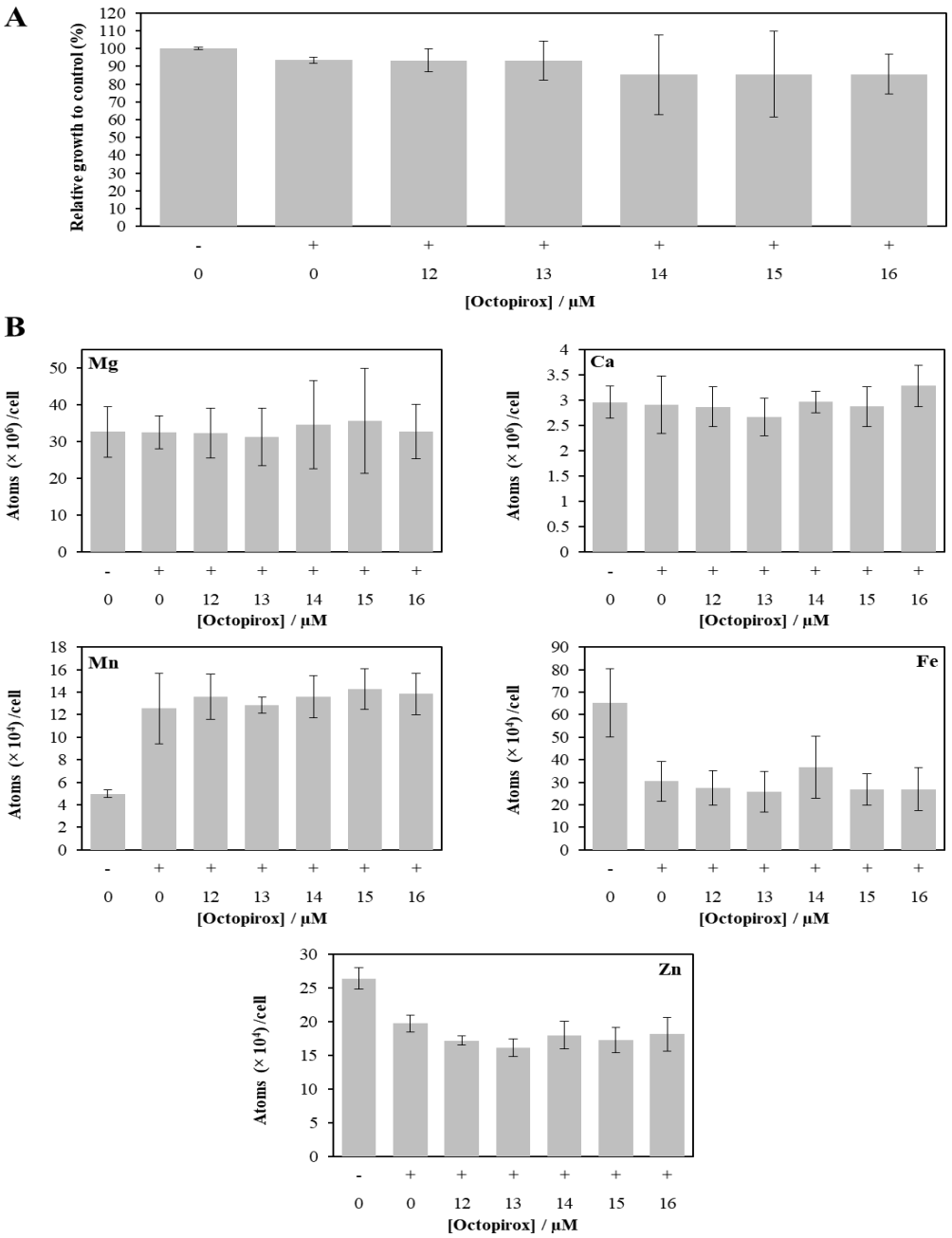

Figure 4-5. Effect of DTPMP and Octopirox in combination on bacterial growth and cellular metal content. A) Inhibition profile of *E. coli* cells in the presence (+) or absence (-) of 10 µM DTPMP and in the presence or absence of 12-16 µM DTPMP as indicated. B) ICP-MS metal analysis of *E. coli* cells in mid-log phase of growth at 37˚C in the presence or absence of DTPMP at 10 µM (indicated by + or – symbol) and with or without 12-16 µM Octopirox. Each graph represents different biologically relevant metals and their abundance shown in atoms per cell. Depending on elemental abundance, the axes differ in scale (10^X values). Mg = magnesium, Ca = calcium, Fe = iron, Mn = manganese and Zn = zinc

4.4. Discussion

Out of the 55 possible combinations tested using the microdilution chequerboard assay, 25 proved to be synergistic, 15 additive, 13 indifferent and 2 antagonistic (summarised in **Figure 4-6**). The synergistic combinations uncovered by the study involved 4 combinations between chelators that had the same *in vivo* metal cellular content profiles and 21 combinations with differing profiles. Hence, chelators with different profiles have an increased likelihood of being synergistic, which suggests that the capacity to recognise and selectively bind different metals results in increased antibacterial activity against *E. coli*. Chelators sharing the same metal profiles are likely to be less effective, as seen with FIC indexes ranging from high at 0.5 (GLDA and MGDA) to low at 0.078 (DTPMP and Octopirox).

	BCS									
CHA	1.02	CHA								
Catechol	0.75	1	Catechol							
DTPA	0.156	0.035	0.35	DTPA						
DTPMP	1.25	0.094	0.063	0.06	DTPMP					
EDTA	0.96	0.094	0.188	1.5	1.5	EDTA				
GLDA	0.5	0.5	0.125	0.2	2	0.3	GLDA			
HBED	2	1.25	1.02	0.53	0.188	1.5	0.516	HBED		
MGDA	2	0.625	0.625	1	1.5	0.75	0.5	1.02	MGDA	
TPEN	1.02	0.188	0.156	0.156	0.125	0.141	0.312	0.5	0.28	TPEN
Octopirox	2	1	1	0.039	0.078	0.063	0.75	0.516	0.75	0.562

synergistic ≤0.5 | additive >0.5-1.0 | indifferent >1.0-≤4.0 | antagonistic >4

Figure 4-6. All possible combinations of chelators used in the study and their FIC indexes determined against *E. coli*. The colours highlight the relationship (synergistic, additive, indifferent or antagonistic) between each chelator pair as defined. The two antagonistic combinations showed synergistic or indifferent effects at some of the concentrations tested, but also antagonism at others. See appendix 3 for representative data.

It might be expected that a combined attack on cellular metal stores, both internally and externally, would be difficult to administer in terms of ensuring enzymes attract the correct metals they require for function. Another possibility is that one of a pair of chelators forms a low affinity complex from which metals readily dissociate. The other chelator in the combination could form a much tighter complex, compensating for the other in combination and resulting in greater overall inhibition. The ranges of growth inhibition according to chelant

concentration suggest that metal affinities, or even the *in vivo* metal profiles, are certainly not the only factor in antimicrobial activity and this aspect requires further investigation. CHA and Catechol stand out as behaving very like each other in combination with other chelants and being additive together (**Figure 4-6**). Hence they are likely to share a similar mode of action, although it remains unclear which metals they actually target in the cell.

The 15 additive combinations, incorporated 10 chelant pairings which showed different cellular metal content effects (Chapter 3), with the remainder derived from combinations grouped into the same *in vivo* metal profile. Six out of the 15 additive pairs involve the known antimicrobial chelator, Octopirox (Piérard *et al.*, 1996; Sigle *et al.*, 2006). Given that many of these combinations involve chelators with apparently different functionality, it is surprising that more synergistic combinations were not found with Octopirox.

Similarly, the indifferent combinations consisted primarily of chelators from different metal profile categories, particularly those that showed no apparent change in metal profile. Both BCS and HBED produced five indifferent pairings that were indifferent, while DTPMP yielded four. BCS exhibited no change in metal profile and no antimicrobial activity alone at the concentrations used here. HBED and DTPMP show a similar metal profile, causing a decrease in iron and increase in manganese. This suggests that BCS, a known copper chelator (Mohindru, Fisher and Rabinovitz, 1983) and HBED, a known iron chelator (Bergeron, Wiegand and Brittenham, 1998) do not function particularly well with the other chelators tested and are generally poor antimicrobials, although HBED and DTPMP do form a synergistic pairing (**Figure 4-6**).

The *in vivo* metal profiles for two synergistic pairs, DTPA / Octopirox and DTPMP / Octopirox, were investigated further. Highlighted in **table 4-5** are metal content values that increased or decreased two fold in relation to the control. The results showed that the cellular metal content profile differed little from the data obtained in Chapter 3 of each of the chelators individually.

Table 4-5. Cellular metal content of *E. coli* during exponential phase with combinations of chelants. The fold-change in metal content relative to a control with no chelators present is indicated with standard deviation values shown. Pink filled boxes indicate decreased metal content (≤0.5) and green filled boxes show increased metal content (≥1.5).

		Fold-change relative to control				
DTPA/Octopirox combinations	Inhibition	**Calcium**	**Iron**	**Magnesium**	**Manganese**	**Zinc**
16 µM DTPA	12%	1.0 ±0.23	0.8 ±0.08	1.0 ±0.15	0.4 ±0.12	0.8 ±0.15
16 µM DTPA + 0.5 µM Octopirox	23%	1.1±0.03	0.6±0.15	1.0±0.07	0.2±0.02	0.9±0.03
14 µM Octopirox	9%	1.0±0.10	0.6±0.10	1.0±0.20	2.7±0.60	0.9±0.10
6 µM DTPA + 14 µM Octopirox	23%	1.1±0.03	0.5±0.10	1.1±0.20	2.8±0.30	0.9±0.10
10 µM DTPA + 14 µM Octopirox	14%	1.1±0.02	0.6±0.20	0.6±0.02	2.8±0.61	0.7±0.04
DTPMP/Octopirox combinations	Inhibition	**Calcium**	**Iron**	**Magnesium**	**Manganese**	**Zinc**
10 µM DTPMP	7%	1.0±0.11	0.5±0.10	1.0±0.07	2.5±0.57	0.7±0.05
10 µM DTPMP + 12 µM Octopirox	6%	1.0±0.06	0.4±0.11	1.0±0.01	2.7±0.26	0.7±0.05
10 µM DTPMP + 16 µM Octopirox	14%	1.1±0.26	0.4±0.09	1.0±0.04	2.8±0.25	0.7±0.13
15 µM Octopirox	13%	1.1±0.24	0.9±0.22	1.0±0.02	1.6±0.22	0.9±0.04
15 µM Octopirox + 5 µM DTPMP	27%	1.1±0.21	0.5±0.25	1.1±0.03	2.6±0.11	0.7±0.01
15 µM Octopirox + 10 µM DTPMP	34%	0.9±0.19	0.5±0.33	1.0±0.04	3.2±0.57	0.6±0.03

The ratio of each chelant in combination seems to be an important factor since the chelator used at a fixed concentration was always present at a higher amount than the other chelant whose concentration was varied. For example, changes in manganese levels were evident in the DTPA / Octopirox combination depending on which chelator was at a higher concentration. With DTPA, manganese levels decrease with a fold change relative to control

of 0.4 and with the addition of Octopirox this trend continues to 0.2 and is considered significant ($p = 0.0465$). When the order of chelants is reversed and Octopirox is kept at a constant and higher concentration, manganese levels increase 2.7-fold more than the control with a slight increase detected with DTPA at 2.8, although this difference is not significant (**Table 4-5**).

Looking specifically at the DTPA / Octopirox combination at 10 µM DTPA + 14 µM Octopirox where the concentrations are similar, the level of magnesium decreases; a feature not apparent with either DTPA or Octopirox by themselves (**Table 4-5** and Chapter 3). This feature may indicate that certain chelator combinations may target different metals together than they do when acting singularly. This might explain why certain combinations categorised into different metal profile categories (Chapter 3) still cause growth inhibition and produce synergistic effects.

With the DTPA / Octopirox pairing, both chelants have different metal profiles, whereas DTPMP and Octopirox both decrease iron levels but increase manganese. The reason why this synergistic pairing was so effective, producing an FIC index of 0.078, is not known. With DTPMP, zinc levels decrease slightly in combination and alone (**Table 4-5**), which was not detected in the metal content data collected in Chapter 3. However, of the chelators assessed in combination, DTPMP was only examined at a single concentration and not at a range as with the others. It is possible that a minor reduction in zinc could have been missed previously. The only occasion where zinc levels decreased below the cut off of ≤0.6-fold was with 15 µM Octopirox and 10 µM DTPMP which inhibited growth by 34% (**Table 4-5**). Chelation of zinc and iron is not a new phenomenon in terms of inhibition of bacterial growth. In the innate immune response, nutritional immunity involves the sequestration and tight regulation of these two metals to restrict bacterial proliferation (Kehl-Fie and Skaar, 2010). Chelants may offer a way to mimic this nutritional immunity, simultaneously starving bacteria of iron and zinc and offering a new approach to block the growth of undesirable microorganisms.

4.5. Concluding remarks and further work

This chapter reveals that the inhibition of bacterial growth using combinations of metal chelators offers significant antibacterial potential. Chelants appear to have different effects on metal homeostasis pathways that cannot be predicted based solely on their metal affinities in solution. *E. coli* metal content analysis by ICP-MS using two chelant combinations has provided an initial insight into the potential mechanisms of multiple metal starvation. Since only two combinations were assessed, additional chelant combinations are needed to provide a more comprehensive exploration of metal bioavailability. A wider concentration range could be evaluated although this has to be balanced with cell viability and integrity which could skew the results. An alternative approach to monitoring cellular metal content would be beneficial, perhaps to define whether metals are trapped by chelants at the surface or manage to penetrate intracellularly. With respect to chelants with similar cellular metal profiles, an RT-PCR or RNA-SEQ approach to measure metal sensor expression could prove useful in evaluating the bacterial response to metal depletion. In addition, selected mutants deficient in in metal regulatory and related stress pathways could be probed for any increase in sensitivity to chelators. These potential avenues are explored in the next two chapters.

Chapter 5. Effect of Ethylenediaminetetraacetic acid exposure on *E. coli* gene expression

5.1. Introduction

To understand the effects of chelants further, we decided to study the bacterial transcriptional response to help identify genes that might be involved in tolerance. The effect of EDTA on *Escherichia coli* was therefore investigated by RNA-SEQ. RNA-SEQ is a Next Generation Sequencing (NGS) technique used to monitor changes in gene expression of organisms by sequencing cDNAs derived from the transcribed region of their genomes. The methodology and nomenclature were proposed in 2008 with a number of papers published that year using the technique on eukaryotic organisms (Cloonan *et al.*, 2008; Lister *et al.*, 2008; Marguerat, Wilhelm and Bähler, 2008; Mortazavi *et al.*, 2008). This approach was not a new concept, it was first proposed and explored in 1975 as a way of defining bacterial phylogenetic relationships (Doolittle *et al.*, 1975; Ehresmann *et al.*, 1975; Shine and Dalgarno, 1975; Zablen *et al.*, 1975). However, this analysis focussed only on 16S ribosomal RNA using laborious techniques that were limited in scope (Fox *et al.*, 1980; Böttger, 1989; Weisburg *et al.*, 1991). By 2009, a number of groups had begun to adapt the RNA-SEQ technology to determine changes in prokaryote transcriptomes (Oliver *et al.*, 2009; Passalacqua *et al.*, 2009; Perkins *et al.*, 2009; Sharma and Vogel, 2009).

Before the development of RNA-SEQ, transcriptional analysis was conducted using microarrays. The microarray technique involved the immobilisation of a fluorescent cDNA or equivalent oligonucleotide corresponding to known genes onto a stable surface. Gene expression is measured as a direct fluorescence output as labelled probe and labelled mRNA samples hybridise (Kane *et al.*, 2000; Relogio *et al.*, 2002; PREMIER Biosoft, 2005). It is an affordable and robust technique but prone to bias depending on the species examined and variation in the transcript specificity of probes. It is also limiting due to background and low-end signal saturation due to the cross-hybridisation or non-specific hybridisation. By comparison RNA-SEQ has enhanced specificity and sensitivity offering a broader dynamic

range and can also detect weakly expressed genes (Wang, Gerstein and Snyder, 2009; Zhao *et al.*, 2014).

RNA-SEQ requires ribosomal depletion of total RNA extracted from a bacterial cell culture, which is converted into a double stranded cDNA by reverse transcription. The resulting library is fragmented which allows adaptors to be attached to either or both ends of the cDNA. The adaptors are recognised by the NGS instrument, so the attached cDNA can be sequenced. The sequences, or reads, are assembled by overlapping sequences or aligned with a reference genome (Croucher and Thomson, 2010; Trapnell *et al.*, 2012; Chen *et al.*, 2014). In this chapter gene expression data obtained from the RNA-SEQ technique will be presented and discussed. The gene expression is in direct response to 0.08 mM EDTA on *E. coli* BW25113 cells to understand the effect of this chelator on biological pathways. In addition to a summary of the differences found in gene expression in response to EDTA, a hypothesis concerning the likely mechanism of action is proposed and discussed.

All RNA-SEQ data within this chapter was done by Dr. Darren Smith's group at Northumbria University. The results are preliminary, however, and validation of these results by RT-PCR is required before embarking upon experiments to test this hypothesis.

5.2. Identification of differentially expressed genes (DEGs)

Total RNA was isolated from BW25113 cell cultures in triplicate using an untreated control alongside those exposed to 0.08 mM EDTA, included in the media from the outset. The EDTA treatment resulted in a growth reduction of ~10%, similar to that used to determine total metal content of *E. coli*. The protocol used is described in Chapter 2.5.1. An RNA integrity number (RIN) of >7 for *E. coli* samples undergoing RNA-SEQ method is generally recommended (Gallego Romero *et al.*, 2014). All samples achieved a RIN score of ≥9.0, except for one of the EDTA-treated samples which gave a borderline acceptable RIN value of 7.1; this data set (R1) was omitted from analysis due to initial PCA plots showing it as an outlier (far right R1 value, **Figure 5-1A**). The other R1 data set from the untreated control was also omitted for similar reasons. The final duplicate data set selected yielded more robust results in the PCA

analysis (**Figure 5-1B**). The combined data identified 5308 genes expressed by *E. coli* in the presence and absence of EDTA. Of these genes, 1646 passed the Q-value statistical criteria employed to judge whether there was a significant difference in gene expression (Chapter 2.5.1.). Q-values are P values of <0.01% adjusted further to account for the potential of a false discovery rate. Data fitting using these significance criteria returned 490 predicted RNA sequences (containing antisense sequences or unknown genes), 261 hypothetical genes and 893 annotated genes. The change in expression level for a selection of these genes is represented in the heatmap in **Figure 5-2**. Annotated genes were further scrutinised using fold change values of ≥1.40 and ≤0.8. The application of these baselines in fold expression change meant that only 141 up-regulated genes were analysed in detail. None of the down-regulated genes met the cut-off using these criteria with the level of change deemed unlikely to be significant.

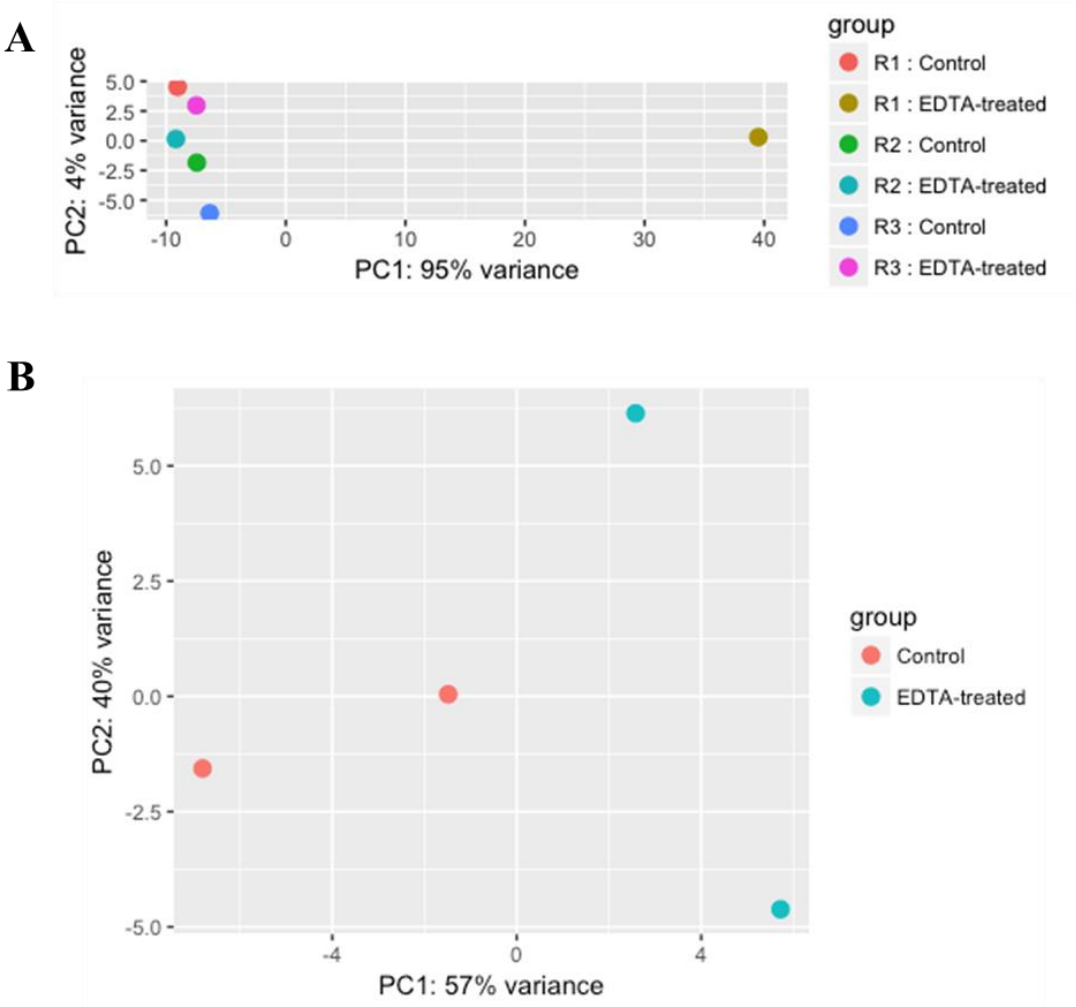

Figure 5-1. Principle component analysis (PCA) plots of triplicate data sets (A) and duplicate data sets (B) of the untreated control and EDTA treated *E. coli* and subsequently recovered cellular RNA.

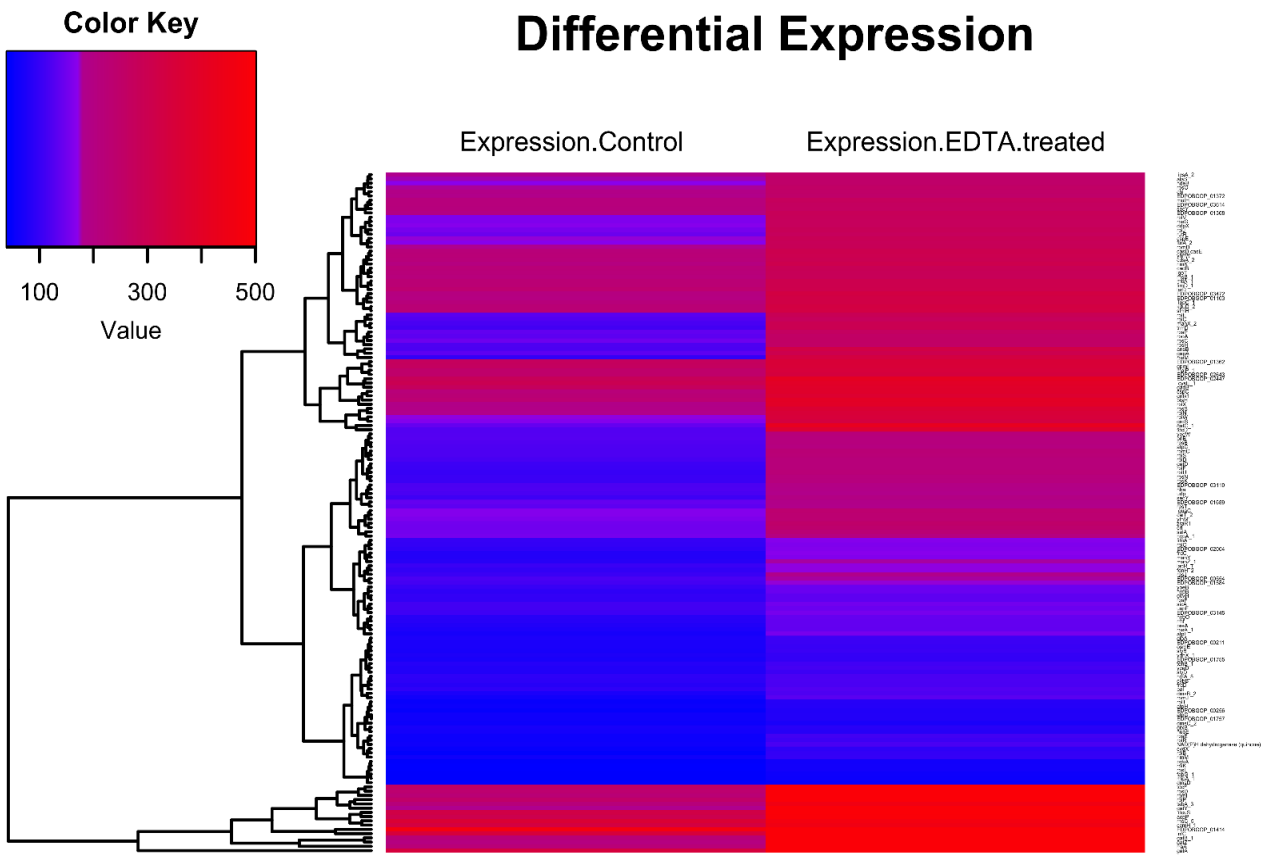

Figure 5-2. Heat map of genes analysed by RNA-SEQ with q-values of ≤0.01. Only the top 160 genes based on these q-values are shown. The colour key can be found in the top left of the **Figure** and represents transcripts from 0 to 500.

5.3 Overview of RNA-SEQ data

5.3.1 Gene ontology analysis

The genes selected from the RNA-SEQ data were subjected to gene ontology (GO) enrichment analysis using the Gene Ontology Consortium online tool (Ashburner *et al.*, 2000; The Gene Ontology Consortium, 2017). The biological processes upregulated by EDTA exposure were identified by assigning GO terms to the DEGs listed. GO terms are a system of classification in which genes are assigned to a set of predefined groups based on functional characteristics. A drawback to this method is the difficulty in analysis, visualisation and redundancies found in the GO term lists. Consequently, secondary analysis of GO terms using the online tool REVIGO was used to help represent the data in a simplified form. Clusters of GO terms are formed by grouping similar functions which REVIGO then assigns to generate a treemap diagram that is easier to interpret (Supek *et al.*, 2011). The treemap displays the clusters as rectangles (**Figure** 5-3 – check numbering of all **Figure**s), whose size is based on $\log_{10}$ p-values and allocates colours based on superclusters.

5.3.2 Biological processes affected by EDTA

The biological processes revealed by the GO enrichment analysis to be upregulated following exposure to EDTA are illustrated in the treemap in **Figure** 5-3. Of the superclusters depicted, translation (GO:0006412; $\log_{10}$ p-value = -14.57) was the most significantly upregulated process by addition of EDTA. The translation supercluster comprises 14 groups, defined by QuickGo (QuickGo, 2001a) as '*The cellular metabolic process in which a protein is formed, using the sequence of a mature mRNA or circRNA molecule to specify the sequence of amino acids in a polypeptide chain*'.

The second largest group in this supercluster is cellular amide metabolic process (GO:0043603, $\log_{10}$ p-value = -11.49) and describes cellular reactions that involve an amide, including any product where an oxoacid has an amino replaced by an acidic hydroxy group (QuickGo, 2006). Several other related gene clusters associated with nitrogen were also upregulated, such as the cellular nitrogen compound biosynthetic and metabolic processes

(GO:0044271, $\log_{10}$ p-value = -5.22; GO:0034641, $\log_{10}$ p-value = -4.80) comprises any reactions and pathways that result in organic or inorganic nitrogenous compound formation (QuickGo, 2004c). Similarly, the organonitrogen compound biosynthetic and compound metabolic processes (GO:1901566, $\log_{10}$ p-value = -4.67; (GO:1901564, $\log_{10}$ p-value = -3.66)) matches the previous group with the exception that it solely incorporates organonitrogen compound synthesis (QuickGo, 2012b)(QuickGo, 2008b, 2012a).

Similarly, cellular macromolecule biosynthetic process (GO:0034645, $\log_{10}$ p-value = -5.92) and macromolecule biosynthetic process (GO:0009059, $\log_{10}$ p-value = -5.88) were also significant pathways affected by EDTA. The terms encompass any reaction or pathway which results in a macromolecule forming from repeating units of smaller molecules (QuickGo, 2001d). The cellular aspect is the generally identical with the added stipulation of '*carried out by individual cells*' (QuickGo, 2008c). Macromolecules includes proteins, phospholipids, polysaccharides and nucleic acids (Patrzykat *et al.*, 2002; Ulvatne *et al.*, 2004); the GO terms for these groups therefore includes all these molecules with the exception of proteins. Other macromolecular translation processes affected are those specific to the metabolism of these macromolecules; cellular macromolecule metabolic process (GO:0044260, $\log_{10}$ p-value = -3.33) and macromolecule metabolic process (GO:0043170, $\log_{10}$ p-value = -4.13), however the latter process forms its own supercluster unrelated to the translation supercluster (QuickGo, 2004a, 2004b). Further analysis of the genes affected is needed to understand precisely what macromolecules are being formed or metabolised in cells exposed to EDTA.

The 'gene expression' term in GO is defined as '*the process in which a gene's sequence is converted into a mature gene product or products (proteins or RNA)*' including production of RNA transcripts, any processes to form mature RNA products and the translation of RNA into proteins (QuickGo, 2007a). This cluster incorporates many genes upregulated in response to EDTA (GO:0010467, $\log_{10}$ p-value = -7.42). Its placement in the translation supercluster implies gene expression that affects or regulates translation. Another similar regulatory mechanism, post-transcriptional regulation of gene expression (GO:0010608, $\log_{10}$ p-value =

-3.43), also resides within this supercluster (QuickGo, 2008a). Maintenance of translational fidelity (GO:1990145, $\log_{10}$ p-value = -4.31) was another biological process linked to the translation supercluster (QuickGo, 2013).

Protein metabolic process (GO:0019538, , $\log_{10}$ p-value = -7.35), defined as chemical pathways and reactions involving a protein, including protein modification (QuickGo, 2001h) which is general and encompasses various proteins. This is different to the other grouping identified as cellular protein metabolic process (GO:0044267, $\log_{10}$ p-value = -7.85) which is largely the same as the definition of protein metabolic process but "the chemical reactions and pathways involve a specific protein, rather than of proteins in general, occurring at the level of an individual.

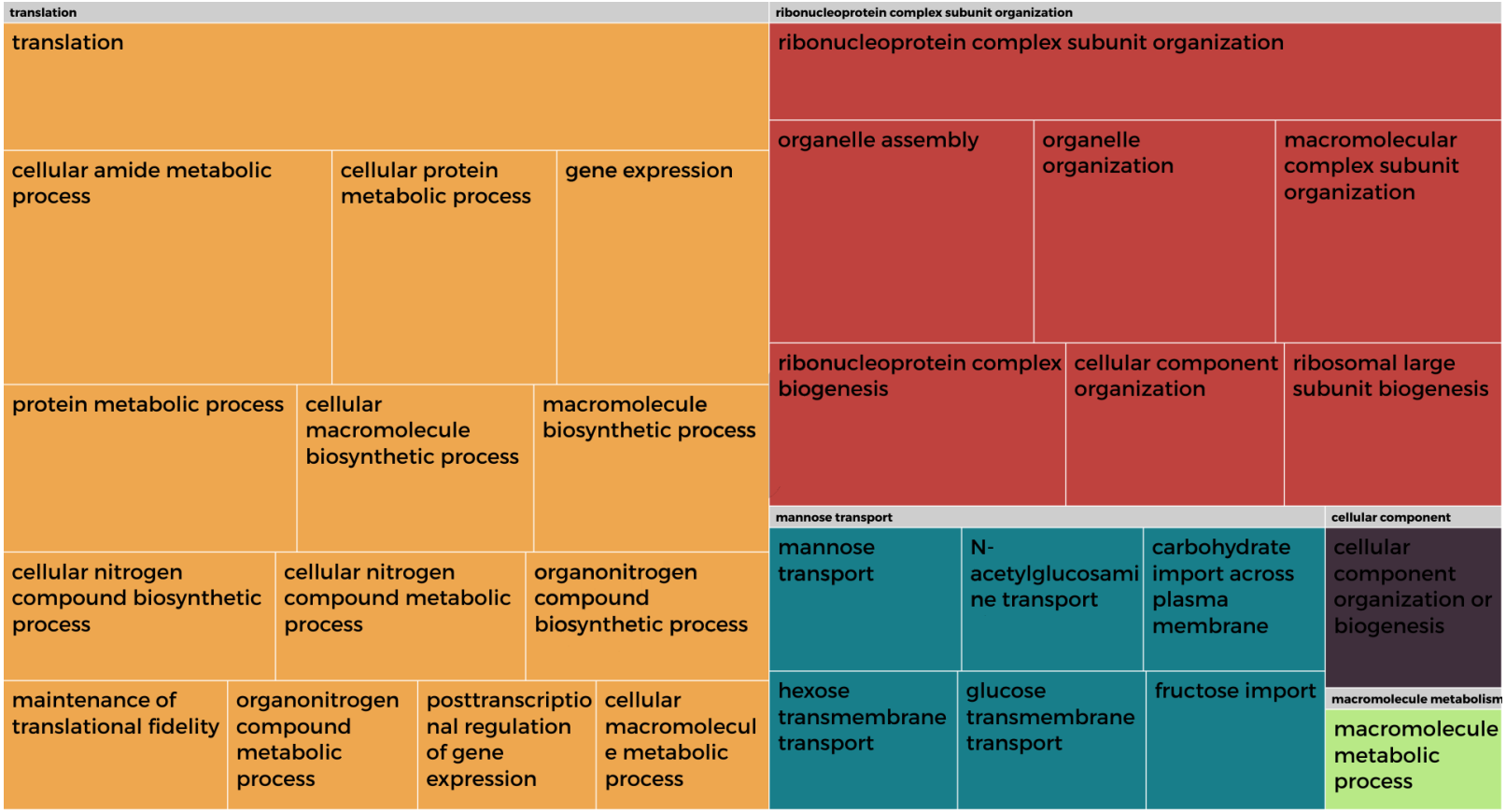

Figure 5-3. Treemap output from REVIGO (Supek et al., 2011) of *E. coli* genes significantly upregulated following exposure to 0.08 mM EDTA based on P-values of ≤0.05 and a fold change of ≥1.2. Each rectangle represents a GO term cluster and each colour represents a supercluster of related clusters based on a biological process. Sizes of rectangles relate to the $\log_{10}$ P-value of each cluster. Move **Figure** closer to where it is first mentioned.

The treemap, **Figure** 5-2, shows a significant upregulation of genes in the super cluster called ribonucleoprotein (RNP) complex subunit organization (GO:0071826, $\log_{10}$ p-value = -10.81). This process is defined as "Any process in which macromolecules aggregate, disaggregate, or are modified, resulting in the formation, disassembly, or alteration of a ribonucleoprotein complex" (Binns *et al.*, 2009; Rouillard *et al.*, 2016). These complexes are integral in biological processes such as DNA replication, the regulation of gene expression and regulation of metabolism of RNA (Hogan *et al.*, 2008; Lukong *et al.*, 2008). These were split into 8 further sub-clusters that are associated with organisation, assembly and biogenesis.

One such grouping if the RNP complex biogenesis (GO:0022613, $\log_{10}$ p-value = -7.34) which describes the process which concerns the macromolecules containing RNA and proteins specifically any process that is involved in its synthesis, organization or assembly. This also includes any alterations to the production or assembly of the a RNP complex (QuickGo, 2007b).

Macromolecular/protein-containing complex subunit organization (GO:0043933, $\log_{10}$ p-value = -7.65), which is defined as "any process in which macromolecules aggregate, disaggregate, or are modified, resulting in the formation, disassembly, or alteration of a protein complex" (QuickGo, 2008d). This is closely related to another function in the group called the ribosomal large subunit biogenesis. Which abridged is any process which involves the synthesis of macromolecule components, construction and arrangement of parts of the large ribosomal subunit which consists of the movement to sites of protein synthesis (QuickGo, 2002). The final group in the supercluster labelled translation is the cellular component organization (GO:0016043, $\log_{10}$ p-value = -5.41) which is any "process that results in the assembly, arrangement of constituent parts, or disassembly of a cellular component" (QuickGo, 2001g).

Other groups in this supercluster relate to bacterial organelles specifically their assembly and organisation. Examples of bacterial organelles include the nucleolus, bacterial microcompartments (vesicles), cytoskeleton and ribosomes; unlike eukaryotes these are all

protein-based (Mélèse and Xue, 1995; Cameron *et al.*, 2013). Organelle assembly (GO:007092, $\log_{10}$ p-value = -8.95) specifically relates to the organelle formation through clustering, composition and binding of components (QuickGo, 2009). The organization of organelles is identical to the assembly definition but includes the disassembly as well (GO:0006996, $\log_{10}$ p-value = -8.17) (QuickGo, 2001b).

Mannose transport is another supercluster of groups shown by treemap data (**Figure** 5-2) and is the last group with consisting of multiple clusters. Mannose transport, under QuickGo definitions, is the transportation of mannose across a lipid bilayer, it does not clarify whether the process is acquisition or exportation (QuickGo, 2001e). Mannose is a sugar monomer and a C-2 epimer of glucose which is transported through *E. coli* membranes using a phosphotransferase system (Erni, Zanolari and Kochers, 1987). It can be used in both glycolysis and amino and nucleotide sugar metabolism. The latter pathway is linked to peptidoglycan and lipopolysaccharide biosynthesis but can also produce Fru-6P from mannose which can also be used in glycolysis/gluconeogenesis (Kanehisa and Goto, 2000; Kanehisa *et al.*, 2016, 2017).

The supercluster consists of 6 groupings; mannose transport (GO:0015761, $\log_{10}$ p-value = -4.32), N-acetylglucosamine transport (GO:0015764, $\log_{10}$ p-value = -4.08), carbohydrate import across plasma membrane (GO:0098704, $\log_{10}$ p-value = -4.08), hexose transmembrane transport (GO:0035428, $\log_{10}$ p-value = -4.08), glucose transmembrane transport (GO:1904659, $\log_{10}$ p-value = -4.08) and fructose import (GO:0032445, $\log_{10}$ p-value = -3.88). Fructose and mannose metabolism are closely linked and play a role in key processes such as amino and nucleotide sugar metabolism, peptidoglycan synthesis and glycolysis and pyruvate metabolism (Kanehisa *et al.*, 2017; Kanehisa Laboratories, 2017). Despite being two different monosaccharides, they are placed in this supercluster together because of this close link.

Another cluster involved is N-acetylglucosamine transport which is described as "the directed movement of N-acetylglucosamine into, out of or within a cell, or between cells, by means of some agent such as a transporter or pore" (QuickGo, 2001f). N-acetylglucosamine, after

glucose, is the best carbon source for *E. coli* in terms of growth yield and It along with mannose is a part of the phosphotransferase system of sugars (Erni, Zanolari and Kochers, 1987; Alvarez-Añorve, Calcagno and Plumbridge, 2005). The phosphorylated N-acetylglucosamine is important as it is used to synthesise lipopolysaccharide and murein (Uehara and Park, 2004); which suggests that the import of this compound maybe to supplement these processes.

Carbohydrate import across plasma membrane is also a group in the supercluster and it is used to describe "the directed movement of a carbohydrate from outside of a cell, across the plasma membrane and into the cytosol" (Binns *et al.*, 2009). This is a broad term therefore a study of genes to understand what carbohydrates could be included in this terminology looked at.

The hexose and glucose transmembrane transport are defined as the movement of hexose or glucose through a membrane (QuickGo, 2001c; QuickGO, 2015). A specific look at the genes that fit into these groups would be ideal to ascertain the exact translational products being produced.

The final supercluster was the cellular component organization or biogenesis (GO:0071840, $\log_{10}$ p-value = -4.66) which is specifically "A process that results in the biosynthesis of constituent macromolecules, assembly, arrangement of constituent parts, or disassembly of a cellular component". This is a closely related term to macromolecule biosynthetic process or organization.

The analysis of GO enrichment is useful to generate hypotheses regarding biological processes altered due to EDTA exposure. However, the understanding of these changes regarding other aspects must be done, such as metal co-factors and structural metal elements which are of interest due to EDTA's chelation abilities. This information may confirm hypotheses, help elucidate the mechanism of action of the chelator or help design future investigative experiments.

5.4. Upregulated gene data analysis

5.4.1. Ribosomal associated genes

The RNA-SEQ data reveal that a large proportion of the genes grouped into the RNP (ribonucleoprotein) complex supercluster are associated with the ribosome and translation. The largest group of DEGs were ribosomal-associated (68 in total; **Table 5-1**), consisting of gene products that assemble to form the ribosome. Three of the top twenty genes (based on fold increase between control and EDTA treated samples) were ribosomal-associated proteins; *rpsM* (3.47-fold) was the third most upregulated gene, while *rpmL* and *rpsD* were seventeenth and eighteenth, both showing a 2.4-fold increase in *E. coli* cells exposed to EDTA relative to the untreated control (See **Appendix 1**).

The rate of ribosomal protein synthesis, in exponentially grown *E. coli* cells, is similar to the rate of ribosome accumulation and is regulated by competition between rRNA and mRNA for interaction with ribosomal proteins (Nomura *et al.*, 1980). Hence, the large number of RNP genes upregulated by EDTA may indicate that the cell is stressed, perhaps by an insufficiency of key proteins required for metabolism. It has previously been shown that under osmotic stress *E. coli* adapts to the environment by slower translation rates, this is offset by the cell increasing ribosome levels (X. Dai *et al.*, 2018).

Table 5-1. Genes upregulated by EDTA that belong to the ribosomal-associated genes category. The gene name and its product are listed. Values for expression level are provided for the untreated control and EDTA-treated samples with the fold difference in the two conditions indicated.

Gene	Gene Product	Control	EDTA	Fold Change
rpsM	30S ribosomal protein S13	96	333	3.47
trmD	tRNA (guanine-N(1)-)-methyltransferase	149	383	2.57
rpmI	50S ribosomal protein L35	225	541	2.40
rpsD	30S ribosomal protein S4	239	565	2.36
rplC	50S ribosomal protein L3	123	276	2.24
rplE	50S ribosomal protein L5	130	288	2.22
rplU	50S ribosomal protein L21	100	220	2.20
rpmJ	50S ribosomal protein L36	62	131	2.11
rpsH	30S ribosomal protein S8	122	256	2.10

rplX	50S ribosomal protein L24	190	396	2.08
rplF	50S ribosomal protein L6	104	214	2.06
rpsN	30S ribosomal protein S14	103	211	2.05
rplB	50S ribosomal protein L2	47	96	2.04
rplW	50S ribosomal protein L23	172	346	2.01
rpsK	30S ribosomal protein S11	103	207	2.01
rplP	50S ribosomal protein L16	253	502	1.98
rpsE	30S ribosomal protein S5	56	110	1.96
rpsP	30S ribosomal protein S16	137	265	1.93
rpoA	DNA-directed RNA polymerase subunit α	133	257	1.93
rpsS	30S ribosomal protein S19	191	367	1.92
rplR	50S ribosomal protein L18	55	105	1.91
leuS	Leucine-tRNA ligase	85	161	1.89
rplN	50S ribosomal protein L14	187	354	1.89
rplD	50S ribosomal protein L4	115	216	1.88
rpmC	50S ribosomal protein L29	120	224	1.87
rpsA_1	30S ribosomal protein S1	74	137	1.85
rplS	50S ribosomal protein L19	120	221	1.84
rplJ	50S ribosomal protein L10	155	285	1.84
rplL	50S ribosomal protein L7/L12	408	732	1.79
rpsJ	30S ribosomal protein S10	103	182	1.77
rpsC	30S ribosomal protein S3	147	259	1.76
rplV	50S ribosomal protein L22	160	279	1.74
rpsG	30S ribosomal protein S7	161	275	1.71
rpsL	30S ribosomal protein S12	37	63	1.70
fusA	Elongation factor G	100	169	1.69
rpsB	30S ribosomal protein S2	123	207	1.68
rplO	50S ribosomal protein L15	97	161	1.66
rimM	Ribosome maturation factor RimM	60	99	1.65
rmf	Ribosome modulation factor	84	138	1.64
rplT	50S ribosomal protein L20	52	84	1.62
crl	Sigma factor-binding protein Crl	149	240	1.61
rpmD	50S ribosomal protein L30	180	285	1.58
rplK	50S ribosomal protein L11	40	63	1.58
rplM	50S ribosomal protein L13	192	283	1.47
yceD	Large ribosomal RNA subunit accumulation protein YceD	78	113	1.45
rpsO	30S ribosomal protein S15	179	258	1.44
rpsQ	30S ribosomal protein S17	78	111	1.42
rpsF	30S ribosomal protein S6	95	135	1.42
hfq	RNA-binding protein Hfq	207	289	1.40

5.4.2. Translation, protein localization and chaperone genes

Fourteen genes were assigned to this group. The largest fold-change was noted with *groS* which showed a 2.05-fold increase compared to the control (**Table 5-2**); the gene has several synonyms: *groES*, *mopB* and *cpn10* (Keseler *et al.*, 2013). GroS/GroES is a heat shock chaperonin that assists protein folding, GroES works together with GroEL to correctly assemble a large number of proteins and in an *rpoH* deletion mutant prevents protein aggregation (Gragerov *et al.*, 1992; Mou *et al.*, 1996). GroS is essential for growth and thus plays a fundamental role in cell physiology (Fayet, Ziegelhoffer and Georgopoulos, 1989). The doubling in transcript levels in response to EDTA implies that there are increased amounts of protein misfolding that is compensated by elevating *groS* expression.

Table 5-2. Genes upregulated by EDTA that belong to the maintenance of translational fidelity genes category. The gene name and its product are listed. Values for expression level are provided for the untreated control and EDTA-treated samples with the fold difference in the two conditions indicated.

Gene Name	Gene Product	Control Expression	EDTA-Treated Expression	Fold-Change
groS	10 kDa chaperonin	164	337	2.05
infC	Translation initiation factor IF-3	350	693	1.98
secY	Protein translocase subunit SecY	107	198	1.85
fkpA	FKBP-type peptidyl-prolyl cis-trans isomerase FkpA	187	290	1.55
hdeB	Acid stress chaperone HdeB	170	250	1.47
dmsD	Tat proofreading chaperone DmsD	35	51	1.46
ycdY	Chaperone protein YcdY	114	165	1.45
sspB	Stringent starvation protein B	36	51	1.42

The second most upregulated gene in this group was *infC* (1.98-fold), encoding a translation initiation factor (IF-3) that has multiple functional roles (Keseler *et al.*, 2013). These include, but are not limited to, recycling of stalled ribosomes (Singh *et al.*, 2005)(Singh *et al.*, 2008). and destabilising inappropriate ribosomal initiation complexes (Risuleo, Gualerzi and Pon, 1976).

The *fkpA* gene was the fourth most upregulated gene (1.55-fold). Its product is a combined PPIase and chaperone (Saul *et al.*, 2004) found in the *E. coli* periplasm which assists folding

of newly translocated polypeptides and is a component of the heat shock induced protein family. FkpA also helps prevent the formation of inclusion bodies (Arié, Sassoon and Betton, 2001). The fifth highest upregulated gene in the translation group was *hdeB* (1.46-fold). an acid stress chaperone. The gene belongs to the *hdeAB* acid stress operon involved in protecting the periplasm from acid stresses by alleviating protein aggregation (Kern *et al.*, 2007). The upregulation of *hdeB*, alongside *skp* and *fkpA* suggests that the periplasmic proteins may susceptible to misfolding or aggregation in the periplasm as a consequence of EDTA exposure.

The Tat proof-reading chaperone gene, *dmsD,* was upregulated by 1.46-fold when compared to control levels and is a protein required for dimethyl sulphoxide (DMSO) reductase synthesis in bacteria. DmsD shares homology with the TorD chaperone and binds the catalytic subunit of the DMSO reductase and is needed for its translocation into the periplasm (Qiu *et al.*, 2008). The *ycdY* gene showed a 1.45-fold increase and also belongs to the TorD family of chaperones. It is hypothesised that YcdY is a specific chaperone involved in correctly inserting zinc into the catalytic site of YcdX, a phosphatase involved in swarming motility in *E. coli* (Redelberger *et al.*, 2011).

The *sspB* gene showed a 1.42-fold increase in expression with addition of EDTA and encodes Stringent starvation protein B. SspB contributes to the degradation of stalled or incomplete proteins by binding to a signal peptide (SsrA), which in turn activates degradation by the ClpXP protease (Levchenko *et al.*, 2000). The last gene in this cluster is *secY* which increased by 1.85-fold and is a component of a protein translocation channel integral to the transport of proteins across the cytoplasmic membrane (Sugano *et al.*, 2017).

5.4.3. Transcriptional regulators

Understanding and examining the contribution of transcriptional factors is an important aspect in investigating cellular responses to conditional experiments. This section focuses on the differentially regulated genes in this class to help interpret the global transcriptional effects on *E. coli* following EDTA exposure. Twenty-four transcriptional regulators were upregulated in

cells exposed to EDTA during exponential growth, including factors linked to specific cellular processes and pathways in *E. coli* (**Appendix 1**).

Table 5-3. Genes upregulated by EDTA that belong to the transcriptional regulator genes category. The gene name and its product are listed. Values for expression level are provided for the untreated control and EDTA-treated samples with the fold difference in the two conditions indicated.

Gene Name	Gene Product	Control	EDTA	Fold-Change
rraA	Regulator of ribonuclease activity A	222	913	4.11
hns	DNA-binding protein H-NS	506	919	1.82
cspC	Cold shock-like protein CspC	219	385	1.76
yedW / *hprR*	putative transcriptional regulatory protein YedW	72	122	1.69
cspE	Cold shock-like protein CspE	173	290	1.68
lacI_1	Lactose phosphotransferase system repressor	103	172	1.67
hha	Hemolysin expression-modulating protein Hha	121	192	1.59
cspA	Cold shock protein CspA	381	565	1.48
dksA	RNA polymerase-binding transcription factor DksA	170	250	1.47

The 4.11-fold increase between control and EDTA samples was seen with *rraA*, the largest change of all those found in the RNA-SEQ data (Appendix and **Table 5-3**). RraA, along with DskA, regulates RNA-specific processes within the cell. Increased expression of *rraA* by EDTA could result in a decrease in cellular RNA degradation. RraA inhibits the expression of RNase E (Rne) (Zhao *et al.*, 2006), an integral component of the degradosome as it performs the initial step of RNA decay. RraA acts on Rne by preventing the autoregulatory mechanism of the enzyme, thus allowing RNase E target transcripts to accumulate and not be degraded (Lee *et al.*, 2003). Overproduction of RNaseE causes growth arrest in *E. coli* which can only be rescued through increasing levels of RraA (Yeom and Lee, 2006).

There was a modest 1.47-fold change in *dskA* expression in response to EDTA. DskA has a dual function in *E. coli* as both repressor and activator, affecting the expression of a diverse range of different genes (Uniprot, 2005; Bateman *et al.*, 2017). For example, it negatively

regulates rRNA gene expression by binding directly to RNA polymerase (RNAP) (Paul *et al.*, 2004). DksA is an essential component of the ppGpp-dependent stress regulon; ppGpp is an alarmone which also regulates RNAP activity (Perederina *et al.*, 2004). DksA promotes the inhibitory effect of the alarmone on RpoS production and this interaction is an integral regulator in the stringent (amino-acid starvation) response in *E. coli* (Brown *et al.*, 2002; Edwards *et al.*, 2011; Ross *et al.*, 2016). DksA also stimulates recombinational repair of DNA double-strand breaks via an interaction with RecN (Meddows *et al.*, 2005). The slight increase in expression of DksA and its pleiotropic on transcription means that it cannot be evaluated in isolation when considering the possible influences of EDTA.

Hha associates with H-NS and modulates its activity; the complex is thought to regulate episomal haemolysin expression (Nieto *et al.*, 1997; Juárez *et al.*, 2000).It is regulated by the transcriptional regulator *cspA* and acts a transcriptional repressor itself. It is found in relatively high abundance, approximately 20,000 copies per cell (Dorman, 2004).

The transcriptional factors listed in **Table 5-3** include three genes, *cspE, cspA* and *cspC,* whose products belong to the cold shock family. The mRNA for *cspA* is normally expressed in all phases of *E .coli* growth in addition to being cold-induced (Brandi and Pon, 2012). CspA affects the expression of two other cold shock genes as well as *hns* and *gyrA* (Jones *et al.*, 1992; Giangrossi, Gualerzi and Pon, 2001), see Section 5.3.4 below. CspA acts as an RNA chaperone preventing secondary RNA structures from forming (Jiang, Hou and Inouye, 1997) and can also inhibit production of non-cold shock proteins (Jiang, Fang and Inouye, 1996). Increased expression of *cspA* needs to be considered in parallel with *hns* as they are functionally connected. CspC despite sequence similarity to CspA, is not induced by cold-shock conditions and its precise function has not yet been clarified (Lee *et al.*, 1994). However, studies have indicated that it has transcription antiterminator activity at ρ-independent terminators both *in vitro* and *in vivo* and appears to upregulate certain genes regulated by RpoS by stabilising *rpoS* mRNA (Bae *et al.*, 2000; Phadtare and Inouye, 2001). The final cold shock-like gene is *cspE* which increased from 173 transcripts to 290, a 1.68-fold change. It is

expressed at low levels during normal growth conditions but increases significantly under cold temperatures (Uppal, Akkipeddi and Jawali, 2008) and like CspC is a transcription antiterminator at ρ-independent terminators (Bae *et al.*, 2000). The *cspE* gene product affects many cellular processes, the most studied being its involvement in resistance of chromosome decondensation and supercoiling of plasmids in *E. coli* (Hu *et al.*, 1996; Sand *et al.*, 2003). Due to its high affinity for ssDNA, CspE may condense DNA by dimerising from separate and distant regions of the DNA (Johnston *et al.*, 2006). Further work is needed to understand the functional significance of these cold shock genes after EDTA exposure.

The *yedW* gene, also known as *hprR*, showed 1.69-fold increased expression in EDTA treated cells. HprR (YedW) with HprS (YedV) comprises a unique two-component system in *E. coli* that controls the transcription of five operons, including the copper sensing *cusSR* and *cusCFBA* operons. The HprSR and CusSR two component systems recognise identical operator sequences and together regulate the same promoters. They differ primarily in the environmental conditions they sense, with HprSR sensing hydrogen peroxide and CusSR detecting copper (II), although there is cross-talk been the two systems (Urano *et al.*, 2015, 2017). Overexpression of HprSR in β-lactam sensitive strains conferred an increase in resistance to the antibiotic (Hirakawa *et al.*, 2003). An informed hypothesis based on the literature, would be that EDTA increases the expression of *hprR* in response to increased hydrogen peroxide or Cu^{2+} (due to cross-talk) in the environment. Such a possibility would be in keeping with the known activity of EDTA as a metal chelator that could also influence the redox state of the cell.

The *lacR* gene increased from 103 to 172 transcripts (1.67-fold) between the untreated control and EDTA-treated cells. In *E. coli*, the *lacI* gene encodes LacR, which negatively regulates expression of the *lac* operon and also functions in an autoregulatory capacity (Griffiths *et al.*, 2000; Oehler, 2009). In response to low levels of glucose, bacterial cells will often switch to alternative carbohydrate utilisation strategies, such as lactose, to support growth (Ozbudak *et*

al., 2004). Increased expression of LacR following addition of EDTA suggests that transport and metabolism of lactose are being repressed.

5.4.4. Nucleoid-associated proteins (NAPs)

NAPs function in bacterial chromosome condensation and contribute to global gene expression, supercoiling, nucleoid architecture and macromolecular crowding (Dame, 2005). The genes affected by EDTA that derive from the NAP functional category are listed in **Table 5-4**. The largest fold increase was seen with *hns*, which showed a 1.82-fold increase in transcription in response to EDTA. Its product, H-NS, functions as both a nucleoid-associated protein (NAP) and a transcriptional regulator. H-NS is a global silencer of AT-rich genes, which constitutes about 5% of *E. coli* genes (Dame, Wyman and Goosen, 2000; Hommais *et al.*, 2001; Dorman, 2004). It fulfils an role in responding and adapting to environmental stressors (Falconi *et al.*, 1993) and influences the expression of a wide range of genes, including those involved in synthesis of bacterial motility proteins (Bertin *et al.*, 1994; Donato and Kawula, 1999), the osmotic response (Lucht *et al.*, 1994; Bouvier *et al.*, 1998), general acid resistance (Shin *et al.*, 2005), glutamic acid- and glutamate-specific acid resistance (De Biase *et al.*, 1999; Giangrossi *et al.*, 2005), alternative carbon sources instead of glucose (Rimsky and Spassky, 1990) and the type II secretory pathway (Francetic *et al.*, 2000). It is unclear from these myriad responses why *hns* expression would be switched on by EDTA exposure, although it may be in response to a general stress response due to metal starvation.

The gene encoding Hha also showed increased expression with a fold-change of 1.59. Hha shares some features with NAPs, affecting the expression of various genes and causing pleiotropic effects which are exacerbated by osmolarity changes (Balsalobre *et al.*, 1999). Hha binds DNA relatively non-specifically and can affect DNA-supercoiling (Juárez *et al.*, 2000; Nieto *et al.*, 2000). It has another function as well, as a DNA binding protein used in *E. coli* to maintain nucleoid structure (Higashi *et al.*, 2016). Binding of H-NS forms distinctive and acute bends in DNA and preferentially interacts with regions with natural curvature (Yamada, Muramatsu and Mizuno, 1990). The protein binds to both gene or intergenic regions of DNA

but does not affect all gene expression in the cell and therefore its primary function is nucleoid structure and not regulatory (Higashi *et al.*, 2016).

Table 5-4. Genes upregulated by EDTA that belong to nucleoid associated protein genes category. The gene name and its product are listed. Values for expression level are provided for the untreated control and EDTA-treated samples with the fold difference in the two conditions indicated.

Gene Name	Gene Product	Control Expression	EDTA-Treated Expression	Fold-Change
hns	DNA-binding protein H-NS	506	919	1.82
priB	Primosomal replication protein N	127	208	1.64
tomB	Hha toxicity modulator TomB	199	284	1.43
hupB	DNA-binding protein HUβ	327	460	1.41

The *hupA* and *hupB* genes were upregulated by 1.32 and 1.41-fold, respectively, in EDTA relative to the control and their gene products (HUα–HUβ) function as a heterodimer (*hupA* showed 1.32-fold increased expression). They are histone-like proteins that prevent the denaturation of DNA under extreme environments by wrapping DNA and thus stabilising the structure (Bonnefoy and Rouviere-Yaniv, 1991). The upregulation of these genes suggest that *E. coli* exposed to EDTA is experiencing problems in nucleoid organisation or stability.

5.4.5. Sugar and amino acid pathways

The 28 genes assigned to this category (**Table 5-5**) encode products involved in sugar and amino acid uptake, export, biosynthesis, phosphorylation or degradation in *E. coli*. Six of this group are *gat* genes that display 2.04-3.60-fold increased expression in response to EDTA. The *gat* genes are responsible for the transport and metabolism of galactitol in *E. coli* and are coordinately produced from the *gatYZABCDR* operon (Nobelmann and Lengeler, 1996).

Another six of the EDTA-upregulated genes belong to *tdcABCDEFG* operon, with *tdcE* showing the third highest increase within the sugar/amino acid pathway cluster. The genes, *tdcB, tdcC, tdcD, tdcE, tdcF* and *tdcG*, all showed increased expression by 2-3-fold (**Table 5-5**).

Table 5-5. Genes upregulated by EDTA that belong to sugar and amino acid pathway genes category. The gene name and its product are listed. Values for expression level are provided for the untreated control and EDTA-treated samples with the fold difference in the two conditions indicated.

Gene Name	Gene Product	Control Expression	EDTA-Treated Expression	Fold-Change
gatA	PTS system galactitol-specific EIIA component	344	1238	3.60
gatZ	D-tagatose-1,6-bisphosphate aldolase subunit GatZ	206	682	3.31
gatC_1	PTS system galactitol-specific EIIC component	140	419	2.99
tdcE	PFL-like enzyme TdcE	186	556	2.99
gatB_1	PTS system galactitol-specific EIIB component	226	670	2.96
tdcD	Propionate kinase	125	370	2.96
gatY	D-tagatose-1,6-bisphosphate aldolase subunit GatY	181	509	2.81
ansB	L-asparaginase 2	119	323	2.71
manX_2	PTS system mannose-specific EIIAB component	116	294	2.53
tdcG	L-serine dehydratase TdcG	164	412	2.51
tdcB	L-threonine dehydratase catabolic TdcB	254	631	2.48
tdcF	Putative reactive intermediate deaminase TdcF	260	567	2.18
manZ_1	PTS system mannose-specific EIID component	85	178	2.09
gatD	Galactitol-1-phosphate 5-dehydrogenase	106	216	2.04
manY	PTS system mannose-specific EIIC component	81	163	2.01
tdcC	Threonine/serine transporter TdcC	157	312	1.99
treB	PTS system trehalose-specific EIIBC component	119	223	1.87
talB	Transaldolase B - membrane	203	377	1.86
treC	Trehalose-6-phosphate hydrolase	107	198	1.85
lamB	Maltoporin	164	302	1.84
ptsH	Phosphocarrier protein HPr	232	402	1.73
udp	Uridine phosphorylase	117	186	1.59
gcvT	Aminomethyltransferase	67	99	1.48
gcvH	Glycine cleavage system H protein	96	135	1.41

The *tdcABCDEFG* operon is induced under anaerobic conditions and is negatively regulated in the presence of glucose, specifically by the cAMP-activated global transcriptional regulator, CRP (Sawers, 2004). The operon encodes two pathways of L-threonine transport and

degradation under anaerobic conditions (Selinger *et al.*, 2003). Another gene, *rhtC*, which was also induced (1.33-fold) is involved in threonine resistance by facilitating efflux of the amino acid (Zakataeva *et al.*, 1999). Since *rhtC* falls below the 1.4-fold cut-off, it was not included in **Table 5-5**.

All three genes in the *manXYZ* operon, which belong to the phosphotransferase system that transports sugars (Okochi *et al.*, 2007), showed 2.0-2.5-fold increased expression in response to EDTA. The products of this operon encode a transporter for a range of sugars, including but not limited to, amino sugars, mannose, glucose, N-acetylglucosamine and glucosamine (Plumbridge, 1998). Similarly, the *treBC* operon is induced 2-fold (**Table 5-5**). TreB transports trehalose into the cell, while TreC breaks down trehalose into a glucose polymer and a single glucose unit. Their expression allows the cell to utilise trehalose as an alternative carbon and energy source when glucose is unavailable (Strom and Kaasen, 1993).

Three genes, *ptsH*, *crr* and *ptsG*, encode a phosphotransferase system for the uptake and phosphorylation of D-glucose. The Crr and PtsG form the two subunits of the II^{Glc} phosphorotransferase (Zeppenfeld *et al.*, 2000), while PtsH catalyses the phosphorylation of the sugar. The *ptsH* and *crr* are cotranscribed, whereas *ptsG* is located further downstream (De Reuse and Danchin, 1988). The *ptsG* and *crr* genes only show a 1.37 and 1.33-fold change, respectively and are therefore not shown in **Table 5-5**.

Additional sugar metabolism genes which also showed increased expression were *talB*, *lamB* and *udp*. The *udp* gene allows the utilization of uridine as a carbon and energy source (Leer, Hammer-Jespersen and Schwartz, 1977) and restricts the cellular level of uridine monophosphate (Reaves *et al.*, 2013). The *talB* gene codes for transaldolase B, which participates in the formation of metabolites involving fructose in the pentose-phosphate pathway (Sprenger *et al.*, 1995). The *lamB* gene produces a maltoporin that is a discriminate transporter for malto-oligosaccharides (Heine, Kyngdon and Ferenci, 1987).

E. coli possesses two L-asparaginases, a low affinity endogenous enzyme (I) and a high-affinity exogenous enzyme (II). The latter is encoded by *ansB* (Jennings and Beacham, 1990) which showed a 2.71-fold increase in response to EDTA. AnsB is used to degrade L-asparagine, which in *E. coli* is a source of carbon and nitrogen (and is induced under anaerobic conditions by Fnr (Spring *et al.*, 1986; Jerlström, Liu and Beacham, 1987).

Two genes, *gcvHT*, were weakly induced (1.41 and 1.48-fold; **Table 5-5**) and are involved in the glycine cleavage system (Okamura-Ikeda *et al.*, 1993). The cleavage of glycine is one of two routes for the biosynthesis of one-carbon products needed for biological processes (Plamann, Rapp and Stauffer, 1983).

5.4.6. Energy production and metabolism

The 33 genes allocated to this category are related to glycolysis, gluconeogenesis, anaerobic or aerobic respiration (**Table 5-6**). The *frdABCD* operon showed increased expression from 1.39-2.65-fold, with *frdAB* representing the top two upregulated genes in this category; *frdD* was only induced 1.39-fold. The *frdABCD* operon produces a fumarate reductase, which uses fumarate as a final electron acceptor and is needed for anaerobic respiration and anaerobic oxidative phosphorylation (Jones and Gunsalus, 1987).

Another group of genes of interest are those necessary to make the ATP synthase complex (Futai, Noumi and Maeda, 1989). ATP synthase catalyses the production of ATP from ADP and phosphate in a reaction that can be conducted under either aerobic or anaerobic conditions using the proton gradient of the membrane (Senior, 1988). It can also catalyse the hydrolysis of ATP to generate a proton gradient for cellular functions during fermentation (Trchounian, 2004). The genes, *atpACFH*, increased in expression by 1.42, 1.70, 1.52 and 2.31-fold, respectively. The other components of this operon, *atpB* and *atpG*, were also significantly induced following EDTA exposure (1.4-fold), although they failed to meet the threshold set for the study. The genes *dmsA* and *dmsB* also showed increased transcription from 1.48 and 1.69-fold. These genes encode a dimethyl sulfoxide reductase expressed under anaerobic

conditions that is used as an alternative terminal electron acceptor (Weiner *et al.*, 1988; Sambasivarao *et al.*, 1990).

Several genes with modestly increased transcription (1.48-1.75-fold) are related to cytochrome production, specifically *cydA* and *cydX*, which encode for a cytochrome *bd* ubiquinol oxidase needed to establish a membrane proton gradient and electron transport (Hoeser *et al.*, 2014). All cytochrome complexes are regularly required by bacteria for respiration during electron transfer reactions (Trumpower and Gennis, 1994).

Other upregulated genes include those involved in electron transfer such as the *hybO* gene, which encodes a constituent of hydrogenase 2 (Vignais and Colbeau, 2004). The *fdnH_2* gene increased by 1.81-fold and produces a subunit of a formate dehydrogenase that acts as an electron conduit (Berg *et al.*, 1991; Jormakka *et al.*, 2002). The *gapA* gene codes for glyceraldehyde 3-phosphate dehydrogenase A which is used in *E. coli* during glycolysis and gluconeogenesis (Boyer, 1976). GapA, alongside 3-phosphoglycerate kinase (PGK) and fructose-1,6-biphosphate adolase (FBA), are essential for carbon metabolism (Bardey *et al.*, 2005). The latter is encoded by the *fabA* gene which also showed increased expression in response to EDTA.

Several differentially expressed genes are associated with pyruvate metabolism. The *pykA* gene encodes a pyruvate kinase, the enzyme that catalyses the phosphorylation step in ATP synthesis. The enzymatic reaction forms ATP and pyruvate from phosphoenolpyruvate and ADP. Two enzymes co-exist in *E. coli* and have different kinetic, chemical and physical properties (Malcovati, Valentini and Kornberg, 1973; Mattevi *et al.*, 1995; Valentini *et al.*, 2000). Another gene, *eno*, codes for enolase which catalyses the reversible reaction of 2-phosphoglycerate to phosphoenolpyruvate necessary for both gluconeogenesis and glycolysis (Thomson *et al.*, 1979; Kaga *et al.*, 2002). The *lpdA* gene encodes a lipoamide dehydrogenase, a subunit of the pyruvate dehydrogenase complex that helps control intracellular levels of pyruvate (Li *et al.*, 2006).

Table 5-6. Genes upregulated by EDTA that belong to energy production and metabolism genes category. The gene name and its product are listed. Values for expression level are provided for the untreated control and EDTA-treated samples with the fold difference in the two conditions indicated.

Gene Name	Gene Product	Control Expression	EDTA-Treated Expression	Fold-Change
frdA	Fumarate reductase flavoprotein subunit	111	294	2.65
frdB	Fumarate reductase	121	301	2.49
atpF	ATP synthase subunit b	67	155	2.31
gapA	Glyceraldehyde-3-phosphate dehydrogenase A (NAD+)	134	306	2.28
frdC	Fumarate reductase subunit C	81	168	2.07
ackA	Acetate kinase - ATP+Acetate = ADP+Acetylphosphate	140	280	2.00
fdnH_2	Formate dehydrogenase, nitrate-inducible	95	172	1.81
cydX	Cytochrome bd-I ubiquinol oxidase subunit X	52	91	1.75
atpC	ATP synthase epsilon chain	121	206	1.70
dmsB_2	Anaerobic dimethyl sulfoxide reductase chain B	72	122	1.69
icd_1	Isocitrate dehydrogenase	102	171	1.68
hybO	Hydrogenase-2 small chain	86	140	1.63
adhE	Aldehyde-alcohol dehydrogenase	74	120	1.62
fbaA	Fructose-bisphosphate aldolase class 2	127	198	1.56
lpdA	Dihydrolipoyl dehydrogenase	90	139	1.54
atpH	ATP synthase subunit delta	54	82	1.52
tpiA	Triosephosphate isomerase	164	245	1.49
eno	Enolase	132	196	1.48
cydA	Cytochrome bd-I ubiquinol oxidase subunit 1	104	154	1.48
pykA	Pyruvate kinase II	42	62	1.48
dmsA	Dimethyl sulfoxide reductase DmsA	61	90	1.48
dcuD_1	Putative cryptic C4-dicarboxylate transporter DcuD	92	134	1.46
pta	Phosphate acetyltransferase	53	77	1.45
atpA	ATP synthase subunit alpha	91	129	1.42
ppa	Inorganic pyrophosphatase	121	172	1.42
ydhY	putative ferredoxin-like protein YdhY (4Fe-4S)	100	141	1.41

A gene for anaerobic growth of *E. coli* called *dcuD* encodes for a transmembrane transport for C4 dicarboxylates that is used under anaerobic conditions and when fumarate respiration is no

longer contributing to bacterial growth (Zientz, Six and Unden, 1996). Following EDTA exposure this gene was seen to increase by 42 transcripts, a 1.45 fold change.

Genes for acetate metabolism also showed increased expression, specifically *pta* (a1.45-fold change) whose product is a phosphate acetyltransferase (Pta). The enzyme catalyses both directions of a reversible reaction that includes acetyl-CoA and acetyl phosphate. The bias of the equilibrium depends on media conditions (Shi, Stansbury and Kuzminov, 2005). Another gene *ackA* was seen to increase by 2-fold when cells were exposed to EDTA and whilst being an acetate kinase (AckA) and propionate kinase also functions in threonine metabolism (Hesslinger, Fairhurst and Sawers, 1998) and flagellar rotation (Barak, Abouhamad and Eisenbach, 1998). AckA facilitates the reversible reaction of acetyl phosphate (produced by Pta) to acetate which causes the formation of ATP from ADP (Kakuda *et al.*, 1994).

The product of the *icd* gene, isocitrate dehydrogenase, can induce changes between the glyoxalate bypass and TCA pathways in *E. coli* (LaPorte, Walsh and Koshland, 1984; McKee and Nimmo, 1989). The enzyme's activity in this role is controlled by direct phosphorylation (Walsh and Koshland, 1985). The *icd* gene showed 1.68-fold increased expression in response to EDTA.

The *adhE* gene showed 1.62-fold change in expression. It encodes an aldehyde-alcohol dehydrogenase which is used in several pathways controlled by iron inside the cell. These include coenzyme A-dependent acetaldehyde dehydrogenase (Lo *et al.*, 2015) and an alcohol dehydrogenase (Jörnvall, 1977). Its functional versatility means it contributes to a number of metabolic pathways, including ethanol degradation (Aristarkhov *et al.*, 1996), L-threonine degradation (Karp *et al.*, 2014) and mixed acid fermentation (Membrillo-Hernández *et al.*, 2000).

The *tpiA* gene is implicitly involved in gluconeogenesis (Alvarez *et al.*, 1998) and in this study increased by 1.49-fold following EDTA treatment. Another gene, *ppa*, whose product is an inorganic pyrophosphatase contributing to energy metabolism an (Lahti *et al.*, 1990) was

upregulated by1.42-fold. Finally, *ydhY* showed an increase of 1.41-fold and encodes a putative electron transporter involved in respiration (Partridge *et al.*, 2008).

5.4.7. Fatty acid synthesis and lipoproteins

The genes in this group participate in the biosynthesis of fatty acids that may be utilised in the formation of the lipid bilayer or stability of the membrane under stressful conditions. Six genes were assigned to this category and are listed in **table 5-7**.

The most highly induced gene in this category (1.63-fold) was *acpP*. The *acpP* gene is co-transcribed with *fabG,* producing the acyl carrier protein (ACP) and 3-ketoacyl-ACP reductase (Rawlings and Cronan, 1992). The *fabG2* also appears in **table 5-7**, with a 1.51-fold increased expression in response to EDTA. ACP and coenzyme A are needed for transportation of the fatty acid chain between synthesising enzymes, one of which is FabG (Magnuson *et al.*, 1993).

The rest of the genes and their products in this group relate to integral membrane proteins. The *tsx* gene encodes a porin embedded in the outer membrane responsible for import of deoxynucleosides and nucleosides (Hantke, 1976; Maier *et al.*, 1988). Transcripts from this gene increased from 85 to 126, a 1.48-fold change (Otto *et al.*, 2001). The *ompX* gene also encodes an outer membrane protein whose function is not yet known. However, its expression is induced in response to osmotic, acid, alkali and pressure conditions and repressed slightly when fimbrae are produced (Nakashima, Horikoshi and Mizuno, 1995; Stancik *et al.*, 2002). Under the experimental conditions described here, *ompX* showed a 1.42-fold increase in expression. The *osmE* gene also showed a 1.42-fold change; it encodes a lipoprotein expressed in response to osmotic stress or stationary phase growth (Gutierrez, Gordia and Bonnassie, 1995; Conter, Menchon and Gutierrez, 1997). The final gene in this group, *slyB,* produces an outer membrane lipoprotein with unknown function in *E. coli* (Minagawa *et al.*, 2003) but in other organisms is known to maintain cell envelope integrity (Plesa *et al.*, 2006). Expression of *slyB* increased 1.49-fold following EDTA exposure.

Table 5-7. Genes upregulated by EDTA that belong to fatty acid synthesis and lipoproteins genes category. The gene name and its product are listed. Values for expression level are provided for the untreated control and EDTA-treated samples with the fold difference in the two conditions indicated.

Gene Name	Gene Product	Control Expression	EDTA-Treated Expression	Fold-Change
acpP	Acyl carrier protein fatty acid biosynthesis	304	496	1.63
fabG2	Putative oxidoreductase	97	146	1.51
slyB	Outermembrane protein	69	103	1.49
tsx	Nucleoside-specific channel-forming protein Tsx	85	126	1.48
ompX	Outer membrane protein X	133	189	1.42
osmE	Osmotically-inducible putative lipoprotein OsmE	71	101	1.42

5.4.8 Metal homeostasis

The genes in this category specifically relate to cellular metal homeostasis, including import, export, storage and metal chaperones in *E. coli* (see **Table 5-8**). The grouping incorporates six genes which showed significant change in gene expression above the 1.4-fold threshold. The largest increase in expression (1.70-fold) was the *ftnA_2* gene, which encodes a non-heme ferritin that acts as a storage reserve for iron (Abdul-Tehrani *et al.*, 1999; Stillman *et al.*, 2001).

The *hypB* gene increased 1.57-fold, the second most highest gene in this category, and its product inserts nickel into a nickel/iron hydrogenase with the assistance of HypA (Lacasse, Douglas and Zamble, 2016). The *yfeX* gene encodes a peroxidase needed for the oxidation of precursor porphyrins to their final porphyrin structure (Dailey *et al.*, 2011) and increased expression by 1.52-fold in response to EDTA. Porphyrin can complex with metals and in the case of manganese-porphyrin complexes, can be substituted for *in vivo* for Mn-superoxide dismutase as a protectant against oxidative stress (Faulkner, Liochev and Fridovich, 1994).

The *ynjE* gene (1.46-fold change) is needed for the synthesis of molybdopterin an essential component for the use of molybdenum as a cofactor (Dahl *et al.*, 2011). Another gene, *moaA*,

showed 1.43-fold increased expression and is also involved in the biosynthesis of molybdenum cofactors (Mehta *et al.*, 2013).

Table 5-8. Genes upregulated by EDTA that belong to metal homeostasis genes category. The gene name and its product are listed. Values for expression level are provided for the untreated control and EDTA-treated samples with the fold difference in the two conditions indicated.

Gene Name	Gene Product	Control Expression	EDTA-Treated Expression	Fold-Change
ftnA_2	Bacterial non-heme ferritin	167	284	1.70
hypB	Hydrogenase isoenzymes nickel incorporation protein HypB	92	144	1.57
yfeX	putative deferrochelatase/peroxidase YfeX	82	125	1.52
ynjE	Thiosulfate sulfurtransferase YnjE molybdenum cofactor synthesis	52	76	1.46
moaA	GTP 3',8-cyclase Mo cofactor	93	133	1.43

5.4.9. Miscellaneous

The genes allocated to this category could not be accommodated within any of the groupings discussed above.The six genes in this miscellaneous category are listed in **table 5-9**. The largest change (2.14-fold) was seen with *tabA_3*, which is involved in biofilm dispersal and may be regulated by toxin-antitoxin systems and KdgR (Kim *et al.*, 2009).

The gene, *fimA*, increased from 99 to 165, corresponding to a 1.67 fold-change. The *fimA* product is a structural constituent of the bacterial pilus/fimbria (Orndorff and Falkow, 1985) which promotes *E. coli* adherence to surfaces and can thus contribute to pathogenicity (Connell *et al.*, 1996) but is not needed for biofilm development (Reisner *et al.*, 2003). The *preA* gene was upregulated 1.75-fold encodes a predicted dehydrogenase (Reed *et al.*, 2003) that is thought to be needed for swarming motility (Inoue *et al.*, 2007). Another gene, *uspE*, increases cell motility by decreasing adhesion (Nachin, Nannmark and Nystrom, 2005); it also confers resistance to UV radiation and other environmental stresses, hence its name: universal stress protein E (Gustavsson, Diez and Nyström, 2002). Expression of *uspE* increased from 84 to 131 transcripts, a 1.56-fold.

Table 5-9. Genes upregulated by EDTA that belong to miscellaneous genes category. The gene name and its product are listed. Values for expression level are provided for the untreated control and EDTA-treated samples with the fold difference in the two conditions indicated.

Gene Name	Gene Product	Control Expression	EDTA-Treated Expression	Fold-Change
tabA_3	Toxin-antitoxin biofilm protein TabA	215	461	2.14
preA	NAD-dependent dihydropyrimidine dehydrogenase subunit PreA	79	138	1.75
fimA	Type-1 fimbrial protein, A chain	99	165	1.67
uspE	Universal stress protein E	84	131	1.56
ahpC	Alkyl hydroperoxide reductase subunit C	163	247	1.52
gloA	Lactoylglutathione lyase	74	106	1.43

The *ahpC* (1.52-fold) and *gloA* (1.43-fold) genes also showed significantly increased expression following EDTA treatment. The product of *ahpC* is alkyl hydroperoxide reductase which is needed for breakdown of hydrogen peroxide (Dip, Kamariah, Nartey, *et al.*, 2014; Dip, Kamariah, Subramanian Manimekalai, *et al.*, 2014). The *gloA* gene encodes an enzyme (a nickel glyoxalase I), which is integral to the conversion of methylgloxal into D-lactate (Clugston *et al.*, 1998).

5.5. Metal requirements of DEGs

EDTA is a known metal chelator that readily forms complexes with metal ions (Oviedo and Rodríguez, 2003). It has also been shown to chelate calcium and magnesium in bacterial outer membranes (Leive, 1965; Leive, Shovlin and Mergenhagen, 1968). The chelating capabilities of EDTA would therefore be expected to have specific effects on genes involved in metal homeostasis or whose products utilise metal cofactors. This section therefore seeks to examine those genes based on this premise and attempt to understand if EDTA influences the metal selected by *E. coli* cells. A total of 24 metal-associated DEGs were identified, comprising 20.6% of the 141 genes considered to be significantly up-regulated following EDTA exposure.

These genes were further subdivided based on the type of metal associated with their products, specifically iron, magnesium, zinc, nickel, manganese and molybdenum.

Table 5-10. Genes and gene products associated with metal binding or homeostasis that were upregulated in response to EDTA treatment.

Name	Metal associated
dksA	Zn finger
gatY	Zn^{2+} cofactor
gatD	Zn binding
fbaA_2	Zn^{2+} cofactor
hypB	Ni/Zn binding
gloA	Ni^{2+} cofactor
tdcG	Fe-S cluster
ydhY	Fe-S cluster
frdB	Fe-S cluster
fdnH_2	Fe-S cluster
preA	Fe-S cluster
ftnA_2	Fe storage
preT	Fe-S cluster
hybO	Fe-S cluster
ynfF	Fe-S cluster/Mo-bis(molybdopterin guanine dinucleotide)
yfeX	haem
cydA	haem
dmsA	Fe-S clusters/Mo-bis(molybdopterin guanine dinucleotide)
moaA	Mo cofactor synthesis
tdcD	Mg^{2+} cofactor
ppa	Mg^{2+} cofactor/Zn^{2+} ion binding
ackA	Mg^{2+} cofactor/ Mn^{2+} cofactor
icd_1	Mg^{2+} cofactor/ Mn^{2+} cofactor
eno	Mg^{2+} cofactor

Twelve of the DEGs contained iron-sulphur clusters, iron co-factors or contributed to iron homeostasis and formed the largest subgroup (**Figure 5-3**). Thus, 8.5% were associated with iron and of these, nine were iron-sulphur cluster proteins. Two gene products had haem cofactors and one associated with iron homeostasis, specifically storage. A full list of genes and associated metals is provided in **table 5-10**. However, two of these twelve also contained a molybdenum cofactor needed for the structure and function of the protein product. Only one

gene product needed molybdenum alone and functions in molybdenum cofactor synthesis (**table 5-10**).

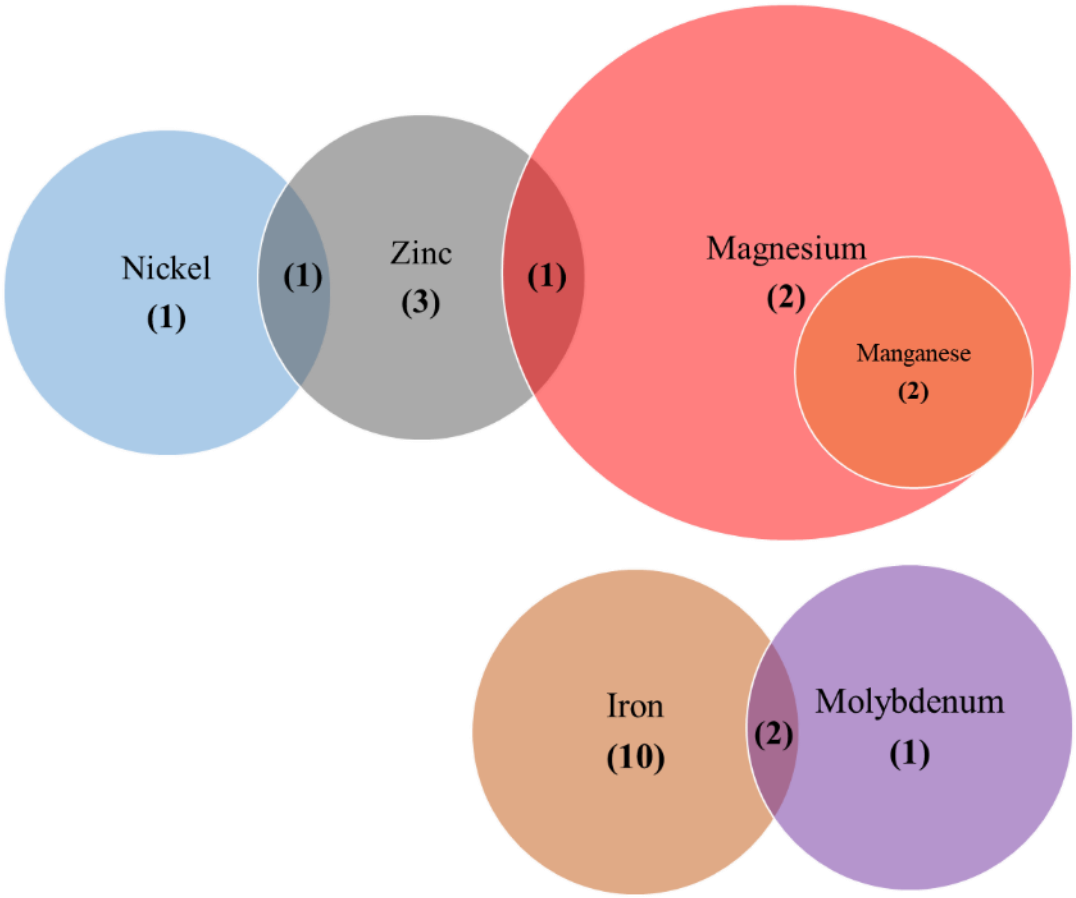

Figure 5-3. Venn-diagram showing metal associated gene products and their frequency (highlighted in bold below each metal). Overlap between circles indicates genes/gene products that require or are involved with both metals; numbers in bold in the overlap indicate frequency of genes. Circles entirely encompassed by other circles indicate that the DEG metal requirements require or possess both metals in the gene product.

Five magnesium-associated genes all utilised the metal as a cofactor in their products, two of which can also accommodate manganese into their active sites and one protein also being able to bind zinc (Katayama *et al.*, 2002). Of the five gene products containing zinc, two require this metal as a cofactor for catalysis, one required the metal as part of a zinc finger motif and the final two proteins readily bind zinc (**Figure 5-3**). One of the zinc binding proteins could also bind nickel (II). The only other protein also associated with nickel uses the metal as a catalytic cofactor.

5.5. Discussion

5.5.1. Biological processes and cellular component analysis

The detailed analysis of specific EDTA-upregulated genes revealed that they participate in the degradation, uptake or synthesis of amino-acids which need nitrogen for their formation. For example, the *tdc* genes which are needed for threonine/serine transport and degradation and *ansB*, required for L-asparagine degradation (Jennings and Beacham, 1990; Hesslinger, Fairhurst and Sawers, 1998). Furthermore, several of these gene products utilise NADH and FAD for electron transport for respiration (Kim *et al.*, 2016), including those encoded by the *frd* operon, *preA* and *icd* which either interact with NAD or FAD (Walsh and Koshland, 1985; Reed *et al.*, 2003; Reaves *et al.*, 2013). Additionally, Hua *et al.* (2004) showed that in glucose and ammonia-limited media, only ~10% of the expressed genes in *E. coli* were involved in amino-acid metabolism, cell envelope synthesis and carbon and energy metabolism. A similar subset of genes were expressed in the *E. coli* cultures grown with EDTA. The carbon and amino-acid genes (**table 5-8**) and those involved in mannose-transport, upregulation of fatty acid synthesis (*fab* and *acpP*) (Rawlings and Cronan, 1992) and the energy metabolism and synthesis genes (section 5.3.6) suggests that EDTA exerts a general restrictive influence on bacterial growth.

Several translation fidelity genes were also upregulated by EDTA, including those products associated with the periplasm either as chaperones or regulation of translocation, such as *groS*, *hdeB* and *fkpA*, which were all involved in preventing protein aggregation (Arié, Sassoon and Betton, 2001; Culotta, Yang and O'Halloran, 2006; Kern *et al.*, 2007). Addition of EDTA may therefore promote problems with protein folding or aggregation in the periplasmic space. Previous studies revealed that the chelation capabilities of EDTA destabilises the outer membrane of *E. coli* (Leive, 1965), which might be likely to be affect the periplasmic space and the proteins therein. Upregulation of periplasmic translocation genes, such as *secY* and *dmsD* (Qiu *et al.*, 2008; Sugano *et al.*, 2017), does indicate that there would be increased protein movement as well into this compartment. This is corroborated by the increase in

membrane associated proteins such as *atpACFH* (Futai, Noumi and Maeda, 1989), *tabA* (Kim *et al.*, 2009), *osmE* (Gutierrez, Gordia and Bonnassie, 1995), *ompX* (Nakashima, Horikoshi and Mizuno, 1995), *slyB* (Ludwig *et al.*, 1995), *lamB* (Benz, Schmid and Vos-Scheperkeuter, 1987) and *fimA* (Donato and Kawula, 1999).

Protein biosynthesis is regulated by two mechanisms in bacteria: molecular organisation, controlled by structural genes, and genetic elements that control the rate of translation, called regulators (Jacob and Monod, 1961). Bacterial gene regulation is a complex process whereby transcriptional elements play an important part, affecting activation or repression of genes (Payankaulam, Li and Arnosti, 2010). This feature was discussed in section 5.3.3 where the genes for eight transcriptional regulators were discussed, each with a different regulatory mechanism and target. Several genes are associated with environmental stresses, such as the cold-shock proteins (*csp*), *hns*, and *dksA* (Hu *et al.*, 1996; De Biase *et al.*, 1999; Ross *et al.*, 2016). Further support for stress resulting from EDTA exposure was found with the up-regulation of *uspE* and *hdeB* which are both induced following general or acidic stress conditions (Gustavsson, Diez and Nyström, 2002; Nachin, Nannmark and Nystrom, 2005; Kern *et al.*, 2007). Similarly, genes expressed during osmotic stress, *ompX* and *osmE*, (Gutierrez, Gordia and Bonnassie, 1995; Nakashima, Horikoshi and Mizuno, 1995) were also differentially expressed, presumably by adverse conditions caused by metal chelation by EDTA. Increases in ribosomal gene synthesis also fits with a cellular response to growth restriction and an effort to overcome this by making more ribosomes to increase translation. An increase in *rraA* transcripts (**table 5-6**) would also promote additional mRNA productionby repression of the degradosome (Lee *et al.*, 2003). Another possibility is that the existing ribosomal complexes are not functioning appropriately. The nearly two-fold increase in expression of the *infC* gene which is needed for stalled ribosomal recycling and initiation of ribosomal complexes would support this notion (Singh *et al.*, 2005). Up-regulation of the *sspB* gene involved in degradation of stalled and truncated proteins inside the cell (Levchenko *et al.*, 2000) also fits with this hypothesis.

5.5.2. Metal associated genes

The effect of EDTA on the cellular metal content of *E. coli* was analysed and discussed in chapter 3 of this thesis and is summarised in **table 5-10**. The cells were grown in the same conditions (125 rpm, 37˚C until mid-log phase of growth) as the RNA-SEQ experiments and metal content analysed using ICP-MS. Two metals (molybdenum and nickel) associated with the genes up-regulated by EDTA in section 5.5 were not analysed by ICP-MS in chapter 3. Five gene products bind to these two metals, however, they both have interchangeable functionality with other metals; molybdenum can be replaced with iron, while nickel could be substituted with zinc.

Nickel is important for anaerobic growth when hydrogenases are expressed. These enzymes need both nickel and iron for activity (Ballantine and Boxer, 1985). Nickel is imported into *E. coli* using a broad substrate transport system, such as the magnesium transporter CorA or the zinc transporter ZupT. At lower concentrations, the cell harnesses the NikACBED uptake system, which has nickel specificity (Koch, Nies and Grass, 2007). Only one gene, *hypB*, which encodes a Ni-Fe hydrogenase maturation protein was induced by EDTA. It, along with *slyD*, promotes insertion of nickel into the Ni-Fe hydrogenase, although the complex can also bind zinc (Khorasani-Motlagh, Lacasse and Zamble, 2017).

Molybdenum was the only other relevant metal that was not analysed by ICP-MS. This metal is essential for *E. coli* and is often employed because of its varied oxidation states (IV, V and VI), useful under a range of different conditions (Leimkühler, 2014). Its bioavailability, as a molybdenate, is relatively high and makes it an excellent choice as an enzymatic cofactor (Hille, 2002). Many enzymes that catalyse metabolic reactions with sulphur, nitrogen or carbon involve a molybdenum cofactor for transfer of either two electrons or an oxo group from a product or substrate (Iobbi-Nivol and Leimkühler, 2013). Two forms of molybdenum cofactor exist, a novel molybdenum-iron-sulphur cluster, called a FeMoco, and a standard molybdenum cofactor (Moco). The FeMoco is usually only found in molybdenum nitrogenases and has a $[Fe_4S_3]$-(bridging-S)$_3$-$[MoFe_3S_3]$ (Rajagopalan, Johnson and Hainline,

1982; Hille, 2002). The Moco factor is more prevalent and found in proteins needed for catalysis of a range of pathways, however, the transfer of electrons is often helped or regulated by other cofactor domains that have Fe-S, FAD/FMN or cytochromes (Iobbi-Nivol and Leimkühler, 2013; Leimkühler, 2014).

Both intracellular nickel and molybdenum require iron to facilitate and mediate reactions. However, under the same growth conditions as RNA-SEQ, the cellular content of iron is around 40% less with EDTA than in the untreated bacterial cultures (**table 5-11**). Interestingly, 12 out of the 29 genes highlighted by the transcriptional analysis were connected to iron. If iron was limiting following EDTA exposure, up-regulation of *ftnA* should not be observed, since this gene is positively regulated by the Fur protein when levels of iron are plentiful (Massé and Gottesman, 2002).

Table 5-11. Cellular content analysis of EDTA exposed *E. coli* cells during mid-phase of growth.

Fold-change relative to control at 10-15% growth inhibition					
Chelant	**Calcium**	**Iron**	**Magnesium**	**Manganese**	**Zinc**
EDTA	0.8 ±0.04	0.6 ±0.09	0.9 ±0.21	0.1 ±0.02	0.6 ±0.06

Zinc levels are also similarly decreased by around 40% and increased expression of several enzymes that utilise zinc structurally or catalytically were suggested by the transcriptome analysis. However, no specific zinc uptake, regulatory or export genes were upregulated. From the results obtained, there does not appear to be a particular deficit in cellular zinc concentration reflected in the up-regulated genes, unless the results reflect a state where the cells have managed to adapt to these conditions through a more generalised metabolic response.

The small number of genes linked to manganese did not preferentially associate with this ion and all preferentially bind to magnesium (Bateman *et al.*, 2017). Since EDTA depletes the cell of approximately 90% of the normal levels of manganese (**table 5-11**), this suggests that no manganese-specific proteins are made in response to this starvation. This could be an inability

to respond to manganese deprivation and hence why this metal is targeted in nutritional immunity. The magnesium cofactored proteins included five up-regulated genes, although no significant changes in this metal were detected by ICP-MS following addition of EDTA. Similarly, no calcium related genes were seen to be affected by the presence of EDTA which corresponds to the modest reduction (20%) in calcium determined by ICP-MS, suggesting that this metal ion is not affected under the conditions employed.

5.6. Future work

The RNA-SEQ analysis suggests that a complex array of stress responses are induced in *E. coli* cells exposed to EDTA, although it is not clear whether this arises from metal deprivation or membrane damage, or both factors. The experiment described in this chapter focussed on the exponential phase of growth with EDTA incorporated from the outset. Future work could monitor gene expression after a shorter period of chelant exposure to monitor the initial response to EDTA. This may identify additional upregulated genes and potentially some that are switched off by chelant treatment. qPCR could be used to validate the changes in selected metal response genes, alongside others identified in this work. Determining the cellular levels of nickel and molybdenum would be helpful in evaluating the effect of EDTA on the proteins that utilise these two metals. It would also be of interest to investigate the cellular response to other chelants, such as Octopirox, that have a different effect on cellular iron and manganese concentrations

Chapter 6. Effect of chelators on *E. coli* single-gene deletion mutants

All experiments in this chapter were repeated 6 times unless otherwise stated. All bacterial strains used were obtained from the Keio Collection Library (a generous gift from Dr. David Weinkove, Durham University)..

6.1. Introduction

The Keio collection consists of 3985 mutants of the *E. coli* K-12 strain with single, non-essential gene deletions made using a kanamycin cassette (Baba *et al.*, 2006). Each deletion is positioned between the second codon and the seventh from last codon in the open reading frame (Yamamoto *et al.*, 2009). The mutant collection has been used in multiple studies, for example, Liu *et al*. (2010) tested 14 antibiotics, including ciprofloxacin, streptomycin, chloramphenicol and triclosan, to investigate variations in antibiotic sensitivity. The study identified 283 mutants with increased sensitivity and concluded that these strains could be used to help determine drug targets and probe multidrug resistance mechanisms (Liu *et al.*, 2010). In a different approach, the collection was used to identify genes that promote formation of persister cells (Hansen, Lewis and Vulić, 2008). In this chapter, we decided to analyse a selection of mutants from the collection to hopefully identify genes important for sensitivity or resistance to chelators.

The RNA-SEQ data from Chapter 5 showed that a large number of genes were upregulated in response to EDTA at a 10-15% inhibition range from initial inoculation up to the mid-exponential phase of growth. It typically took *E. coli* cells 3-4 hours at 37˚C to reach mid-log phase meaning that the information gained represented a longer-term adaptive response of bacterial cultures to EDTA. Hence, the initial response of *E. coli* to EDTA exposure has not been characterised. It is important to recognise that genes affected in an initial response to a stimulus may well be different from genes required for viability following prolonged exposure to a specific condition. For example, *Lactobacillus plantarum* treated with 8% ethanol for 10 or 30 minutes results in downregulation of the *dak1A* gene, whereas after 24 hours in 8% ethanol this gene is upregulated; the converse occurs with the *dnaJ* gene (van Bokhorst-van de Veen *et al.*, 2011). Mutants from the Keio collection can therefore be used to examine effects at any stage in the growth of *E. coli*. To ascertain genes needed for initial response and survival, we

monitored bacterial growth after the addition of a chelator at the beginning of logarithmic growth. Comparisons were made between the *E. coli* WT strain BW25113 and the isogenic single-gene deletion mutant strains using doubling time to measure responses with or without chelators. Doubling times were calculated after the addition of EDTA at 0.2 OD_{650} using values between 0.2 and 1.0 to provide a simple way to represent growth rate. We focussed our efforts on 47 mutants selected because of their contribution to replication, recombination, oxidative stress, metal homeostasis and periplasmic stress informed by the relevant literature and the RNA-SEQ data obtained in Chapter 5. The upregulation of genes involved in metal regulation, nucleoid formation, oxidative stress and the periplasm were the main factors influencing the choice of mutants tested.

The close relationship between metals and oxidative stress was considered when deciding upon mutants. For example, iron engages in the Fenton reaction with hydrogen peroxide to generate highly toxic reactive oxygen species (Touati, 2000). Two superoxide dismutases which are key in the oxidative stress response pathway are regulated by the ferric uptake regulator *fur* (Niederhoffer *et al.*, 1990) and all three *E. coli* superoxide dismutases possess metal cofactors, either iron (Cozi, Yost and Fridovich, 1973), manganese (Keele, Mccord and Fridovich, 1970) or copper and zinc (Benovs and Fridovichg, 1994). Inducible genes of the oxidative stress response can also be regulated by the SOS response and *vice versa* (Vanbogelen, Kelley and Neidhardt, 1987), providing an overlap in genes coordinated for DNA damage repair (Farr and Kogoma, 1991). This dynamic between metals, oxidative stress and DNA repair is of interest in further understanding the global response of *E. coli* to chelators, metal starvation and the identification of potential susceptibility and resistance genes.

Three chelators, EDTA, DTPMP and Octopirox, were selected for this study. EDTA was chosen as it appears to primarily reduce manganese levels in the cell. In contrast, Octopirox and DTPMP were chosen as they have similar metal chelation profiles, reducing iron but increasing manganese; however, when combined they produce a synergistic effect and have a similar metal chelation profile both singly and in combination (Chapters 3 and 4). The deletion mutants may prove useful in discerning differences in mechanism of action or metal bioavailability by each of these chelants. A list of mutants and the function of the relevant gene products is provided in **Table 2-1**.

6.2. Doubling time of single-gene deletion mutants exposed to EDTA

6.2.1. DNA repair and recombination

WT BW25113 and 17 single gene deletion mutants were tested with and without 0.08 mM EDTA at 37˚C, with shaking at 200 rpm and growth monitored over 16 hours (see Appendix 2). The mutants tested were *recABCDFJNQ* (tested in triplicate), *ruvABC*, *uvrAC*, *mutMTY*, *sbcB* and *nth* (**Figure 6-1**). The WT showed a slight reduction in doubling time with EDTA under the conditions used. Only four of the mutant strains in this grouping showed p-values of ≤0.05 denoting statistical significance with reference to the deletion mutant growing in control conditions vs the addition of EDTA in deletion mutant cultures. The Δ*recB* mutant (p = 0.0001) had an average doubling time of 68.5 minutes in the absence of EDTA and 251.7 minutes in its presence. This was the only *rec* mutant that showed a substantial effect, suggesting that end processing of DNA breaks, but not genetic exchange (since *recA* is unaffected), may be important in tolerating EDTA. The *mutT* and *mutY* mutants showed p-values of 0.0189 and 0.0135. The average doubling time for Δ*mutT* without EDTA was 28.0 minutes, increasing to 52.8 minutes with EDTA, a 24.8 minute increase in doubling time. The Δ*mutY* strain saw an increase in average doubling time from 34.7 to 68.5 minutes with addition of EDTA. The final statistically significant mutant was Δ*uvrA* strain with a p-value = 0.0086. The average doubling time decreased by 32.7 minutes, from 99.4 to 66.7 minutes with addition of EDTA. This was the only mutant in this group that showed an improved growth rate with exposure to the chelant. Interestingly, *mfd* (involved in transcription-coupled nucleotide excision repair) showed a similar pattern, whereas *uvrC* did not, despite its involvement in the same DNA repair pathway.

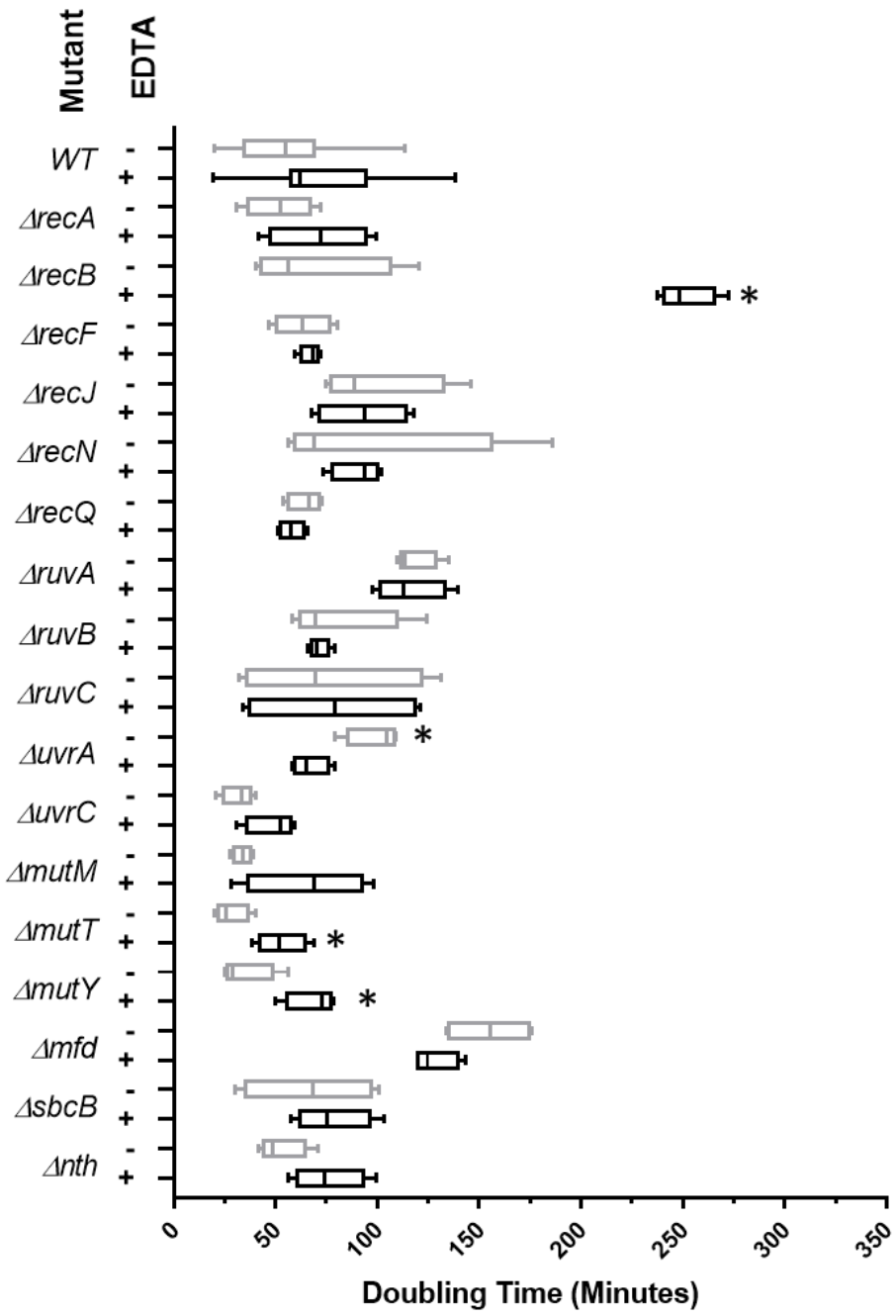

Figure 6-1. Box and whisker plots of *E. coli* DNA recombination and repair mutants. Deletion mutants are labelled on y-axis and doubling time on the x-axis. The presence (+), black box and whisker plot) or absence of EDTA (–), light grey box and whisker plot) are indicated. An asterisk denotes p-values of ≤0.05; statistical analysis conducted using unpaired t-test. Whiskers represent the lowest and highest values in the data set whilst the box is the lowest quartile, the median and the highest quartile in the data set.

6.2.2. Oxidative stress gene deletion

Five genes associated with the oxidative stress response were tested against 0.08 mM EDTA (**Figure 6-2**). The genes included the mutants corresponding to the three metal cofactored superoxide dismutases (*ΔsodA*, *ΔsodB* and *ΔsodC*) and the *ahpC* alkyl hydroperoxidase and the *katG* catalase. Only the *ΔkatG* strain in this grouping showed a significant p-value (0.045), increasing in mean doubling time from 32 to 55.2 minutes with addition of EDTA.

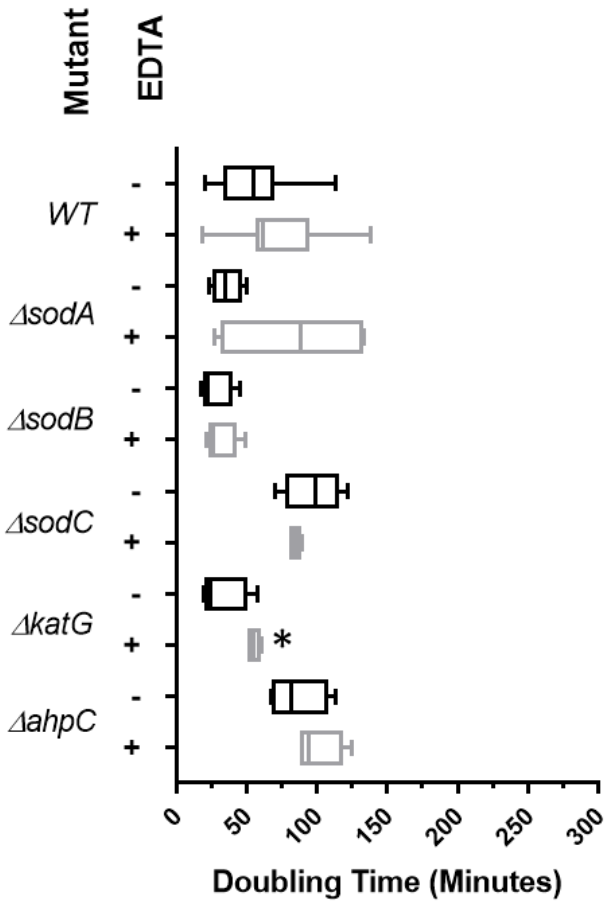

Figure 6-2. Box and whisker plots of *E. coli* Oxidative stress mutants. Deletion mutants are labelled on y-axis and doubling time on the x-axis. The presence (+), black box and whisker plot) or absence of EDTA (–), light grey box and whisker plot) are indicated. An asterisk denotes p-values of ≤0.05; statistical analysis conducted using unpaired t-test.

Additional experiments were conducted with the superoxide dismutases using a native PAGE assay to assess their activities using the deletion mutants to help identify each protein (**Figure 6-3**). The assay

tests for activity of the SODs from *E. coli* grown with and without EDTA to assay if they are still active and expressed inside the cells. The slowest migrating band is the manganese-superoxide dismutase (SodA), while the fastest migrating band corresponds to the iron-superoxide dismutase, which is present in larger amounts (SodB). A faint band migrating between SodA and SodB is a heterodimeric form of the two superoxide dismutases (Hassan and Irwin Fridovich, 1977). The SodC nickel/copper-superoxide dismutase could not be detected, as the gene is only expressed in the stationary phase of growth (Gort, Ferber and Imlay, 1999); these experiments used cells in mid-exponential phase of growth. The assay revealed a significant reduction in superoxide dismutase in SodA and SodB in the WT exposed to EDTA (**Figure 6-3)**. This indicates that these superoxide dismutases either cannot access their requisite metals due to chelation or they become mismetallated and therefore non-functional.

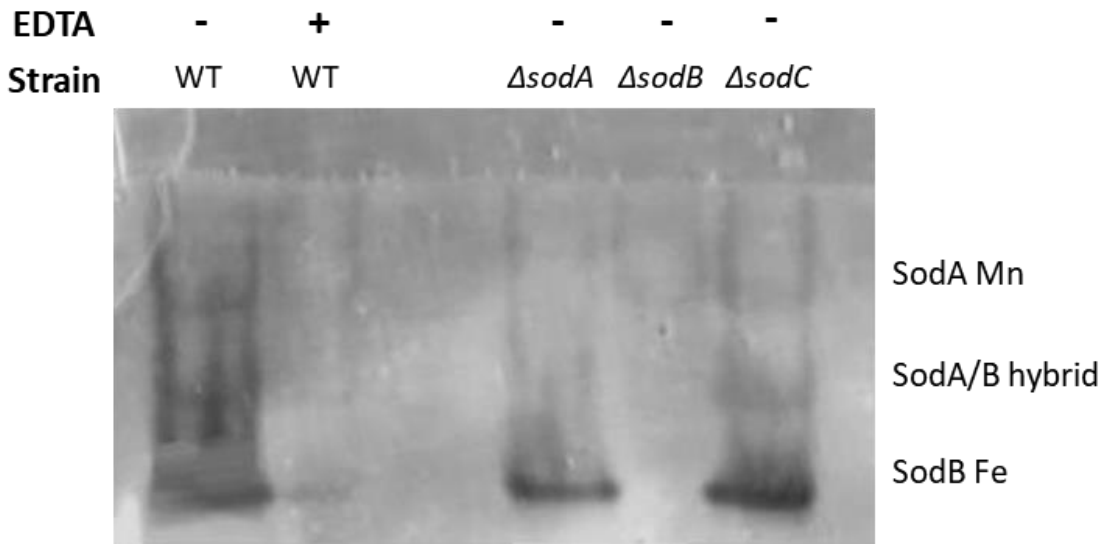

Figure 6-3. Native PAGE of total cellular proteins stained with by negative staining for hydrogen peroxide production using riboflavin/nitro-blue tetrazolium to monitor superoxide dismutase activity. The presence (+) or absence (–) of EDTA is indicated and lanes containing WT *E. coli* or mutant proteins are labelled. The position of each superoxide dismutase is also indicated on the right of the gel. This is a representative gel of results obtained in triplicate.

6.2.3. Metal homeostasis

This grouping consists of 20 mutants whose products are involved in iron, manganese, copper, zinc, nickel and other aspects of metal homeostasis, including several that utilise these metals as cofactors in

cellular processes. These mutants are further subdivided based on the metals they utilise with data presented in **Figures 6-4, 6-5** and **6-6**.

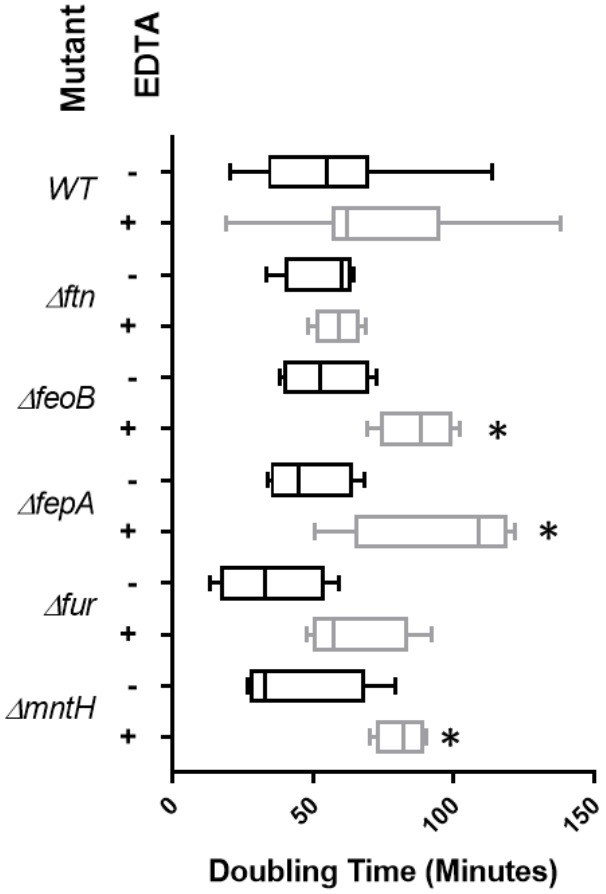

Figure 6-4. Box and whisker plots of *E. coli* metal homeostasis mutants of manganese and iron systems. Deletion mutants are labelled on y-axis and doubling time on the x-axis. The presence (+), black box and whisker plot) or absence of EDTA (–), light grey box and whisker plot) are indicated. An asterisk denotes p-values of ≤0.05; statistical analysis conducted using unpaired t-test.

Mutants affecting iron and manganese homeostasis were examined together because of the close relationship they share in bacterial systems (Niederhoffer *et al.*, 1990). Five mutants, are associated with iron homeostasis and one affecting manganese regulation were tested (**Figure 6-4**). Only three of these strains showed statistically significant differences in a paired t-test, *ΔfeoB* ($p = 0.0215$), *ΔfepA* ($p = 0.0315$) and *ΔmntH* ($p = 0.0261$). The *ΔfeoB* (Fe^{2+} transporter) strain increased in average doubling time from 54 to 87.1 minutes following addition of EDTA. The *ΔfepA* (ferrienterobactin receptor) mutant showed an increase in doubling time from 47.9 to 97.6 minutes. The *ΔmntH* (a divalent metal

cation transporter, especially of manganese and iron) strain had an increased doubling time from 42.9 to 81.2 minutes when EDTA was added.

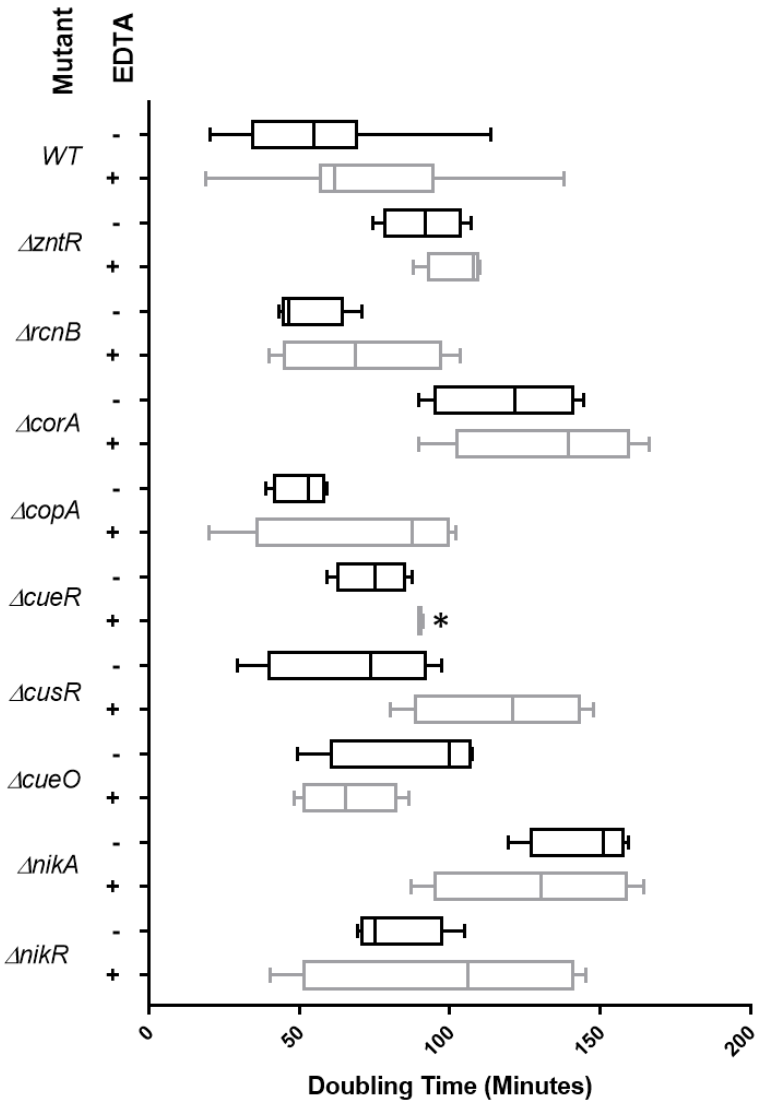

Figure 6-5. Box and whisker plots of *E. coli* metal homeostasis mutants of copper, nickel, cobalt, zinc and magnesium systems. Deletion mutants are labelled on y-axis and doubling time on the x-axis. The presence (+), black box and whisker plot) or absence of EDTA (–), light grey box and whisker plot) are indicated. An asterisk denotes p-values of ≤0.05; statistical analysis conducted using unpaired t-test.

The next group incorporates nine mutants affecting zinc, copper, nickel, cobalt and magnesium homeostasis (**Figure 6-5**). Only one of these mutants (*ΔcueR*, p = 0.0432) showed a statistically significant difference in growth rate, with an increased mean doubling time from 74.4 to 89.9 minutes.

CueR is a transcriptional regulator that induces the expression of tolerance systems in response to copper stress, including *copA* which was also included in this screen (**Figure 6-5**).

The final group comprise five mutant genes that affect metal binding proteins required for a variety of cellular functions. Four of these deletion mutants showed statistically significant differences in growth with EDTA relative to the untreated control (**Figure 6-6**).

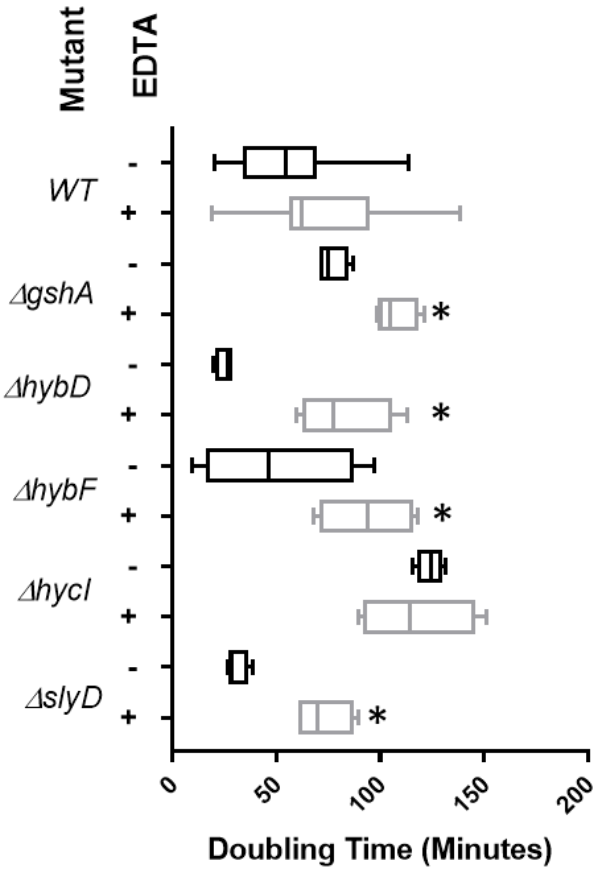

Figure 6-6. Box and whisker plots of *E. coli* metal various cellular function mutants. Deletion mutants are labelled on y-axis and doubling time on the x-axis. The presence (+), black box and whisker plot) or absence of EDTA (–), light grey box and whisker plot) are indicated. An asterisk denotes p-values of ≤0.05; statistical analysis conducted using unpaired t-test.

The *ΔgshA* (glutamate-cysteine ligase) mutant showed an increased doubling time from 76.8 to 107.3 minutes (p = 0.0033). Strain, *ΔslyD* (FKBP-type peptidyl-prolyl cis-trans isomerase), also showed a large increase in doubling time from 30.9 to 72.4 minutes (p = 0.0018). Similarly, two other mutants, *ΔhybD* (p-value = 0.003) and *ΔhybF* (p-value = 0.0957) showed significantly increased doubling times

following addition of EDTA. The *hybD* (hydrogenase 2 maturation protease) deletion increased from 25.5 to 81.9 minutes. The doubling time of the *hybF* (hydrogenase maturation factor) deletion increased from 43.6 to 93.6 minutes. The results observed with the metal homeostasis and associated mutants fits with problems arising in cells due to specific metal depletion as a consequence of EDTA exposure.

6.2.4. Periplasmic stress

Four periplasmic stress associated mutants were exposed to EDTA and their growth and doubling times analysed. These gene deletion strains were repeated 10 times. Three of these, involved in the Cpx two-component envelope stress response system, showed statistically significant differences in growth rate (**Figure 6-7**).

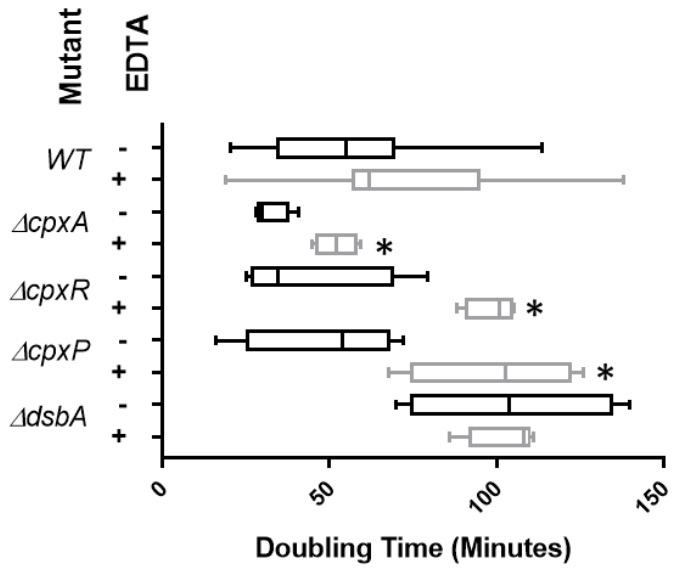

Figure 6-7. Box and whisker plots of *E. coli* periplasmic stress mutants. Deletion mutants are labelled on y-axis and doubling time on the x-axis. The presence (+), black box and whisker plot) or absence of EDTA (–), light grey box and whisker plot) are indicated. An asterisk denotes p-values of ≤0.05; statistical analysis conducted using unpaired t-test.

Deletion of the *cpxA* gene (the histidine kinase sensor in the Cpx two-component regulatory system) in *E. coli* showed an increased doubling time from 19.9 to 52 minutes (p = 0.0043). The *ΔcpxR* (response regulator of the Cpx two-component regulatory system) mutant showed an increased doubling time from 43.4 to 98.8 minutes (p = 0.0051). The final mutant, *ΔcpxP*, (the auxiliary protein in the Cpx two-

component regulatory system) had an average doubling time of 49.1 minutes increasing to 99.6 minutes ($p = 0.0266$) with addition of EDTA. The results suggest that EDTA induces periplasmic stress that requires the Cpx response system to help promote tolerance.

6.3. Growth rate of single-gene deletion mutants exposed to Octopirox

6.3.1. DNA repair and recombination

As with EDTA, the 17 DNA repair and recombination mutants (*recABCDFJNQ*, *ruvABC*, *uvrAC*, *mutMTY*, *sbcB* and *nth*) were tested in the presence or absence of Octopirox at 0.01625 mM added during early exponential phase and incubated at 37˚C, with shaking at 200 rpm for a total of 16 hours (**Figure 6-8**). Only four mutant strains showed statistically significant growth rate reductions with Octopirox and these mutants differed from those affected by EDTA (**Figure 6-1**). The *ΔrecA* (the recombinase responsible for homologous pairing and strand exchange to produce Holliday junctions) showed the greatest increase in average doubling time following addition of Octopirox, from 26.2 to 71.1 minutes ($p = 0.0404$). Two of the components (*ruvB* and *ruvC*) of the tripartite RuvABC Holliday junction resolvase system also showed increased doubling times. The average doubling time for *ΔruvB* without was 109.5 minutes and this increased to 161.4 minutes with Octopirox ($p= 0.0034$). The *ΔruvC* strain saw an increase from 116.6 to 176.4 minutes ($p = 0.0368$). Surprisingly, the *ruvA* deletion showed no significant differences following chelant exposure, with doubling times of 66.9 and 72.7 minutes ($p = 0.6953$).

The final mutant of this grouping that displayed statistically significant difference in growth rate was *ΔmutY* (encoding adenine DNA glycosylase, which helps deal with oxidatively damaged bases), decreasing from 83.9 to 103.8 minutes with exposure to Octopirox ($p = 0.0115$). In contrast, the related mutator mutants *mutT* (8-oxo-dGTP diphosphatase) and *mutM* (formamidopyrimidine-DNA glycosylase) showed no significant differences in growth rate in the presence or absence of chelant. The effect on *mutY* may indicate an increase in oxidative damage to DNA arising from Octopirox treatment.

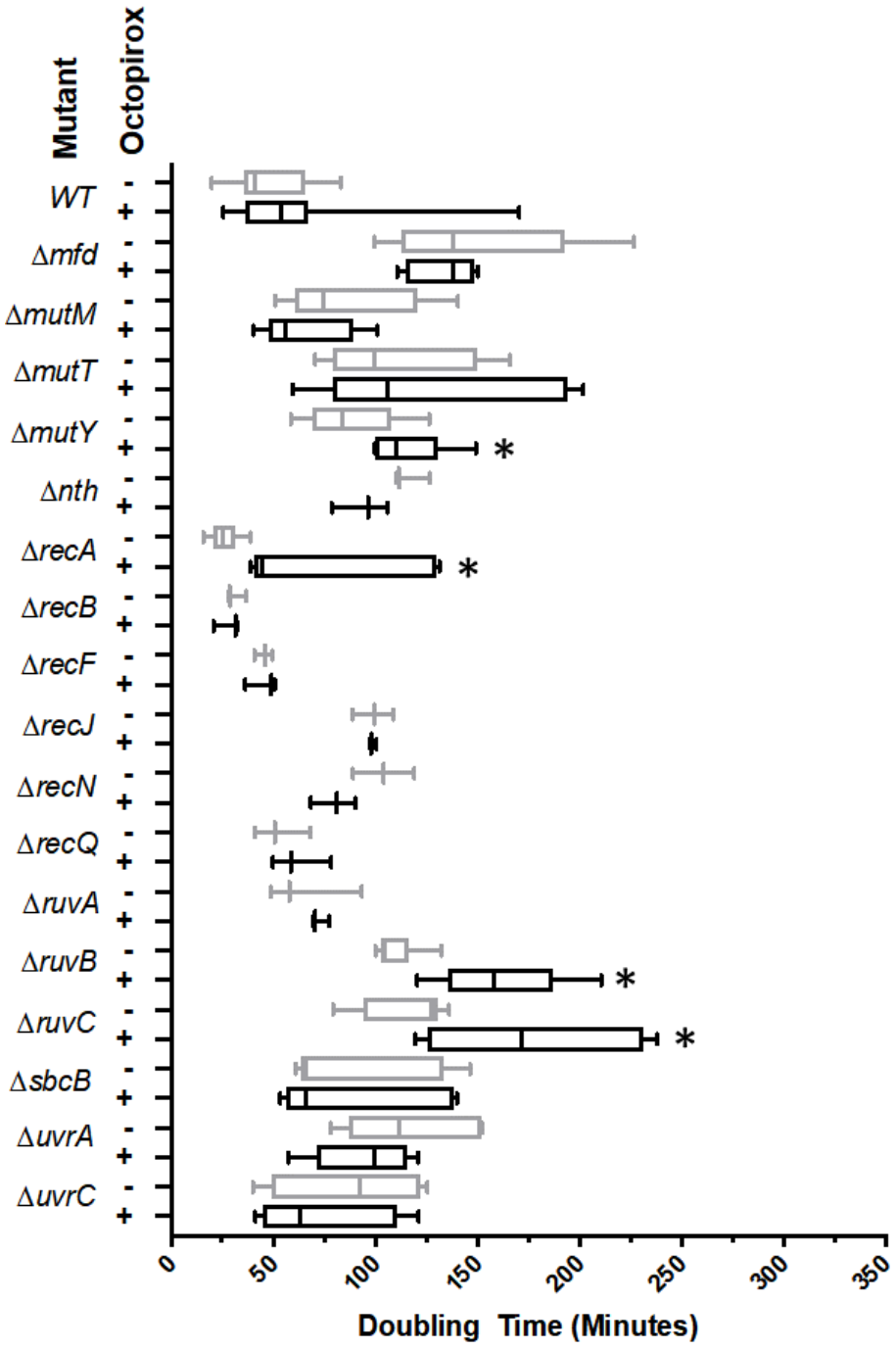

Figure 6-8. Box and whisker plots of *E. coli* DNA recombination and repair mutants. Deletion mutants are labelled on y-axis and doubling time on the x-axis. The presence (+), black box and whisker plot) or absence of Octopirox (–), light grey box and whisker plot) are indicated. An asterisk denotes p-values of ≤0.05; statistical analysis conducted using unpaired t-test.

6.3.2. Oxidative stress

Five genes associated with the oxidative stress response were tested against 0.01625 mM Octopirox (**Figure 6-9**). The genes included the deletion mutants for the three metal co-factored superoxide dismutase genes (*ΔsodA*, *ΔsodB* and *ΔsodC*) and the deletion mutants for *ahpC* and *katG*. Three of these mutants showed a significant change in average doubling time

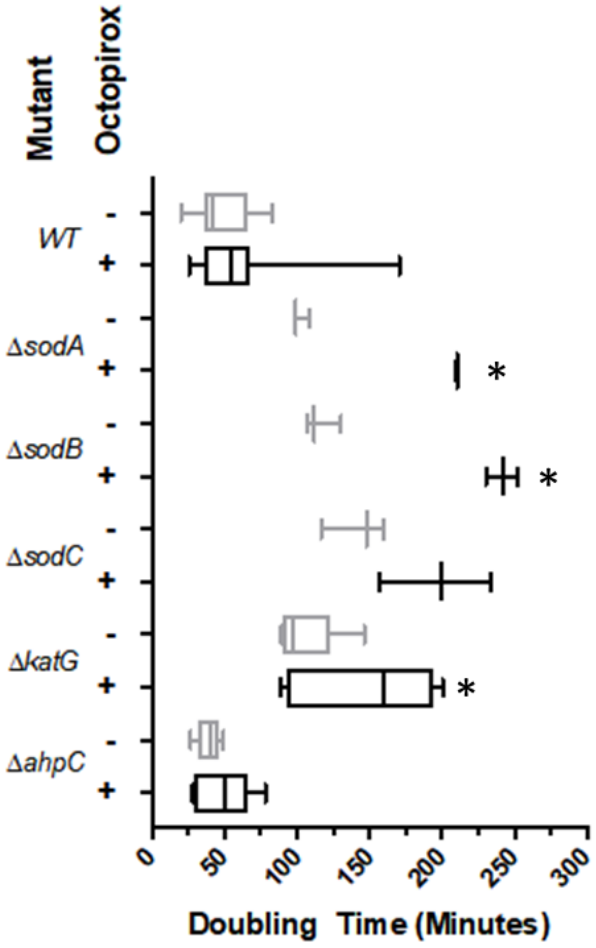

Figure 6-9. Box and whisker plots of *E. coli* oxidative stress mutants. Deletion mutants are labelled on y-axis and doubling time on the x-axis. The presence (+), black box and whisker plot) or absence of Octopirox (–), light grey box and whisker plot) are indicated. An asterisk denotes p-values of ≤0.05; statistical analysis conducted using unpaired t-test.

with Octopirox. The *ΔsodA* and the *ΔsodB strains* showed p-values of 0.0001 and 0.0002 with doubling time increases of 107.7 and 125.0 minutes with the chelant present. The average doubling time of *ΔkatG* increased by 90.4 minutes from 92.5 to 182.9 minutes with the addition of Octopirox.

6.3.3. Metal homeostasis gene deletion

Five iron and manganese mutants were investigated, four associated with iron homeostasis and one affecting manganese regulation (**Figure 6-10**). Only two mutant strains showed statistically significant differences when analysed using a paired t-test. These were *ΔfepA* (p-value = 0.048) and *ΔmntH* (p-value = 0.0112). The *ΔfepA* strain had an increased doubling time of 92 minutes, from 71 to 162 minutes, while the *ΔmntH* doubling time increased by 117 minutes, from 73 to 190 minutes.

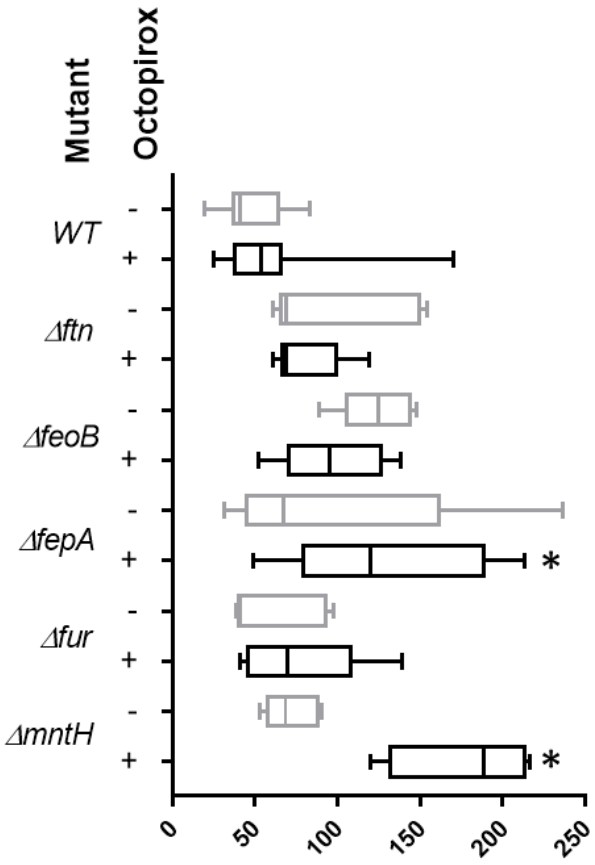

Figure 6-10. Box and whisker plots of *E. coli* metal homeostasis mutants of manganese and iron systems. Deletion mutants are labelled on y-axis and doubling time on the x-axis. The presence (+), black box and whisker plot) or absence of Octopirox (–), light grey box and whisker plot) are indicated. An asterisk denotes p-values of ≤0.05; statistical analysis conducted using unpaired t-test.

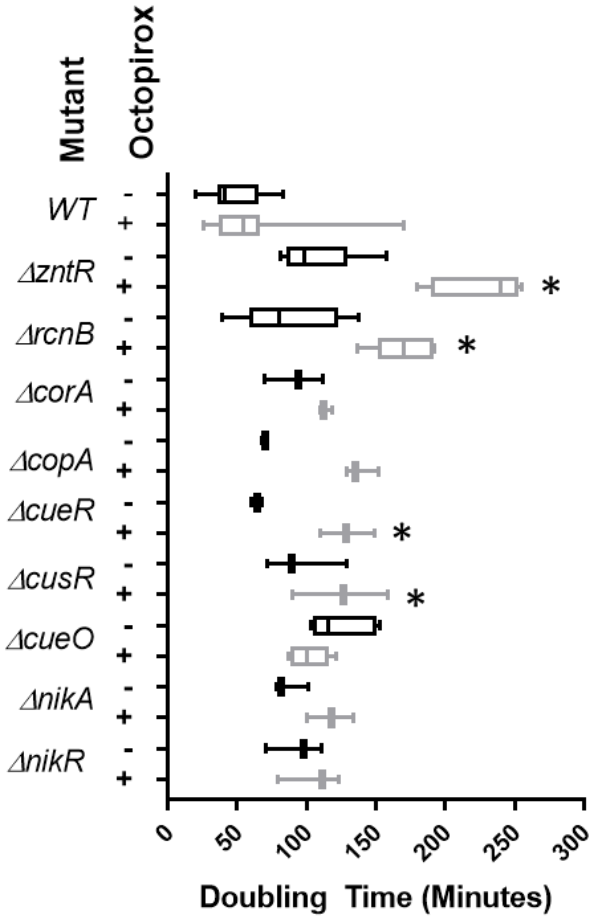

Figure 6-11. Box and whisker plots of *E. coli* metal homeostasis mutants of copper, nickel, cobalt, zinc and magnesium systems. Deletion mutants are labelled on y-axis and doubling time on the x-axis. The presence (+), black box and whisker plot) or absence of Octopirox (–), light grey box and whisker plot) are indicated. An asterisk denotes p-values of ≤0.05; statistical analysis conducted using unpaired t-test.

The deletion strains involved in zinc, copper, nickel, cobalt and magnesium homeostasis are shown in **Figure 6-11**. Four out of the nine deletion mutants in this group showed statistically significant changes in doubling time. These included two involved in regulating copper homeostasis, *ΔcueR* and *ΔcusR*. Deletion of the *cueR* (p-value = 0.0006) resulted in a 68.6 minute increase in doubling time, from 70 to 138.6 minutes. The *cusR* mutant increased in doubling time from 64.2 to 129.1 minutes, an increase of 64.8 minutes (p-value of 0.0048). The remaining two strains were *ΔzntR* and *ΔrcnB* showed p-values of 0.0001 and 0.0058 respectively. The *zntR* mutant with a 90.9 minute doubling time without chelant, increased to 248.6 minutes with addition of Octopirox, a difference of 157.7 minutes. The *rcnB* mutant showed a similar increase of 91.9 minutes in doubling time, from 65.9 to 157.7 minutes.

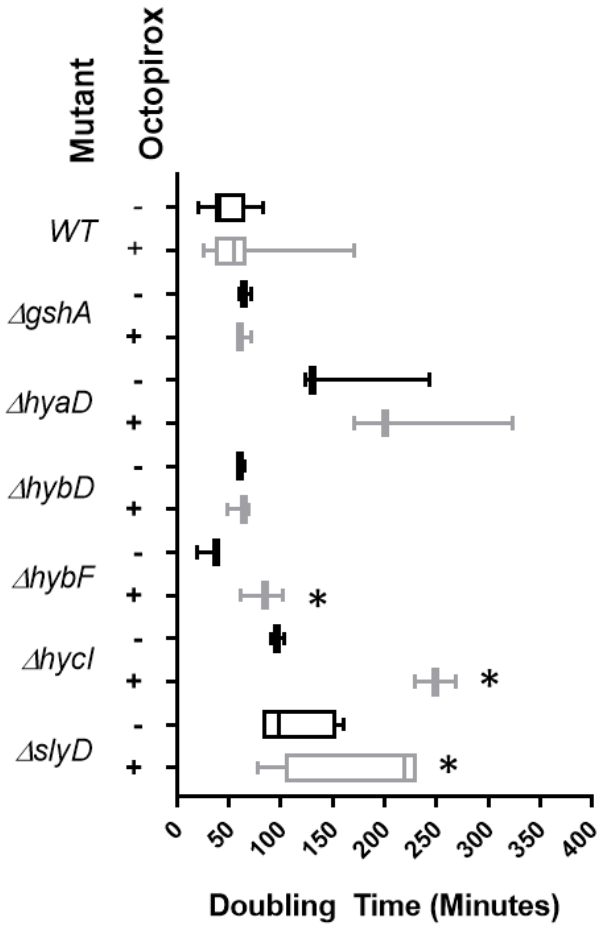

Figure 6-12. Box and whisker plots of *E. coli* metal various cellular function mutants. Deletion mutants are labelled on y-axis and doubling time on the x-axis. The presence (+), black box and whisker plot) or absence of Octopirox (–), light grey box and whisker plot) are indicated. An asterisk denotes p-values of ≤0.05; statistical analysis conducted using unpaired t-test.

Out of the metal cofactored mutants tested with Octopirox, only three strains were adversely affected by chelant addition (**Figure 6-12**). Deletion of *hybF* resulted in an average doubling time of 31.0 minutes that increased to 82.6 minutes after the addition of Octopirox (an increase of 51.5 minutes; p-value = 0.0184). The *ΔhycI* mutant doubling time increased by 152.6 minutes, from 96.8 to 249.5 minutes (p-value = 0.0002). The *ΔslyD* mutant also showed an increased doubling time, from 87.2 to 227.0 minutes, an an increase of 139.7 minutes (p-value = 0.0001).

6.3.4. Periplasmic stress

All mutants in this category showed a significant change in doubling time following addition of Octopirox (**Figure 6-13**) and were repeated a total of 10 times. A *cpxA* deletion, unusually, resulted in

a decreased doubling time (-11.4 minutes) from 54.5 to 43.2 minutes with chelant addition (p-value = 0.0263). In contrast, *ΔcpxR* increased in doubling time from 59.6 to 114.2 minutes, a 65.6 minute difference (p-value = 0.0002). The *cpxP* mutant showed an increased doubling time of 59.8 minutes, from 62.4 to 122.2 minutes (p-value = 0.0006). The final strain, *ΔdsbA*, displayed a 52.3 minute increased doubling time in cultures without and with Octopirox (p-value 0.0006).

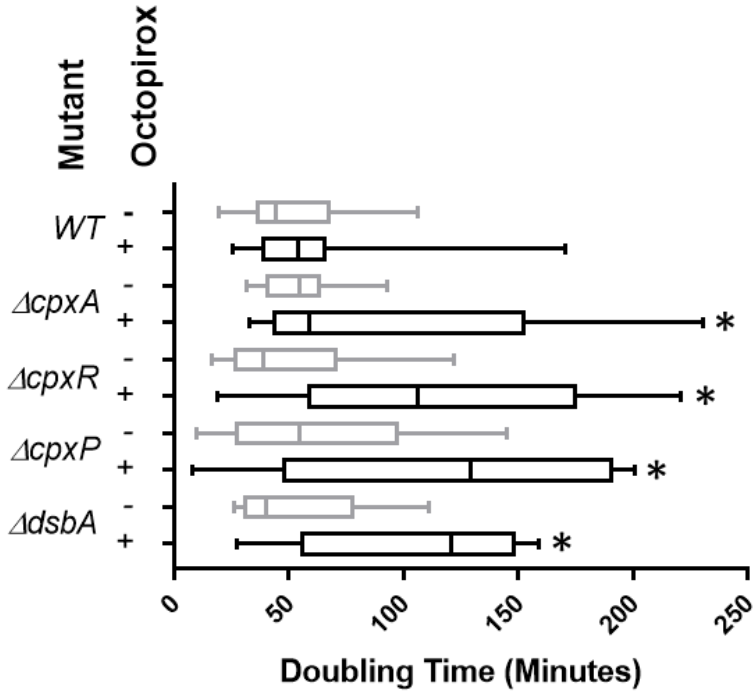

Figure 6-13. Box and whisker plots of *E. coli* periplasmic stress mutants. Deletion mutants are labelled on y-axis and doubling time on the x-axis. The presence (+), black box and whisker plot) or absence of Octopirox (–), light grey box and whisker plot) are indicated. An asterisk denotes p-values of ≤0.05; statistical analysis conducted using unpaired t-test.

6.4. Doubling times of deletion mutants exposed to DTPMP

6.4.1. DNA repair and recombination

Out of the 17 DNA recombination and repair mutants exposed to 0.05 mM DTPMP in early exponential phase, only four showed significant differences in growth rate (**Figure 6-14**).

The affected mutants included *recB*, which showed a modest increase in doubling time of 12.9 minutes from 32.5 to 45.3 minutes (p-value = 0.0496). This was the only one of the six *rec* mutants tested that showed an effect on growth after addition of DTPMP. The *ΔruvB* strain had an increased doubling time

of 35.7 minutes, from 110.6 to 146.3 minutes (p-value = 0.0004) and was the only *ruv* mutant affected by chelant addition. The *ΔruvA* and *ΔruvC* strains had p-values of 0.3262 and 0.0685 that are not significant when analysed by the paired t-test.

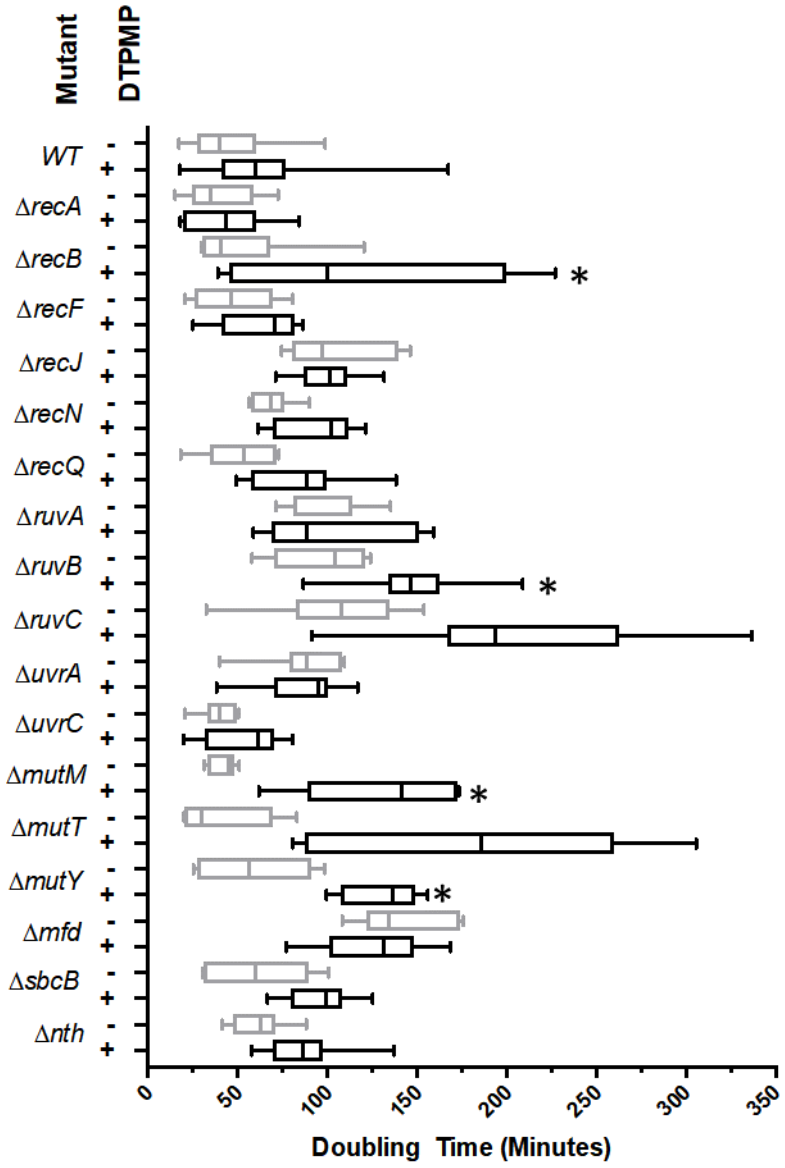

Figure 6-14. Box and whisker plots of *E. coli* DNA recombination and repair mutants. Deletion mutants are labelled on y-axis and doubling time on the x-axis. The presence (+), black box and whisker plot) or absence of DTPMP (–), light grey box and whisker plot) are indicated. An asterisk denotes p-values of ≤0.05; statistical analysis conducted using unpaired t-test.

The final two genes that showed an increase in average doubling time validated by statistical analysis were *ΔmutY* and *ΔmutM*. Deletion of *mutY* resulted in a doubling time of 91.8 minutes that increased to

148.69 minutes when exposed to chelant, an increase of 55.1 minutes (p-value = 0.0012). The *ΔmutM* strain showed a 33.7 minute increase in doubling time from 46.3 to 80.0 minutes (p-value = 0.0253). No significant change was detected with any of the other mutants, including *ΔmutT* which gave a p-value of 0.1741.

6.4.2. Oxidative stress gene deletion

Five oxidative stress mutants were tested with DTPMP and all but *ΔahpC* (p-value = 0.2997) showed a significantly reduced growth rate following chelant exposure (**Figure 6-15**). The *ΔkatG* strain had an average doubling time of 74.9 minutes that increased to 132.7 minutes with addition of DTPMP an increase of 57.8 minutes (p-value of 0.0115).

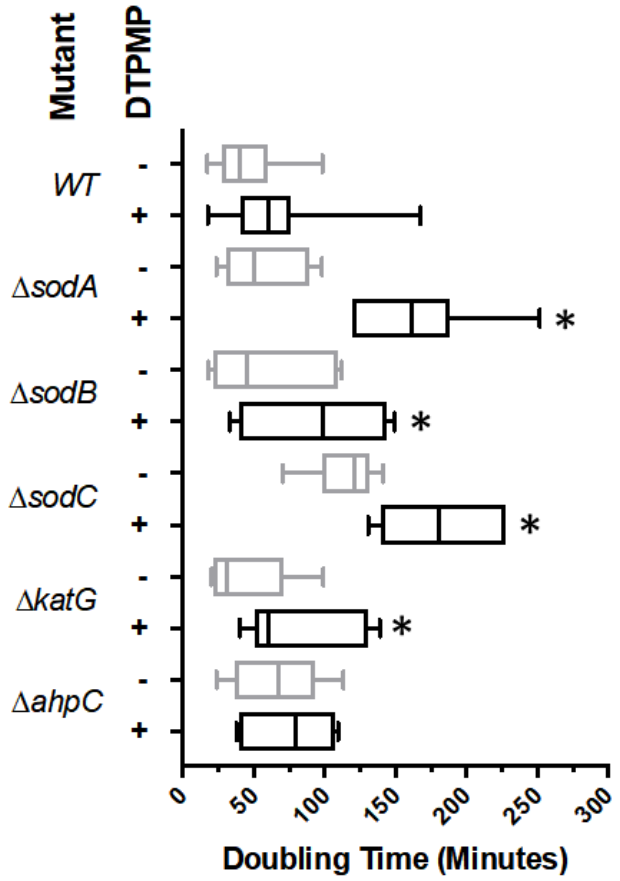

Figure 6-15. Box and whisker plots of *E. coli* oxidative stress mutants. Deletion mutants are labelled on y-axis and doubling time on the x-axis. The presence (+), black box and whisker plot) or absence of DTPMP (–), light grey box and whisker plot) are indicated. An asterisk denotes p-values of ≤0.05; statistical analysis conducted using unpaired t-test.

The *E. coli ΔsodA* strain showed an increase in doubling time of 33.4 minutes, from 89.3 to 122.8 minutes (p-value = 0.0051). The *ΔsodB* strain behaved similarly, with an increase in doubling time of 40.5 minutes, from 103.6 to 144.1 minutes (p-value = 0.0054). The final mutant in this group (*ΔsodC*) increased doubling time by 80.3 minutes, from 131.5 minutes to 211.7 minutes (p-value = 0.0093).

6.4.3. Metal homeostasis gene deletion

Only one of the five mutants involved in iron and manganese homeostasis was affected by addition of 0.05 mM DTPMP in early exponential phase (**Figure 6-16**). This deletion strain was *ΔfeoB* which increased in average doubling time by 77 minutes from 28 to 106 minutes (p-value = 0.0364).

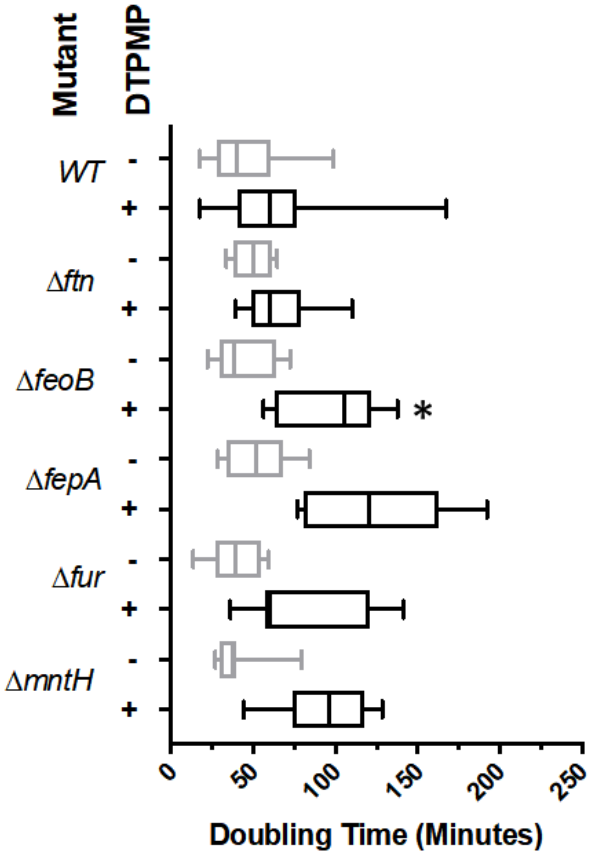

Figure 6-16. Box and whisker plots of *E. coli* metal homeostasis mutants of manganese and iron systems. Deletion mutants are labelled on y-axis and doubling time on the x-axis. The presence (+), black box and whisker plot) or absence of DTPMP (–), light grey box and whisker plot) are indicated. An asterisk denotes p-values of ≤0.05; statistical analysis conducted using unpaired t-test.

Other iron metal homeostasis single gene deletion mutants all had p-values above 0.05, *Δftn* (0.4934), *ΔfepA* (0.0973) and *Δfur* (0.3579), while the only manganese homeostasis mutant, *ΔmntH*, had a p-value of 0.1008.

Nine mutant strains were analysed involved in copper, zinc, cobalt, nickel and magnesium ion regulation (**Figure 6-17**). Out of these genes, the paired t-test analysis of the doubling time data suggested that only a single strain, *ΔcopA*, showed a significant difference. This strain increased in doubling time from 46.7 and 104.4 minutes with addition of DTPMP, an increase of 57.6 minutes (p-value = 0.0054).

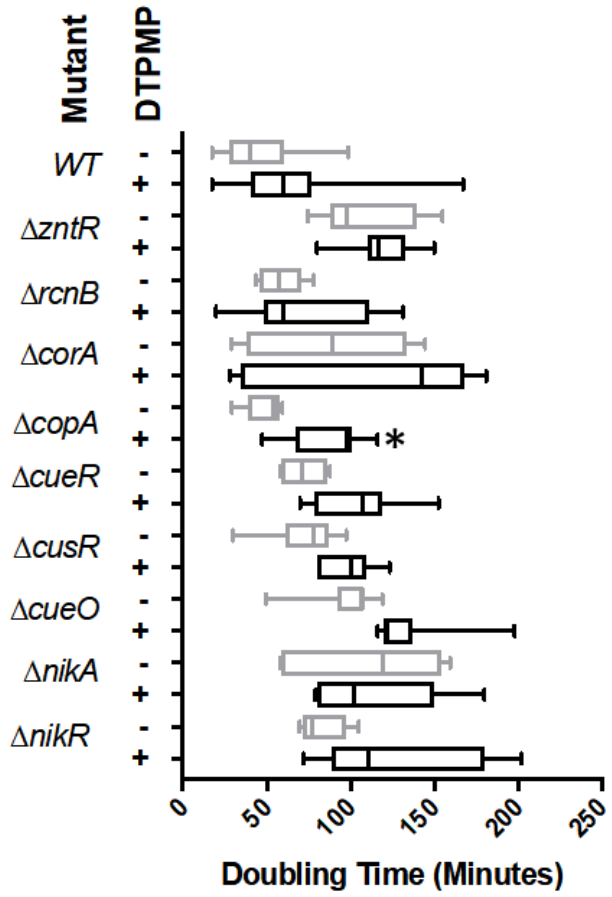

Figure 6-17. Box and whisker plots of *E. coli* metal homeostasis mutants of copper, nickel, cobalt, zinc and magnesium systems. Deletion mutants are labelled on y-axis and doubling time on the x-axis. The presence (+), black box and whisker plot) or absence of DTPMP (–), light grey box and whisker plot) are indicated. An asterisk denotes p-values of ≤0.05; statistical analysis conducted using unpaired t-test.

Of the other six metal homeostasis genes investigated, only two showed statistically significant differences in doubling times (**Figure 6-18**). These were *ΔgshA* and *ΔslyD* which had p-values of 0.0102 and 0.0007, with increases of 20.2 minutes and 35.6, respectively. Without chelator the deletion of *gshA* and *slyD* had average doubling times of 91.0 and 53.0 minutes that increased to 73.2 and 126.6 minutes, respectively.

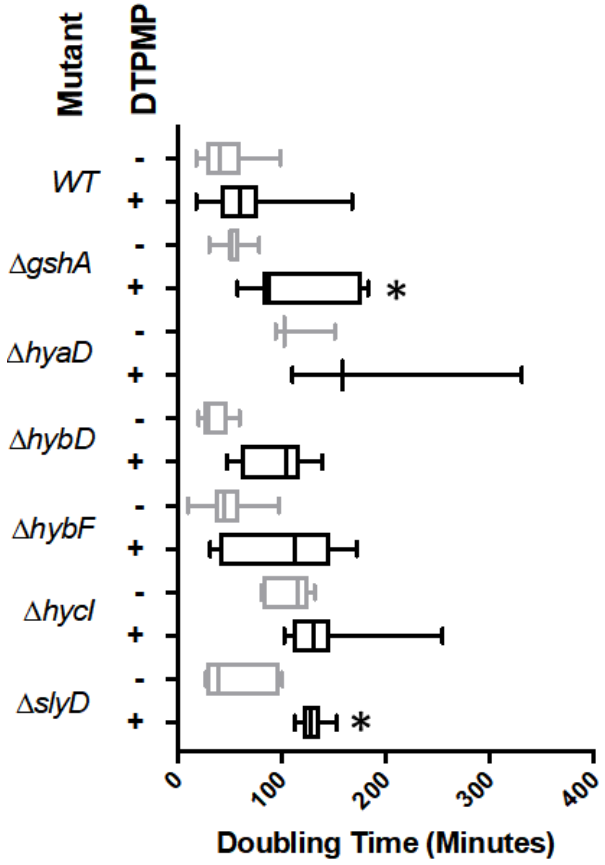

Figure 6-18. Box and whisker plots of *E. coli* metal various cellular function mutants. Deletion mutants are labelled on y-axis and doubling time on the x-axis. The presence (+), black box and whisker plot) or absence of DTPMP (–), light grey box and whisker plot) are indicated. An asterisk denotes p-values of ≤0.05; statistical analysis conducted using unpaired t-test.

6.4.4. Periplasmic stress

Only two out of the four periplasmic stress mutants were significantly affected by DTPMP and were repeated a total of 10 times. These gene deletions were *cpxA* and *cpxP* which had increases in average

doubling times of 35.6 (p-value = 0.0367) and 21.5 (p-value = 0.0198) minutes. See **Figure 6-19** for further details.

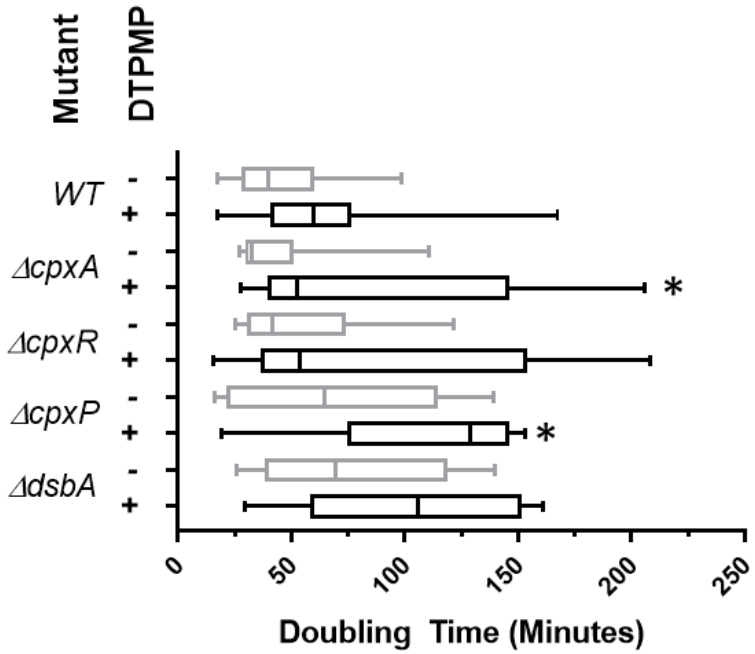

Figure 6-19. Box and whisker plots of *E. coli* periplasmic stress mutants. Deletion mutants are labelled on y-axis and doubling time on the x-axis. The presence (+), black box and whisker plot) or absence of DTPMP (–), light grey box and whisker plot) are indicated. An asterisk denotes p-values of ≤0.05; statistical analysis conducted using unpaired t-test.

6.5. Discussion

The three different chelators (EDTA, Octopirox and DTPMP) investigated in this chapter showed different effects on the mutant strains examined from the Keio collection. Of the 47 strains tested, 28 displayed an effect on growth rate due to the presence of the chelant and only five of these were affected by all three chelants (**Table 6-1**). These effects are discussed further below, comparing the three chelators in each of the assigned functional categories.

Table 6-1. Difference in average doubling time of *E. coli* deletion mutants exposed to different chelators added during early exponential phase of growth. Asterisks indicate differences where p-values were ≤0.05 which were evaluated using unpaired t-tests.

	Average doubling time difference		
Deletion mutant	**EDTA**	**DTPMP**	**Octopirox**

ΔahpC	14.7	5.6	19.8
ΔcopA	23.4	57.6*	28.4
ΔcorA	14.5	45.1	21.8
ΔcpxA	19.9*	20.2*	-11.4*
ΔcpxP	50.6*	20.6*	59.8*
ΔcpxR	55.4*	2.0	65.6*
ΔcueO	-22.7	19.2	-5.1
ΔcueR	15.5*	12.6	68.6*
ΔcusR	48.9	10.9	64.8*
ΔdsbA	-1.1	11.3	52.3*
ΔfeoB	33.2*	77.3*	-43.0
ΔfepA	49.7*	51.2	91.8*
Δftn	4.3	4.5	3.8
Δfur	29.0	15.2	13.8
ΔgshA	30.5*	20.1*	-1.9
ΔhybD	56.4*	5.7	-1.2
ΔhybF	43.6*	-10.8	51.5*
ΔhycI	-7.0	37.1	152.6*
ΔkatG	23.2*	57.8*	90.4*
Δmfd	-27.1	-22.2	-25.3
ΔmntH	38.4*	33.4	117.1*
ΔmutM	32.5	33.7*	14.5
ΔmutT	24.8*	34.1	-1.7
ΔmutY	33.8*	55.1*	-19.9*
ΔnikA	-17.1	21.2	30.6
ΔnikR	18.3	3.4	11.2
Δnth	23.6	-1.8	-22.5
ΔrcnB	18.2	-24.2	91.9*
ΔrecA	19.1	-1.1	44.9*
ΔrecB	183.2*	12.9*	-2.9
ΔrecF	3.6	12.8	-0.1
ΔrecJ	-6.3	-17.5	-0.5
ΔrecN	-4.2	8.4	-24.0
ΔrecQ	-6.8	12.8	9.2
ΔruvA	-2.3	-17.1	5.8
ΔruvB	-9.0	35.7*	51.9*
ΔruvC	2.7	41.7	59.8*
ΔsbcB	11.0	29.1	4.5
ΔslyD	41.6*	35.6*	139.7*
ΔsodA	48.5	33.4*	107.7*
ΔsodB	3.8	40.5*	125.0*
ΔsodC	-12.7	80.3*	55.3
ΔuvrA	-32.8*	-1.7	-14.6
ΔuvrC	16.7	-12.1	-12.9
WT	19.1*	18.4*	13.3*

ΔzntR	12.1	-23.9	157.7*

6.5.1. Copper homeostasis

Three mutants (*copA*, *cueR* and *cusR*) related to copper homeostasis were adversely affected by chelant addition, although none showed an effect with all three chelators **(table 6-1)**. In *E. coli*, copper utilisation is paramount for cell viability, however, even low levels can be toxic so the metal concentration is tightly regulated (Grass and Rensing, 2001). Copper toxicity is primarily associated with iron-sulphur cluster dehydratases that are integral to the formation of certain amino acids. Iron in these enzymes can be displaced by the more reactive copper ion and this is prevented in a number of ways, such as export and chelation by glutathione (Macomber and Imlay, 2009). It is also thought that aerobic conditions contribute to copper toxicity, whereby the metal associates with the cytoplasmic membrane and generates hydroperoxide (Grey and Steck, 2001).

The primary factor in *E. coli* copper homeostasis is CopA which is an inner membrane exporter of Cu(I) ions (Rensing and Grass, 2003). CueO, a multicopper oxidase that reacts with siderophores and iron-sulphur clusters, limits free iron availability within the periplasm, providing a protective effect if copper is present (Kim *et al.*, 2001). The oxidase also oxidises the highly reactive Cu(I) into the less reactive and more manageable Cu(II) ion (Chaturvedi and Henderson, 2014). Both CopA and CueO are simultaneously controlled at the transcriptional level by *cueR* (Stoyanov and Brown, 2003), which activates their expression following copper binding (Grass and Rensing, 2001; Stoyanov, Hobman and Brown, 2001). *E. coli* possess an alternative copper sensing and regulatory system provided by CusRS (Yamamoto and Ishihama, 2005). These two proteins form a two-component system (Munson *et al.*, 2000) that regulates expression of a tripartite exporter (CusCFBA) which spans the cell envelope in *E. coli*. The exporter works in conjunction with *cueO* to protect the periplasm from copper toxicity (Rensing and Grass, 2003). Deletion of either *cueR* or *cusR* regulators confers copper sensitivity in either aerobic or anaerobic conditions (Outten *et al.*, 2001). It is important to note that the machinery used for copper import in *E. coli* has yet to be identified but it has been predicted that it is regulated by a putative transporter (Rensing and Grass, 2003).

None of the three chelators used in this chapter had any effect on growth of the *cueO* mutant, suggesting that oxidation of iron-containing elements in the periplasm, preventing an increase in free iron levels, is not important in the antibacterial mode of action. This could be due to compensatory mechanisms, such as the CusCFBA exporter, that act in the absence of *cueO*. Deletion of *copA* only resulted in a significant growth rate reduction in the presence of DTPMP, whereas neither EDTA nor Octopirox showed any discernible differences relative to the control. This suggests that CopA plays an important role in the initial tolerance mechanism of *E. coli* to DTPMP, however, a mutant in its transcriptional regulator, *cueR*, was unaffected by this chelant. It has been suggested that *copA* transcription could also be influenced by the periplasmic stress regulator *cpxR* (Outten *et al.*, 2000) and this could potentially explain this discrepancy.

In contrast to DTPMP, the *cueR* mutant did exhibit a 15.5 minute increase in doubling time with EDTA and a 68.6 minute increase with Octopirox. The *cusR* strain was only affected by the latter with an increase in doubling time of 64.8 minutes. With addition of Octopirox, the absence of either of the two copper regulatory systems is detrimental to growth, suggesting they are both important in tolerating the effects of this chelant and do not entirely substitute for each other. Other factors regulated by CueR and CusR may be important as loss of either of the copper export pathways (CopA or CueO) did not affect bacterial growth when exposed to Octopirox. With EDTA, only the *ΔcueR* mutant was negatively affected, indicating that the *cue* copper regulon is needed for tolerance as neither CopA or CueO deficiency alone showed any detrimental growth effects. Consistent with this notion, the absence of the *cusR* system was also not important with EDTA. Overall, the results suggest that copper homeostasis is important for an adequate cellular response to metal chelation but this response is different depending on the chelant used.

6.5.2. Iron and manganese homeostasis

Iron exists in the natural environment in two differently charged forms, Fe^{2+} (ferrous) and Fe^{3+} (ferric), where the former ion is more soluble than the latter. While the two states offer versatility in functionality, it also makes the metal more difficult to transport into the cytosol, since the insoluble ferric form predominates over the ferrous. Access to iron is critically important for bacterial cell

viability, however, if not strictly regulated fluctuations in concentration could prove toxic. This toxicity arises in the presence of oxygen from the production of reactive oxygen species from hydrogen peroxide through the Fenton reaction (Touati, 2000). As a result, DNA, proteins and lipids are susceptible to damage and hence bacteria have evolved a complex homeostasis system to manage iron levels (Andrews, Robinson and Rodríguez-Quiñones, 2003). The system in *E. coli* is regulated by Fur (ferric uptake regulation) which controls expression of a large group of genes, some of which do not specifically influence iron homeostasis. Binding of iron by Fur present in the cytosol induces a conformational change which promotes binding to operator sequences adjacent to the genes it controls (Escolar, Pérez-Martín and de Lorenzo, 1999). Depending on where in the promoter region Fur assembles, this results in an upregulation or downregulation of gene expression (Massé and Gottesman, 2002). For example, Fur regulates the *mntH* gene which is required for uptake of manganese (Patzer and Hantke, 2001). Some iron regulated genes, such as *fepA*, *feoB* and *ftn*, are directly controlled by the Fur-Fe complex. The FepA receptor is involved in recognition and uptake of iron-siderophore complexes (Raymond, Dertz and Kim, 2003). The product of *feoB* is a specific ferrous iron importer that is only expressed under anaerobic conditions and actively repressed by Fur bound to iron (Kammler, Schon and Hantke, 1993). Ftn is an iron storage protein that assembles into a hollow sphere that can accommodate over 2000 iron atoms within the interior of the structure (Hudson *et al.*, 1993). Expression of *ftn* is reliant on the presence of Fur-Fe and is typically more highly expressed in the stationary phase of growth rather than exponential (Nandal *et al.*, 2010).

Out of the three chelators tested against mutants defective in iron and manganese homeostasis, none caused any significant difference in growth rate in Δ*fur* or Δ*ftn* strains. EDTA had a detrimental effect on growth of *ΔfeoB*, *ΔfepA* and *ΔmntH* suggesting that the chelant deprives the cell of iron since these genes are only expressed when Fur lacks iron as it functions as a repressor of their transcription. The *mntH* gene is also repressed by the Mn-MntR complex when manganese is plentiful, so an *mntH* deletion would be expected to be detrimental if cellular manganese levels are low. The data documented in Chapter 4, shows that EDTA reduces both iron and manganese which fits with the effects observed on mutants involved in these pathways.

DTPMP only had a detrimental growth effect on the *feoB* gene which suggests that the import of ferrous iron into the cell is key for tolerating this chelant. Deletion of the genes comprising the ferric uptake system were unaffected by DTPMP, indicating that the ferric ion not similarly important for survivability. The only mutants with significantly altered growth rates with Octopirox, were those involving the siderophore receptor FepA and the manganese uptake transporter MntH. ICP-MS analysis of cells in mid-log phase of growth with this chelator showed a reduction in iron levels concomitant with an increase in manganese (Chapter 4). Uptake of manganese is presumed to compensate for iron depletion which fits with a requirement to acquire these metals and the connection with FepA and MntH function. Why DTPMP and Octopirox affect different mutants when they both have the same effect on cellular iron and manganese concentrations is not clear.

6.5.3. Other metal homeostasis systems

The mutants in this group correspond to specific mechanisms involved in magnesium, zinc, cobalt and nickel homeostasis. No changes were observed with *corA*, *nikA* or *nikR* when exposed to any of the three chelants. The *corA* gene is responsible for import and export of Mg^{2+} ions (Smith *et al.*, 1993). Nickel transport in *E. coli* is conducted by low affinity and high affinity import systems, with the latter co-ordinated by the *nik* system (Eitinger and Mandrand-Berthelot, 2000). This *nik* system consists of a transcriptional regulator, NikR, which controls the *nikA* gene encoding an ABC-transporter that can import and export nickel. The other metal homeostasis mutants (**table 6-1**) tested also failed to show significant changes in growth with either EDTA or DTPMP suggesting that these chelators do not target these metals. However, addition of Octopirox did severely restrict growth in an Δ*rcnB* and Δ*zntR* mutants. RcnB indirectly influences nickel and cobalt homeostasis (Bleriot *et al.*, 2011), while ZntR encodes a regulatory protein needed for induction of the ZntA zinc efflux pump (Brocklehurst *et al.*, 1999).

6.5.4. Metal cofactor proteins

The mutants selected that utilise specific metals as cofactors all showed an increase in average doubling time, with the exception of *ΔhyaD* which was unaffected. HyaD is a protease needed for maturation of hydrogenase isoenzyme 3 (Menon *et al.*, 1991), HybF is involved in nickel insertion in the Ni-Fe

hydrogenases 1 and 2 (Hube, Blokesch and Böck, 2002), while HybD and HycI are endopeptidases required for maturation of hydrogenases 2 and 3, respectively (Rossmann *et al.*, 1995). The *gshA* gene is integral to the production of glutathione as it encodes a γ-glutamate-cysteine ligase which is a catalyst for the first step in the biosynthetic pathway (Apontoweil and Berends, 1975). The *slyD* gene is a chaperone for nickel insertion into Ni-Fe hydrogenase complexes (Kaluarachchi, Zhang and Zamble, 2011) and *in vivo* binds both nickel and zinc (Wülfing, Lombardero and Plückthun, 1994). The *ΔslyD* showed significant growth impairment following exposure to EDTA, DTPMP or Octopirox, the only mutant in this grouping to show this susceptibility. This could indicate that specific insertion of nickel into hydrogenases by this chaperone is adversely affected by all of these chelants, perhaps highlighting the importance of correct nickel delivery or a wider disruption metal homeostasis. In addition, EDTA negatively affected *gshA*, *hybD* and *hybF* mutants indicating that maturation of hydrogenases and biosynthesis of glutathione are important in tackling the problems imparted by this chelant. DTPMP conferred significant growth inhibition only in the *gshA* mutant. Octopirox, however, did not alter growth in this mutant, but did increase doubling time with both *hycI* and *hybF*. This suggests that hydrogenases 1 and 2 are a target for Octopirox chelation or are prone to the indirect effects of metal chelation.

6.5.5. DNA repair and recombination

Three *E. coli* mutants (*mutMTY*) from this group relate to avoidance and repair of guanine oxidation (Tajiri, Maki and Sekiguchi, 1995). MutY is an adenine DNA glycosylase that removes adenine mispaired with either guanine or 7,8-dihydro-8-oxoguanine (8-oxo-dGTP) (Zhang *et al.*, 1998). All three chelators caused a significant increase in doubling time of the *mutY* mutant, with DTPMP causing the greatest lag and Octopirox the least. Formation of 8-oxo-dGTP arises from the spontaneous or induced production of oxygen free radicals that escape detoxification by antioxidant pathways of the cell (Sekiguchi *et al.*, 2013). The enhanced sensitivity of *ΔmutY* with these chelators indicates that they bring about an increase in the intracellular levels of reactive oxygen species. MutM (formamidopyrimidine-DNA glycosylase) overlaps with MutY in functionality by removing 8-oxo-dGTP and other oxidised purines incorporated in the genome (Seeberg, Eide and Bjørås, 1995). DTPMP

was the only chelator to affect the doubling time of the *ΔmutM* strain. MutT is a diphosphatase which removes 8-oxo-dGTP from the nucleotide pool to prevent misincorporation during DNA replication (Maki and Sekiguchi, 1992). The only chelant to affect growth rate of the *ΔmutT* strain was EDTA. Overall the effect of chelants on this DNA repair and tolerance system suggests that the chelators cause increased oxidative damage in the cell.

Several other DNA repair and tolerance systems, namely mutants in the *rec*, *uvr* and *ruv* genes (Michel, 2005), were also affected by the presence of chelant added in early exponential phase. Some of the components of these *E. coli* repair and recombination pathways are regulated as part of the SOS response, which is controlled by the LexA transcriptional repressor and activated by RecA binding to exposed ssDNA. RecBCD (exonuclease V) forms a helicase-nuclease complex that processes dsDNA breaks and helps load RecA to initiate recombinational repair (Hickson *et al.*, 1985). RecFOR can also act as a complex and facilitates nucleation of RecA at ssDNA gaps, particularly assisting with replication fork restart (Rangarajan, Woodgate and Goodman, 2002). In addition to its role in the SOS response, RecA mediates homologous pairing and strand exchange between ssDNA and an undamaged chromosome to form a Holliday junction that is an essential intermediate for restoring the damaged template. Octopirox addition was the only chelator to slow the growth of the *recA* mutant. Addition of EDTA or DTPMP, but not Octopirox, retarded the growth of the *ΔrecB* strain. None of the other *rec* mutants showed any change in growth when the chelant was added. The primary resolution pathway in *E. coli* is encoded by the *ruvABC* genes (Eggleston, Mitchell and West, 1997; Yamada, Ariyoshi and Morikawa, 2004). RuvAB helps dissociate the RecA filament and promotes branch migration of the Holliday junction DNA (Adams and West, 1995). RuvC is an endonuclease that resolves the Holliday junction to separate the interlinked chromosomes (Connolly *et al.*, 1991; Dunderdale *et al.*, 1991). Out of the chelators tested, EDTA did not affect any of the *ruv* mutants, DTPMP only reduced growth in a *ΔruvB* strain and Octopirox had a detrimental on both *ΔruvB* and *ΔruvC*. The sensitivity of *recA*, *recB*, *ruvB* and *ruvC* strains is in keeping with DNA damage that either causes breaks or interrupts replisome progression. However, the variety of effects with each of the chelants and the absence of effect in some cases, such as *ruvA*, cannot be interpreted simply.

The only gene in the *uvrABC* group affected by a chelant (EDTA) was *uvrA* and it induced an acceleration of *E. coli* growth. UvrA works with UvrB and UvrC to recognise bulky adducts in DNA and mediate nucleotide excision repair (Sancar and Sancar, 1988). Lesion recognition requires a UvrA-UvrB complex (Stracy *et al.*, 2016), while excision of an oligonucleotide containing the damaged bases or bases is performed by the UvrC endonuclease (Verhoeven *et al.*, 2000). The 32.8-minute decrease in average doubling time with EDTA strongly suggests that UvrA may be a target for the chelant. Interestingly, UvrA possesses two zinc finger motifs involved in DNA binding (Truglio *et al.*, 2006) that could be affected directly by metal chelation by EDTA. Nucleotide excision repair does not deal with damage induced by reactive oxygen species.

6.5.6. Oxidative stress

The three chelators showed different effects on the oxidative stress mutants, Δ*sodA*, Δ*sodB*, Δ*sodC*, Δ*ahpC* and Δ*katG*. The *ahpC* mutant was unaffected by each chelant. The *katG* gene encodes hydroperoxidase I and functions as a peroxidase and a catalase (Loewen and Switala, 1986). KatG acting as a catalase, harnesses a ferric haem group to convert two hydrogen peroxide molecules into water and oxygen (Hillar *et al.*, 2000; Kumar, Tabor and Richardson, 2004). The peroxidase reaction only detoxifies a single hydrogen peroxide molecule using an alternative electron donor (Hillar *et al.*, 2000). All three chelants slowed the growth rate of *ΔkatG*, with the largest effect seen with Octopirox (**table 6-1**). These findings show that hydroperoxidase I is important in tolerating these chelants, consistent with a general problem associated with hydrogen peroxide production. The effect of chelants on reactive oxygen species also accords with the results with the superoxide dismutase mutants.

E. coli carries three superoxide dismutases with different metal cofactors, each scavenging O_2^- to protect against oxygen toxicity (Parker and Blake, 1988). They differ in primary structure, and in the case of SodC, cellular location. SodC is found in the periplasm and contains both copper and zinc as cofactors (Hassan and I Fridovich, 1977; Gort, Ferber and Imlay, 1999). SodA and SodB are manganese and iron superoxide dismutase, respectively, with partially overlapping activities in the cytosol (Hopkin, Papazian and Steinman, 1992; Dubrac and Touati, 2000). EDTA did not adversely influence the growth of any of these three deletion mutants. This was unexpected as EDTA renders SodA and SodB non-

functional, presumably due to mismetallation. Whereas, DTPMP caused significantly increased doubling times in these three strains. Octopirox caused significant changes only in cells lacking the cytoplasmic superoxide dimutases, SodA and SodB. Thus, DTPMP may result in oxidative damage in both cytosol and periplasm. Octopirox, however, appears to only present oxidative damage problems within the *E. coli* cytoplasm, affecting only strains defective in SodA and SodB.

6.5.7. Periplasmic stress proteins

Cell envelope stress is regulated and sensed by a two-component system comprised of CpxA and CpxR (Batchelor *et al.*, 2005). The system responds to a large number of stimuli, including periplasmic, osmotic and oxidative stress, in addition to heat shock, alkali pH, membrane disruption and envelope protein misfolding and aggregation (De Wulf and Lin, 2000; Weatherspoon-Griffin *et al.*, 2014). CpxP interacts with CpxA to inactivate the system under normal conditions (Tschauner *et al.*, 2014). The Cpx periplasmic stress response regulates a large number of *E. coli* genes (Weatherspoon-Griffin *et al.*, 2014), including *dsbA*, which encodes a disulphide bond catalyst which aids folding of transmembrane proteins (Raivio, 2005)(Kishigami and Ito, 1996). The *ΔcpxA* strain showed a reduced growth rate with EDTA and DTPMP, while Octopirox increased growth implying resistance to the chelant (**Table 6-**1). The *ΔcpxR* and *ΔcpxP* strain showed increased differences in doubling time with EDTA and Octopirox, but not DTPMP. Out of all chelators tested, only Octopirox affected the *dsbA* deletion mutant, again causing a decrease in growth. Overall, the results for these mutants imply that EDTA and Octopirox cause significant cell envelope stress. However, the *cpxA* mutant exposed to Octopirox caused the doubling time to accelerate. There is cross-talk between the Cpx two component system and biofilm factors, which could potentially induce CpxR in the absence of CpxA (Landini, 2009).

6.6. Overall trends

Out of the deletion mutants tested only 4 deletions showed a difference in growth when any chelators were present. The first gene deletion mutant *ΔslyD* showed an increase in growth when any chelator was applied to culture and is needed for protein re-folding and the insertion of nickel into hydrogenases as well as a hypothetical role in the regulation of which hydrogenases are synthesised within the *E. coli* cell (Scholz *et al.*, 2006; Pinske, Sargent and Sawers, 2015).

The other gene deletion mutant affected by all three chelators was *ΔmutY* which performs an integral function as a mis-match repair gene for when guanosinee is oxidised under oxidative damage and pairs to adenine (Martinez and Kolter, 1997). However, unlike other genes init's operon *mutY* is upregulated by Fur and other proteins and not down regulated like *mutM* and *mutT* (Yoon *et al.*, 2003). The effect of EDTA and DTPMP showed an increase on doubling time for *ΔmutY* however, Octopirox showed a decrease.

Finally, two gene (*cpxA* and *cpxP*) deletion mutant strains showed to be affected by the presence of any chelators. The two proteins CpxA and CpxP encoded by these genes are needed for periplasmic stress (Tschauner *et al.*, 2014). The *ΔcpxP* strain has increased growth when either EDTA, DTPMP or Ovtopirox is added to culture and this suggests that the *cpxP*. The *ΔcpxA* strain however, shows increase in growth for 2 chelators (EDTA and DTPMP) but a decrease in doubling time when Octopirox is present.

6.7. Future work

The results in this chapter highlight the sensitivity of *E. coli* mutants to EDTA, DTPMP and Octopirox and suggest that systems other than metal homeostasis are important in tolerating chelators. Further work is needed to investigate the phenotypic effects of the three chelants and more fully understand why they affect some mutants and not others. RNA-SEQ experiments with DTPMP and Octopirox would help to assess the cellular transcriptional response to these chelators. Monitoring effects on DNA, protein and lipid oxidation would also be of interest.

Chapter 7. Discussion

This study provides a considerable amount of new information on chelant antibacterial efficacy and how this relates to cellular metal content. In terms of antimicrobial activity, most chelators proved relatively weak at inhibiting *E. coli* growth, many requiring millimolar concentrations to prevent bacterial proliferation. However, in combination the chelants frequently proved highly effective, offering significant potential for industrial and medical applications. Insight into the metals each chelant affects in the bacterial cell also expands the opportunity for their use as research tools to interrogate metal homeostasis.

7.1. Cellular metal content of *E. coli* in the presence of chelant

The majority of the 11 chelants tested resulted in some effect on *E. coli* metal content with the exception of three, CHA, Catechol and BCS, which produced no apparent change in calcium, copper, iron, magnesium, manganese or zinc levels. This result was unexpected as these chelators are known to preferentially associate with specific metals in solution (**Table 7-1**). For example, CHA is produced naturally by plants to chelate iron (Nenortiene, Sapragoniene and Stankevicius, 2002), as does Catechol (Rogers, 1973), while BCS is known to chelate copper from eukaryotic cells (Coloso, Drake and Stipanuk, 1990). There several possible explanations for why these chelants display no measurable effect on cellular metal levels. It could be that they deprive cells of metals that were not readily detectable using ICP-MS parameters, such as nickel, cobalt, copper or molybdenum. Copper levels were monitored but because the number of atoms per cell is low in *E. coli* (approximately 1.4×10^4), the results were somewhat variable. However, no significant differences were detected in copper concentrations with these three chelants or any of the others tested in this study. Alternatively, these three chelators do sequester specific metal ions but these are unavailable to the enzymes that require them for function. These metals could be bound at the cell surface, associated elsewhere within the envelope or be located in the cytosol but tightly bound. It is possible that they actually do not chelate metals under the conditions used, perhaps by being swamped by the large concentration of other metals in the media, such as calcium or magnesium. However, CHA and Catechol do inhibit bacterial growth

at relatively low concentrations (MIC of 2500 µM) and it seems likely that this is due to their chelant activities.

Table 7-1. Metal affinities of chelants selected in this study. The stability or equilibrium constant (K), expressed as log K are shown. Values obtained from the literature were determined at 25°C, I = 0.1 M. The first value for BCS with Cu^{2+} and Zn^{2+} refers to ML (metal-ligand) complex formation (also for BCS with Fe^{2+}), the second refers to ML_2 complex formation; BCS with Ca^{2+} refers to ML_3 complex formation. Octopirox is the ethanolammonium salt of piroctone and is predicted to be a strong iron chelator. Affinity data was obtained from the IUPAC metal affinity database (Pettit, 2006).

Ligand	**Mg^{2+}**	**Ca^{2+}**	**Mn^{2+}**	**Fe^{2+}**	**Fe^{3+}**	**Cu^{2+}**	**Zn^{2+}**
BCS		18.8		20.3		7.1,10.8	10.1,14.9
CHA					11.24		
Catechol	1.98	1.7	7.52		18.52	8.09	9.50
DTPA	9.3	10.7	14.31	15.97	28.7	21.5	18.61
DTPMP	6.4	7.11	11.15			19.47	16.45
EDTA	8.83	10.61	13.81	14.27	25.0	18.7	16.44
GLDA	5.2	5.9	7.6	–	15.35	13.1	11.5
HBED	10.51	9.29	14.78		39	22.95	18.95
MGDA	5.8	7.0	8.4		16.5	13.9	10.9
TPEN	–		10.27	14.6		20.6	15.58
Octopirox							

The other eight chelators could be placed into three distinct categories according to similarities in the metals they affected in *E. coli* at 10-15% growth inhibition. The first category incorporating DTPMP, Octopirox and HBED reduces cellular iron concentrations by about half, while simultaneously elevating levels of manganese by 2.5-3-fold relative to the untreated controls. A second category contains the chelators DTPA, EDTA, GLDA and MGDA, which primarily depletes cells of manganese by as much as 10-fold. The third category contains only TPEN, which predominately reduces zinc concentration in *E. coli*.

These cellular effects differ markedly from those expected from the published data from the IUPAC metal affinity database available for ten of these chelants (**Table 7-1**). Most of the chelants, including Octopirox, are predicted to bind preferentially to iron (either ferric or ferrous). TPEN in solution has a higher affinity for copper or zinc. The results from the experiments described in this thesis, mean that

caution should be expressed in assuming that the affinities defined in solution correspond to the metals actually affected when chelants are mixed with bacterial cultures in rich media.

7.2. Effects of EDTA chelation on *E. coli*

Previous studies on the antibacterial properties of EDTA are rather limited in scope and suggest that the chelant primarily disrupts envelope permeability by affecting LPS stability in the outer leaflet of the bacterial outer membrane (Leive, 1965). However, subsequent work indicated that outer membrane stress was not the key factor in its antibacterial effects (Alakomi, Saarela and Helander, 2003). EDTA is widely used as a chelator, including in the phytoextraction of heavy metals in soils (Luo, Shen and Li, 2005), biomodification of tooth roots through removal of the smear layer (Grover, Yadav and Nanda, 2011) and as a potentiator of antimicrobial preservatives, increasing their efficacy (Finnegan and Percival, 2015). This has meant that EDTA is used widely in many household products and industrial processes (Oviedo and Rodríguez, 2003). However, the lack of biodegradability of EDTA using conventional wastewater treatment approaches means that it tends to persist in the environment (Nörtemann, 1999). Hence this chelant has one of the highest concentrations of any compound made by humans in European waters (Oviedo and Rodríguez, 2003).

The prominence and importance of EDTA in industrial processes and commercial products makes it an important candidate for further investigation into its mode of action. The analysis of EDTA began with an exploration of its impact on the cellular metal content of *E. coli*. Despite the expectation from affinity data that it would preferentially sequester iron, EDTA in fact produced a 10-fold reduction in manganese, alongside more modest decreases in iron and zinc. Supplementation of the culture media with manganese allowed restoration of growth in the presence of EDTA, indicating that availability of manganese is a key factor in growth inhibition. No decrease was detected with calcium or magnesium, which is surprising as these two ions were proposed as the main mechanism of cellular membrane destabilisation (Leive, Shovlin and Mergenhagen, 1968; Goldberg *et al.*, 1983; Lugtenberg and Van Alphen, 1983; Marvin, Ter Beest and Witholt, 1989).

EDTA-treated *E. coli* cells during the mid-log phase of growth were subjected to gene expression analysis by RNA-SEQ to help investigate the cellular response to chelant exposure. Only modest

changes in gene expression were detected, although a large number of genes were significantly upregulated in samples treated with EDTA. The gene showing the largest change in transcription was *rraA*, which showed a 4.11-fold increase in expression. RraA encodes an inhibitor of RNase E, a major component of the mRNA degradation system which also processes a range of structural RNAs (Lee *et al.*, 2003). Degradation of mRNA clearly would have a direct impact on the number of transcripts within the cell and consequently a detrimental influence on the amount of proteins translated by ribosomes (Grunberg-Manago, 1999). Elevated expression of RraA would be expected therefore to inhibit this degradative pathway, elevating transcript stability and allowing increased protein production in response to environmental changes (Górna *et al.*, 2010), perhaps similar to the cellular stresses induced by metal chelation. Further experiments could be undertaken to ascertain mRNA quantity and quality at different time points following EDTA exposure to monitor efficiency of RNase E inhibition on the degradosome or production of structural RNAs. In addition, an *E. coli* mutant deficient in either RraA or RNase E production could be assayed for any enhanced sensitivity to this chelant.

Other noteworthy upregulated genes included the *gat* regulon, which allow galactitol utilisation as an alternative carbon source for glycolysis. The *gat* gene products participate in transportation, phosphorylation and subsequent degradation of metabolites for glycolysis I, a process typically adopted under anaerobic conditions (Nobelmann and Lengeler, 1996; Mayer and Boos, 2005). Thus exposure of cells to EDTA, either directly or indirectly influences the use of galactitol instead of glucose as a carbon source. This allows the switch from an aerobic catabolic pathway to its aerobic counterpart. It would be of interest to culture *E. coli* in the presence of chelant to compare growth and viability under aerobic and anaerobic conditions. Increased expression of the galactitol utilisation pathway should promote better growth of *E. coli* in anaerobic conditions with EDTA. Further experiments could involve assessing the impact of EDTA on cells deficient in these pathways. Minimal media supplemented with either or both of these sugars could also be used to assess *E. coli* growth when EDTA is present, again in aerobic or anaerobic environments.

Genes from the *tdcABCDEFG* operon were also upregulated when *E. coli* was treated with EDTA. The products of the *tdc* genes facilitate the breakdown of L-serine and L-threonine into pyruvate and other

intermediates (Sawers, 2004). Pyruvate is an important metabolite in fatty acid synthesis, glycolysis, amino acid metabolism and gluconeogenesis (Akita, Nakashima and Hoshino, 2016). Upregulation of both *tdc* and *gat* operons again suggests that glycolysis and alternative carbon sources are being used by *E. coli* in response to EDTA. The involvement of pyruvate in fatty acid production potentially provides a link to previously published works indicating that the LPS layer is susceptible to destabilisation when exposed to EDTA (Leive, Shovlin and Mergenhagen, 1968). Assessment of the importance of glycolysis and fatty acid metabolism would merit further study. Other genes involved in alternative carbon metabolism induced in response to EDTA include the *manXYZ* operon, involved in mannose biosynthesis (Erni, Zanolari and Kochers, 1987).

EDTA also caused upregulation of *groS*, which encodes GroES a chaperone involved in stress induced mutagenesis in the presence of magnesium and ATP (Laminet *et al.*, 1990)(Al Mamun *et al.*, 2012). The increase in *groS* expression suggests that EDTA induces problems with protein folding as a result of cellular stress. Interestingly, relatively few metal regulatory systems or oxidative damage and avoidance systems showed increased expression with EDTA. However, these included a number of genes encoding iron binding or iron-sulphur cluster proteins, notably *frdAB*, *tdcG*, *fdnH*, *preA*, *ftnA*, *dmsAB*, *hybO*, *ynfF*, *hypB*, *lpdA* and *ahpC*). These effects indicate that EDTA may well deprive cells of iron or induce oxidative stress, potentially related to its severe effects on manganese depletion.

In parallel with the transcriptome analysis, a series of mutants involved in expected relevant pathways were examined for the effect of EDTA on growth rate when EDTA was added at mid-log phase, rather than at the beginning of culturing in the RNA-SEQ experiments. Deletion mutants in the periplasmic stress sensory system (*cpx* genes) exhibited an increase in doubling time when EDTA was present. This fits with previous studies linking EDTA to effects on cellular membrane permeability and shedding of LPS (Vaara, 1992; Pelletier, Bourlioux and Van Heijenoort, 1994). While the Cpx system is associated with periplasmic stress, it specifically responds to problems in protein folding in this compartment, promotes adaptation and preserves membrane integrity (Ruiz and Silhavy, 2005; MacRitchie *et al.*, 2008; Raivio, Leblanc and Price, 2013). It also plays a minor role in antibiotic resistance and virulence regulation (Raivio, Leblanc and Price, 2013). The EDTA susceptibility of *cpx* deletion mutants suggests

that the chelant causes protein misfolding in the periplasmic space. A direct effect of EDTA on *E. coli* membrane permeability was recently confirmed *in vivo* using live/dead staining (Mulla *et al.*, 2018).

Mutants defective in metal homeostasis genes also exhibited increased doubling times in contact with EDTA (Grass and Rensing, 2001; Outten *et al.*, 2001). These included two iron uptake system genes, either *feoB* and *fepA*, needed for the import of ferrous iron and enterobactin bound to iron (Hantke, 2001). Uptake of manganese via the manganese pump, MntH, (Patzer and Hantke, 2001) also seemed to be important in tolerating EDTA treatment. Effects on iron and manganese homeostasis is corroborated by the cellular metal content analysis which revealed that iron was reduced almost by half by EDTA, while manganese levels dropped 10-fold.

Deletion of the gene for the copper regulator, CueR, also caused a lag in doubling time, however, neither of the genes it regulates, *cueO* nor *copA*, when mutated, caused a significant effect. The alternative export system for copper, the *cus* operon (Outten *et al.*, 2001) when absent also failed to show any change in growth rate. This poses the question of whether *cueR* could control the expression of other, unspecified genes required for viability in response to metal chelation. The genes responsible for copper import are not yet known in *E. coli* although several candidates have been postulated (Grass and Rensing, 2001)(Rensing and Grass, 2003). Some pathogenic *E. coli* strains can produce the siderophore yersiniabactin to bind copper ions and actively import the complex into the cell; the yersiniabactin is recycled for use after metal delivery (Koh *et al.*, 2017). EDTA could potential be starving cells of copper, although there was no evidence for this when this was investigated, although the results were variable.

Deletion of the *gshA* gene, required for production of the antioxidant glutathione (Apontoweil and Berends, 1975) (Ferguson and Booth, 1998), also showed an increased doubling time when EDTA was added. Hence glutathione provides a protective intracellular effect against EDTA, suggesting that this chelant does induce reactive oxygen species. Mutants in *katG*, *sodA* and *sodB*, but not *sodC*, also showed a reduced growth rate when exposed to EDTA, consistent with their role in detoxification of toxic oxygen species. In addidtion, both SodA and Sod B activities appeared to be deactivated by EDTA, possibly via mis-metallation. Overall the results with EDTA fit with a small number of

antibacterial effects involving damage to the bacterial outer membrane and periplasm, depriving cells of metals (especially manganese) and stimulation of reactive oxygen species.

7.3. Effect of DTPMP and Octopirox on *E. coli*

With respect to effects on cellular metal content of *E. coli*, DTPMP showed remarkably similar properties to Octopirox. This finding was unexpected as DTPMP is structurally related to other chelants such as EDTA, DTPA, GLDA and MGDA (**Figure 7-1**), all of which behave very differently from Octopirox in terms of impact on metal composition. The presence of an amide backbone means DTPMP is most closely related to DTPA, differing in addition of phosphate groups at the termini of the compound instead of carboxylates. Octopirox or Piroctone olamine is an ethanolamine salt of the hydroxamic acid derivative piroctone and is most structurally similar to HBED and CHA. The difference being in HBED two phenol rings attached to the opposite termini of the compound whilst Octopirox has only one ring structure and this being a pyridine derivative with a hydroxy group attached at the nitrogen atom. Both chelate iron and exposing cells to HBED produces a lower level of iron than Octopirox (see chapter 3) however, both chelants increase the levels of manganese present inside cells. CHA is similar to Octopirox in regard to the short carbon chain with amide and hydroxy group attached to opposite termini. CHA is a much longer carbon chain with the hydroxylamine group attached to one terminus with the adjacent carbon also containing a double bond to oxygen. The other chelant to produce this result was DTPMP but it has a radically different chemical structure when compared to either compounds HBED or Octopirox (**Figure 7-1**).

Despite the structural differences between DTPMP and Octopirox, they behave very similarly in their cellular effects, both lowering the cellular levels of iron but increasing the levels of manganese by three-fold (see chapter 3). Concentrations of iron and manganese are co-ordinately controlled in bacterial cells growing in either aerobic conditions or iron-deprived media. Substitution of iron for manganese can occur in several ways, for instance iron can be exchanged for manganese within a polypeptide or an alternative protein that utilises manganese as a cofactor can substitute (Cotruvo and Stubbe, 2012). This switch in metal usage could explain the increase in manganese, whereby as iron is depleted, manganese levels increase to populate the proteins requiring this metal for function.

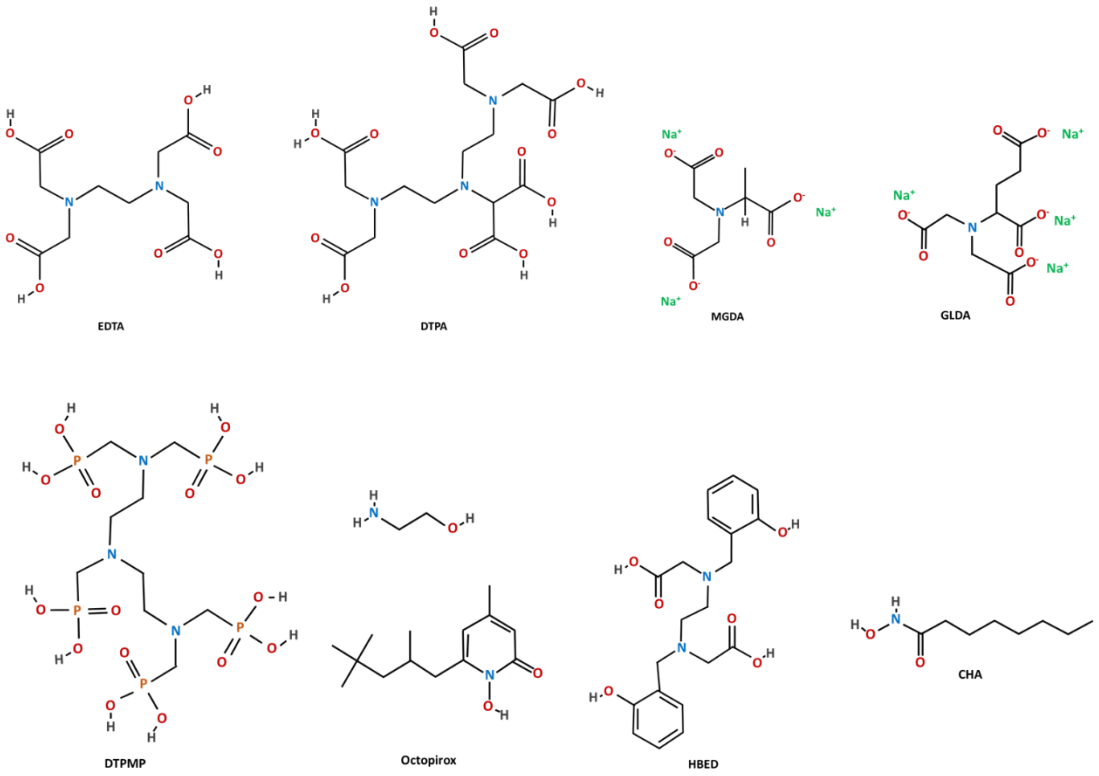

Figure 7-1. Structure of EDTA, DTPA, MGDA, GLDA, DTPMP, Octopirox, HBED and CHA. Nitrogen atoms are represented in blue, phosphorous in orange, oxygen in red, sodium in green and hydrogen in grey. Adapted from the PubChem: open database (Kim *et al.*, 2016).

To ascertain if there was any mechanistic difference between the two chelators, deletion mutants were assessed for resistance or sensitivity in terms of growth. Differing effects were observed between DTPMP and Octopirox with a number of *E. coli* mutant strains. Deletion of *feoB*, the gene needed for ferrous uptake, showed no significant change in growth rate following addition of Octopirox but did show decelerated growth with DTPMP. The opposite effect was observed with the *fepA* mutant, which encodes the importer for the Fe^{3+}-enterobactin complex. These results indicate that DTPMP and Octopirox may chelate different iron states found in the media, DTPMP binding Fe^{2+} and Octopirox binding Fe^{3+}. The deletion of the manganese uptake gene, which would render *E. coli* unable to increase cellular levels of manganese, showed only a significant lag in growth when Octopirox was introduced (note that DTPMP also increased doubling time in the deletion strain however the p-value was not significant). This showed that the increase in manganese uptake by bacteria when this chelant is present is protective.

There was also some effect of these chelators on *E. coli* mutants affecting copper homeostasis. The *copA* mutant showed reduced growth only with DTPMP, while the two copper regulator mutants, *cusR* and *cueR*, showed delayed growth rate only with Octopirox. Further investigation of these differential effects is warranted, especially since no copper cellular metal content data was obtained by ICP-MS for these two chelants.

Deletion of *zntR* also resulted in a significant decreased doubling time with Octopirox, whereas DTPMP did not affect growth. Octopirox could be causing effects on zinc levels in this mutant through its involvement in regulating the zinc exporter, ZntA. However, no significant changes in zinc concentration were detected in *E. coli* exposed to either DTPMP or Octopirox, although when added together a slight decrease in zinc levels was apparent.

Another feature that merits discussion with respect to the mode of action of these two chelants was there effect *cpx* mutants defective in genes involved in detecting periplasmic stress and avoiding periplasmic protein aggregation. Octopirox negatively affected growth in all of the *cpx* mutants tested, except for *cpxA*), suggesting that this system is critical for surviving exposure to this chelant. In contrast, DTPMP only affected the deletion mutant affecting the *cpxA* gene. This indicates that Octopirox may be more disruptive to cell membranes than DTPMP. The reason for the accelerated growth rate seen with the *cpxA* mutant exposed to Octopirox would be interesting to examine further.

Mutants in the manganese and iron superoxide dismutases (*sodA* and *sodB*, respectively) were also affected by the presence of both Octopirox and DTPMP, though the former tended to produce longer delays in doubling time than the latter. DTPMP was the only chelator to reduce growth with the copper-zinc SOD mutant. This SOD is encoded by *sodC* and, unlike the other two SODs, is located in the periplasm and only produced in stationary phase. Its main function is to protect the cell from exogenous sources of superoxide (Imlay and Imlay, 1996). The results suggest that both chelators affect the oxidative stress pathway, specifically SODs, as a consequence of their chelating ability since these proteins require metal cofactors for function. Alternatively, their activities help detoxify elevated levels of superoxide resulting from treatment with these chelators. A fuller understanding is needed regarding the role of SODs in the presence of these chelators and their effect on expression of the *sod* genes.

Many recombination and repair gene mutants also showed extended doubling times especially with Octopirox. This chelant caused a delay in growth of *recA*, *ruvB*, *ruvC* and *mutY* mutants. RecA is involved in signalling DNA damage as part of the SOS response and is responsible for the initiation step in homologous recombination (Kuzminov, 1999; Courcelle and Hanawalt, 2003). The *mutY* gene product excises adenine mispaired to oxidatively damaged guanine to avoid G:C to T:A mutations. MutM behaves similarly as a DNA glycosylase but eliminates oxidatively damaged purines in DNA (Michaels *et al.*, 1992). The *ruvB* and *ruvC* genes encode components of the RuvABC system involved in branch migration and resolution of Holliday junction recombination intermediates (van Gool *et al.*, 1999). DTPMP behaved similarly to Octopirox but only resulted in slower growth rates with *mutY*, *ruvB* and *recB* deletion mutants. RecB forms a complex with RecC and RecD (exonuclease V) which functions in processing double stranded DNA breaks for recombinational repair (Hickson *et al.*, 1985; Shi, Stansbury and Kuzminov, 2005). The susceptibility of these mutants indicates that DNA damage occurs in *E. coli* cells exposed to these chelants. Effects on *mutM* and *mutY* implicates oxygen radical damage as a likely factor resulting from DTPMP and Octopirox exposure, which is consistent with the effects seen with mutants lacking superoxide dismutases. Further studies could be undertaken using these chelants in combination with DNA damaging agents, such as UV light or hydrogen peroxide, to probe their activities against *E. coli* mutants with deficiencies in oxidative damage tolerance and metal homeostasis pathways.

From the deletion mutant experiments in chapter 6, DTPMP and Octopirox, although they have remarkably similar effects on cellular metal content, appear to have subtly different mechanisms of action. This is especially obvious when they are combined in a chequerboards assay in which they exhibit a synergistic interaction. It would be of interest to examine the transcriptional response of *E. coli* to these chelants to help define further any nuances in their mode of action. Ultimately it would be helpful to identify their extracellular or intracellular targets, whether in the external environment, outer or inner membranes, periplasmic space or cytosol and this would inform future chelant design and potentially improve their antibacterial effects.

7.4. Antimicrobial activity of chelants individually and in combination

The 11 chelants investigated in this study did not exhibit particularly impressive antibacterial activities when used on their own. Of those rested, three chelants (BCS, HBED and MGDA) did not produce any notable antimicrobial activity. BCS and HBED are known chelators with specificity and high affinity for copper and iron, respectively (Bergeron, Wiegand and Brittenham, 1998; Chen *et al.*, 2016). MGDA is biodegradable which may have contributed to its poor antibacterial activity (Kolodyńska, Jachula and Hubicki, 2009; Jachula, Kolodyńska and Hubicki, 2011). In combination with other chelants, these three chelators also did not produce many synergistic pairings, BCS (2), HBED (3) and MGDA (1). This may be partly due to an inability to precisely define MIC values due to their limited inhibitory effects alone; hence FIC values may not be accurate and truly reflect the microbial efficacy of these chelants.

Four distinct categories of chelant were characterised in this study based on the effect on cellular metal levels when *E. coli* growth is reduced by 10–15%. These groups showed: 1) no apparent change in metal content (BCS, CHA, Catechol), 2) a substantial reduction in manganese (DTPA, EDTA, GLDA, MGDA), 3) a decrease in iron and increase in manganese (DTPMP, HBED, Octopirox) and 4) a decrease in zinc (TPEN). It might have been expected that categories of chelants that displayed similar effects on metals might be additive in combination, while those that target different metals might be predicted to yield synergistic results. This proved not to be the case as can be seen from the summary of chequerboard and metal analysis data presented in **Table 7-2**. There are four examples where chelants induce a similar cellular response to metals yet produce synergistic effects (e.g. DTPA+GLDA, DTPMP+HBED). There are also multiple examples of chelants from different categories showing additive, indifferent or antagonistic effects (e.g. GLDA+HBED, DTPMP+EDTA). The results indicate that there are several different ways that chelants function in depriving cells of metal, even for those that appear to have the same overall effect.

Table 7-2. Comparison of synergistic, additive, indifferent and antagonistic combinations alongside cellular metal concentrations for the chelant categories with shared functionality.

Synergistic		Additive		Indifferent		Antagonistic	
BCS	DTPA	BCS	Catechol	BCS	CHA	BCS	TPEN
BCS	GLDA	BCS	EDTA	BCS	DTPMP	GLDA	TPEN
CHA	DTPA	CHA	Catechol	BCS	HBED		
CHA	DTPMP	CHA	MGDA	BCS	MGDA		
CHA	EDTA	Catechol	MGDA	BCS	Octopirox		
CHA	GLDA	Catechol	Octopirox	CHA	HBED		
CHA	TPEN	DTPA	MGDA	Catechol	HBED		
Catechol	DTPA	EDTA	MGDA	DTPA	EDTA		
Catechol	DTPMP	GLDA	HBED	DTPMP	EDTA		
Catechol	EDTA	GLDA	MGDA	DTPMP	GLDA		
Catechol	GLDA	GLDA	Octopirox	DTPMP	MGDA		
Catechol	TPEN	HBED	Octopirox	EDTA	HBED		
DTPA	DTPMP	MGDA	Octopirox	HBED	MGDA		
DTPA	GLDA	TPEN	Octopirox				
DTPA	HBED	CHA	Octopirox				
DTPA	TPEN						
DTPA	Octopirox						
DTPMP	HBED						
DTPMP	TPEN						
DTPMP	Octopirox						
EDTA	GLDA						
EDTA	TPEN						
EDTA	Octopirox						
HBED	TPEN						
MGDA	TPEN						

↓ Zn	↓ Mn	↓ Fe ↑ Mn	no change

Despite the complexity in interpreting these findings, there are three chelants that have effects radically different from the others and generally yield synergistic combinations when paired with chelants from one of the other categories. TPEN, which reduces zinc levels, functions distinctly from the others as it is synergistic with all but three pairings (BCS, GLDA and Octopirox). CHA and Catechol do not affect metal content at all but behave very similarly in chequerboard assays suggesting that they have similar cellular effects; trapping metals at the cell surface is one possibility. Assuming Octopirox (and perhaps also HBED as both are predicted to be lipophilic) targets the cell surface, this might explain the additive effects seen with Catechol and CHA in combination with Octopirox (and their indifferent response to HBED). Hence, DTPMP (synergistic with Octopirox and therefore likely to function away from the cell surface) is synergistic with both catechol and CHA. HBED and Octopirox are additive with each other but synergistic with DTPMP, which fits if their location differs. Thus chelant combinations that target

different metals within different cellular compartments are likely to be the most effective at bacterial growth inhibition.

Octopirox, TPEN and CHA, all show markedly lower MIC values than the other chelants, similar to known antibiotics tested against the same *E. coli* strain. Most of the other chelators tested have MICs in the millimolar concentration range and may therefore not be applicable in a clinical, domestic or research setting on their own. However, these concentrations can be drastically reduced from millimolar to micromolar when used in certain synergistic combinations, providing significant potential as antibacterial preservatives suitable for a wide range of applications. These chelant combinations should also prove useful as simple tools to probe metal homeostasis systems and cross-talk between metal regulation systems and other biological processes. Further work is needed to characterise the different cellular targets of chelants, identify key metalloenzymes affected and define their different mechanisms of action.

Conclusions and future directions

Chelants are employed in medical and industrial settings and in commercial products as additives that promote microbial hostility. Despite their widespread use, little research has been undertaken to characterise the effect of chelating agents on bacterial growth and biological processes. The assumption has been that metal chelation is the primary mode of action efficacy was related to the metal affinity and specificity. In this study, however, growth inhibition assays using different chelants on *E. coli* WT and mutant strains, cellular metal content analysis and transcriptomic experiments have revealed that the situation is considerably more complicated. Several chelants appear to affect not only metal homeostasis, but other interrelated aspects of cell biology, including of oxidative damage tolerance and repair pathways and cell envelope integrity. Chelants also do not deprive bacterial cells of the specific metals expected from published affinity data. Furthermore, chelants with similar affects on cellular metal levels can have differing antibacterial effects in combination, suggesting separate cellular components are affected, possibly by sequestration of metals at distinct spatial locations in the bacterial cell.

There remain several unanswered questions from this study that would merit further investigation. The effect of chelators on the biologically relevant metals, copper, nickel and molybdenum, would be helpful in determining their importance to bacterial growth and survival. Where in the bacterial cell that chelants exert their effects could potentially be evaluated by using fluorescent chelants to identify cellular location by microscopy or by separating the cytosol and cell envelope to assess where chelants reside. Direct oxidative damage of biological molecules, such as DNA, lipids and proteins by chelants could also be monitored in different ways. The superoxide dismutase assay could be tested with chelants other than EDTA. In addition, assessing the transcriptional response to different chelants by RT-PCR or RNA-SEQ could also prove informative. Additional *E. coli* mutants could be tested and experiments performed to isolate mutants that develop resistance to chelant exposure. Subsequent genome sequencing of resistant strains could help in identifying key cellular targets. It would also be of interest to validate the properties of selected chelants in other bacterial species and whether effects are bacteriostatic or bactericidal.

The 11 chelators studied offer significant potential as biological probes of metal homeostasis, particularly those that have some selectivity for iron (e.g. Octopirox and DTPMP), manganese (EDTA) and zinc (TPEN). These chelants affect numerous systems in addition to metal homeostasis, either indirectly or directly, including membrane integrity, periplasmic stress, DNA recombination and repair, ribosomal complexes, carbon and sugar sources, oxidative stress and energy production. A complete explanation for these pleiotropic effects is not yet available. Although the chelants often showed limited antibacterial efficacy individually, in combination they functioned well in restricting bacterial growth at significantly reduced concentrations and offer significant potential as robust preservatives in both medical and industrial sectors.

Appendix 1

Name	Product	Expression Control	Expression EDTA-treated	log2 fold change	qValue Control vs EDTA-treated
rraA	Regulator of ribonuclease activity A	222	913	2.04	1.56E-88
gatA	PTS system galactitol-specific EIIA component	344	1238	1.85	3.93E-25
rpsM	30S ribosomal protein S13	96	333	1.79	6.84E-78
gatZ	D-tagatose-1,6-bisphosphate aldolase subunit GatZ	206	682	1.73	9.30E-07
gatC_1	PTS system galactitol-specific EIIC component	140	419	1.58	4.04E-10
tdcE	PFL-like enzyme TdcE	186	556	1.58	0.004329614
gatB_1	PTS system galactitol-specific EIIB component	226	670	1.57	4.18E-37
tdcD	Propionate kinase	125	370	1.57	3.96E-17
gatY	D-tagatose-1,6-bisphosphate aldolase subunit GatY	181	509	1.49	3.42E-14
ansB	L-asparaginase 2	119	323	1.44	4.37E-19
trmD	tRNA (guanine-N(1)-)-methyltransferase	111	294	1.41	2.46E-25
frdA	Fumarate reductase flavoprotein subunit	149	383	1.36	0.001071521
manX_2	PTS system mannose-specific EIIAB component	116	294	1.34	6.63E-23
tdcG	L-serine dehydratase TdcG	164	412	1.33	1.81E-05
frdB	Fumarate reductase iron-sulfur subunit	121	301	1.31	8.15E-22
tdcB	L-threonine dehydratase catabolic TdcB	254	631	1.31	3.12E-04
rpmI	50S ribosomal protein L35	225	541	1.27	1.73E-33
rpsD	30S ribosomal protein S4	239	565	1.24	5.68E-11
atpF	ATP synthase subunit b	67	155	1.21	1.55E-27
gapA	Glyceraldehyde-3-phosphate dehydrogenase A	134	306	1.19	2.76E-12
rplC	50S ribosomal protein L3	123	276	1.17	8.71E-17
rplE	50S ribosomal protein L5	130	288	1.15	8.67E-16
rplU	50S ribosomal protein L21	100	220	1.14	1.17E-24
tdcF	Putative reactive intermediate deaminase TdcF	260	567	1.12	1.40E-18
tabA_3	Toxin-antitoxin biofilm protein TabA	215	461	1.10	5.36E-17
rpmJ	50S ribosomal protein L36	62	131	1.08	8.44E-13
rpsH	30S ribosomal protein S8	122	256	1.07	1.26E-23
manZ_1	PTS system mannose-specific EIID component	85	178	1.07	1.49E-13
rplX	50S ribosomal protein L24	190	396	1.06	5.08E-17
frdC	Fumarate reductase subunit C	81	168	1.05	2.09E-21
rplF	50S ribosomal protein L6	104	214	1.04	3.42E-18
groS	10 kDa chaperonin	164	337	1.04	2.67E-22
rpsN	30S ribosomal protein S14	103	211	1.03	8.45E-21
rplB	50S ribosomal protein L2	47	96	1.03	8.26E-21
gatD	Galactitol-1-phosphate 5-dehydrogenase	106	216	1.03	4.07E-14
manY	PTS system mannose-specific EIIC component	81	163	1.01	1.81E-13
rplW	50S ribosomal protein L23	172	346	1.01	1.00E-19
rpsK	30S ribosomal protein S11	103	207	1.01	2.97E-20
ackA	Acetate kinase	140	280	1.00	1.22E-05
-	NAD(P)H dehydrogenase (quinone)	58	116	1.00	3.81E-19
tdcC	Threonine/serine transporter TdcC	157	312	0.99	6.52E-04

rplP	50S ribosomal protein L16	253	502	0.99	5.40E-15
infC	Translation initiation factor IF-3	350	693	0.99	7.95E-07
rpsE	30S ribosomal protein S5	56	110	0.97	1.98E-17
rpsP	30S ribosomal protein S16	137	265	0.95	4.96E-18
rpoA	DNA-directed RNA polymerase subunit alpha	133	257	0.95	5.55E-08
rpsS	30S ribosomal protein S19	191	367	0.94	5.01E-17
rplR	50S ribosomal protein L18	55	105	0.93	9.01E-13
leuS	Leucine--tRNA ligase	85	161	0.92	0.00182305
rplN	50S ribosomal protein L14	187	354	0.92	1.09E-10
rplD	50S ribosomal protein L4	115	216	0.91	2.45E-10
treB	PTS system trehalose-specific EIIBC component	119	223	0.91	6.24E-05
rpmC	50S ribosomal protein L29	120	224	0.90	3.22E-13
talB	Transaldolase B	203	377	0.89	7.69E-04
rpsA_1	30S ribosomal protein S1	74	137	0.89	3.39E-07
secY	Protein translocase subunit SecY	107	198	0.89	1.11E-06
treC	Trehalose-6-phosphate hydrolase	107	198	0.89	3.14E-04
rplS	50S ribosomal protein L19	120	221	0.88	1.24E-16
lamB	Maltoporin	164	302	0.88	0.002542997
rplJ	50S ribosomal protein L10	155	285	0.88	9.53E-10
hns	DNA-binding protein H-NS	506	919	0.86	0.002263458
fdnH_2	Formate dehydrogenase, nitrate-inducible, iron-sulfur	95	172	0.86	2.01E-10
rplL	50S ribosomal protein L7/L12	408	732	0.84	1.22E-05
rpsJ	30S ribosomal protein S10	103	182	0.82	2.66E-14
rpsC	30S ribosomal protein S3	147	259	0.82	5.06E-11
cspC	Cold shock-like protein CspC	219	385	0.81	2.89E-15
cydX	Cytochrome bd-I ubiquinol oxidase subunit X	52	91	0.81	2.27E-06
preA	NAD-dependent dihydropyrimidine dehydrogenase su	79	138	0.80	6.13E-10
rplV	50S ribosomal protein L22	160	279	0.80	4.23E-13
ptsH	Phosphocarrier protein HPr	232	402	0.79	1.81E-10
rpsG	30S ribosomal protein S7	161	275	0.77	7.04E-08
rpsL	30S ribosomal protein S12	37	63	0.77	2.29E-07
atpC	ATP synthase epsilon chain	121	206	0.77	1.97E-13
ftnA_2	Bacterial non-heme ferritin	167	284	0.77	7.42E-08
yedW	putative transcriptional regulatory protein YedW	126	214	0.76	2.50E-09
dmsB_2	Anaerobic dimethyl sulfoxide reductase chain B	72	122	0.76	8.68E-14
fusA	Elongation factor G	100	169	0.76	0.005475324
rpsB	30S ribosomal protein S2	123	207	0.75	9.83E-08
icd_1	Isocitrate dehydrogenase [NADP]	102	171	0.75	2.10E-05
cspE	Cold shock-like protein CspE	173	290	0.75	1.69E-12
lacR_1	Lactose phosphotransferase system repressor	103	172	0.74	1.65E-12
fimA	Type-1 fimbrial protein, A chain	99	165	0.74	3.70E-11
rplO	50S ribosomal protein L15	97	161	0.73	9.01E-13

rimM	Ribosome maturation factor RimM	60	99	0.72	8.58E-12
rmf	Ribosome modulation factor	84	138	0.72	5.95E-07
priB	Primosomal replication protein N	127	208	0.71	5.51E-12
acpP	Acyl carrier protein	304	496	0.71	5.61E-07
hybO	Hydrogenase-2 small chain	86	140	0.70	6.67E-08
adhE_1	Aldehyde-alcohol dehydrogenase	74	120	0.70	0.006198272
rplT	50S ribosomal protein L20	52	84	0.69	5.25E-08
crl	Sigma factor-binding protein Crl	149	240	0.69	9.79E-09
ynfF	putative dimethyl sulfoxide reductase chain YnfF	64	102	0.67	0.00108602
udp	Uridine phosphorylase	117	186	0.67	1.42E-06
hha	Hemolysin expression-modulating protein Hha	121	192	0.67	9.85E-10
rpmD	50S ribosomal protein L30	180	285	0.66	5.38E-11
rplK	50S ribosomal protein L11	40	63	0.66	6.16E-07
hypB	Hydrogenase isoenzymes nickel incorporation protein	92	144	0.65	2.09E-06
uspE	Universal stress protein E	84	131	0.64	3.53E-06
fbaA_2	Fructose-bisphosphate aldolase class 2	127	198	0.64	2.30E-04
fkpA	FKBP-type peptidyl-prolyl cis-trans isomerase FkpA	187	290	0.63	0.001010369
lpdA	Dihydrolipoyl dehydrogenase	90	139	0.63	2.24E-04
yfeX	putative deferrochelatase/peroxidase YfeX	82	125	0.61	9.82E-06
atpH	ATP synthase subunit delta	54	82	0.60	3.99E-09
ahpC	Alkyl hydroperoxide reductase subunit C	163	247	0.60	5.05E-06
aceF	Dihydrolipoyllysine-residue acetyltransferase compon	65	98	0.59	2.93E-04
fabG2	putative oxidoreductase	97	146	0.59	1.24E-05
tpiA	Triosephosphate isomerase	164	245	0.58	3.58E-04
slyB	Outer membrane lipoprotein SlyB	69	103	0.58	2.01E-09
eno	Enolase	132	196	0.57	0.008359875
cspA	Cold shock protein CspA	381	565	0.57	1.88E-05
tsx	Nucleoside-specific channel-forming protein tsx	85	126	0.57	2.13E-05
cydA	Cytochrome bd-I ubiquinol oxidase subunit 1	104	154	0.57	0.005878845
gcvT	Aminomethyltransferase	67	99	0.56	1.91E-05
pykA	Pyruvate kinase II	42	62	0.56	1.11E-06
dmsA	Dimethyl sulfoxide reductase DmsA	61	90	0.56	0.003469136
rplM	50S ribosomal protein L13	192	283	0.56	2.54E-05
hdeB	Acid stress chaperone HdeB	170	250	0.56	2.95E-07
dksA	RNA polymerase-binding transcription factor DksA	170	250	0.56	2.54E-05
ynjE	Thiosulfate sulfurtransferase YnjE	52	76	0.55	1.15E-05
dmsD	Tat proofreading chaperone DmsD	35	51	0.54	1.23E-06
dcuD_1	Putative cryptic C4-dicarboxylate transporter DcuD	92	134	0.54	7.28E-04
pta	Phosphate acetyltransferase	53	77	0.54	5.33E-05
yceD	Large ribosomal RNA subunit accumulation protein Yce	78	113	0.53	8.96E-09
ycdY	Chaperone protein YcdY	114	165	0.53	5.10E-06
rpsO	30S ribosomal protein S15	179	258	0.53	7.97E-09

gloA	Lactoylglutathione lyase	74	106	0.52	3.62E-08
moaA	GTP 3',8-cyclase	93	133	0.52	3.64E-05
tomB	Hha toxicity modulator TomB	199	284	0.51	5.37E-05
yoeB	Toxin YoeB	101	144	0.51	2.41E-07
rpsQ	30S ribosomal protein S17	78	111	0.51	4.28E-06
osmE	Osmotically-inducible putative lipoprotein OsmE	71	101	0.51	6.22E-07
ppa	Inorganic pyrophosphatase	121	172	0.51	1.40E-05
rpsF	30S ribosomal protein S6	95	135	0.51	2.68E-08
ompX	Outer membrane protein X	133	189	0.51	4.83E-05
atpA	ATP synthase subunit alpha	91	129	0.50	0.002343148
sspB	Stringent starvation protein B	36	51	0.50	8.97E-06
ydhY	putative ferredoxin-like protein YdhY	100	141	0.50	1.21E-05
hupB	DNA-binding protein HU-beta	327	460	0.49	9.16E-05
gcvH	Glycine cleavage system H protein	96	135	0.49	6.66E-08
preT	NAD-dependent dihydropyrimidine dehydrogenase su	65	91	0.49	1.15E-04
hfq	RNA-binding protein Hfq	207	289	0.48	2.01E-05
fabF	3-oxoacyl-[acyl-carrier-protein] synthase 2	61	85	0.48	1.36E-04
frdD	Fumarate reductase subunit D	84	117	0.48	1.26E-07
rpsT	30S ribosomal protein S20	134	185	0.47	1.62E-07
crp	cAMP-activated global transcriptional regulator CRP	103	142	0.46	5.72E-05
rpsU	30S ribosomal protein S21	40	55	0.46	3.66E-04
rplQ	50S ribosomal protein L17	32	44	0.46	2.68E-04
atpB	ATP synthase subunit a	72	99	0.46	1.12E-05
proQ	RNA chaperone ProQ	80	110	0.46	3.60E-06
frr	Ribosome-recycling factor	107	147	0.46	1.19E-05
ptsG	PTS system glucose-specific EIICB component	83	114	0.46	0.0011625
fabB	3-oxoacyl-[acyl-carrier-protein] synthase 1	70	96	0.46	2.16E-04
dmsB_1	Anaerobic dimethyl sulfoxide reductase chain B	106	145	0.45	5.47E-05
pykF	Pyruvate kinase I	82	112	0.45	0.001091703
ihfA	Integration host factor subunit alpha	63	86	0.45	1.82E-05
accB	Biotin carboxyl carrier protein of acetyl-CoA carboxylas	154	210	0.45	1.70E-04
tusA_1	Sulfurtransferase TusA	33	45	0.45	3.62E-04
tsf	Elongation factor Ts	123	167	0.44	3.03E-05
fabG_1	3-oxoacyl-[acyl-carrier-protein] reductase FabG	42	57	0.44	4.05E-07
uspA	Universal stress protein A	203	275	0.44	2.72E-04
sicA	Chaperone protein SicA	111	150	0.43	1.89E-06
adk	Adenylate kinase	123	166	0.43	2.93E-04
kstR2	HTH-type transcriptional repressor KstR2	103	139	0.43	2.01E-05
inlJ	Internalin-J	103	139	0.43	1.27E-04
pal	Peptidoglycan-associated lipoprotein	92	124	0.43	2.95E-07
tig	Trigger factor	72	97	0.43	1.36E-04
hypA_1	hydrogenase nickel incorporation protein HypA	153	206	0.43	1.87E-06

slyD	FKBP-type peptidyl-prolyl cis-trans isomerase SlyD	78	105	0.43	2.29E-07
ydcO	Inner membrane protein YdcO	61	82	0.43	2.26E-04
cydB	Cytochrome bd-I ubiquinol oxidase subunit 2	62	83	0.42	2.46E-04
atpG	ATP synthase gamma chain	60	80	0.42	1.06E-06
mipA_1	MltA-interacting protein	42	56	0.42	6.50E-07
grcA	Autonomous glycyl radical cofactor	226	300	0.41	4.59E-04
asd	Aspartate-semialdehyde dehydrogenase	110	146	0.41	0.003984648
crr	PTS system glucose-specific EIIA component	156	207	0.41	3.83E-04
cybB	Cytochrome b561	89	118	0.41	4.29E-07
rhtC_1	Threonine efflux protein	178	236	0.41	6.33E-04
hupA	DNA-binding protein HU-alpha	251	332	0.40	2.92E-04
agp	Glucose-1-phosphatase	90	119	0.40	7.01E-04
skp	Chaperone protein Skp	110	145	0.40	4.96E-06
srlD	Sorbitol-6-phosphate 2-dehydrogenase	70	92	0.39	7.89E-06
tehB_1	Tellurite methyltransferase	83	109	0.39	9.01E-07
nuoE	NADH-quinone oxidoreductase subunit E	64	84	0.39	9.58E-07
mhpC_1	2-hydroxy-6-oxononadienedioate/2-hydroxy-6- oxono	129	169	0.39	5.30E-04
dgkA	Diacylglycerol kinase	71	93	0.39	7.67E-06
uspF	Universal stress protein F	110	144	0.39	7.09E-07
rplY	50S ribosomal protein L25	91	119	0.39	6.77E-06
ariR	putative two-component-system connector protein Ari	52	68	0.39	6.02E-04
ydhX_1	putative ferredoxin-like protein YdhX	75	98	0.39	1.09E-06
dps	DNA protection during starvation protein	137	179	0.39	4.38E-04
mepS_2	Murein DD-endopeptidase MepS/Murein LD-carboxype	108	141	0.38	1.04E-04
pdhR_1	Pyruvate dehydrogenase complex repressor	82	107	0.38	1.52E-04
ihfB	Integration host factor subunit beta	79	103	0.38	2.31E-05
dsrB	Protein DsrB	122	159	0.38	2.22E-05
ndhF	Nicotinate dehydrogenase FAD-subunit	86	112	0.38	5.79E-04
pheT	Phenylalanine--tRNA ligase beta subunit	53	69	0.38	0.007170945
deoB_2	Phosphopentomutase	113	147	0.38	0.00886776
fimD_1	Outer membrane usher protein FimD	103	133	0.37	0.00588219
fldC	(R)-phenyllactyl-CoA dehydratase beta subunit	104	134	0.37	0.007586994
hyfA_5	Hydrogenase-4 component A	91	117	0.36	1.26E-06
grxC	Glutaredoxin 3	116	149	0.36	4.15E-06
gapA1	Glyceraldehyde-3-phosphate dehydrogenase 1	88	113	0.36	3.95E-05
evgA	DNA-binding transcriptional activator EvgA	148	190	0.36	7.60E-04
deoC	Deoxyribose-phosphate aldolase	121	155	0.36	5.23E-04
grxB	Glutaredoxin 2	68	87	0.36	1.43E-06
pheS	Phenylalanine--tRNA ligase alpha subunit	65	83	0.35	2.97E-04
lsrG	(4S)-4-hydroxy-5-phosphonooxypentane-2,3-dione iso	94	120	0.35	1.17E-05
slyX	Protein SlyX	94	120	0.35	9.10E-05
yafW	Antitoxin YafW	160	204	0.35	6.18E-06

miaA	tRNA dimethylallyltransferase	84	107	0.35	0.001043261
grxD	Glutaredoxin 4	95	121	0.35	4.30E-06
dmsC_2	Anaerobic dimethyl sulfoxide reductase chain C	55	70	0.35	2.32E-06
lpfA	putative major fimbrial subunit LpfA	129	164	0.35	3.25E-04
iscU	Iron-sulfur cluster assembly scaffold protein IscU	59	75	0.35	6.71E-05
dcuA	Anaerobic C4-dicarboxylate transporter DcuA	93	118	0.34	0.009651137
serS	Serine--tRNA ligase	91	115	0.34	0.00905589
nlpI	Lipoprotein NlpI	126	159	0.34	0.001177569
nudB	Dihydroneopterin triphosphate diphosphatase	46	58	0.33	4.51E-05
fldA	Flavodoxin 1	69	87	0.33	7.60E-06
tatE	Sec-independent protein translocase protein TatE	154	194	0.33	5.19E-06
yebC	putative transcriptional regulatory protein YebC	131	165	0.33	5.93E-04
yhcB	Inner membrane protein YhcB	193	243	0.33	0.001100798
gpmA	2,3-bisphosphoglycerate-dependent phosphoglycerate	89	112	0.33	7.63E-04
rob_2	Right origin-binding protein	117	147	0.33	3.38E-04
narW	putative nitrate reductase molybdenum cofactor assen	51	64	0.33	9.41E-06
yeeA	Inner membrane protein YeeA	64	80	0.32	0.001322523
nuoC	NADH-quinone oxidoreductase subunit C/D	60	75	0.32	0.001005943
lpoB	Penicillin-binding protein activator LpoB	36	45	0.32	7.11E-05
pepT	Peptidase T	56	70	0.32	0.00140732
ymgF	Inner membrane protein YmgF	69	86	0.32	9.31E-04
oppD_1	Oligopeptide transport ATP-binding protein OppD	69	86	0.32	0.001542867
ribE	6,7-dimethyl-8-ribityllumazine synthase	65	81	0.32	1.04E-05
tsaR_1	HTH-type transcriptional regulator TsaR	61	76	0.32	4.75E-05
prs	Ribose-phosphate pyrophosphokinase	49	61	0.32	1.24E-05
cyoA	Cytochrome bo(3) ubiquinol oxidase subunit 2	94	117	0.32	0.001631488
glnK	Nitrogen regulatory protein P-II 2	94	117	0.32	8.15E-06
-	PhoH-like protein	74	92	0.31	0.001363663
sra	Stationary-phase-induced ribosome-associated protein	194	241	0.31	2.82E-05
ycdZ	Inner membrane protein YcdZ	29	36	0.31	0.001562758
uvrY	Response regulator UvrY	54	67	0.31	9.82E-06
tatA	Sec-independent protein translocase protein TatA	129	160	0.31	1.12E-05
rpmH	50S ribosomal protein L34	71	88	0.31	0.002553147
ddpX	D-alanyl-D-alanine dipeptidase	68	84	0.30	7.89E-06
proA	Gamma-glutamyl phosphate reductase	68	84	0.30	0.002541845
dus	putative tRNA-dihydrouridine synthase	94	116	0.30	0.001768908
yqgF	Putative pre-16S rRNA nuclease	77	95	0.30	1.19E-05
paaF	2,3-dehydroadipyl-CoA hydratase	60	74	0.30	4.61E-06
yjjW	Putative glycyl-radical enzyme activating enzyme YjjW	69	85	0.30	3.62E-04
dkgB_2	2,5-diketo-D-gluconic acid reductase B	65	80	0.30	1.22E-04
fabD	Malonyl CoA-acyl carrier protein transacylase	52	64	0.30	1.68E-05
rpmG	50S ribosomal protein L33	87	107	0.30	0.001249999

srlR_3	Glucitol operon repressor	148	182	0.30	0.005604154
mdh_2	Malate dehydrogenase	122	150	0.30	0.005381897
secG	Protein-export membrane protein SecG	168	206	0.29	1.10E-04
lsrD	Autoinducer 2 import system permease protein LsrD	40	49	0.29	1.91E-05
yefM	Antitoxin YefM	165	202	0.29	9.31E-06
wzzB	Chain length determinant protein	116	142	0.29	0.005874308
gspA_2	General stress protein A	90	110	0.29	0.002141482
msrB	Peptide methionine sulfoxide reductase MsrB	45	55	0.29	4.93E-04
osmC	Peroxiredoxin OsmC	63	77	0.29	4.63E-05
pdxH	Pyridoxine/pyridoxamine 5'-phosphate oxidase	81	99	0.29	7.12E-05
ompG	Outer membrane protein G	77	94	0.29	0.002099191
rlmE	Ribosomal RNA large subunit methyltransferase E	96	117	0.29	4.39E-04
ppiC	Peptidyl-prolyl cis-trans isomerase C	230	280	0.28	0.001136534
dapA	4-hydroxy-tetrahydrodipicolinate synthase	106	129	0.28	0.002003861
yedR	Inner membrane protein YedR	167	203	0.28	2.46E-05
infA	Translation initiation factor IF-1	225	273	0.28	1.79E-05
lptB_1	Lipopolysaccharide export system ATP-binding protein	61	74	0.28	1.24E-05
glpP	Glycerol uptake operon antiterminator regulatory prot	104	126	0.28	3.94E-04
fnr	Fumarate and nitrate reduction regulatory protein	81	98	0.27	6.71E-04
secE	Protein translocase subunit SecE	81	98	0.27	2.33E-05
sfmA	putative fimbrial-like protein SfmA	48	58	0.27	6.71E-05
fadM	Long-chain acyl-CoA thioesterase FadM	198	239	0.27	0.002390948
gap_1	Glyceraldehyde-3-phosphate dehydrogenase	63	76	0.27	1.67E-04
gntR_1	HTH-type transcriptional regulator GntR	97	117	0.27	0.001658021
hokB	Toxin HokB	108	130	0.27	0.001307924
rplA	50S ribosomal protein L1	99	119	0.27	0.003002468
rpmB	50S ribosomal protein L28	124	149	0.26	3.15E-05
srlE	PTS system glucitol/sorbitol-specific EIIB component	106	127	0.26	0.001168273
nikR	Nickel-responsive regulator	66	79	0.26	7.12E-05
ndhC	NAD(P)H-quinone oxidoreductase subunit 3	117	140	0.26	6.76E-05
bvgA_2	Virulence factors putative positive transcription regula	112	134	0.26	3.71E-05
cca	Multifunctional CCA protein	82	98	0.26	0.001323679
rpsR	30S ribosomal protein S18	108	129	0.26	1.68E-04
rapZ	RNase adapter protein RapZ	67	80	0.26	3.12E-04
cbpA	Curved DNA-binding protein	98	117	0.26	0.003273564
cspG_2	Cold shock-like protein CspG	57	68	0.25	0.005878845
secB	Protein-export protein SecB	135	161	0.25	0.001323679
nuoG	NADH-quinone oxidoreductase subunit G	26	31	0.25	0.00415621
speG	Spermidine N(1)-acetyltransferase	89	106	0.25	2.93E-05
pspE	Thiosulfate sulfurtransferase PspE	237	282	0.25	0.003579005
ftsZ	Cell division protein FtsZ	90	107	0.25	0.00118357
ysnE	putative N-acetyltransferase YsnE	106	126	0.25	6.49E-05

hda	DnaA regulatory inactivator Hda	112	133	0.25	0.003808787
yfjZ_2	Putative antitoxin YfjZ	91	108	0.25	5.89E-05
fabA	3-hydroxydecanoyl-[acyl-carrier-protein] dehydratase	70	83	0.25	2.39E-05
cspD	Cold shock-like protein CspD	97	115	0.25	3.62E-04
hybB	putative Ni/Fe-hydrogenase 2 b-type cytochrome subu	81	96	0.25	0.002661623
dmsC_1	Anaerobic dimethyl sulfoxide reductase chain C	49	58	0.24	3.70E-05
tpx	Thiol peroxidase	33	39	0.24	0.001433718
lutA_1	Lactate utilization protein A	144	170	0.24	0.001352871
moaE	Molybdopterin synthase catalytic subunit	61	72	0.24	9.84E-05
ygdR_2	putative lipoprotein YgdR	111	131	0.24	2.56E-04
ygbF	CRISPR-associated endoribonuclease Cas2	389	459	0.24	0.003792232
pfkA	ATP-dependent 6-phosphofructokinase isozyme 1	78	92	0.24	0.00447917
bluR	HTH-type transcriptional repressor BluR	78	92	0.24	4.04E-04
tyrR	Transcriptional regulatory protein TyrR	67	79	0.24	0.001205266
clpX	ATP-dependent Clp protease ATP-binding subunit ClpX	73	86	0.24	0.003755655
cyoD	Cytochrome bo(3) ubiquinol oxidase subunit 4	62	73	0.24	7.29E-04
mgsA	Methylglyoxal synthase	62	73	0.24	9.75E-05
marR	Multiple antibiotic resistance protein MarR	79	93	0.24	5.37E-05
zapB	Cell division protein ZapB	217	255	0.23	1.06E-04
yccA	Modulator of FtsH protease YccA	120	141	0.23	0.004329614
gnd	6-phosphogluconate dehydrogenase, decarboxylating	63	74	0.23	0.00492181
rpoE	ECF RNA polymerase sigma-E factor	132	155	0.23	0.004359372
mocA	Molybdenum cofactor cytidylyltransferase	69	81	0.23	4.81E-05
hdeA	Acid stress chaperone HdeA	150	176	0.23	6.94E-05
aat	Leucyl/phenylalanyl-tRNA--protein transferase	81	95	0.23	4.21E-04
acuI	putative acrylyl-CoA reductase AcuI	81	95	0.23	0.003810657
rpmF	50S ribosomal protein L32	29	34	0.23	0.004012517
lpxC	UDP-3-O-acyl-N-acetylglucosamine deacetylase	35	41	0.23	4.95E-05
cra	Catabolite repressor/activator	94	110	0.23	0.003657994
zinT	Metal-binding protein ZinT	106	124	0.23	0.005105159
arcA	Aerobic respiration control protein ArcA	136	159	0.23	0.002730614
nuoB	NADH-quinone oxidoreductase subunit B	71	83	0.23	4.00E-05
sfmC	putative fimbrial chaperone SfmC	71	83	0.23	4.81E-05
mdtM	Multidrug resistance protein MdtM	89	104	0.22	0.003749243
pepE	Peptidase E	101	118	0.22	0.004215705
ompN_1	Outer membrane protein N	66	77	0.22	0.005151011
sodC	Superoxide dismutase [Cu-Zn]	42	49	0.22	4.88E-04
panD	Aspartate 1-decarboxylase	128	149	0.22	5.38E-05
clsA	Cardiolipin synthase A	55	64	0.22	0.004081176
ampD	1,6-anhydro-N-acetylmuramyl-L-alanine amidase AmpD	196	228	0.22	0.002398238
ybaB	Nucleoid-associated protein YbaB	185	215	0.22	0.001478823
oppB	Oligopeptide transport system permease protein OppB	74	86	0.22	0.003958979

thiL	Thiamine-monophosphate kinase	105	122	0.22	0.002407665
minD	Septum site-determining protein MinD	68	79	0.22	3.94E-04
lexA_3	LexA repressor	87	101	0.22	2.01E-04
tehA	Tellurite resistance protein TehA	56	65	0.22	4.38E-04
bamD	Outer membrane protein assembly factor BamD	106	123	0.21	0.005053588
rseA	Anti-sigma-E factor RseA	63	73	0.21	6.24E-05
gmk	Guanylate kinase	63	73	0.21	6.49E-05
hypD	Hydrogenase isoenzymes formation protein HypD	38	44	0.21	6.70E-05
bsmA	Lipoprotein BsmA	70	81	0.21	4.04E-04
srlR_1	Glucitol operon repressor	51	59	0.21	1.26E-04
sodB	Superoxide dismutase [Fe]	90	104	0.21	1.69E-04
ppiB	Peptidyl-prolyl cis-trans isomerase B	97	112	0.21	5.08E-05
prfB_2	Peptide chain release factor RF2	104	120	0.21	0.005626011
nuoN	NADH-quinone oxidoreductase subunit N	59	68	0.20	0.007200754
uspD	Universal stress protein D	145	167	0.20	0.002159695
lptA	Lipopolysaccharide export system protein LptA	132	152	0.20	0.005840996
rrrD_2	Lysozyme RrrD	66	76	0.20	1.15E-04
yagE_1	putative 2-keto-3-deoxy-galactonate aldolase YagE	53	61	0.20	1.11E-04
dpp5	Dipeptidyl-peptidase 5	80	92	0.20	0.002288507
exoX	Exodeoxyribonuclease 10	60	69	0.20	9.40E-05
maeA	NAD-dependent malic enzyme	60	69	0.20	0.002420652
atoE	Putative short-chain fatty acid transporter	67	77	0.20	0.007337539
mtlR_1	Mannitol operon repressor	101	116	0.20	1.68E-04
coaA_1	Pantothenate kinase	115	132	0.20	0.00675767
hybD	Hydrogenase 2 maturation protease	61	70	0.20	1.15E-04
ybdO_2	putative HTH-type transcriptional regulator YbdO	95	109	0.20	0.006518806
ydfG	NADP-dependent 3-hydroxy acid dehydrogenase YdfG	34	39	0.20	3.11E-04
rihB	Pyrimidine-specific ribonucleoside hydrolase RihB	68	78	0.20	0.004535667
adhP	Alcohol dehydrogenase, propanol-preferring	62	71	0.20	0.002879301
ubiG	Ubiquinone biosynthesis O-methyltransferase	97	111	0.19	0.006177697
minE	Cell division topological specificity factor	77	88	0.19	0.001136534
nudL	putative Nudix hydrolase NudL	21	24	0.19	0.008273679
ycdX	putative phosphatase YcdX	77	88	0.19	7.30E-04
ygiN	putative quinol monooxygenase YgiN	113	129	0.19	1.10E-04
fdnI	Formate dehydrogenase, nitrate-inducible, cytochrom	64	73	0.19	8.74E-05
erfK	putative L,D-transpeptidase ErfK/SrfK	57	65	0.19	4.71E-04
dtd	D-aminoacyl-tRNA deacylase	72	82	0.19	1.56E-04
efeU_2	Ferrous iron permease EfeU	72	82	0.19	2.57E-04
relB	Antitoxin RelB	73	83	0.19	0.002535896
uidB	Glucuronide carrier protein	73	83	0.19	0.00369749
clpS	ATP-dependent Clp protease adapter protein ClpS	190	216	0.19	0.002181591
mtfA	Protein MtfA	95	108	0.19	0.006818611

iscA_2	Iron-binding protein IscA	117	133	0.18	1.26E-04
clpP	ATP-dependent Clp protease proteolytic subunit	96	109	0.18	0.002006272
pflA	Pyruvate formate-lyase 1-activating enzyme	74	84	0.18	6.86E-04
lpxD_1	UDP-3-O-(3-hydroxymyristoyl)glucosamine N-acyltrans	82	93	0.18	0.007867589
ynbA	Inner membrane protein YnbA	45	51	0.18	2.91E-04
fdoI	Formate dehydrogenase, cytochrome b556(fdo) subuni	106	120	0.18	0.007703327
ftsQ	Cell division protein FtsQ	114	129	0.18	0.006345569
ycjG	L-Ala-D/L-Glu epimerase	61	69	0.18	0.002006705
chbG	Chitooligosaccharide deacetylase ChbG	84	95	0.18	0.003582213
selD	Selenide, water dikinase	46	52	0.18	1.36E-04
ribF	Riboflavin biosynthesis protein RibF	100	113	0.18	0.005979548
ispG	4-hydroxy-3-methylbut-2-en-1-yl diphosphate synthas	54	61	0.18	0.001801924
fecD	Fe(3+) dicitrate transport system permease protein Fe	54	61	0.18	2.23E-04
ydhF	Oxidoreductase YdhF	54	61	0.18	1.09E-04
pyrE_1	Orotate phosphoribosyltransferase	93	105	0.18	0.004763294
gadC	putative glutamate/gamma-aminobutyrate antiporter	70	79	0.17	0.006156365
bfr	Bacterioferritin	187	211	0.17	0.008338447
hisS	Histidine--tRNA ligase	78	88	0.17	0.004532485
-	putative NTE family protein	78	88	0.17	0.009982995
artP	Arginine transport ATP-binding protein ArtP	102	115	0.17	0.008967646
nuoJ	NADH-quinone oxidoreductase subunit J	55	62	0.17	2.08E-04
tyrS	Tyrosine--tRNA ligase	55	62	0.17	0.009172612
topA_2	DNA topoisomerase 1	119	134	0.17	0.005220238
pgrR_1	HTH-type transcriptional regulator PgrR	167	188	0.17	0.008192656
bioD1_2	ATP-dependent dethiobiotin synthetase BioD 1	48	54	0.17	2.31E-04
ampH	D-alanyl-D-alanine- carboxypeptidase/endopeptidase	80	90	0.17	0.007857603
apbC	Iron-sulfur cluster carrier protein	48	54	0.17	5.44E-04
rpiA	Ribose-5-phosphate isomerase A	80	90	0.17	4.88E-04
rseB	Sigma-E factor regulatory protein RseB	48	54	0.17	8.12E-05
hpf	Ribosome hibernation promoting factor	105	118	0.17	1.70E-04
ybeY	Endoribonuclease YbeY	90	101	0.17	1.22E-04
pdxA	4-hydroxythreonine-4-phosphate dehydrogenase	41	46	0.17	1.74E-04
gltC_1	HTH-type transcriptional regulator GltC	82	92	0.17	0.008607524
ribD	Riboflavin biosynthesis protein RibD	82	92	0.17	0.008045248
secM	Secretion monitor	74	83	0.17	1.34E-04
trkG	Trk system potassium uptake protein TrkG	74	83	0.17	0.003657994
eutM	Ethanolamine utilization protein EutM	91	102	0.16	3.89E-04
lipA	Lipoyl synthase	58	65	0.16	0.001277019
ompW	Outer membrane protein W	50	56	0.16	1.79E-04
mnaT	L-amino acid N-acyltransferase MnaT	67	75	0.16	2.38E-04
spuE	Spermidine-binding periplasmic protein SpuE	42	47	0.16	2.38E-04
ygbE	Inner membrane protein YgbE	160	179	0.16	3.59E-04

ulaC_2	Ascorbate-specific PTS system EIIA component	118	132	0.16	2.72E-04
rodZ	Cytoskeleton protein RodZ	59	66	0.16	0.002856402
cyoE	Protoheme IX farnesyltransferase	110	123	0.16	0.005888955
ecpB	putative fimbrial chaperone EcpB	144	161	0.16	0.006954481
yqhD	Alcohol dehydrogenase YqhD	51	57	0.16	0.003055637
nanA	N-acetylneuraminate lyase	119	133	0.16	0.005053588
icsA_2	Outer membrane protein IcsA autotransporter	77	86	0.16	0.006963318
dapB	4-hydroxy-tetrahydrodipicolinate reductase	129	144	0.16	0.004520861
frmR	Transcriptional repressor FrmR	130	145	0.16	2.44E-04
ogt	Methylated-DNA--protein-cysteine methyltransferase	87	97	0.16	1.15E-04
fbaA_1	putative fructose-bisphosphate aldolase	96	107	0.16	0.009239049
ptsO	Phosphocarrier protein NPr	131	146	0.16	2.47E-04
cdd	Cytidine deaminase	35	39	0.16	1.44E-04
gadB	Glutamate decarboxylase beta	70	78	0.16	0.006282259
rfbD	dTDP-4-dehydrorhamnose reductase	115	128	0.15	0.005069272
trxB	Thioredoxin reductase	71	79	0.15	0.00905589
srlB	PTS system glucitol/sorbitol-specific EIIA component	116	129	0.15	1.51E-04
fabZ	3-hydroxyacyl-[acyl-carrier-protein] dehydratase FabZ	117	130	0.15	5.84E-04
fklB	FKBP-type 22 kDa peptidyl-prolyl cis-trans isomerase	63	70	0.15	2.97E-04
yhdN_2	General stress protein 69	81	90	0.15	0.009565168
deoD	Purine nucleoside phosphorylase DeoD-type	81	90	0.15	0.002411495
pdxY	Pyridoxal kinase PdxY	27	30	0.15	6.52E-04
rssB	Regulator of RpoS	54	60	0.15	9.80E-04
yeaD	Putative glucose-6-phosphate 1-epimerase	55	61	0.15	2.90E-04
rplI	50S ribosomal protein L9	37	41	0.15	0.005817524
pncA	Nicotinamidase	65	72	0.15	2.31E-04
yehA	putative fimbrial-like protein YehA	103	114	0.15	0.00601469
hslV	ATP-dependent protease subunit HslV	94	104	0.15	2.63E-04
flhE	Flagellar protein FlhE	47	52	0.15	0.003566572
ecpE	putative fimbrial chaperone EcpE	94	104	0.15	0.008037141
tilS	tRNA(Ile)-lysidine synthase	47	52	0.15	0.003894538
ypjF	putative toxin YpjF	160	177	0.15	6.40E-04
mdoH	Glucans biosynthesis glucosyltransferase H	38	42	0.14	0.008115484
ydjZ_2	TVP38/TMEM64 family inner membrane protein YdjZ	38	42	0.14	7.01E-04
hycA	Formate hydrogenlyase regulatory protein HycA	124	137	0.14	0.002010198
pgrR_3	HTH-type transcriptional regulator PgrR	67	74	0.14	0.004125996
lptE	LPS-assembly lipoprotein LptE	29	32	0.14	0.004914207
minC	Septum site-determining protein MinC	58	64	0.14	2.95E-04
artM_1	Arginine ABC transporter permease protein ArtM	78	86	0.14	6.13E-04
btuR	Cob(I)yrinic acid a,c-diamide adenosyltransferase	49	54	0.14	4.38E-04
galU	UTP--glucose-1-phosphate uridylyltransferase	59	65	0.14	7.07E-04
yjiG	Inner membrane protein YjiG	50	55	0.14	0.001569219

proP_1	Proline/betaine transporter	50	55	0.14	0.009973304
rbsD	D-ribose pyranase	91	100	0.14	2.69E-04
pspG	Phage shock protein G	142	156	0.14	2.91E-04
ddpC	putative D,D-dipeptide transport system permease prc	71	78	0.14	0.006518806
hflD	High frequency lysogenization protein HflD	51	56	0.13	3.58E-04
rnlB	Antitoxin RnlB	92	101	0.13	2.97E-04
ddpF	putative D,D-dipeptide transport ATP-binding protein I	41	45	0.13	3.88E-04
cmk	Cytidylate kinase	73	80	0.13	3.16E-04
yeiP	Elongation factor P-like protein	94	103	0.13	9.18E-04
pliG	Inhibitor of g-type lysozyme	105	115	0.13	2.46E-04
abgT	p-aminobenzoyl-glutamate transport protein	63	69	0.13	0.009149367
symE	Toxic protein SymE	53	58	0.13	0.004714704
pgpA	Phosphatidylglycerophosphatase A	107	117	0.13	0.001753613
emrE	Multidrug transporter EmrE	129	141	0.13	2.74E-04
-	Aminodeoxyfutalosine deaminase	54	59	0.13	0.001522451
deaD	ATP-dependent RNA helicase DeaD	54	59	0.13	0.006686107
dsrF	Intracellular sulfur oxidation protein DsrF	65	71	0.13	0.001771418
-	Hydrolase	76	83	0.13	2.46E-04
uspG	Universal stress protein UP12	76	83	0.13	3.14E-04
pdhR_3	Pyruvate dehydrogenase complex repressor	87	95	0.13	0.007351609
luxS	S-ribosylhomocysteine lyase	98	107	0.13	4.08E-04
ispE	4-diphosphocytidyl-2-C-methyl-D-erythritol kinase	33	36	0.13	4.71E-04
srlA	PTS system glucitol/sorbitol-specific EIIC component	110	120	0.13	0.005726671
csrA	Carbon storage regulator	233	254	0.12	2.78E-04
yajI	putative lipoprotein YajI	100	109	0.12	9.93E-04
nfsB	Oxygen-insensitive NAD(P)H nitroreductase	90	98	0.12	0.004274615
hchA	Molecular chaperone Hsp31 and glyoxalase 3	68	74	0.12	0.002512229
kdsB	3-deoxy-manno-octulosonate cytidylyltransferase	57	62	0.12	2.82E-04
roxA	50S ribosomal protein L16 3-hydroxylase	57	62	0.12	0.009454246
bvgA_1	Virulence factors putative positive transcription regula	80	87	0.12	5.39E-04
chaB	Putative cation transport regulator ChaB	149	162	0.12	3.93E-04
kdsA	2-dehydro-3-deoxyphosphooctonate aldolase	46	50	0.12	4.35E-04
ttcA	tRNA 2-thiocytidine biosynthesis protein TtcA	46	50	0.12	2.69E-04
kefF_1	Glutathione-regulated potassium-efflux system ancilla	47	51	0.12	0.001411595
feaR	Transcriptional activator FeaR	59	64	0.12	9.55E-04
moaB	Molybdenum cofactor biosynthesis protein B	83	90	0.12	2.84E-04
sfmF	putative fimbrial-like protein SfmF	83	90	0.12	3.26E-04
rstA	Transcriptional regulatory protein RstA	60	65	0.12	3.44E-04
msrC	Free methionine-R-sulfoxide reductase	61	66	0.11	3.50E-04
nikC	Nickel transport system permease protein NikC	61	66	0.11	7.01E-04
sucD_2	Succinate--CoA ligase [ADP-forming] subunit alpha	61	66	0.11	0.0011625
fur	Ferric uptake regulation protein	98	106	0.11	3.24E-04

nadE	NH(3)-dependent NAD(+) synthetase	75	81	0.11	0.007113506
wbbL_2	Rhamnosyltransferase WbbL	113	122	0.11	0.001506966
-	Outer membrane protein Omp38	101	109	0.11	4.05E-04
gadA	Glutamate decarboxylase alpha	76	82	0.11	0.008338377
mdtK	Multidrug resistance protein MdtK	38	41	0.11	0.001319817
panB	3-methyl-2-oxobutanoate hydroxymethyltransferase	65	70	0.11	9.46E-04
gap_2	Glyceraldehyde-3-phosphate dehydrogenase	143	154	0.11	0.007854146
narV	Respiratory nitrate reductase 2 gamma chain	39	42	0.11	8.62E-04
kdgR_1	Transcriptional regulator KdgR	39	42	0.11	5.12E-04
ndk	Nucleoside diphosphate kinase	66	71	0.11	7.82E-04
bshB1	N-acetyl-alpha-D-glucosaminyl L-malate deacetylase 1	106	114	0.10	0.005501196
appY	HTH-type transcriptional regulator AppY	80	86	0.10	0.005680602
fldI	(R)-phenyllactate dehydratase activator	55	59	0.10	3.81E-04
uppS	Ditrans,polycis-undecaprenyl-diphosphate synthase ((	83	89	0.10	0.007861872
hlyE	Hemolysin E, chromosomal	111	119	0.10	0.009135718
ycgR	Flagellar brake protein YcgR	42	45	0.10	4.19E-04
folE	GTP cyclohydrolase 1	42	45	0.10	9.13E-04
bamC	Outer membrane protein assembly factor BamC	42	45	0.10	2.91E-04
paaD	Putative 1,2-phenylacetyl-CoA epoxidase, subunit D	56	60	0.10	8.13E-04
ynfM	Inner membrane transport protein YnfM	43	46	0.10	0.001650033
sfaS_1	S-fimbrial adhesin protein SfaS	101	108	0.10	6.65E-04
-	putative FAD-linked oxidoreductase	59	63	0.09	0.008985078
cueR	HTH-type transcriptional regulator CueR	104	111	0.09	4.39E-04
paaC	1,2-phenylacetyl-CoA epoxidase, subunit C	60	64	0.09	2.97E-04
lolB	Outer-membrane lipoprotein LolB	75	80	0.09	3.18E-04
ppsR	Phosphoenolpyruvate synthase regulatory protein	60	64	0.09	6.51E-04
immR	HTH-type transcriptional regulator ImmR	122	130	0.09	7.09E-04
mntP	putative manganese efflux pump MntP	61	65	0.09	5.19E-04
mazF	Endoribonuclease MazF	139	148	0.09	4.24E-04
ftsA_2	Cell division protein FtsA	47	50	0.09	5.88E-04
rusA	Crossover junction endodeoxyribonuclease RusA	80	85	0.09	9.34E-04
sapF	Putrescine export system ATP-binding protein SapF	48	51	0.09	9.44E-04
slyA	Transcriptional regulator SlyA	96	102	0.09	4.88E-04
menB	1,4-dihydroxy-2-naphthoyl-CoA synthase	49	52	0.09	4.11E-04
folB	Dihydroneopterin aldolase	66	70	0.08	0.002421623
soxS	Regulatory protein SoxS	132	140	0.08	4.65E-04
yddG	Aromatic amino acid exporter YddG	50	53	0.08	5.23E-04
bssS	Biofilm regulator BssS	100	106	0.08	0.001845648
nagK	N-acetyl-D-glucosamine kinase	50	53	0.08	5.36E-04
sfp	4'-phosphopantetheinyl transferase sfp	68	72	0.08	6.27E-04
csgC	Curli assembly protein CsgC	68	72	0.08	0.002967057
bamB	Outer membrane protein assembly factor BamB	51	54	0.08	0.007072545

yehT	Transcriptional regulatory protein YehT	68	72	0.08	6.34E-04
rcnR	Transcriptional repressor RcnR	158	167	0.08	5.39E-04
ydcU	Inner membrane ABC transporter permease protein Yd	36	38	0.08	8.34E-04
nuoF	NADH-quinone oxidoreductase subunit F	36	38	0.08	5.71E-04
aroK	Shikimate kinase 1	90	95	0.08	5.34E-04
cusR	Transcriptional regulatory protein CusR	55	58	0.08	8.10E-04
yciB	putative intracellular septation protein A	37	39	0.08	0.005928947
rimL	Ribosomal-protein-serine acetyltransferase	74	78	0.08	7.32E-04
galF	UTP--glucose-1-phosphate uridylyltransferase	58	61	0.07	9.86E-04
iraP	Anti-adapter protein IraP	97	102	0.07	0.002134958
fabI	Enoyl-[acyl-carrier-protein] reductase [NADH] FabI	39	41	0.07	9.03E-04
tcyP	L-cystine uptake protein TcyP	40	42	0.07	0.003053668
yccM_2	Putative electron transport protein YccM	62	65	0.07	0.001858546
gltR	HTH-type transcriptional regulator GltR	42	44	0.07	0.001360868
garR_2	2-hydroxy-3-oxopropionate reductase	64	67	0.07	0.006047709
mepH_1	Murein DD-endopeptidase MepH	64	67	0.07	0.001018711
ydgK	Inner membrane protein YdgK	44	46	0.06	0.006523696
htpX	Protease HtpX	67	70	0.06	0.006309221
yddE	putative isomerase YddE	67	70	0.06	0.009309633
grpE	Protein GrpE	90	94	0.06	0.002301012
nikB	Nickel transport system permease protein NikB	46	48	0.06	7.04E-04
menC	o-succinylbenzoate synthase	46	48	0.06	5.30E-04
sprT	Protein SprT	118	123	0.06	0.002805851
fliO	Flagellar protein FliO	126	131	0.06	7.08E-04
ycjU	Beta-phosphoglucomutase	51	53	0.06	9.05E-04
folM	Dihydromonapterin reductase	26	27	0.05	0.007351609
catM	HTH-type transcriptional regulator CatM	52	54	0.05	8.15E-04
yecD	Isochorismatase family protein YecD	78	81	0.05	7.27E-04
trxA_2	Thioredoxin 1	79	82	0.05	0.002542997
nuoI_1	NADH-quinone oxidoreductase subunit I	53	55	0.05	0.001100798
folD	Bifunctional protein FolD protein	54	56	0.05	0.001024503
exbB_1	Biopolymer transport protein ExbB	85	88	0.05	0.009973304
yiaW_2	Inner membrane protein YiaW	143	148	0.05	0.00181272
gatB_2	PTS system galactitol-specific EIIB component	144	149	0.05	0.001171281
fdhE	Protein FdhE	58	60	0.05	0.004030346
-	putative transporter	145	150	0.05	0.00130586
ybjM	Inner membrane protein YbjM	59	61	0.05	0.00601469
hyfA_1	Hydrogenase-4 component A	60	62	0.05	0.001157215
ghoS	Endoribonuclease GhoS	91	94	0.05	0.002534075
ynjC	Inner membrane ABC transporter permease protein Yn	31	32	0.05	0.001559604
relE	mRNA interferase RelE	94	97	0.05	0.002204131
paaG	1,2-epoxyphenylacetyl-CoA isomerase	63	65	0.05	0.001171156

dapD	2,3,4,5-tetrahydropyridine-2,6-dicarboxylate N-succiny	63	65	0.05	0.001801924
lppC_1	Putative lipoprotein LppC	95	98	0.04	0.002295449
slp_2	Outer membrane protein slp	64	66	0.04	0.001208148
ycgZ	putative two-component-system connector protein Yc	96	99	0.04	0.004863792
cynS	Cyanate hydratase	98	101	0.04	7.31E-04
glgS	Surface composition regulator	197	203	0.04	0.001211643
pgpB	Phosphatidylglycerophosphatase B	67	69	0.04	0.001448359
surE	5'/3'-nucleotidase SurE	68	70	0.04	0.002526818
gstB_2	Glutathione S-transferase GST-6.0	34	35	0.04	0.007137669
nuoH	NADH-quinone oxidoreductase subunit H	35	36	0.04	0.001411495
rutE	putative malonic semialdehyde reductase RutE	70	72	0.04	0.001012387
murP	PTS system N-acetylmuramic acid-specific EIIBC compo	36	37	0.04	0.002672528
cobU	Bifunctional adenosylcobalamin biosynthesis protein (	73	75	0.04	0.001177569
hypE	Hydrogenase isoenzymes formation protein HypE	37	38	0.04	0.001208247
yjjP_1	Inner membrane protein YjjP	111	114	0.04	9.29E-04
narK	Nitrate/nitrite transporter NarK	37	38	0.04	0.002343148
cobB	NAD-dependent protein deacylase	38	39	0.04	0.00118357
yjdF	Inner membrane protein YjdF	81	83	0.04	0.001825601
yohK	Inner membrane protein YohK	41	42	0.03	0.00248638
aphA	Class B acid phosphatase	83	85	0.03	0.009998367
cynT	Carbonic anhydrase 1	42	43	0.03	0.002405001
arnF	putative 4-amino-4-deoxy-L-arabinose-phosphoundec	86	88	0.03	0.00130586
ytfP	Gamma-glutamylcyclotransferase family protein YtfP	88	90	0.03	0.001424482
rspR	HTH-type transcriptional repressor RspR	44	45	0.03	0.001575489
ribC	Riboflavin synthase	88	90	0.03	0.006309221
uspC	Universal stress protein C	91	93	0.03	0.001424482
rfbC	dTDP-4-dehydrorhamnose 3,5-epimerase	47	48	0.03	0.003216664
yecS	L-cystine transport system permease protein YecS	47	48	0.03	0.001382172
mazE	Antitoxin MazE	191	195	0.03	0.001177569
ruvA	Holliday junction ATP-dependent DNA helicase RuvA	48	49	0.03	0.002070174
malG	Maltose transport system permease protein MalG	50	51	0.03	0.001136534
nemA	N-ethylmaleimide reductase	50	51	0.03	0.004863792
osmY_1	Osmotically-inducible protein Y	50	51	0.03	0.001749649
ybjP	putative lipoprotein YbjP	100	102	0.03	0.002079602
azoR	FMN-dependent NADH-azoreductase	51	52	0.03	0.00173595
-	2-oxoglutaramate amidase	52	53	0.03	0.001202033
trmB	tRNA (guanine-N(7)-)-methyltransferase	52	53	0.03	0.001749649
rppH	RNA pyrophosphohydrolase	105	107	0.03	0.006625954
ydiV	Putative anti-FlhC(2)FlhD(4) factor YdiV	55	56	0.03	0.001933662
rimI	Ribosomal-protein-alanine acetyltransferase	112	114	0.03	0.002079602
ydeH_2	Diguanylate cyclase YdeH	58	59	0.02	0.002105384
ybcI	Inner membrane protein YbcI	59	60	0.02	0.001674872

hexR	HTH-type transcriptional regulator HexR	62	63	0.02	0.003964385
yegS	Lipid kinase YegS	63	64	0.02	0.008192656
clcD_1	Carboxymethylenebutenolidase	64	65	0.02	0.003479093
tusA_2	Sulfurtransferase TusA	130	132	0.02	0.001555769
sdhC	Succinate dehydrogenase cytochrome b556 subunit	66	67	0.02	0.003045799
hisF	Imidazole glycerol phosphate synthase subunit HisF	69	70	0.02	0.004525409
sfaG_1	S-fimbrial protein subunit SfaG	69	70	0.02	0.001585271
moaC	Cyclic pyranopterin monophosphate synthase	70	71	0.02	0.001852942
rpoZ	DNA-directed RNA polymerase subunit omega	140	142	0.02	0.001750168
ykgO	50S ribosomal protein L36 2	149	151	0.02	0.008536015
ybgI	GTP cyclohydrolase 1 type 2	76	77	0.02	0.008338447
yagT	Putative xanthine dehydrogenase YagT iron-sulfur-bin	79	80	0.02	0.005016093
nusG	Transcription termination/antitermination protein Nus	82	83	0.02	0.001424482
aroL	Shikimate kinase 2	83	84	0.02	0.001464602
atpI	ATP synthase protein I	85	86	0.02	0.001818407
cheW	Chemotaxis protein CheW	96	97	0.01	0.001465968
ybiA	N-glycosidase YbiA	99	100	0.01	0.001260273
osmB	Osmotically-inducible lipoprotein B	131	132	0.01	0.002475175
paaE	1,2-phenylacetyl-CoA epoxidase, subunit E	49	49	0.00	0.004530053
rlmA	23S rRNA (guanine(745)-N(1))-methyltransferase	30	30	0.00	0.005499913
ridA	2-iminobutanoate/2-iminopropanoate deaminase	86	86	0.00	0.002130752
ubiH	2-octaprenyl-6-methoxyphenol hydroxylase	35	35	0.00	0.002204131
fabH	3-oxoacyl-[acyl-carrier-protein] synthase 3	37	37	0.00	0.001353314
garL	5-keto-4-deoxy-D-glucarate aldolase	72	72	0.00	0.008181743
accD	Acetyl-coenzyme A carboxylase carboxyl transferase su	43	43	0.00	0.002189229
lsrC	Autoinducer 2 import system permease protein LsrC	37	37	0.00	0.00182305
wbbI	Beta-1,6-galactofuranosyltransferase WbbI	51	51	0.00	0.002860304
ftsB	Cell division protein FtsB	86	86	0.00	0.003767819
nrfB	Cytochrome c-type protein NrfB	49	49	0.00	0.003064393
fecC	Fe(3+) dicitrate transport system permease protein Fe	42	42	0.00	0.002148498
mglC	Galactoside transport system permease protein MglC	50	50	0.00	0.002204131
glnP	Glutamine transport system permease protein GlnP	76	76	0.00	0.002396158
ccmB	Heme exporter protein B	47	47	0.00	0.002246499
dmlR_2	HTH-type transcriptional regulator DmlR	55	55	0.00	0.002304076
hyfA_4	Hydrogenase-4 component A	74	74	0.00	0.002204131
ydcV_3	Inner membrane ABC transporter permease protein Yd	44	44	0.00	0.002024022
ytfT	Inner membrane ABC transporter permease protein Ytf	41	41	0.00	0.00288637
ynjF	Inner membrane protein YnjF	50	50	0.00	0.001708699
sdaA	L-serine dehydratase 1	35	35	0.00	0.002076254
mltD	Membrane-bound lytic murein transglycosylase D	44	44	0.00	0.006918588
nusB	N utilization substance protein B	74	74	0.00	0.002553147
ptsN	Nitrogen regulatory protein	67	67	0.00	0.002384009

abgA	p-aminobenzoyl-glutamate hydrolase subunit A	37	37	0.00	0.002006705
paaK	Phenylacetate-coenzyme A ligase	39	39	0.00	0.004272146
purN	Phosphoribosylglycinamide formyltransferase	67	67	0.00	0.002424747
proS_2	Proline--tRNA ligase	55	55	0.00	0.004128499
entH	Proofreading thioesterase EntH	85	85	0.00	0.002145651
arnE	putative 4-amino-4-deoxy-L-arabinose-phosphoundec	88	88	0.00	0.002681757
yfjZ_1	Putative antitoxin YfjZ	63	63	0.00	0.009239049
ddpD	putative D,D-dipeptide transport ATP-binding protein I	41	41	0.00	0.001888377
ybhK	Putative gluconeogenesis factor	55	55	0.00	0.001933662
yedA	putative inner membrane transporter YedA	52	52	0.00	0.00163494
rsuA	Ribosomal small subunit pseudouridine synthase A	52	52	0.00	0.002288507
rpoH	RNA polymerase sigma factor RpoH	68	68	0.00	0.009554086
sfaH_1	S-fimbrial protein subunit SfaH	56	56	0.00	0.002407969
gabD	Succinate-semialdehyde dehydrogenase [NADP(+)] Ga	28	28	0.00	0.002919648
setB	Sugar efflux transporter B	45	45	0.00	0.006308116
-	Ureidoglycolate lyase	51	51	0.00	0.002475175
yhaH	Inner membrane protein YhaH	104	103	-0.01	0.002671091
yphA	Inner membrane protein YphA	102	101	-0.01	0.002409402
arsC_3	Arsenate reductase	93	92	-0.02	0.002596062
gadE	Transcriptional regulator GadE	86	85	-0.02	0.002024022
rpe_2	Ribulose-phosphate 3-epimerase	85	84	-0.02	0.007162132
coaD	Phosphopantetheine adenylyltransferase	84	83	-0.02	0.003214594
rsmG	Ribosomal RNA small subunit methyltransferase G	83	82	-0.02	0.003669309
gspB	Putative general secretion pathway protein B	82	81	-0.02	0.002396158
leuE	Leucine efflux protein	78	77	-0.02	0.003214594
btuE	Thioredoxin/glutathione peroxidase BtuE	78	77	-0.02	0.002343148
ssuE	FMN reductase (NADPH)	77	76	-0.02	0.002660359
holC	DNA polymerase III subunit chi	74	73	-0.02	0.002514108
torR	TorCAD operon transcriptional regulatory protein TorR	72	71	-0.02	0.002640655
bcp	Putative peroxiredoxin bcp	71	70	-0.02	0.002553147
yedP	Mannosyl-3-phosphoglycerate phosphatase	68	67	-0.02	0.00917916
fdoG_2	Formate dehydrogenase-O major subunit	66	65	-0.02	0.002646865
ispD	2-C-methyl-D-erythritol 4-phosphate cytidylyltransfera	65	64	-0.02	0.00221742
chrR	Chromate reductase	63	62	-0.02	0.003243733
ecpA	Common pilus major fimbrillin subunit EcpA	63	62	-0.02	0.003477816
iscR	HTH-type transcriptional regulator IscR	63	62	-0.02	0.002956829
upp	Uracil phosphoribosyltransferase	62	61	-0.02	0.002672593
cpoB	Cell division coordinator CpoB	60	59	-0.02	0.002906626
ydcZ	Inner membrane protein YdcZ	60	59	-0.02	0.00571082
cdsA_2	Phosphatidate cytidylyltransferase	59	58	-0.02	0.004331716
ylaC	Inner membrane protein YlaC	58	57	-0.03	0.005409405
rluB	Ribosomal large subunit pseudouridine synthase B	58	57	-0.03	0.003718965

dppC	Dipeptide transport system permease protein DppC	57	56	-0.03	0.003575203
yijD	Inner membrane protein YijD	111	109	-0.03	0.002956829
epd	D-erythrose-4-phosphate dehydrogenase	54	53	-0.03	0.007316107
yebZ	Inner membrane protein YebZ	54	53	-0.03	0.002900517
yfiH	Laccase domain protein YfiH	54	53	-0.03	0.002978599
hycG_1	Formate hydrogenlyase subunit 7	52	51	-0.03	0.003214594
ydhX_2	putative ferredoxin-like protein YdhX	52	51	-0.03	0.003643144
pgl	6-phosphogluconolactonase	51	50	-0.03	0.004739469
ccmA	Cytochrome c biogenesis ATP-binding export protein C	51	50	-0.03	0.003591368
mukE	Chromosome partition protein MukE	49	48	-0.03	0.002982054
narL_2	Nitrate/nitrite response regulator protein NarL	48	47	-0.03	0.002470024
galM_1	Aldose 1-epimerase	47	46	-0.03	0.003187798
dhaK	PEP-dependent dihydroxyacetone kinase, dihydroxyac	47	46	-0.03	0.003131275
glsA2	Glutaminase 2	46	45	-0.03	0.002542997
ydjM	Inner membrane protein YdjM	46	45	-0.03	0.005467142
comR	HTH-type transcriptional repressor ComR	45	44	-0.03	0.003333841
astE	Succinylglutamate desuccinylase	45	44	-0.03	0.002330123
csgE	Curli production assembly/transport component CsgE	88	86	-0.03	0.003362395
cpdA	3',5'-cyclic adenosine monophosphate phosphodiester	42	41	-0.03	0.003244
potA_3	Spermidine/putrescine import ATP-binding protein Po	42	41	-0.03	0.003958979
sdhD	Succinate dehydrogenase hydrophobic membrane ancl	124	121	-0.04	0.002823913
gltA	Citrate synthase	41	40	-0.04	0.005928947
tusB	Protein TusB	121	118	-0.04	0.003618605
rsxA	Electron transport complex subunit RsxA	40	39	-0.04	0.00775142
plsX	Phosphate acyltransferase	40	39	-0.04	0.003479093
yagS	Putative xanthine dehydrogenase YagS FAD-binding su	40	39	-0.04	0.003811578
kdpE	KDP operon transcriptional regulatory protein KdpE	79	77	-0.04	0.006514863
msrQ	Protein-methionine-sulfoxide reductase heme-bindin	38	37	-0.04	0.009883211
alkA	DNA-3-methyladenine glycosylase 2	37	36	-0.04	0.002660301
yfcQ	putative fimbrial-like protein YfcQ	110	107	-0.04	0.007888488
tsaD	tRNA N6-adenosine threonylcarbamoyltransferase	36	35	-0.04	0.005557623
flhD	Flagellar transcriptional regulator FlhD	71	69	-0.04	0.008228753
cmoA	Carboxy-S-adenosyl-L-methionine synthase	35	34	-0.04	0.005867686
fliP	Flagellar biosynthetic protein FliP	35	34	-0.04	0.008361598
puuB	Gamma-glutamylputrescine oxidoreductase	35	34	-0.04	0.00303763
ybaN	Inner membrane protein YbaN	70	68	-0.04	0.007137669
mhpC_2	2-hydroxy-6-oxononadienedioate/2-hydroxy-6- oxono	138	134	-0.04	0.003363124
slmA	Nucleoid occlusion factor SlmA	69	67	-0.04	0.004227996
kanE	Alpha-D-kanosaminyltransferase	34	33	-0.04	0.003115512
hybE	Hydrogenase-2 operon protein HybE	101	98	-0.04	0.004000098
ubiE_3	Ubiquinone/menaquinone biosynthesis C-methyltrans	65	63	-0.05	0.002879301
ansA	L-asparaginase 1	32	31	-0.05	0.003131275

pgsA	CDP-diacylglycerol--glycerol-3-phosphate 3-phosphati	63	61	-0.05	0.003804555
ydcV_1	Inner membrane ABC transporter permease protein Yd	62	60	-0.05	0.006001885
yeiG	S-formylglutathione hydrolase YeiG	62	60	-0.05	0.004714399
argR	Arginine repressor	61	59	-0.05	0.004678709
cho	Excinuclease cho	30	29	-0.05	0.006818611
ydiB	Quinate/shikimate dehydrogenase	30	29	-0.05	0.009883211
cbpM	Chaperone modulatory protein CbpM	88	85	-0.05	0.007015017
gmhA	Phosphoheptose isomerase	57	55	-0.05	0.004050591
puuD	Gamma-glutamyl-gamma-aminobutyrate hydrolase Pu	56	54	-0.05	0.003657994
fliT	Flagellar protein FliT	83	80	-0.05	0.004669783
-	PKHD-type hydroxylase	80	77	-0.06	0.009545165
iaaA	Isoaspartyl peptidase	53	51	-0.06	0.006514863
hyaC	putative Ni/Fe-hydrogenase 1 B-type cytochrome subu	53	51	-0.06	0.004906624
tatB	Sec-independent protein translocase protein TatB	105	101	-0.06	0.009687352
dcd	dCTP deaminase	52	50	-0.06	0.003928836
rbsC_2	Ribose import permease protein RbsC	52	50	-0.06	0.006514863
yidG	Inner membrane protein YidG	129	124	-0.06	0.004128499
yghB	Inner membrane protein YghB	77	74	-0.06	0.005053588
astA	Arginine N-succinyltransferase	51	49	-0.06	0.007258485
fucA_1	L-fuculose phosphate aldolase	51	49	-0.06	0.003682137
yedK	Putative SOS response-associated peptidase YedK	74	71	-0.06	0.004511101
rnhB	Ribonuclease HII	73	70	-0.06	0.003813614
fdhF_2	Formate dehydrogenase H	72	69	-0.06	0.005680602
thiD	Hydroxymethylpyrimidine/phosphomethylpyrimidine	48	46	-0.06	0.004550738
sixA	Phosphohistidine phosphatase SixA	71	68	-0.06	0.005659652
yhdT	putative membrane protein YhdT	138	132	-0.06	0.004297457
znuC	Zinc import ATP-binding protein ZnuC	46	44	-0.06	0.005662171
hemR	Hemin receptor	135	129	-0.07	0.009998367
anmK	Anhydro-N-acetylmuramic acid kinase	44	42	-0.07	0.004903016
entB	Enterobactin synthase component B	44	42	-0.07	0.005227754
eco	Ecotin	109	104	-0.07	0.009239049
ydhP_2	Inner membrane transport protein YdhP	43	41	-0.07	0.005883569
ulaD_1	3-keto-L-gulonate-6-phosphate decarboxylase UlaD	42	40	-0.07	0.007580287
chuR_1	Anaerobic sulfatase-maturating enzyme	42	40	-0.07	0.00643132
purU	Formyltetrahydrofolate deformylase	42	40	-0.07	0.004392561
pyrF	Orotidine 5'-phosphate decarboxylase	63	60	-0.07	0.005699193
lrp	Leucine-responsive regulatory protein	62	59	-0.07	0.004388471
pilE1	Fimbrial protein	61	58	-0.07	0.007678568
-	D-psicose 3-epimerase	40	38	-0.07	0.006783278
eutD	Ethanolamine utilization protein EutD	40	38	-0.07	0.004550738
nikD	Nickel import ATP-binding protein NikD	60	57	-0.07	0.004359372
rnc	Ribonuclease 3	59	56	-0.08	0.00542009

cusB	Cation efflux system protein CusB	39	37	-0.08	0.007107342
bdcA	Cyclic-di-GMP-binding biofilm dispersal mediator prot	39	37	-0.08	0.006563971
yfhL	putative ferredoxin-like protein YfhL	115	109	-0.08	0.006481108
murQ	N-acetylmuramic acid 6-phosphate etherase	57	54	-0.08	0.00917916
thiK	Thiamine kinase	38	36	-0.08	0.007007929
yhbY	RNA-binding protein YhbY	169	160	-0.08	0.006707443
yqaA	Inner membrane protein YqaA	75	71	-0.08	0.005867686
rluA	Ribosomal large subunit pseudouridine synthase A	75	71	-0.08	0.006563971
artM_2	Arginine transport ATP-binding protein ArtM	37	35	-0.08	0.009317132
hcaR_1	Hca operon transcriptional activator HcaR	37	35	-0.08	0.00616181
ydgI	Putative arginine/ornithine antiporter	37	35	-0.08	0.006778713
araC	Arabinose operon regulatory protein	55	52	-0.08	0.005888955
plsY	putative glycerol-3-phosphate acyltransferase	55	52	-0.08	0.005414601
ccmE	Cytochrome c-type biogenesis protein CcmE	91	86	-0.08	0.005105159
sfaG_2	S-fimbrial protein subunit SfaG	54	51	-0.08	0.008811662
lpxH	UDP-2,3-diacylglucosamine hydrolase	53	50	-0.08	0.00509857
rsmE	Ribosomal RNA small subunit methyltransferase E	69	65	-0.09	0.007703327
yccX	Acylphosphatase	102	96	-0.09	0.0087193
flgD	Basal-body rod modification protein FlgD	68	64	-0.09	0.004936569
araD	L-ribulose-5-phosphate 4-epimerase AraD	51	48	-0.09	0.006645123
ynhG	putative L,D-transpeptidase YnhG	34	32	-0.09	0.007693049
pcm	Protein-L-isoaspartate O-methyltransferase	67	63	-0.09	0.006392553
yigZ	IMPACT family member YigZ	50	47	-0.09	0.006653305
amiD	N-acetylmuramoyl-L-alanine amidase AmiD	50	47	-0.09	0.005501196
hycG_2	Formate hydrogenlyase subunit 7	66	62	-0.09	0.007703327
hisD	Histidinol dehydrogenase	33	31	-0.09	0.004016565
pntA	NAD(P) transhydrogenase subunit alpha	33	31	-0.09	0.005878845
yciK	putative oxidoreductase YciK	49	46	-0.09	0.005666202
cutA	Divalent-cation tolerance protein CutA	114	107	-0.09	0.007015017
eutS	Ethanolamine utilization protein EutS	97	91	-0.09	0.005864597
csgA	Major curlin subunit	97	91	-0.09	0.005666599
ispF	2-C-methyl-D-erythritol 2,4-cyclodiphosphate synthase	64	60	-0.09	0.007899281
cutC_2	Copper homeostasis protein CutC	48	45	-0.09	0.007997838
yqjI	Transcriptional regulator YqjI	80	75	-0.09	0.00685639
artQ	Arginine ABC transporter permease protein ArtQ	63	59	-0.09	0.007150584
tauB	Taurine import ATP-binding protein TauB	63	59	-0.09	0.006309221
zipA	Cell division protein ZipA	31	29	-0.10	0.005410236
fcl	GDP-L-fucose synthase	31	29	-0.10	0.005291432
lolA	Outer-membrane lipoprotein carrier protein	77	72	-0.10	0.005826059
lolD_1	Lipoprotein-releasing system ATP-binding protein LolD	46	43	-0.10	0.00612315
lsrR	Transcriptional regulator LsrR	46	43	-0.10	0.006715839
ykgM	50S ribosomal protein L31 type B	167	156	-0.10	0.005862629

arcC2_1	Carbamate kinase 2	45	42	-0.10	0.005878845
ybiS	putative L,D-transpeptidase YbiS	45	42	-0.10	0.006258809
narI	Respiratory nitrate reductase 1 gamma chain	45	42	-0.10	0.007107342
satP	Succinate-acetate/proton symporter SatP	90	84	-0.10	0.009239049
rcsF	Outer membrane lipoprotein RcsF	89	83	-0.10	0.007621338
can	Carbonic anhydrase 2	74	69	-0.10	0.007150584
ycjP	Inner membrane ABC transporter permease protein Yc	59	55	-0.10	0.008140862
mutH	DNA mismatch repair protein MutH	58	54	-0.10	0.006653305
fliS	Flagellar protein FliS	114	106	-0.10	0.006514863
arsC_1	Arsenate reductase	83	77	-0.11	0.009517873
queC	7-cyano-7-deazaguanine synthase	55	51	-0.11	0.007194735
phoB	Phosphate regulon transcriptional regulatory protein P	55	51	-0.11	0.007560921
dut	Deoxyuridine 5'-triphosphate nucleotidohydrolase	96	89	-0.11	0.006818611
pspF	Psp operon transcriptional activator	41	38	-0.11	0.008351352
yiaW_1	Inner membrane protein YiaW	95	88	-0.11	0.00863779
ycjO	Inner membrane ABC transporter permease protein Yc	54	50	-0.11	0.006178877
maa	Maltose O-acetyltransferase	81	75	-0.11	0.006653305
truD	tRNA pseudouridine synthase D	40	37	-0.11	0.008192656
lexA_2	LexA repressor	93	86	-0.11	0.008841181
nfsA	Oxygen-insensitive NADPH nitroreductase	53	49	-0.11	0.007885332
fdnH_1	Formate dehydrogenase, nitrate-inducible, iron-sulfur	39	36	-0.12	0.007678568
hisC	Histidinol-phosphate aminotransferase	39	36	-0.12	0.00917916
cof	HMP-PP phosphatase	52	48	-0.12	0.007566646
yhdE	Maf-like protein YhdE	65	60	-0.12	0.008841181
crcB	Putative fluoride ion transporter CrcB	77	71	-0.12	0.009239049
yohD	Inner membrane protein YohD	64	59	-0.12	0.009573798
rihC	Non-specific ribonucleoside hydrolase RihC	51	47	-0.12	0.008178625
yjjP_2	Inner membrane protein YjjP	89	82	-0.12	0.008826285
nimR	HTH-type transcriptional regulator NimR	38	35	-0.12	0.007678568
deoR_1	Deoxyribose operon repressor	63	58	-0.12	0.009274723
puuR	HTH-type transcriptional regulator PuuR	63	58	-0.12	0.008338447
soxR	Redox-sensitive transcriptional activator SoxR	87	80	-0.12	0.00905589
nsrR	HTH-type transcriptional repressor NsrR	85	78	-0.12	0.009484737
carE	Caffeyl-CoA reductase-Etf complex subunit CarE	36	33	-0.13	0.008126328
dapF	Diaminopimelate epimerase	60	55	-0.13	0.00863779
purR_2	HTH-type transcriptional repressor PurR	36	33	-0.13	0.007008938
hycI	Hydrogenase 3 maturation protease	72	66	-0.13	0.009916411
lpxD_2	UDP-3-O-(3-hydroxymyristoyl)glucosamine N-acyltrans	107	98	-0.13	0.00929694
gmhB	D-glycero-beta-D-manno-heptose-1,7-bisphosphate 7-	81	74	-0.13	0.00813931
ydaF	Putative ribosomal N-acetyltransferase YdaF	69	63	-0.13	0.009949508
atoA	Acetate CoA-transferase subunit beta	57	52	-0.13	0.009713416
tqsA_1	AI-2 transport protein TqsA	34	31	-0.13	0.008013616

mukF	Chromosome partition protein MukF	34	31	-0.13	0.00863779
rlmB_1	23S rRNA (guanosine-2'-O-)-methyltransferase RlmB	45	41	-0.13	0.009078651
mcbR	HTH-type transcriptional regulator McbR	45	41	-0.13	0.009900032
mhpD	2-keto-4-pentenoate hydratase	56	51	-0.13	0.008384258
cysC	Adenylyl-sulfate kinase	56	51	-0.13	0.009545165
ftsL	Cell division protein FtsL	89	81	-0.14	0.0099533
mzrA_2	Modulator protein MzrA	120	109	-0.14	0.009902035
ygdR_1	putative lipoprotein YgdR	201	182	-0.14	0.009787005
fliM	Flagellar motor switch protein FliM	42	38	-0.14	0.009483819
xynB	Beta-xylosidase	31	28	-0.15	0.009565168
cysA_2	Sulfate/thiosulfate import ATP-binding protein CysA	39	35	-0.16	0.009573798

Appendix 2

Appendix 2.1 - EDTA growth curve data

Control (-) and 0.08 mM EDTA (+) exposure at approx. 0.2 A_{650nm} of *WT E. coli* with monitoring every 30 minutes for 16 hours.

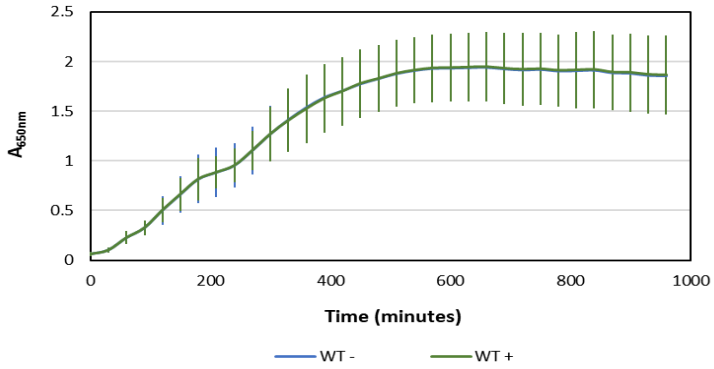

Control (-) and 0.08 mM EDTA (+) exposure at approx. 0.2 A_{650nm} of *ΔrecA E. coli* with monitoring every 30 minutes for 16 hours.

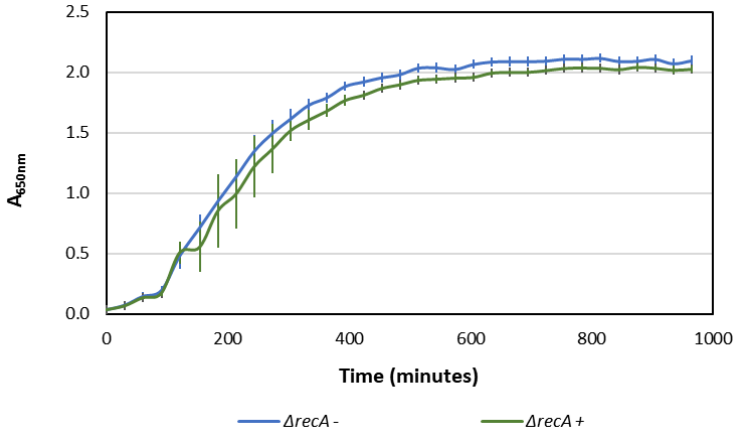

Control (-) and 0.08 mM EDTA (+) exposure at approx. 0.2 A_{650nm} of *ΔrecB E. coli* with monitoring every 30 minutes for 16 hours.

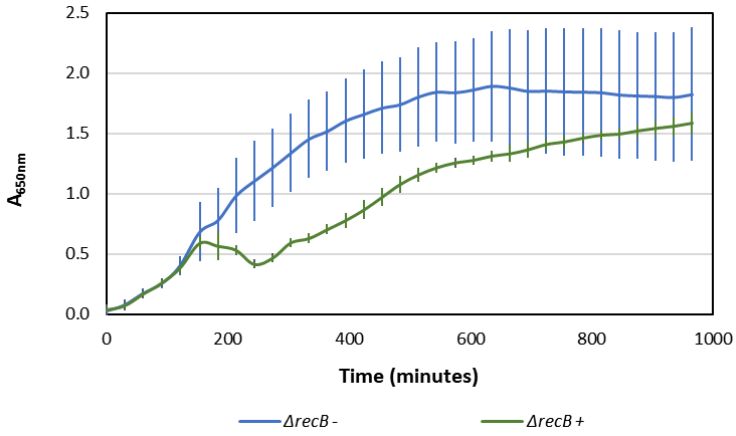

Control (-) and 0.08 mM EDTA (+) exposure at approx. 0.2 A_{650nm} of *ΔrecF E. coli* with monitoring every 30 minutes for 16 hours.

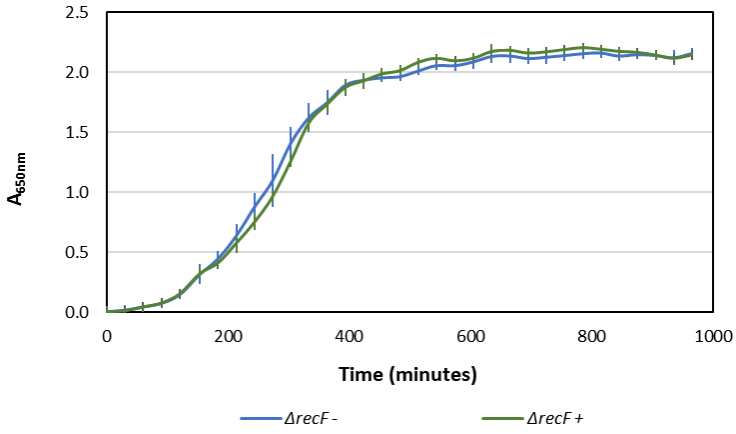

Control (-) and 0.08 mM EDTA (+) exposure at approx. 0.2 A_{650nm} of *ΔrecJ E. coli* with monitoring every 30 minutes for 16 hours.

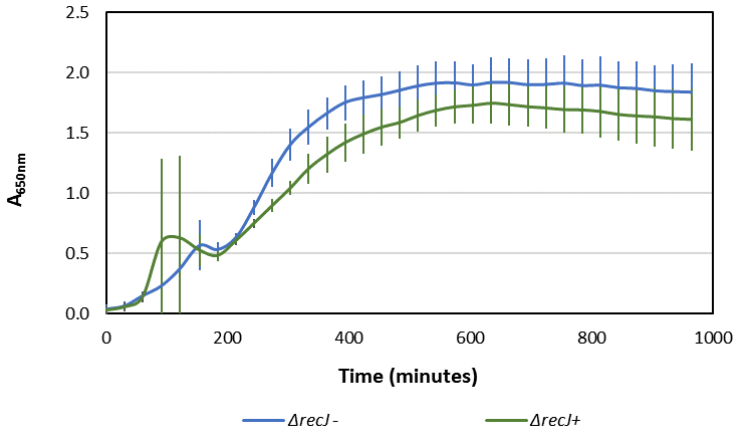

Control (-) and 0.08 mM EDTA (+) exposure at approx. 0.2 A_{650nm} of *ΔrecN E. coli* with monitoring every 30 minutes for 16 hours.

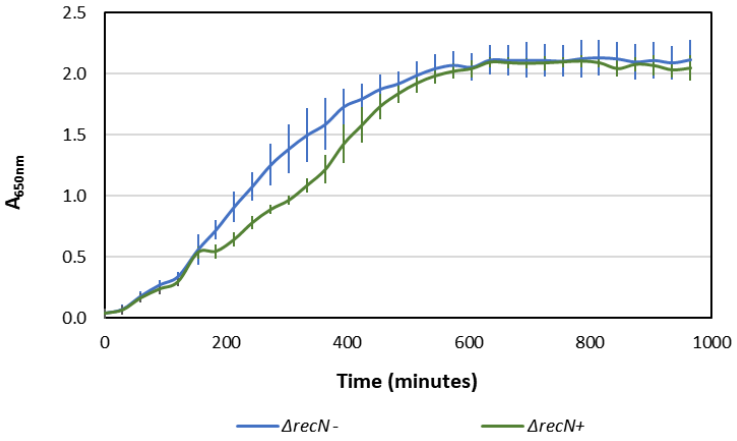

Control (-) and 0.08 mM EDTA (+) exposure at approx. 0.2 A_{650nm} of *ΔrecQ E. coli* with monitoring every 30 minutes for 16 hours.

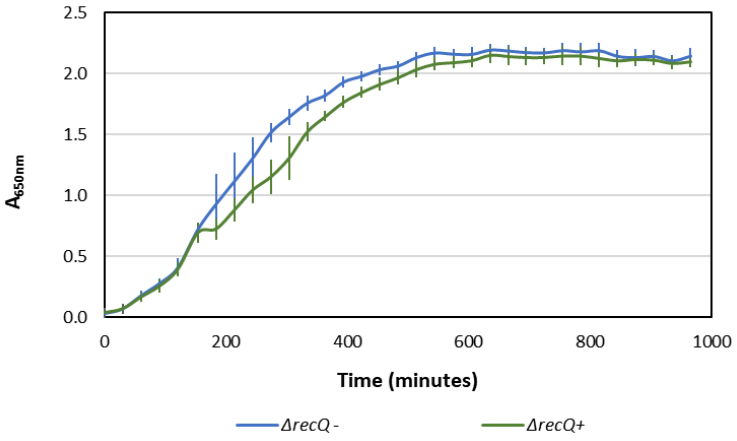

Control (-) and 0.08 mM EDTA (+) exposure at approx. 0.2 A_{650nm} of *ΔruvA E. coli* with monitoring every 30 minutes for 16 hours.

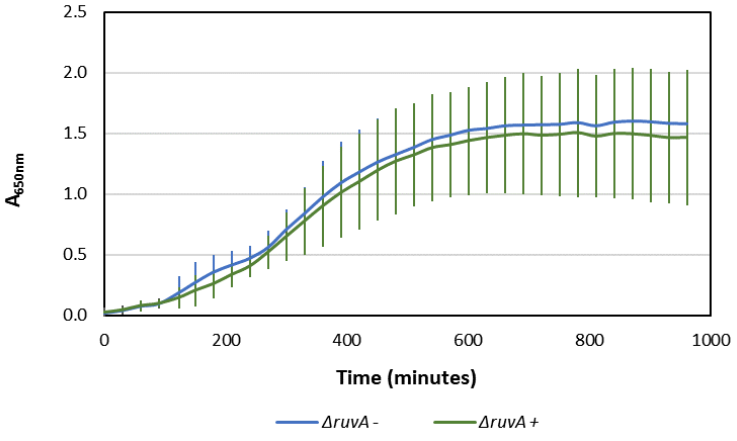

Control (-) and 0.08 mM EDTA (+) exposure at approx. 0.2 A_{650nm} of *ΔruvB E. coli* with monitoring every 30 minutes for 16 hours.

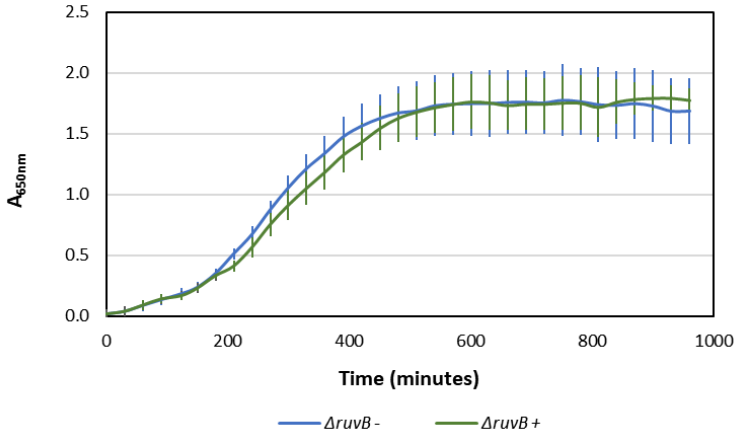

Control (-) and 0.08 mM EDTA (+) exposure at approx. 0.2 A_{650nm} of *ΔruvC E. coli* with monitoring every 30 minutes for 16 hours.

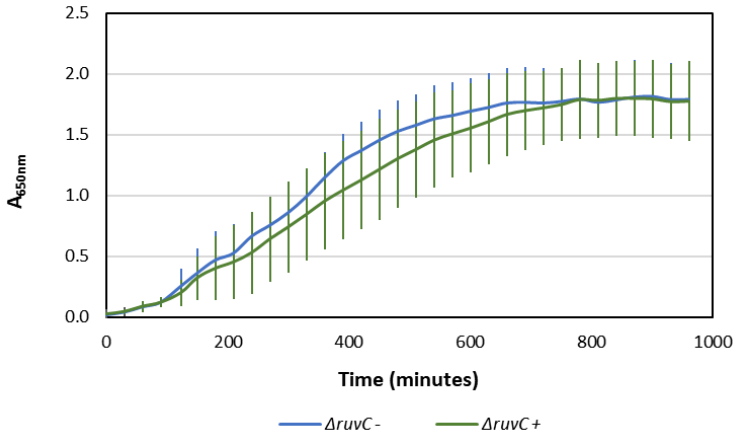

Control (-) and 0.08 mM EDTA (+) exposure at approx. 0.2 A_{650nm} of *ΔuvrA E. coli* with monitoring every 30 minutes for 16 hours.

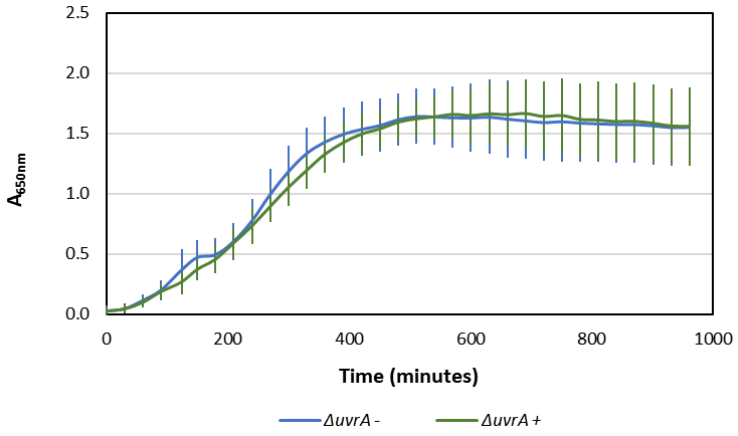

Control (-) and 0.08 mM EDTA (+) exposure at approx. 0.2 A_{650nm} of *ΔuvrC E. coli* with monitoring every 30 minutes for 16 hours.

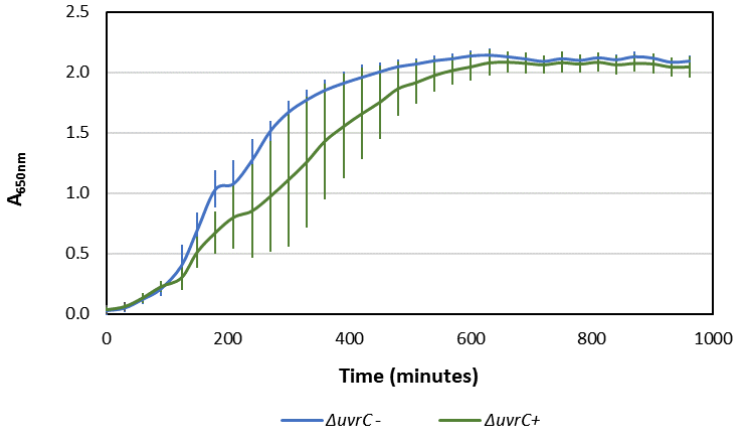

Control (-) and 0.08 mM EDTA (+) exposure at approx. 0.2 A_{650nm} of *ΔmutM E. coli* with monitoring every 30 minutes for 16 hours.

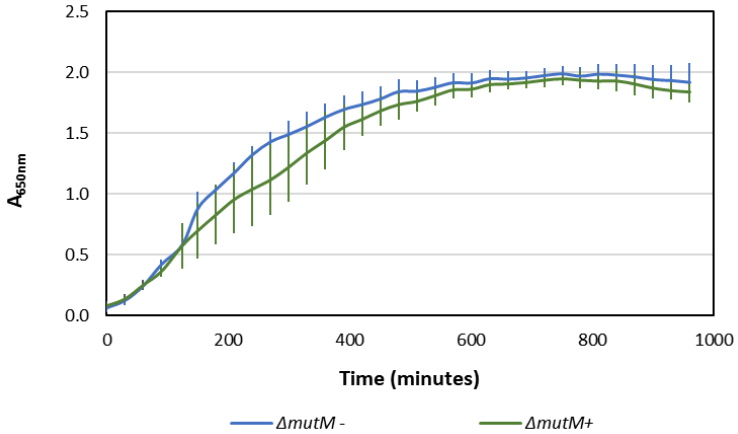

Control (-) and 0.08 mM EDTA (+) exposure at approx. 0.2 A_{650nm} of *ΔmutT E. coli* with monitoring every 30 minutes for 16 hours.

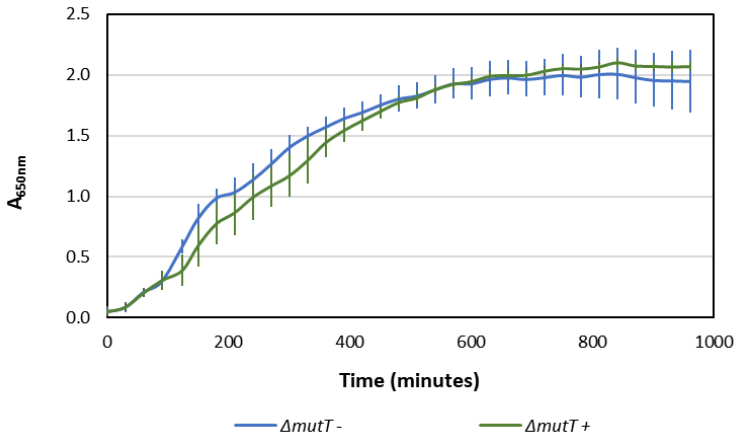

Control (-) and 0.08 mM EDTA (+) exposure at approx. 0.2 A_{650nm} of *ΔmutY E. coli* with monitoring every 30 minutes for 16 hours.

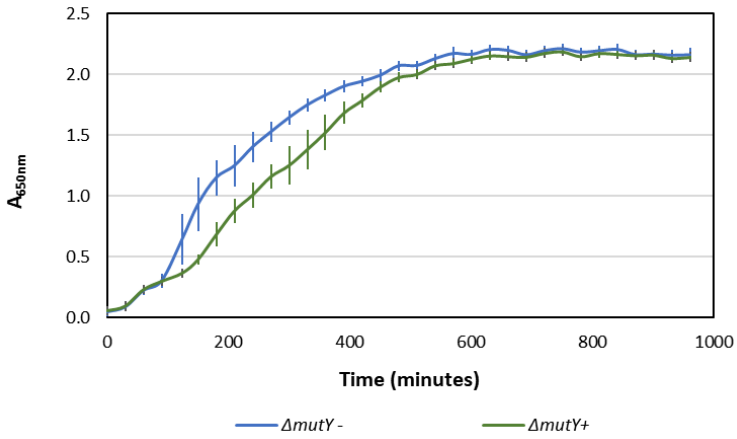

Control (-) and 0.08 mM EDTA (+) exposure at approx. 0.2 A_{650nm} of *Δnth E. coli* with monitoring every 30 minutes for 16 hours.

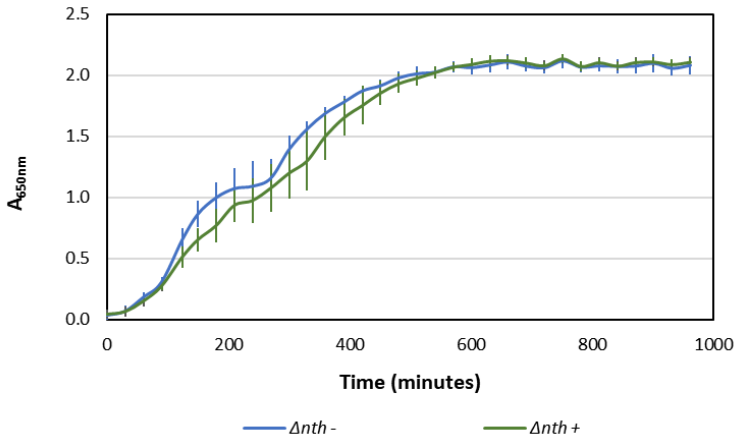

Control (-) and 0.08 mM EDTA (+) exposure at approx. 0.2 A_{650nm} of *Δmfd E. coli* with monitoring every 30 minutes for 16 hours.

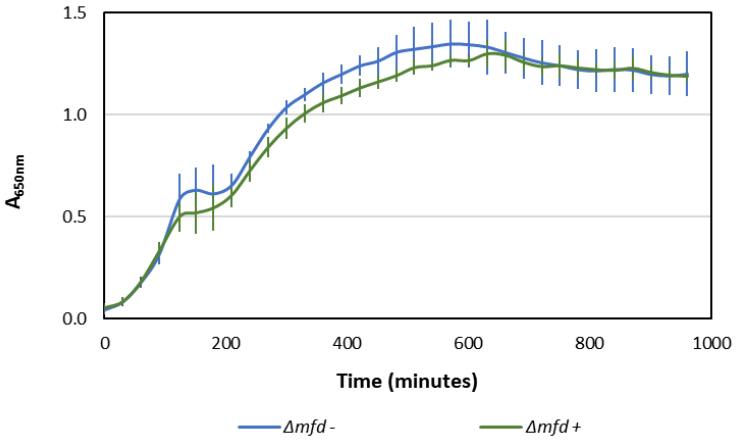

Control (-) and 0.08 mM EDTA (+) exposure at approx. 0.2 A_{650nm} of *ΔsbcB E. coli* with monitoring every 30 minutes for 16 hours.

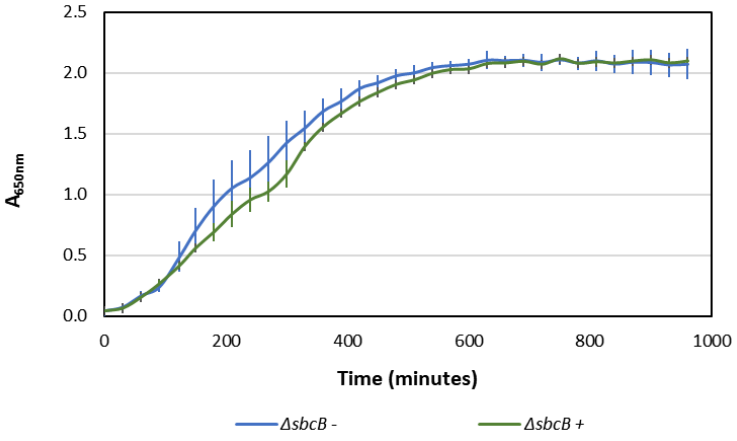

Control (-) and 0.08 mM EDTA (+) exposure at approx. 0.2 A_{650nm} of *ΔahpC E. coli* with monitoring every 30 minutes for 16 hours.

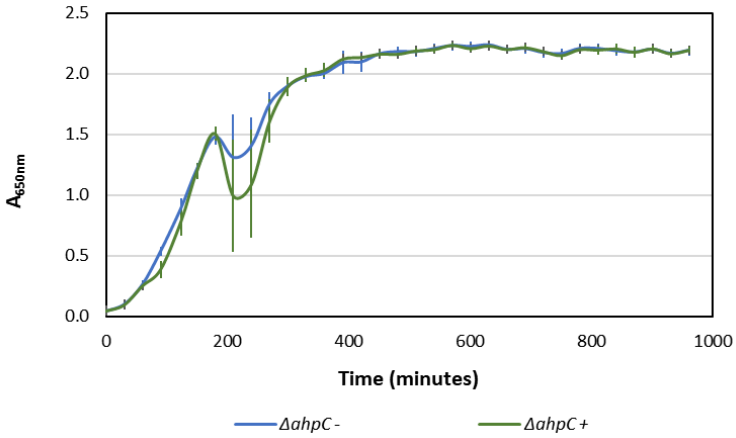

Control (-) and 0.08 mM EDTA (+) exposure at approx. 0.2 A_{650nm} of *ΔkatG E. coli* with monitoring every 30 minutes for 16 hours.

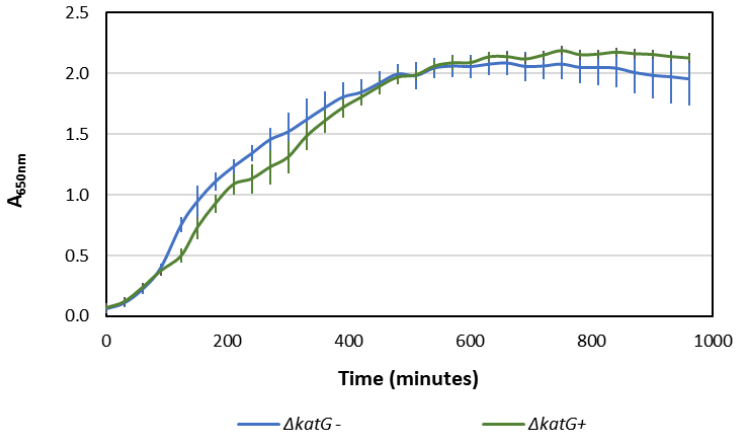

Control (-) and 0.08 mM EDTA (+) exposure at approx. 0.2 A_{650nm} of *ΔsodA E. coli* with monitoring every 30 minutes for 16 hours.

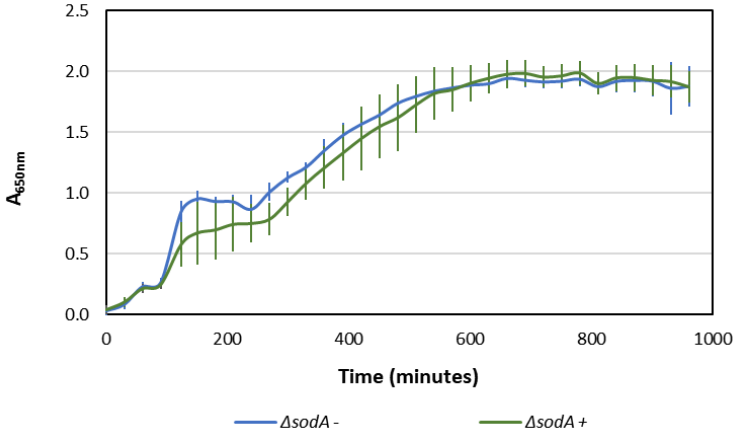

Control (-) and 0.08 mM EDTA (+) exposure at approx. 0.2 A_{650nm} of *ΔsodB E. coli* with monitoring every 30 minutes for 16 hours.

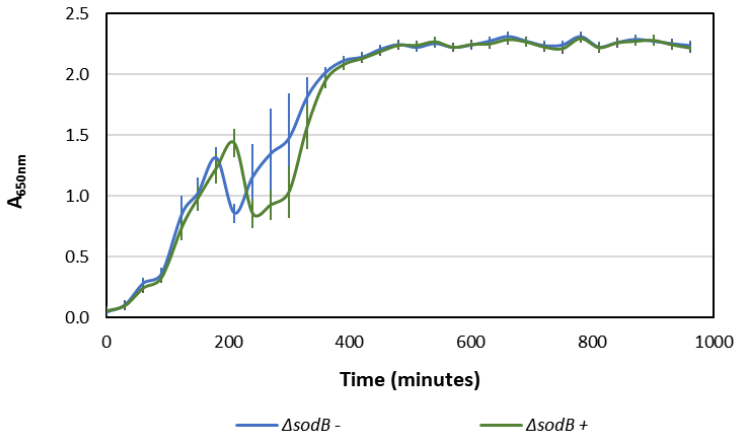

Control (-) and 0.08 mM EDTA (+) exposure at approx. 0.2 A_{650nm} of *ΔsodC E. coli* with monitoring every 30 minutes for 16 hours.

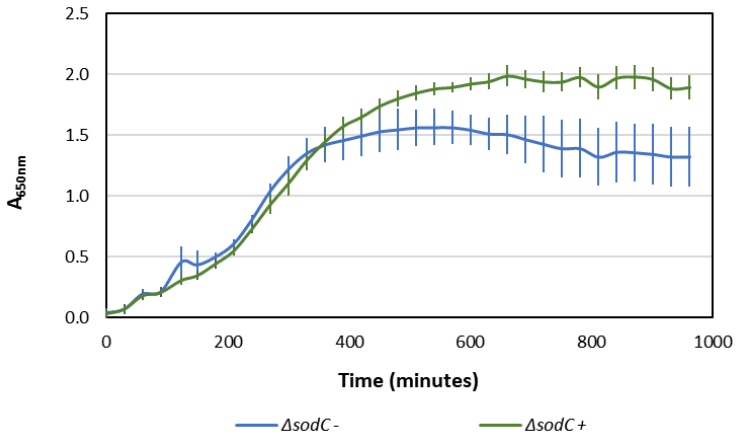

Control (-) and 0.08 mM EDTA (+) exposure at approx. 0.2 A_{650nm} of *ΔfepA E. coli* with monitoring every 30 minutes for 16 hours.

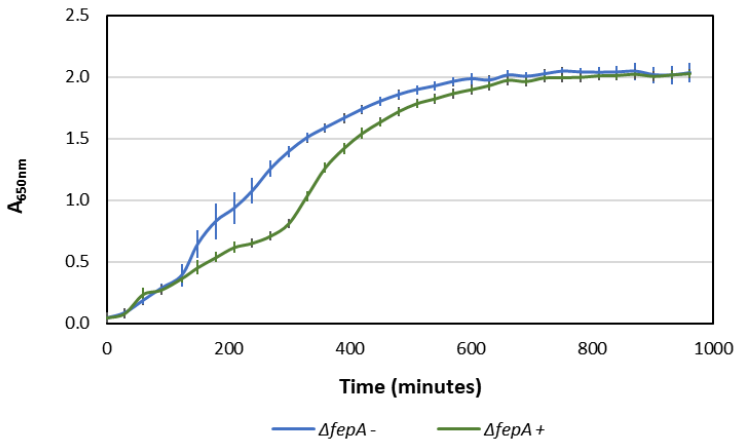

Control (-) and 0.08 mM EDTA (+) exposure at approx. 0.2 A_{650nm} of *ΔfeoB E. coli* with monitoring every 30 minutes for 16 hours.

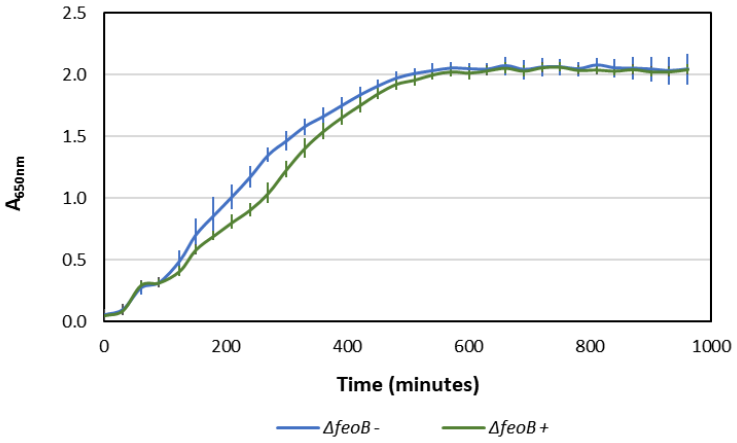

Control (-) and 0.08 mM EDTA (+) exposure at approx. 0.2 A_{650nm} of *Δftn E. coli* with monitoring every 30 minutes for 16 hours.

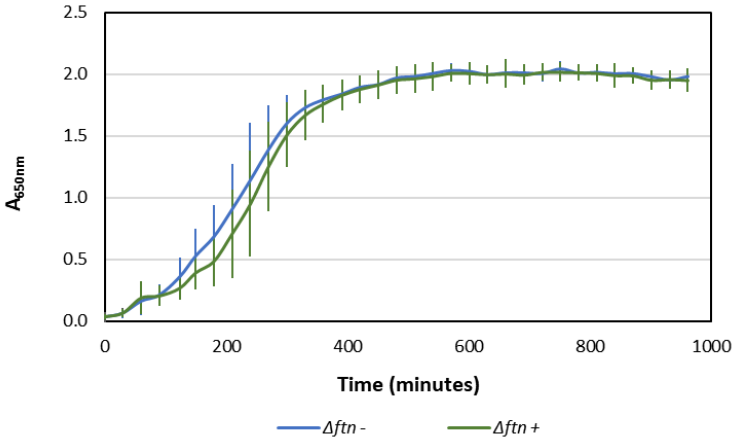

Control (-) and 0.08 mM EDTA (+) exposure at approx. 0.2 A_{650nm} of *Δfur E. coli* with monitoring every 30 minutes for 16 hours.

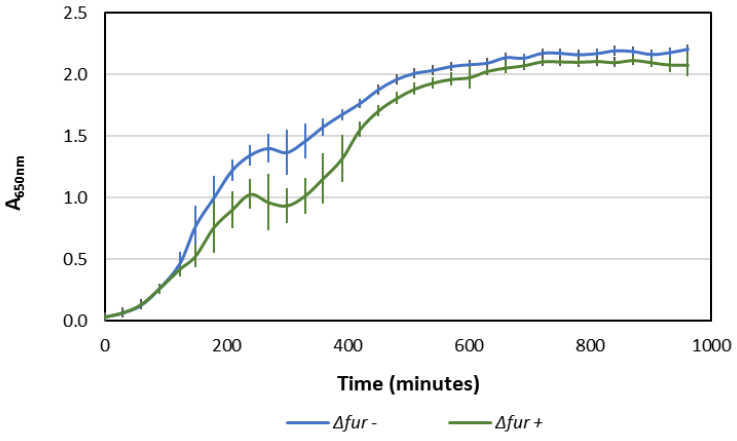

Control (-) and 0.08 mM EDTA (+) exposure at approx. 0.2 A_{650nm} of *ΔmntH E. coli* with monitoring every 30 minutes for 16 hours.

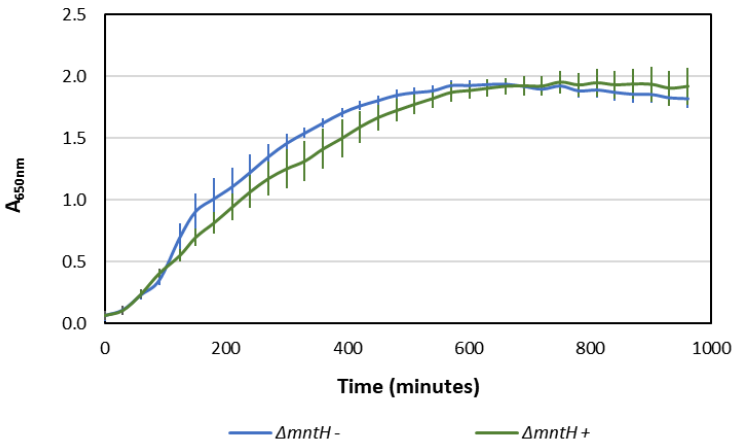

Control (-) and 0.08 mM EDTA (+) exposure at approx. 0.2 A_{650nm} of *ΔcopA E. coli* with monitoring every 30 minutes for 16 hours.

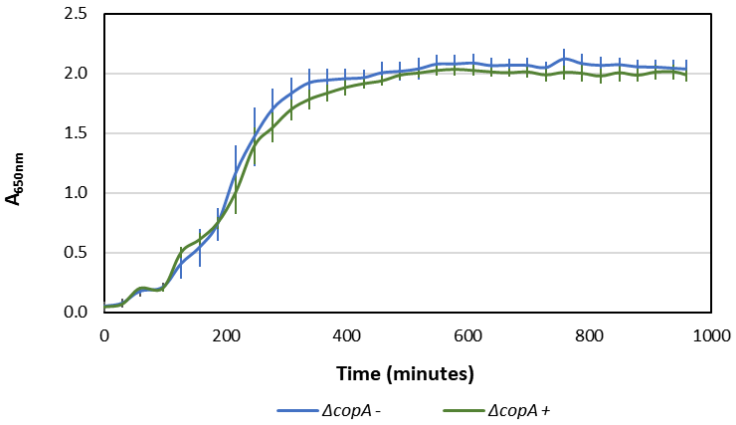

Control (-) and 0.08 mM EDTA (+) exposure at approx. 0.2 A_{650nm} of *ΔcueR E. coli* with monitoring every 30 minutes for 16 hours.

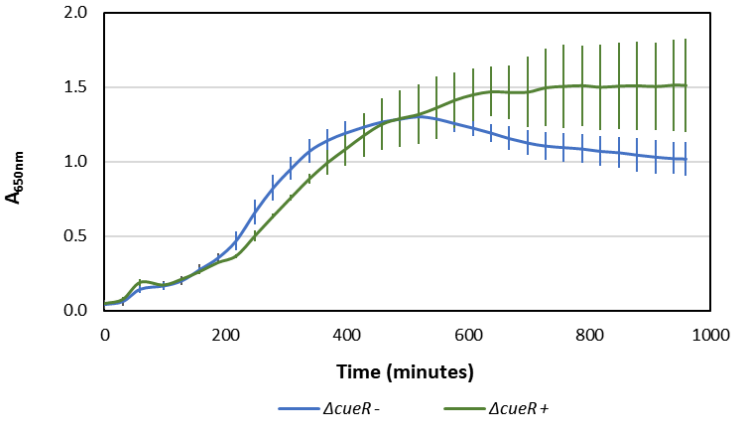

Control (-) and 0.08 mM EDTA (+) exposure at approx. 0.2 A_{650nm} of *ΔcueO E. coli* with monitoring every 30 minutes for 16 hours.

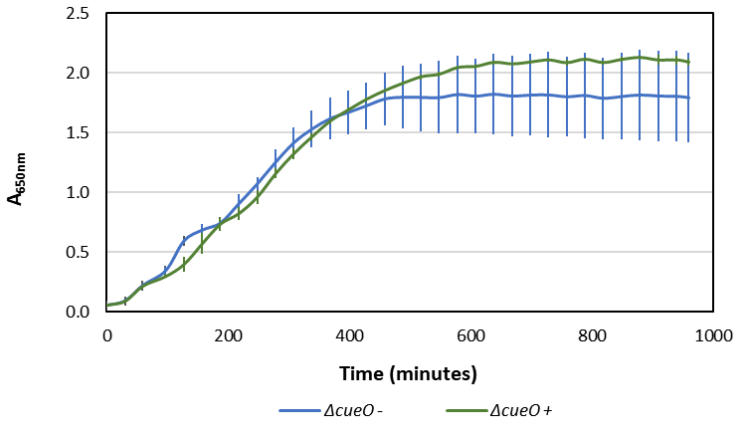

Control (-) and 0.08 mM EDTA (+) exposure at approx. 0.2 A_{650nm} of *ΔcusR E. coli* with monitoring every 30 minutes for 16 hours.

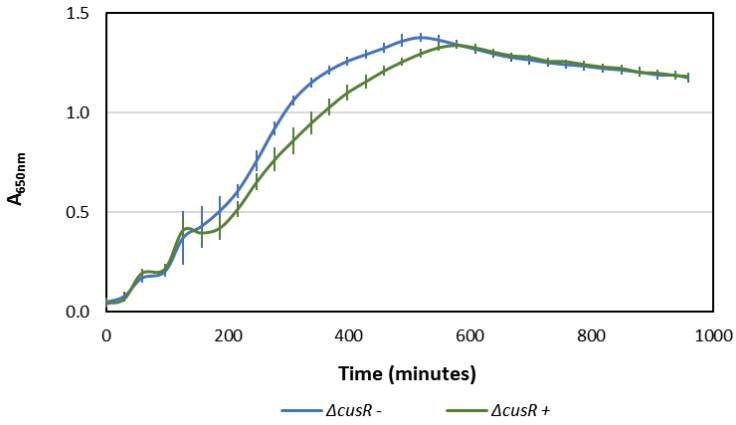

Control (-) and 0.08 mM EDTA (+) exposure at approx. 0.2 A_{650nm} of *ΔcorA E. coli* with monitoring every 30 minutes for 16 hours.

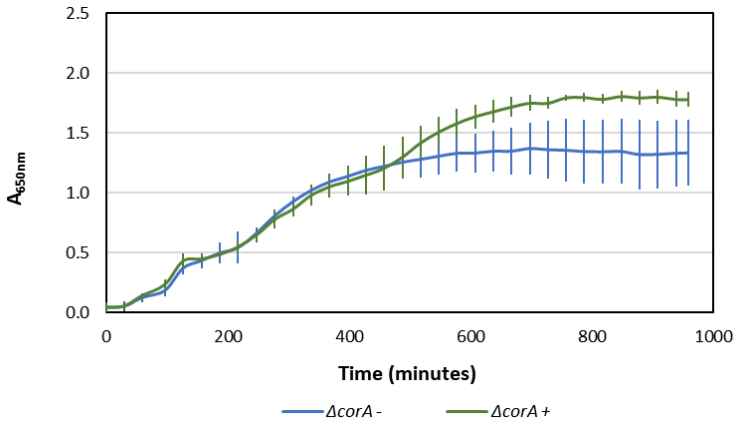

Control (-) and 0.08 mM EDTA (+) exposure at approx. 0.2 A_{650nm} of *ΔnikA E. coli* with monitoring every 30 minutes for 16 hours.

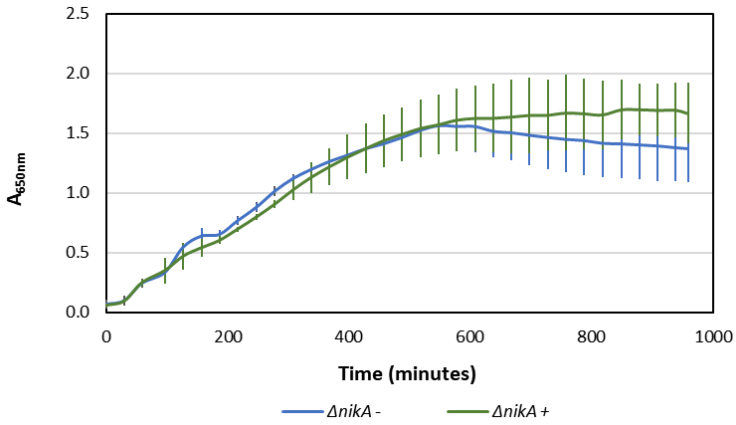

Control (-) and 0.08 mM EDTA (+) exposure at approx. 0.2 A_{650nm} of *ΔnikR E. coli* with monitoring every 30 minutes for 16 hours.

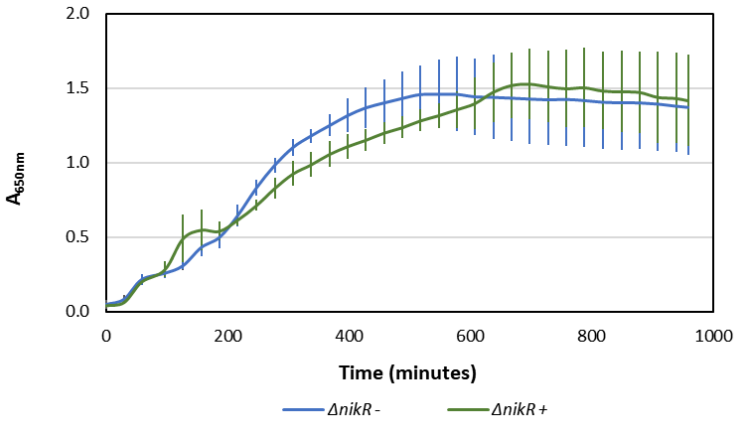

Control (-) and 0.08 mM EDTA (+) exposure at approx. 0.2 A_{650nm} of *ΔrcnB E. coli* with monitoring every 30 minutes for 16 hours.

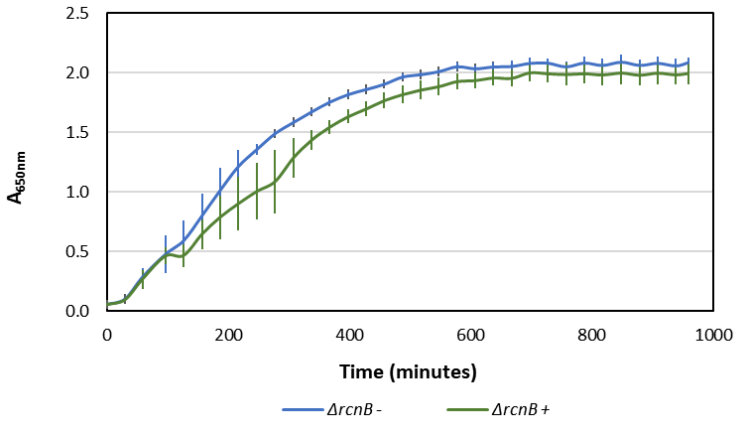

Control (-) and 0.08 mM EDTA (+) exposure at approx. 0.2 A_{650nm} of *ΔzntR E. coli* with monitoring every 30 minutes for 16 hours.

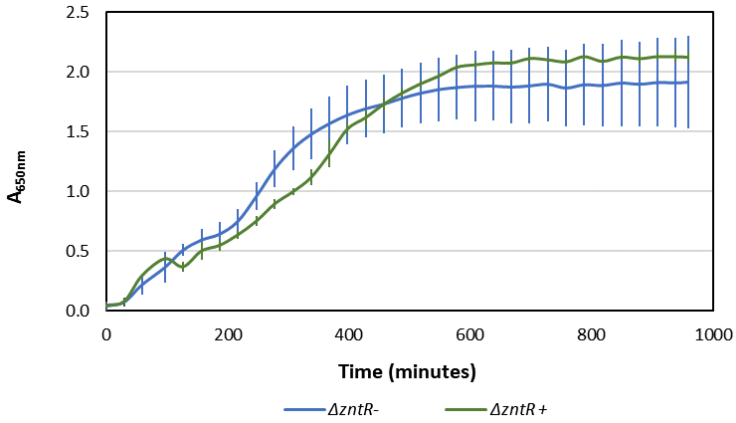

Control (-) and 0.08 mM EDTA (+) exposure at approx. 0.2 A_{650nm} of *ΔgshA E. coli* with monitoring every 30 minutes for 16 hours.

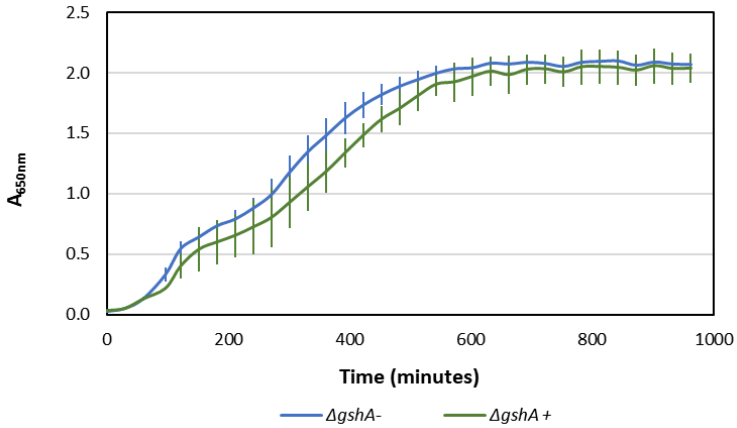

Control (-) and 0.08 mM EDTA (+) exposure at approx. 0.2 A_{650nm} of *ΔhybD E. coli* with monitoring every 30 minutes for 16 hours.

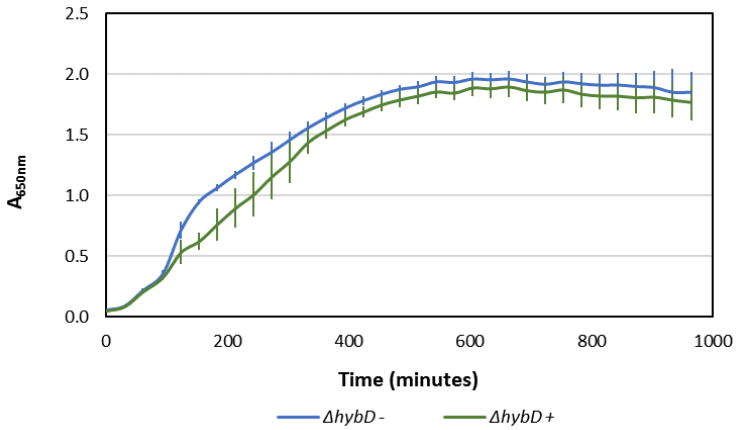

Control (-) and 0.08 mM EDTA (+) exposure at approx. 0.2 A_{650nm} of *ΔhybF E. coli* with monitoring every 30 minutes for 16 hours.

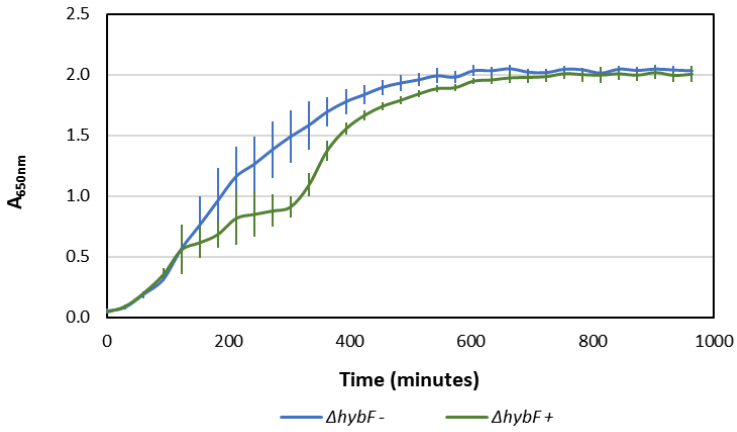

Control (-) and 0.08 mM EDTA (+) exposure at approx. 0.2 A_{650nm} of *ΔhycI E. coli* with monitoring every 30 minutes for 16 hours.

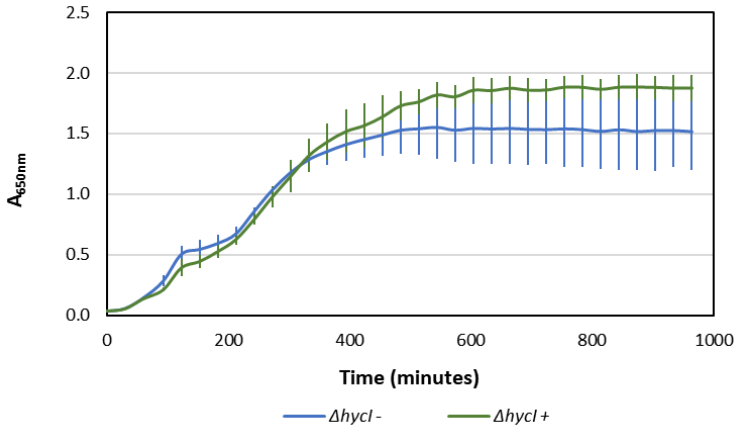

Control (-) and 0.08 mM EDTA (+) exposure at approx. 0.2 A_{650nm} of *ΔslyD E. coli* with monitoring every 30 minutes for 16 hours.

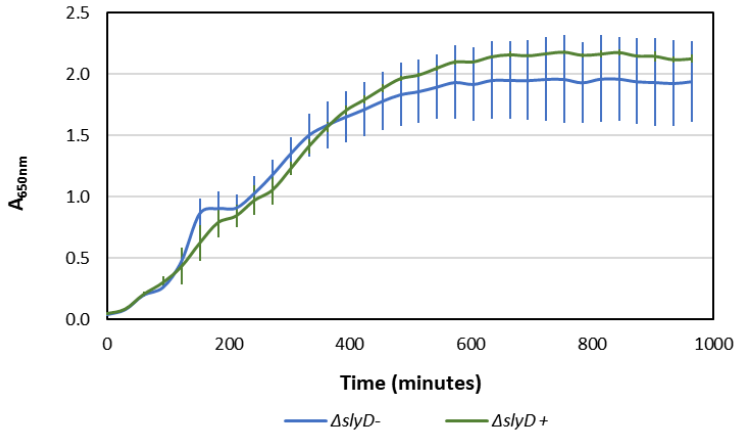

Control (-) and 0.08 mM EDTA (+) exposure at approx. 0.2 A_{650nm} of *ΔcpxA E. coli* with monitoring every 30 minutes for 16 hours.

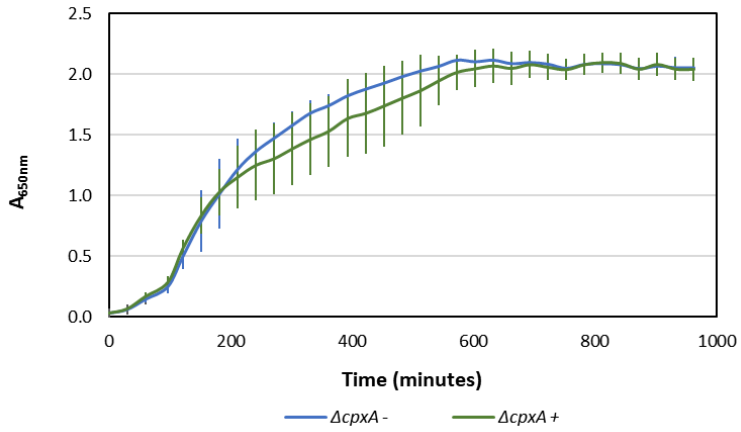

Control (-) and 0.08 mM EDTA (+) exposure at approx. 0.2 A_{650nm} of *ΔcpxR E. coli* with monitoring every 30 minutes for 16 hours.

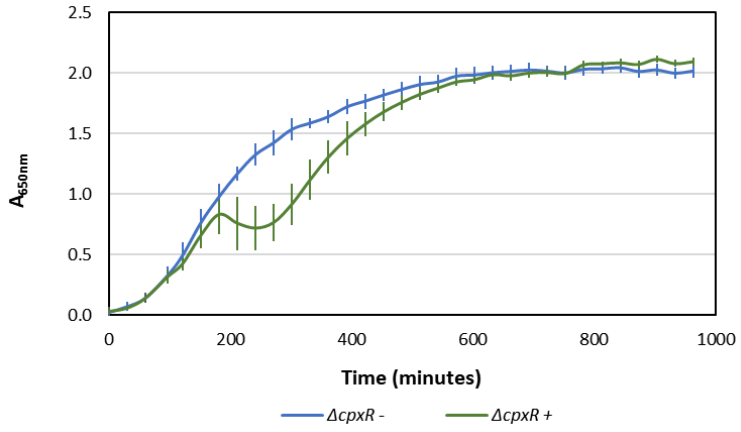

Control (-) and 0.08 mM EDTA (+) exposure at approx. 0.2 A_{650nm} of *ΔcpxP E. coli* with monitoring every 30 minutes for 16 hours.

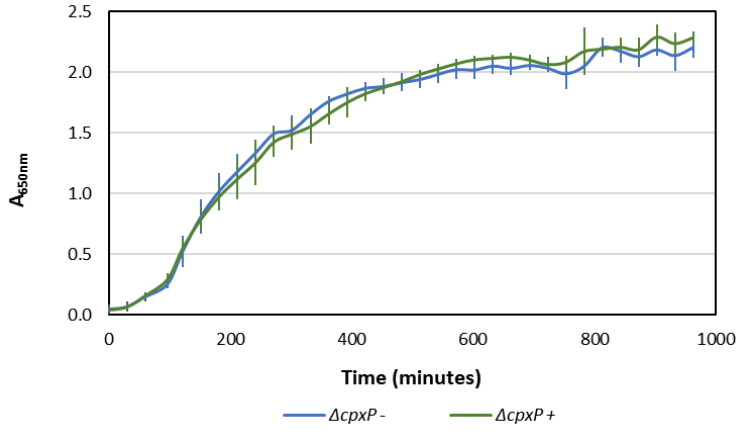

Control (-) and 0.08 mM EDTA (+) exposure at approx. 0.2 A_{650nm} of *ΔdsbA E. coli* with monitoring every 30 minutes for 16 hours.

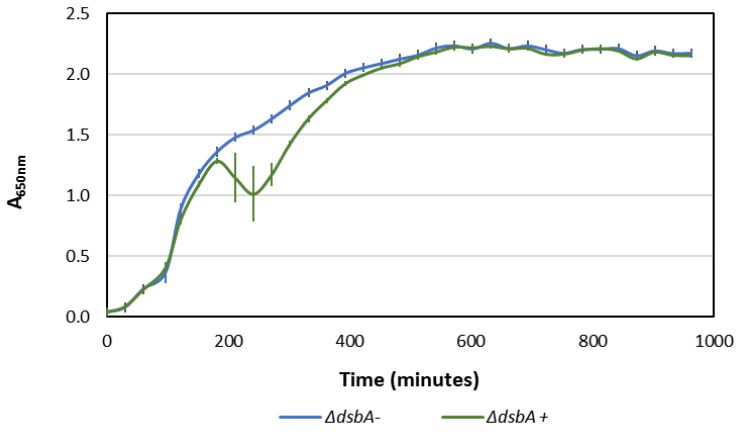

Appendix 2.2 - DTPMP growth curve data

Control (-) and 0.05 mM DTPMP (+) exposure at approx. 0.2 A_{650nm} of *WT E. coli* with monitoring every 30 minutes for 16 hours.

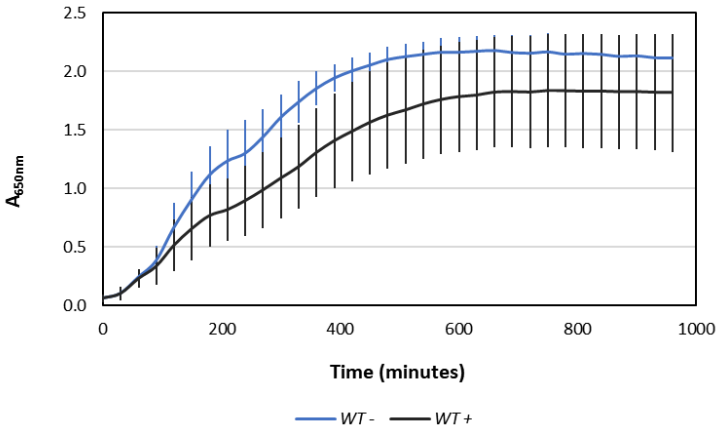

Control (-) and 0.05 mM DTPMP (+) exposure at approx. 0.2 A_{650nm} of *ΔrecA E. coli* with monitoring every 30 minutes for 16 hours.

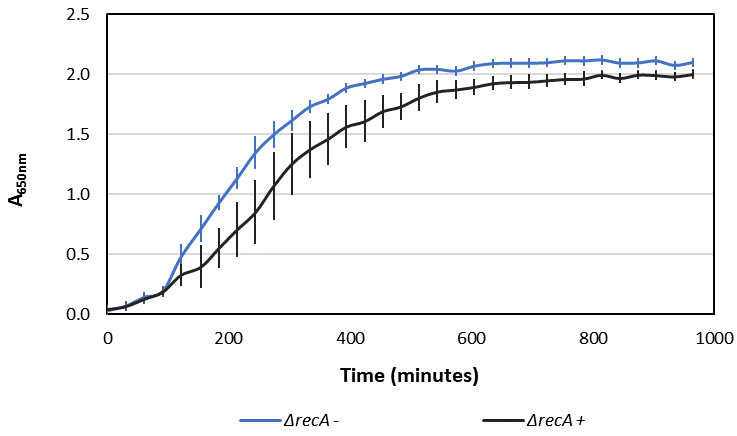

Control (-) and 0.05 mM DTPMP (+) exposure at approx. 0.2 A_{650nm} of *ΔrecB E. coli* with monitoring every 30 minutes for 16 hours.

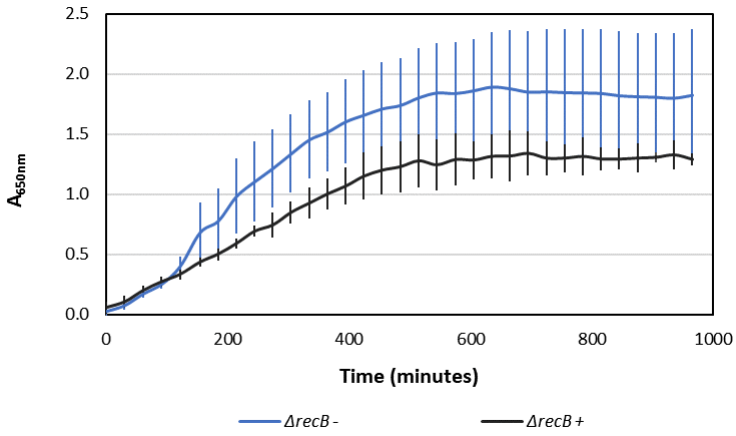

Control (-) and 0.05 mM DTPMP (+) exposure at approx. 0.2 A_{650nm} of *ΔrecF E. coli* with monitoring every 30 minutes for 16 hours.

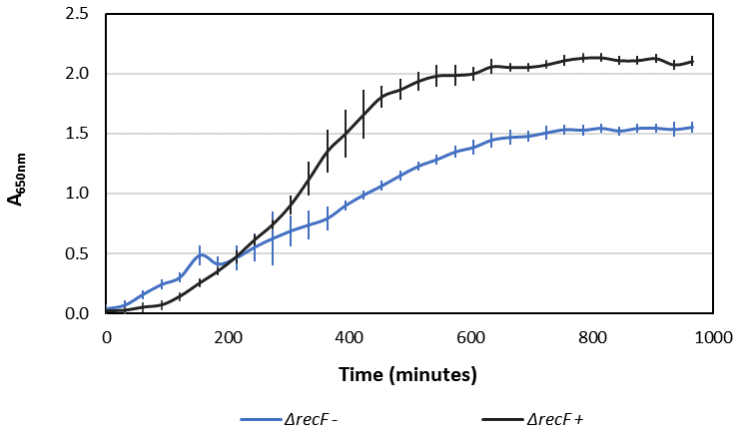

Control (-) and 0.05 mM DTPMP (+) exposure at approx. 0.2 A_{650nm} of *ΔrecJ E. coli* with monitoring every 30 minutes for 16 hours.

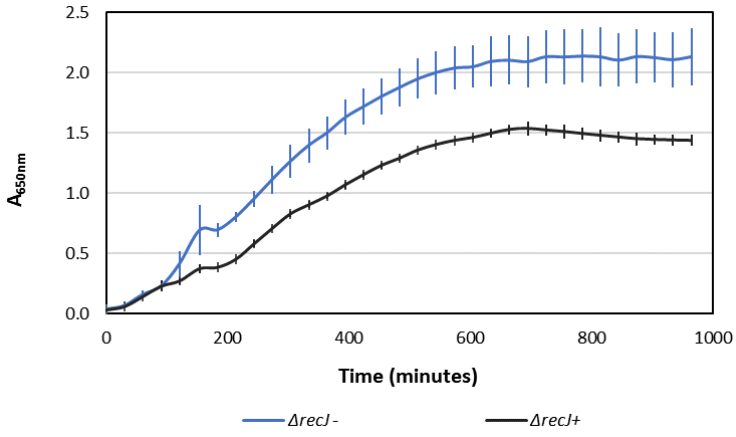

Control (-) and 0.05 mM DTPMP (+) exposure at approx. 0.2 A_{650nm} of *ΔrecN E. coli* with monitoring every 30 minutes for 16 hours.

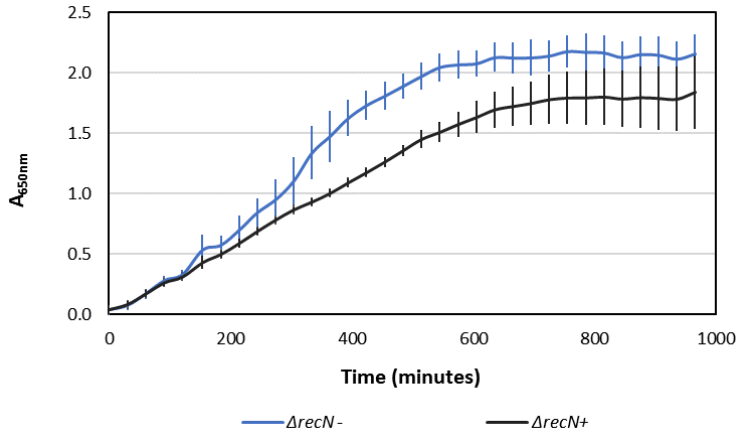

Control (-) and 0.05 mM DTPMP (+) exposure at approx. 0.2 A_{650nm} of *ΔrecQ E. coli* with monitoring every 30 minutes for 16 hours.

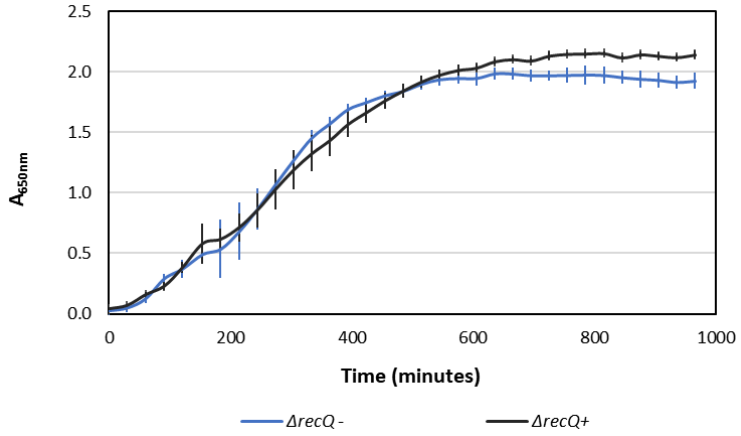

Control (-) and 0.05 mM DTPMP (+) exposure at approx. 0.2 A_{650nm} of *ΔruvA E. coli* with monitoring every 30 minutes for 16 hours.

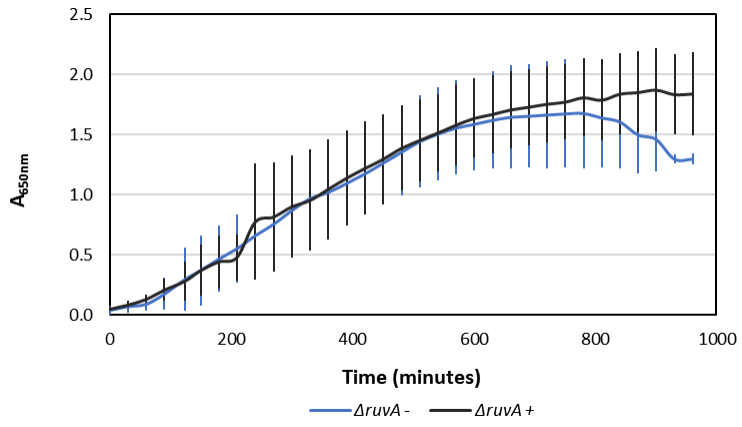

Control (-) and 0.05 mM DTPMP (+) exposure at approx. 0.2 A_{650nm} of *ΔruvB E. coli* with monitoring every 30 minutes for 16 hours.

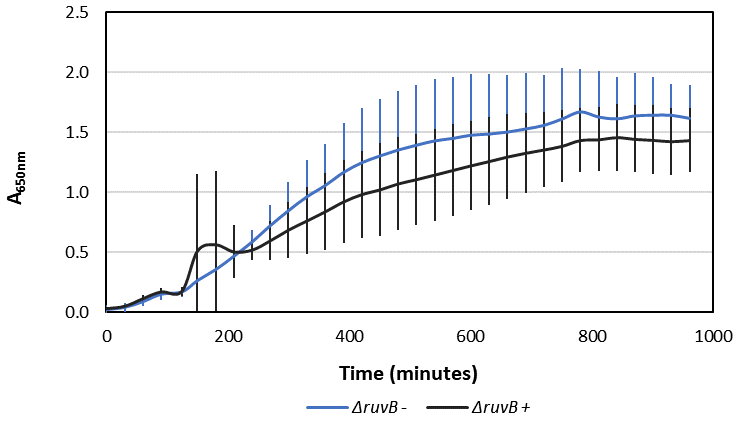

Control (-) and 0.05 mM DTPMP (+) exposure at approx. 0.2 A_{650nm} of *ΔruvC E. coli* with monitoring every 30 minutes for 16 hours.

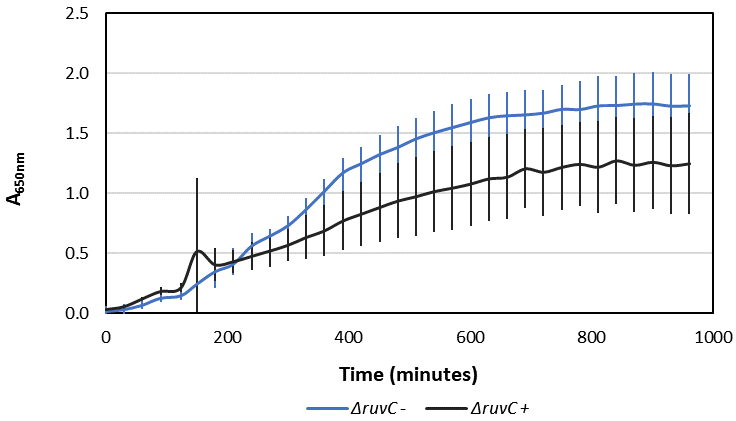

Control (-) and 0.05 mM DTPMP (+) exposure at approx. 0.2 A_{650nm} of *ΔuvrA E. coli* with monitoring every 30 minutes for 16 hours.

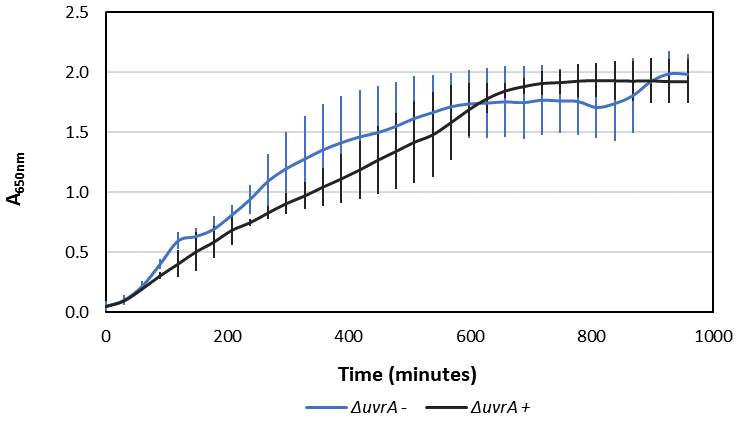

Control (-) and 0.05 mM DTPMP (+) exposure at approx. 0.2 A_{650nm} of *ΔuvrC E. coli* with monitoring every 30 minutes for 16 hours.

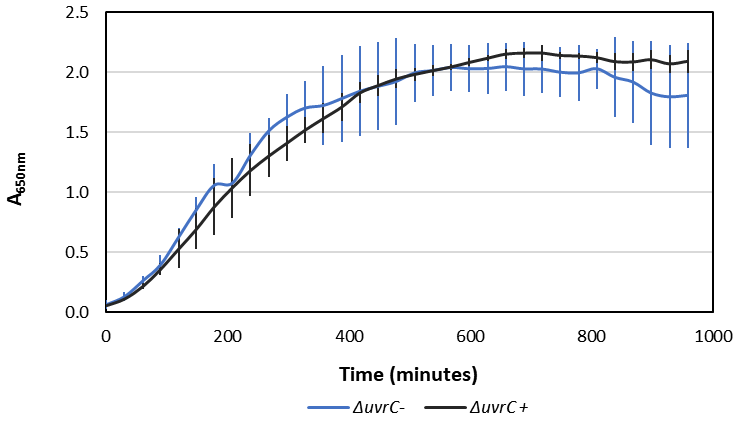

Control (-) and 0.05 mM DTPMP (+) exposure at approx. 0.2 A_{650nm} of *ΔmutM E. coli* with monitoring every 30 minutes for 16 hours.

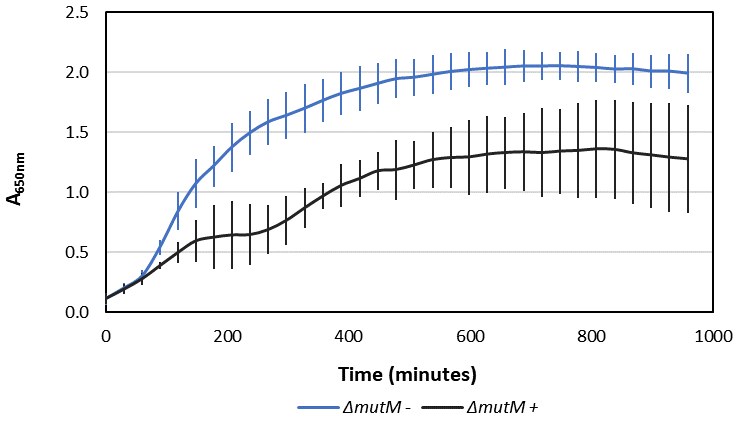

Control (-) and 0.05 mM DTPMP (+) exposure at approx. 0.2 A_{650nm} of *ΔmutT E. coli* with monitoring every 30 minutes for 16 hours.

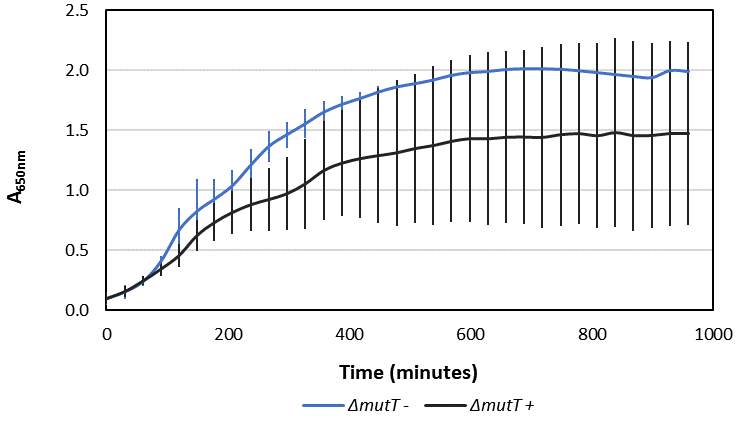

Control (-) and 0.05 mM DTPMP (+) exposure at approx. 0.2 A_{650nm} of *ΔmutY E. coli* with monitoring every 30 minutes for 16 hours.

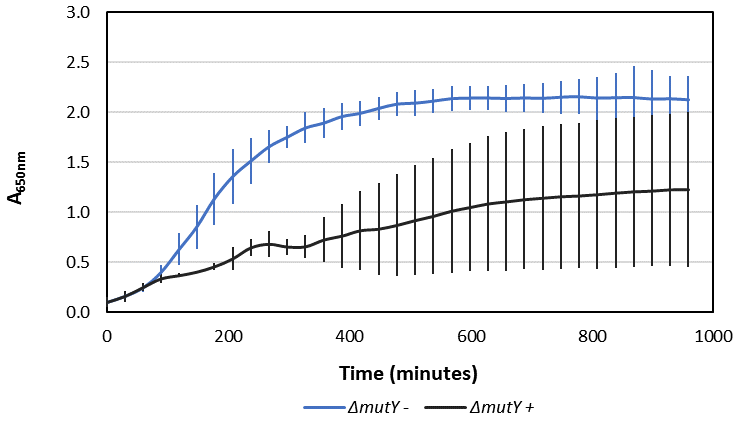

Control (-) and 0.05 mM DTPMP (+) exposure at approx. 0.2 A_{650nm} of *Δnth E. coli* with monitoring every 30 minutes for 16 hours.

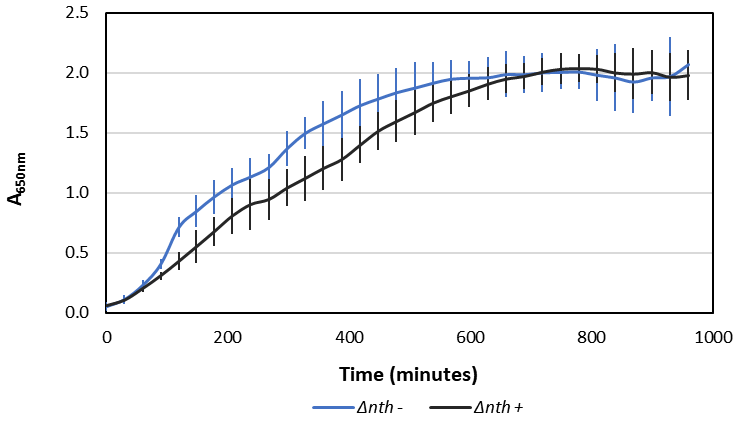

Control (-) and 0.05 mM DTPMP (+) exposure at approx. 0.2 A_{650nm} of *Δmfd E. coli* with monitoring every 30 minutes for 16 hours.

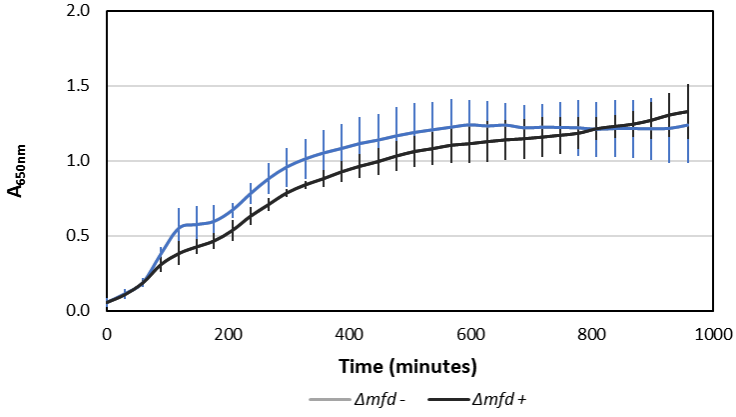

Control (-) and 0.05 mM DTPMP (+) exposure at approx. 0.2 A_{650nm} of *ΔsbcB E. coli* with monitoring every 30 minutes for 16 hours.

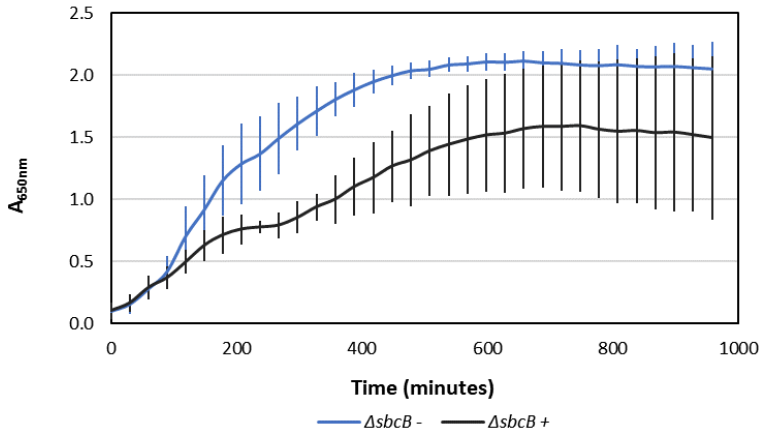

Control (-) and 0.05 mM DTPMP (+) exposure at approx. 0.2 A_{650nm} of *ΔahpC E. coli* with monitoring every 30 minutes for 16 hours.

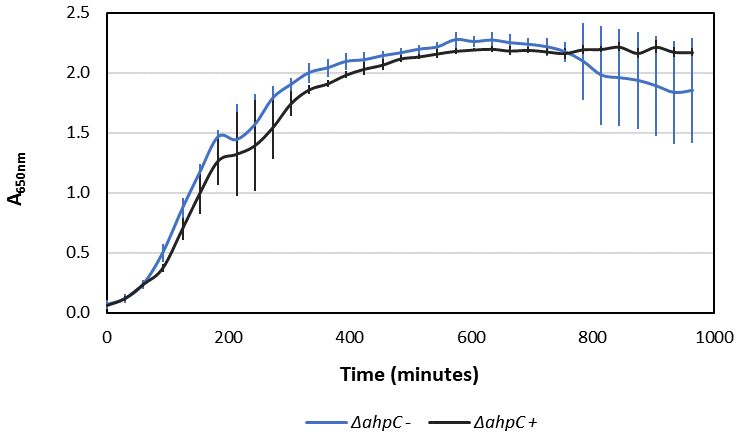

Control (-) and 0.05 mM DTPMP (+) exposure at approx. 0.2 A_{650nm} of *ΔkatG E. coli* with monitoring every 30 minutes for 16 hours.

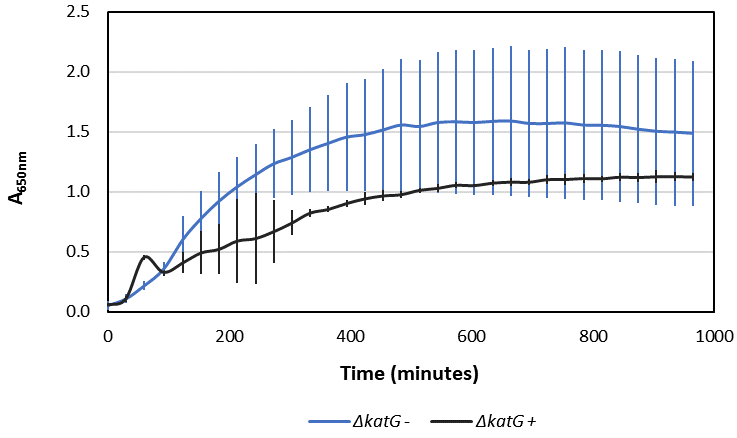

Control (-) and 0.05 mM DTPMP (+) exposure at approx. 0.2 A_{650nm} of *ΔsodA E. coli* with monitoring every 30 minutes for 16 hours.

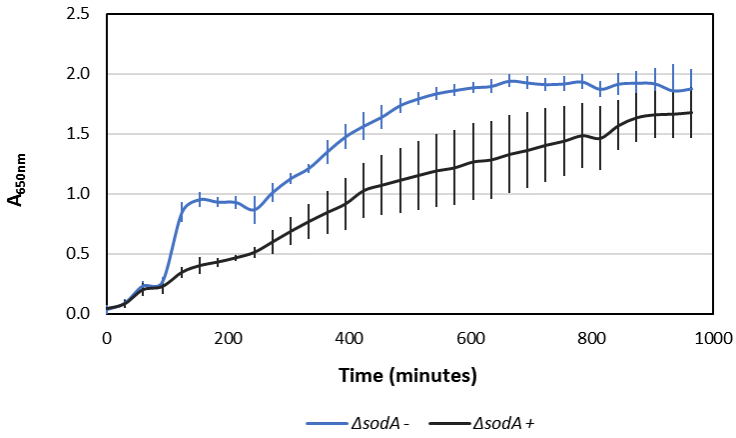

Control (-) and 0.05 mM DTPMP (+) exposure at approx. 0.2 A_{650nm} of *ΔsodB E. coli* with monitoring every 30 minutes for 16 hours.

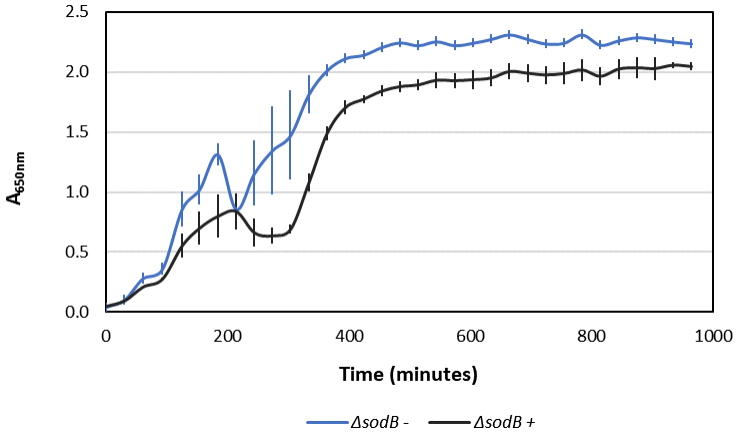

Control (-) and 0.05 mM DTPMP (+) exposure at approx. 0.2 A_{650nm} of *ΔsodC E. coli* with monitoring every 30 minutes for 16 hours.

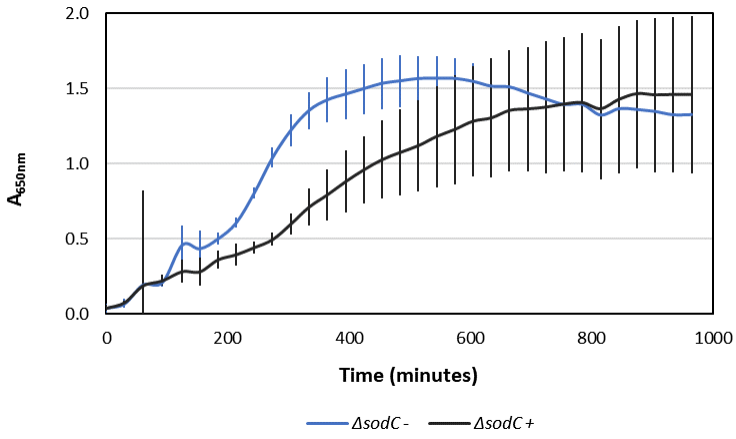

Control (-) and 0.05 mM DTPMP (+) exposure at approx. 0.2 A_{650nm} of *ΔfepA E. coli* with monitoring every 30 minutes for 16 hours.

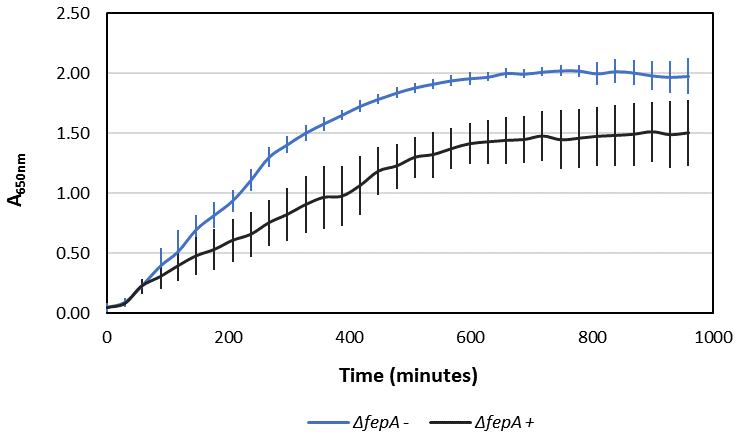

Control (-) and 0.05 mM DTPMP (+) exposure at approx. 0.2 A_{650nm} of *ΔfeoB E. coli* with monitoring every 30 minutes for 16 hours.

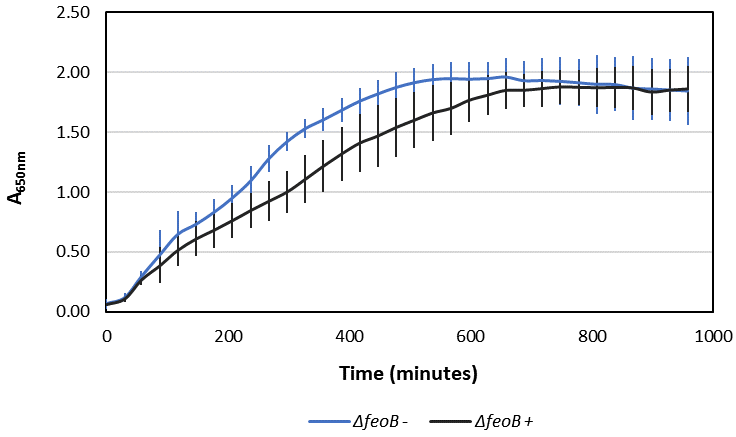

Control (-) and 0.05 mM DTPMP (+) exposure at approx. 0.2 A_{650nm} of *Δftn E. coli* with monitoring every 30 minutes for 16 hours.

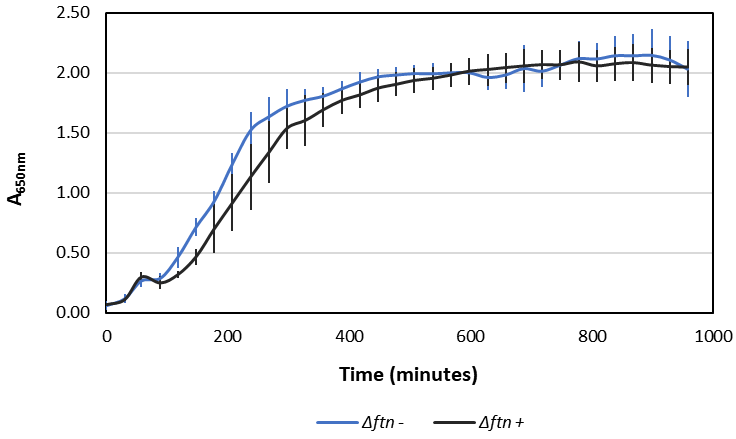

Control (-) and 0.05 mM DTPMP (+) exposure at approx. 0.2 A_{650nm} of *Δfur E. coli* with monitoring every 30 minutes for 16 hours.

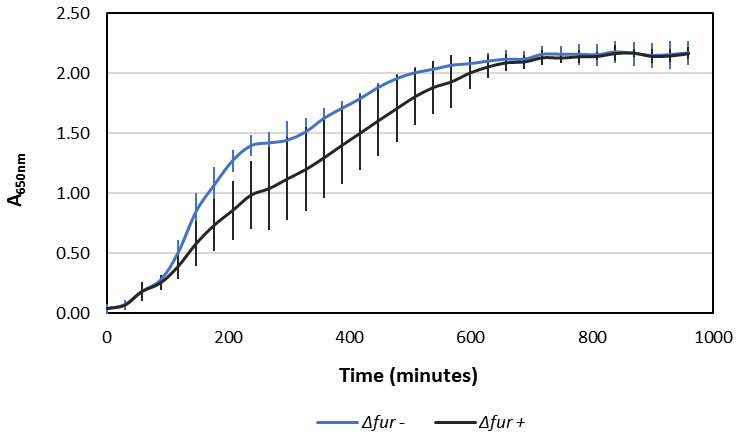

Control (-) and 0.05 mM DTPMP (+) exposure at approx. 0.2 A_{650nm} of *ΔmntH E. coli* with monitoring every 30 minutes for 16 hours.

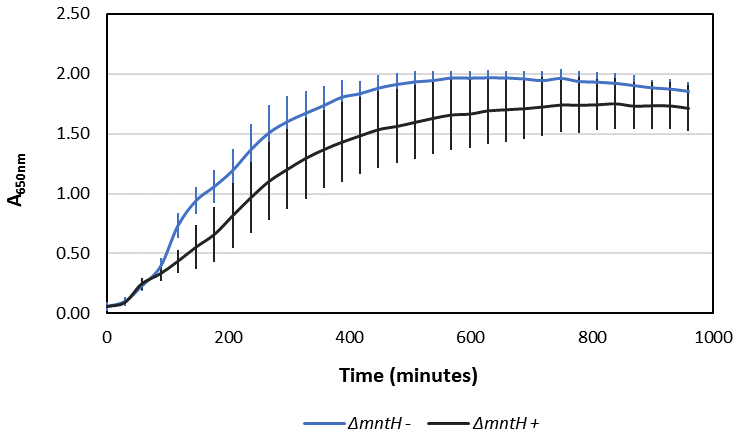

Control (-) and 0.05 mM DTPMP (+) exposure at approx. 0.2 A_{650nm} of *ΔcopA E. coli* with monitoring every 30 minutes for 16 hours.

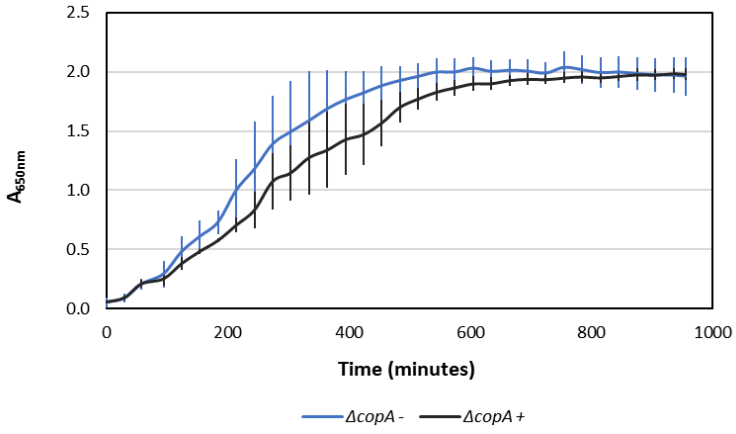

Control (-) and 0.05 mM DTPMP (+) exposure at approx. 0.2 A_{650nm} of *ΔcueR E. coli* with monitoring every 30 minutes for 16 hours.

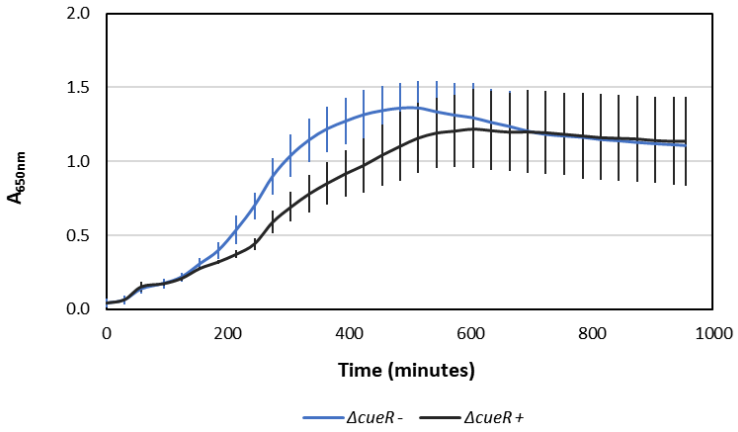

Control (-) and 0.05 mM DTPMP (+) exposure at approx. 0.2 A_{650nm} of *ΔcueO E. coli* with monitoring every 30 minutes for 16 hours.

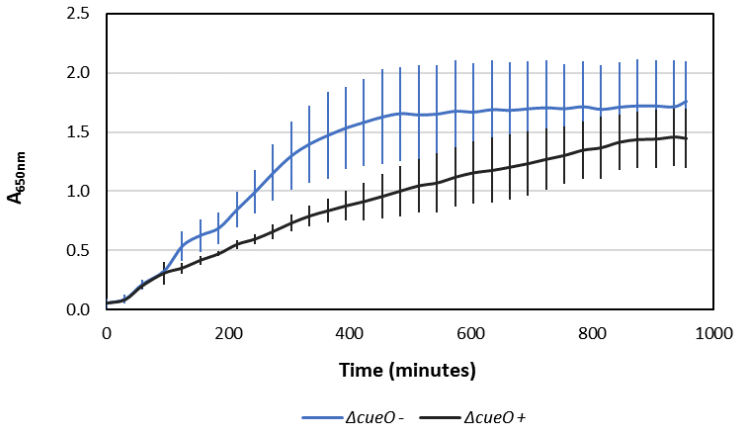

Control (-) and 0.05 mM DTPMP (+) exposure at approx. 0.2 A_{650nm} of *ΔcusR E. coli* with monitoring every 30 minutes for 16 hours.

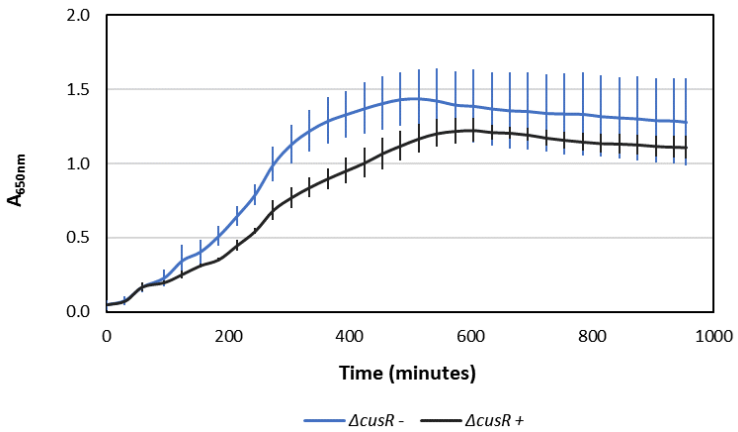

Control (-) and 0.05 mM DTPMP (+) exposure at approx. 0.2 A_{650nm} of *ΔcorA E. coli* with monitoring every 30 minutes for 16 hours.

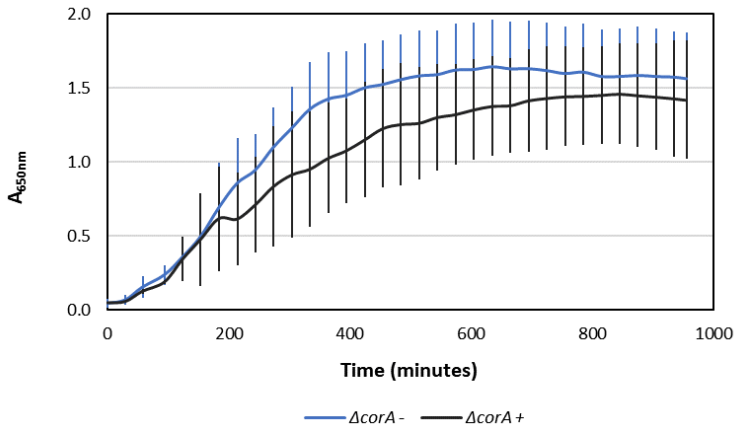

Control (-) and 0.05 mM DTPMP (+) exposure at approx. 0.2 A_{650nm} of *ΔnikA E. coli* with monitoring every 30 minutes for 16 hours.

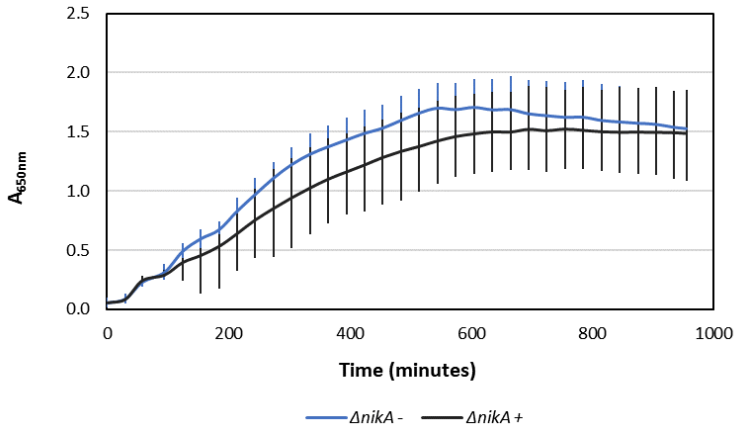

Control (-) and 0.05 mM DTPMP (+) exposure at approx. 0.2 A_{650nm} of *ΔnikR E. coli* with monitoring every 30 minutes for 16 hours.

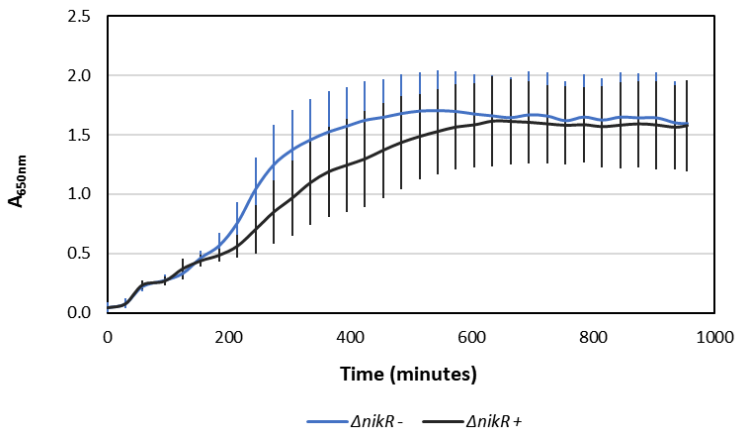

Control (-) and 0.05 mM DTPMP (+) exposure at approx. 0.2 A_{650nm} of *ΔrcnB E. coli* with monitoring every 30 minutes for 16 hours.

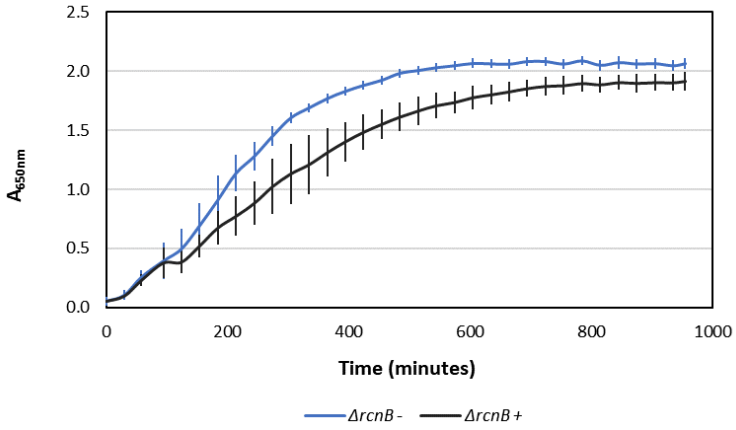

Control (-) and 0.05 mM DTPMP (+) exposure at approx. 0.2 A_{650nm} of *ΔzntR E. coli* with monitoring every 30 minutes for 16 hours.

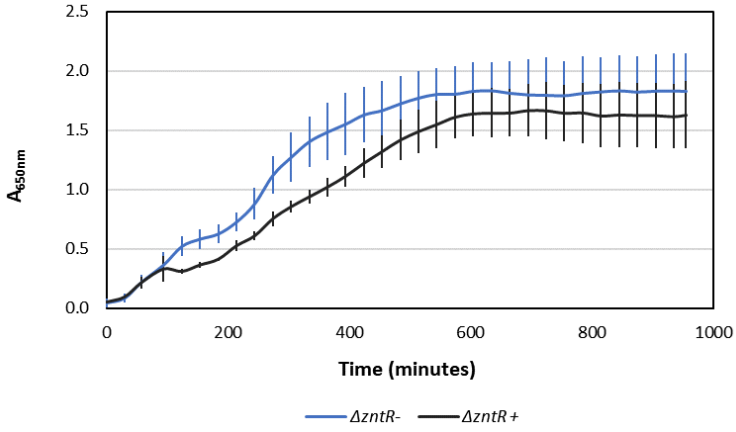

Control (-) and 0.05 mM DTPMP (+) exposure at approx. 0.2 A_{650nm} of *ΔgshA E. coli* with monitoring every 30 minutes for 16 hours.

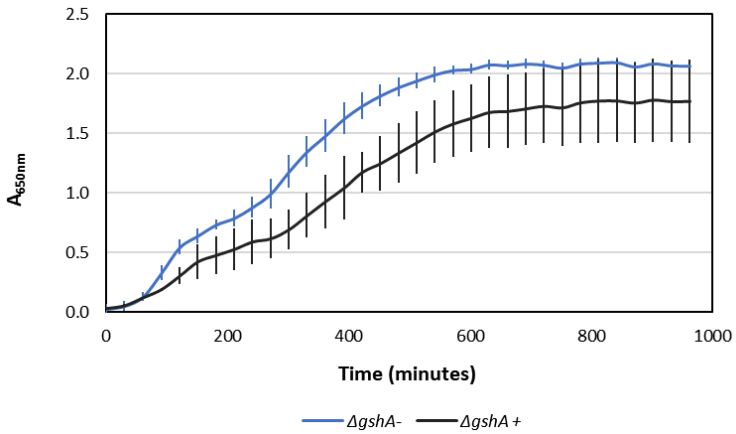

Control (-) and 0.05 mM DTPMP (+) exposure at approx. 0.2 A_{650nm} of *ΔslyD E. coli* with monitoring every 30 minutes for 16 hours.

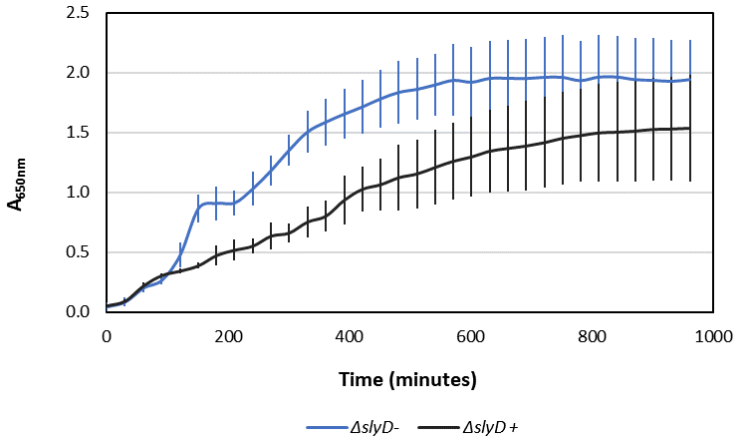

Control (-) and 0.05 mM DTPMP (+) exposure at approx. 0.2 A_{650nm} of *ΔhybD E. coli* with monitoring every 30 minutes for 16 hours.

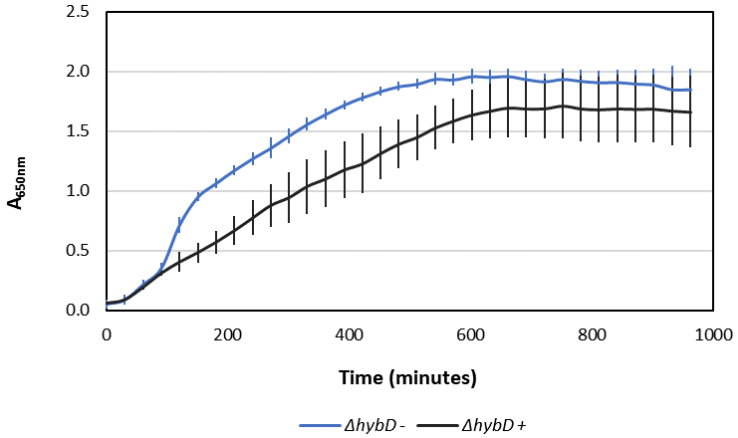

Control (-) and 0.05 mM DTPMP (+) exposure at approx. 0.2 A_{650nm} of *ΔhybF E. coli* with monitoring every 30 minutes for 16 hours.

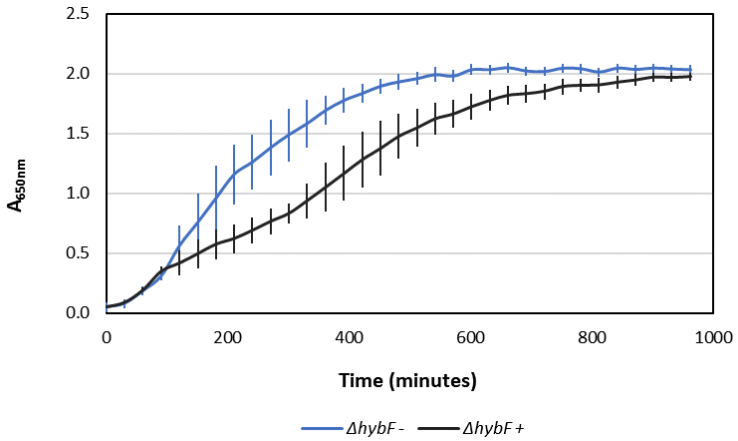

Control (-) and 0.05 mM DTPMP (+) exposure at approx. 0.2 A_{650nm} of *ΔhycI E. coli* with monitoring every 30 minutes for 16 hours.

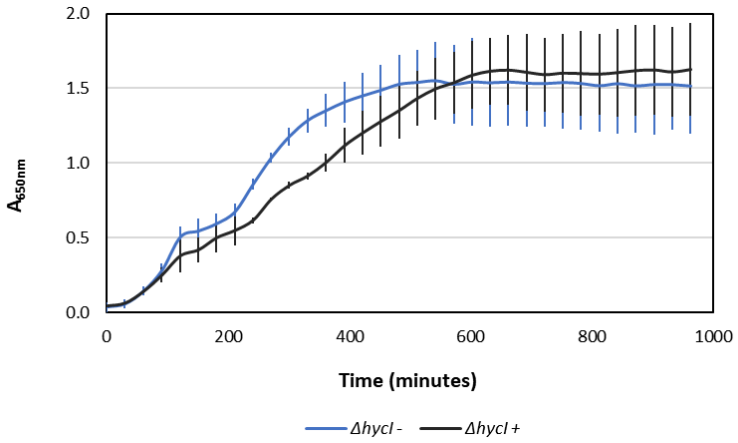

Control (-) and 0.05 mM DTPMP (+) exposure at approx. 0.2 A_{650nm} of *ΔcpxA E. coli* with monitoring every 30 minutes for 16 hours.

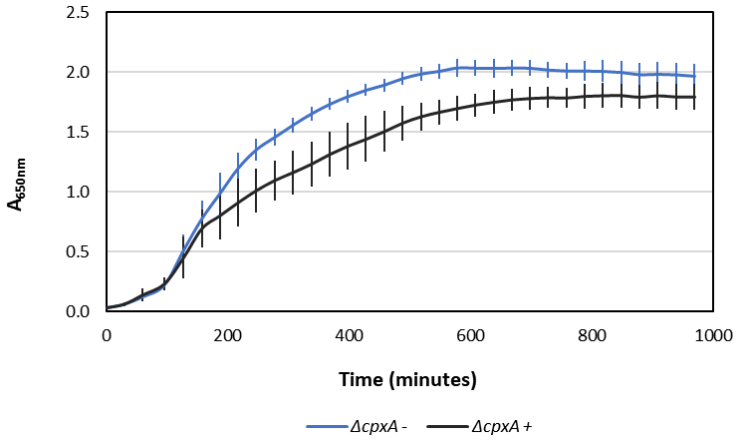

Control (-) and 0.05 mM DTPMP (+) exposure at approx. 0.2 A_{650nm} of *ΔcpxR E. coli* with monitoring every 30 minutes for 16 hours.

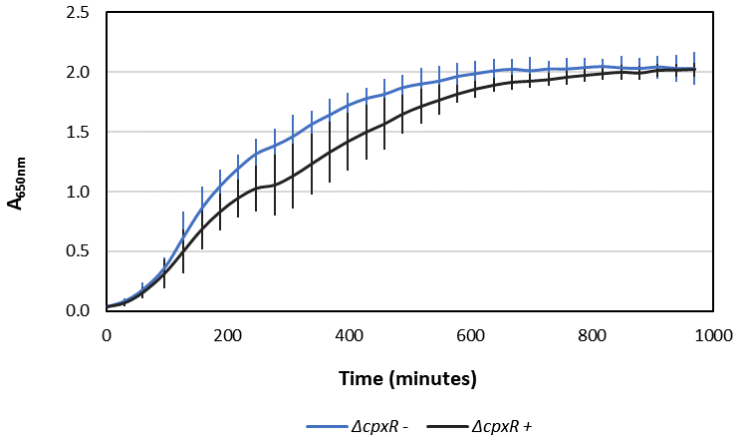

Control (-) and 0.05 mM DTPMP (+) exposure at approx. 0.2 A_{650nm} of *ΔcpxP E. coli* with monitoring every 30 minutes for 16 hours.

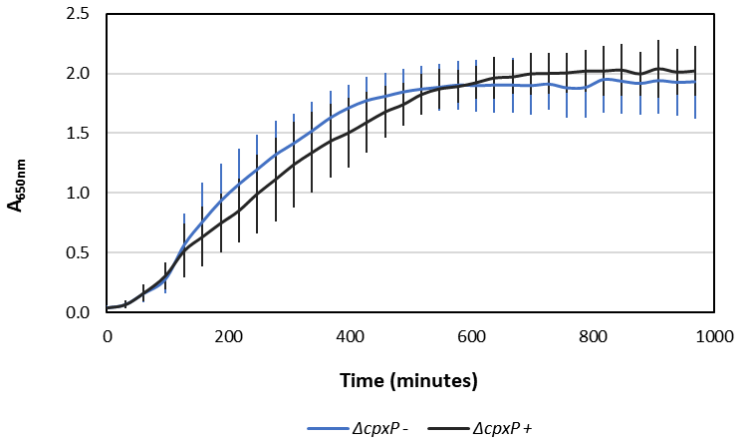

Control (-) and 0.05 mM DTPMP (+) exposure at approx. 0.2 A_{650nm} of *ΔdsbA E. coli* with monitoring every 30 minutes for 16 hours.

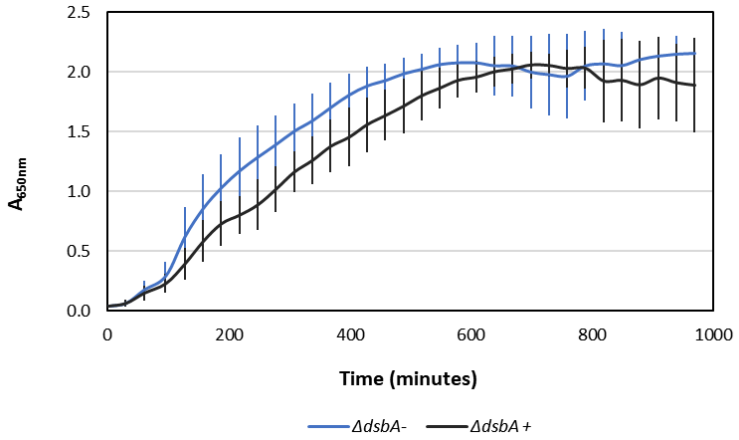

Appendix 2.3 - Octopirox growth curve data

Control (-) and 0.01625 mM Octopirox (+) exposure at approx. 0.2 A_{650nm} of *WT E. coli* with monitoring every 30 minutes for 16 hours.

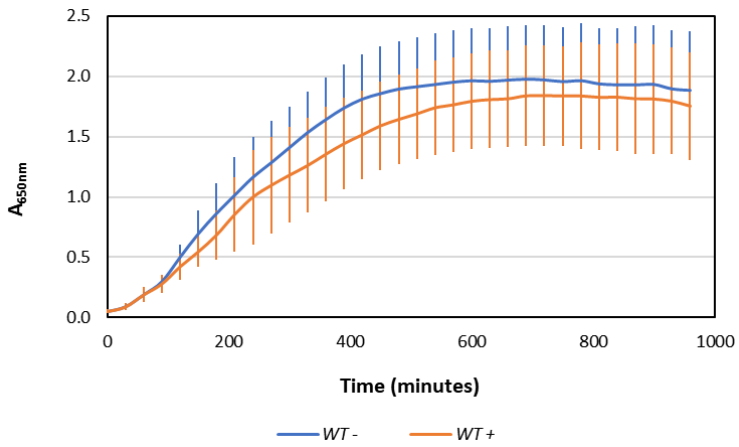

Control (-) and 0.01625 mM Octopirox (+) exposure at approx. 0.2 A_{650nm} of *ΔrecA E. coli* with monitoring every 30 minutes for 16 hours.

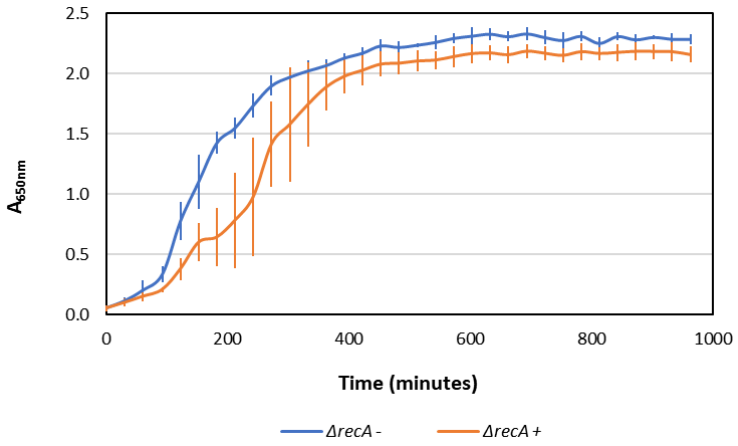

Control (-) and 0.01625 mM Octopirox (+) exposure at approx. 0.2 A_{650nm} of *ΔrecB E. coli* with monitoring every 30 minutes for 16 hours.

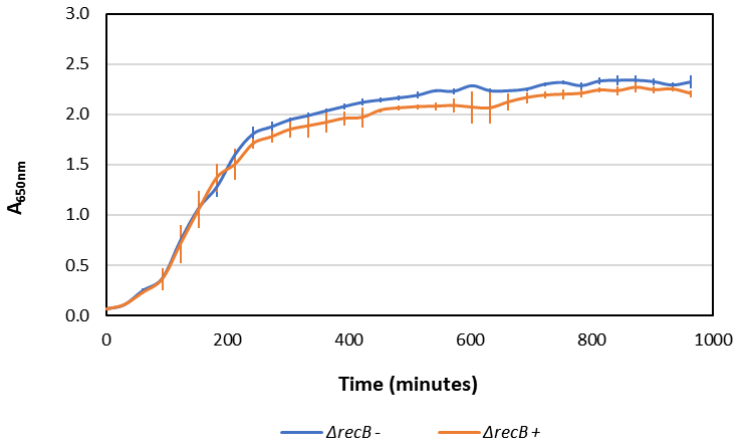

Control (-) and 0.01625 mM Octopirox (+) exposure at approx. 0.2 A_{650nm} of *ΔrecF E. coli* with monitoring every 30 minutes for 16 hours.

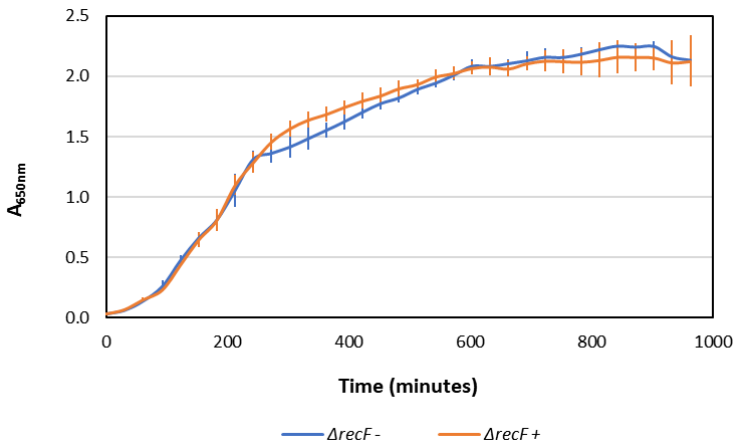

Control (-) and 0.01625 mM Octopirox (+) exposure at approx. 0.2 A_{650nm} of *ΔrecJ E. coli* with monitoring every 30 minutes for 16 hours.

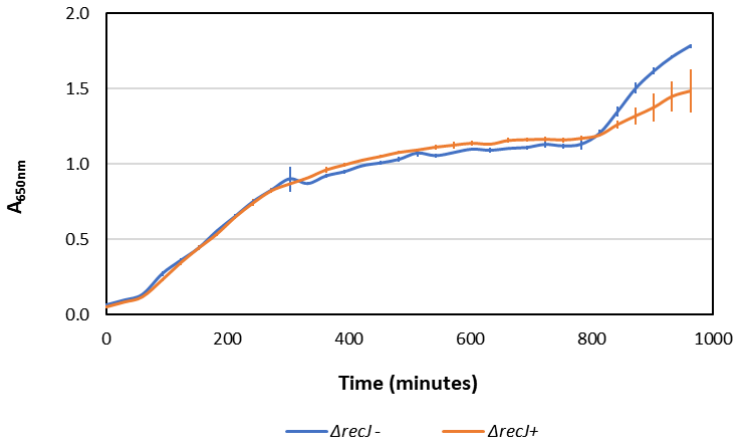

Control (-) and 0.01625 mM Octopirox (+) exposure at approx. 0.2 A_{650nm} of *ΔrecN E. coli* with monitoring every 30 minutes for 16 hours.

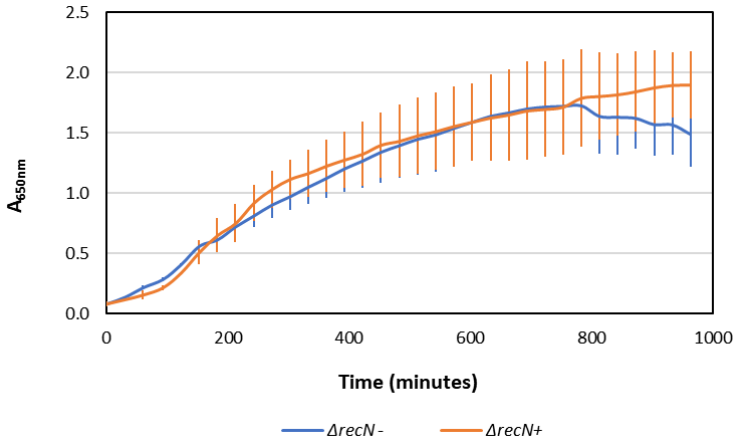

Control (-) and 0.01625 mM Octopirox (+) exposure at approx. 0.2 A_{650nm} of *ΔrecQ E. coli* with monitoring every 30 minutes for 16 hours.

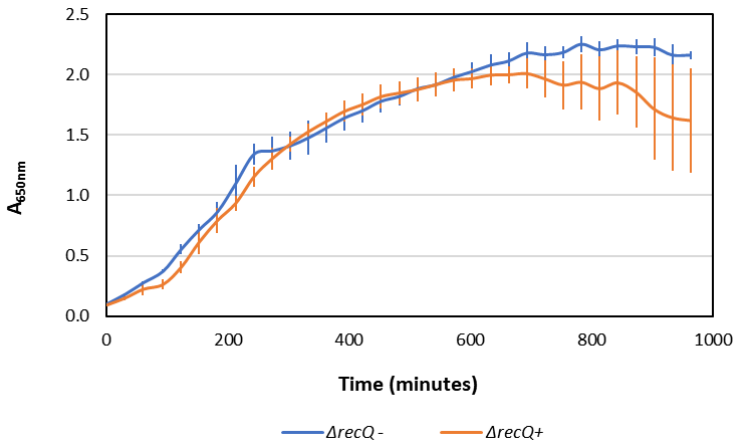

Control (-) and 0.01625 mM Octopirox (+) exposure at approx. 0.2 A_{650nm} of *ΔruvA E. coli* with monitoring every 30 minutes for 16 hours.

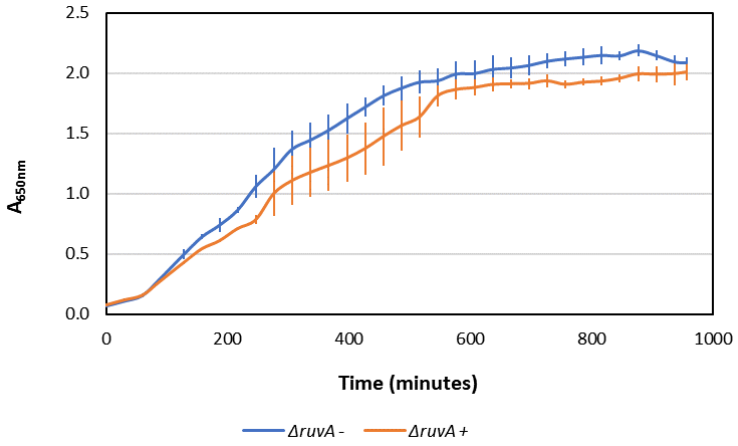

Control (-) and 0.01625 mM Octopirox (+) exposure at approx. 0.2 A_{650nm} of *ΔruvB E. coli* with monitoring every 30 minutes for 16 hours.

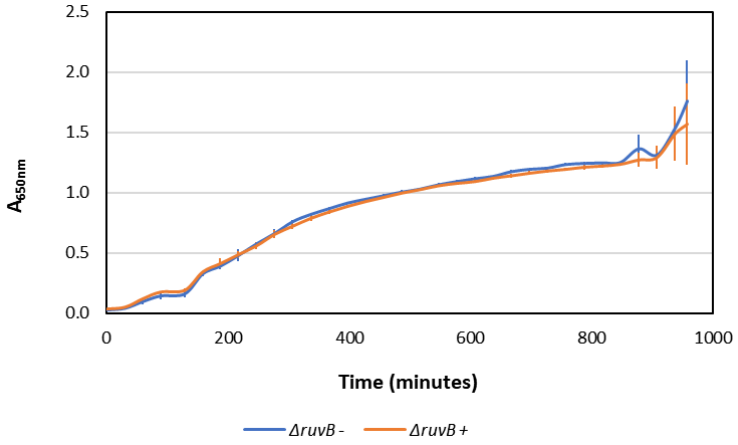

Control (-) and 0.01625 mM Octopirox (+) exposure at approx. 0.2 A_{650nm} of *ΔruvC E. coli* with monitoring every 30 minutes for 16 hours.

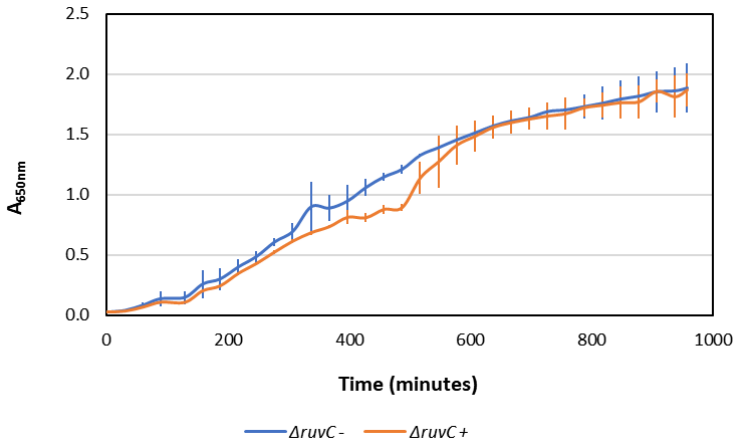

Control (-) and 0.01625 mM Octopirox (+) exposure at approx. 0.2 A_{650nm} of *ΔuvrA E. coli* with monitoring every 30 minutes for 16 hours.

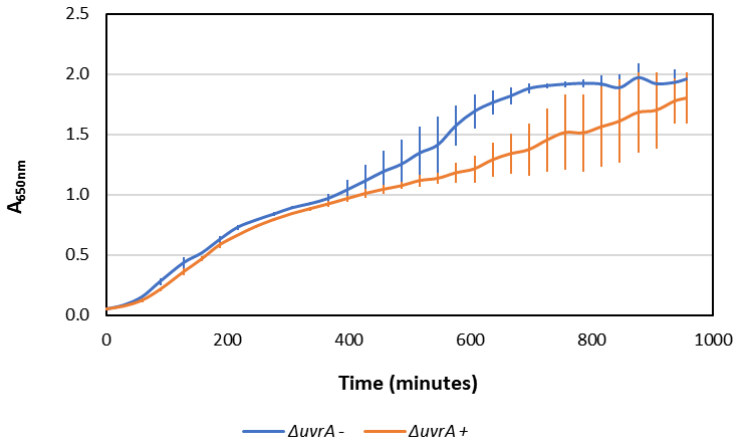

Control (-) and 0.01625 mM Octopirox (+) exposure at approx. 0.2 A_{650nm} of *ΔuvrC E. coli* with monitoring every 30 minutes for 16 hours.

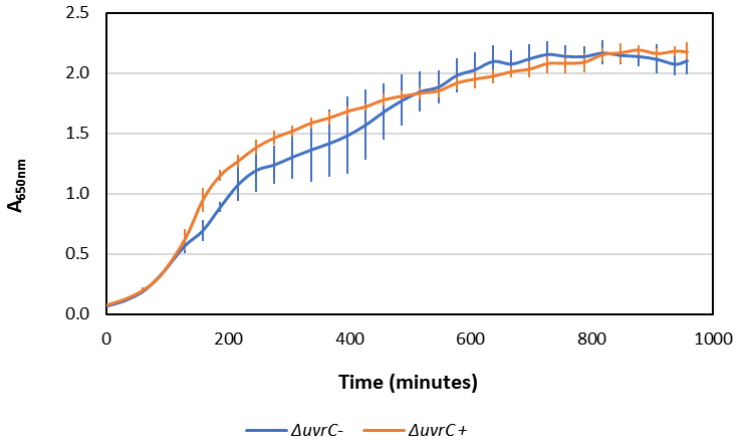

Control (-) and 0.01625 mM Octopirox (+) exposure at approx. 0.2 A_{650nm} of *ΔmutM E. coli* with monitoring every 30 minutes for 16 hours.

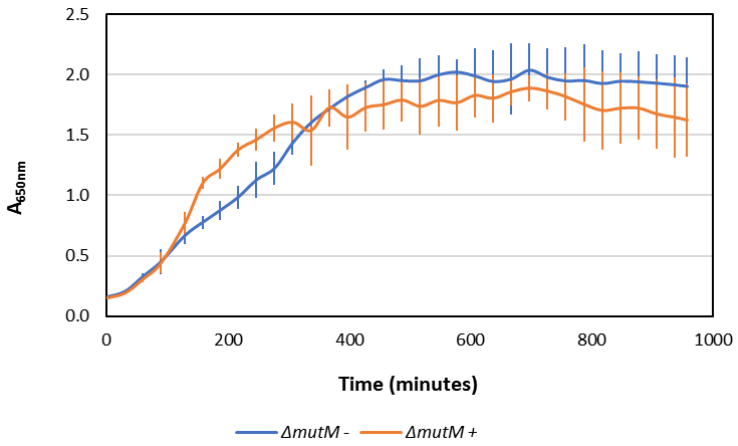

Control (-) and 0.01625 mM Octopirox (+) exposure at approx. 0.2 A_{650nm} of *ΔmutT E. coli* with monitoring every 30 minutes for 16 hours.

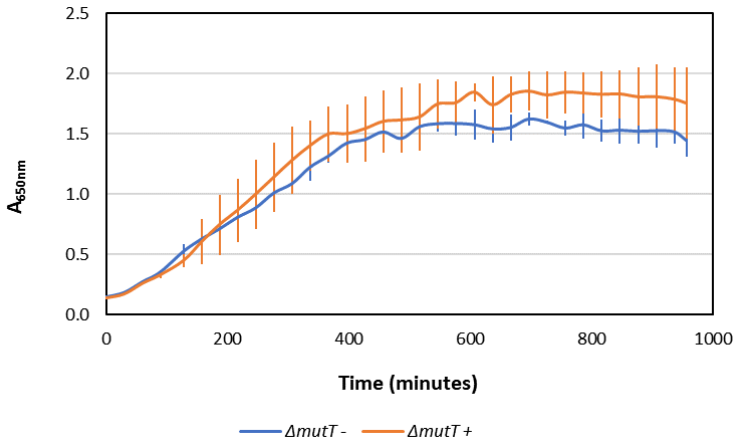

Control (-) and 0.01625 mM Octopirox (+) exposure at approx. 0.2 A_{650nm} of *ΔmutY E. coli* with monitoring every 30 minutes for 16 hours.

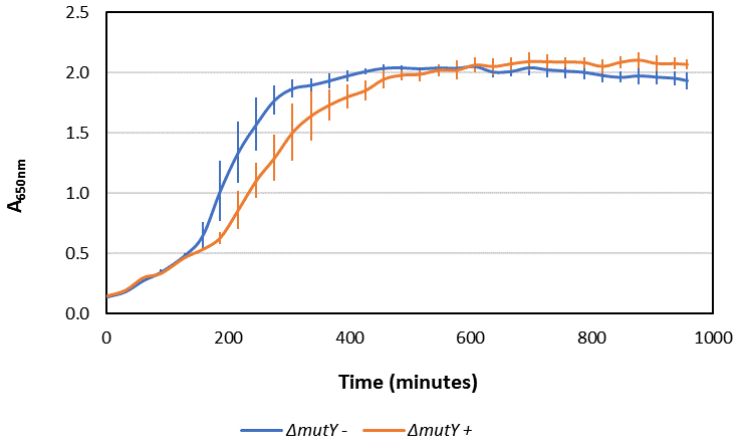

Control (-) and 0.01625 mM Octopirox (+) exposure at approx. 0.2 A_{650nm} of *Δnth E. coli* with monitoring every 30 minutes for 16 hours.

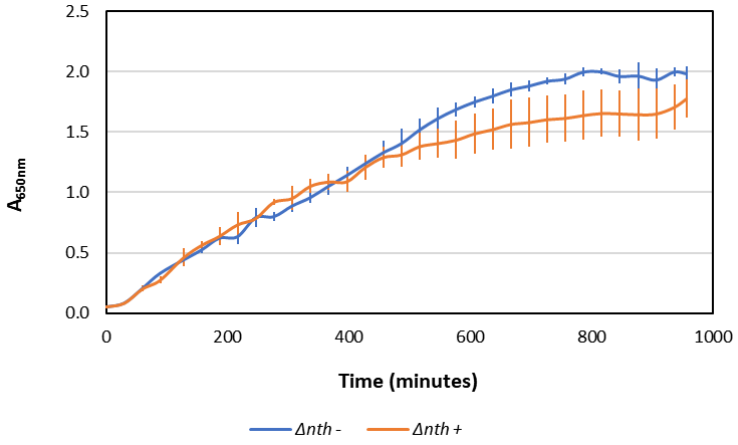

Control (-) and 0.01625 mM Octopirox (+) exposure at approx. 0.2 A_{650nm} of *Δmfd E. coli* with monitoring every 30 minutes for 16 hours.

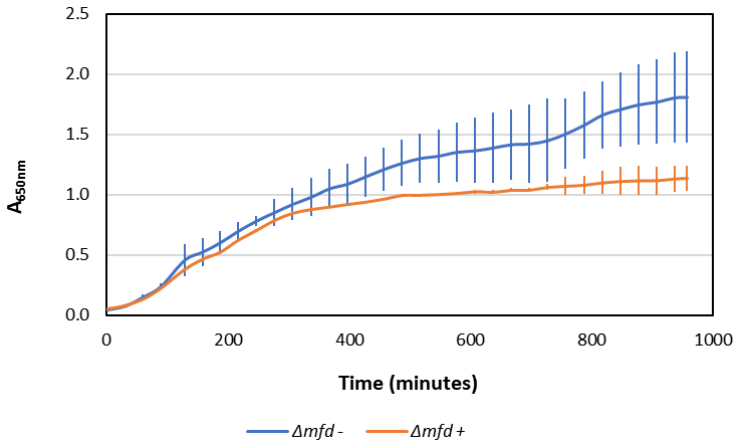

Control (-) and 0.01625 mM Octopirox (+) exposure at approx. 0.2 A_{650nm} of *ΔsbcB E. coli* with monitoring every 30 minutes for 16 hours.

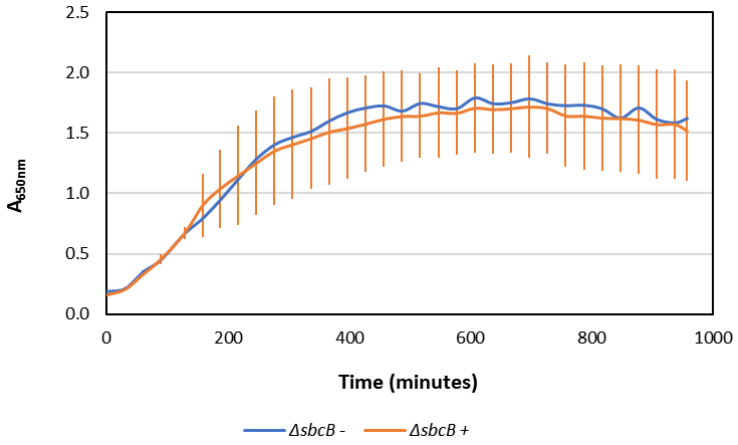

Control (-) and 0.01625 mM Octopirox (+) exposure at approx. 0.2 A_{650nm} of *ΔahpC E. coli* with monitoring every 30 minutes for 16 hours.

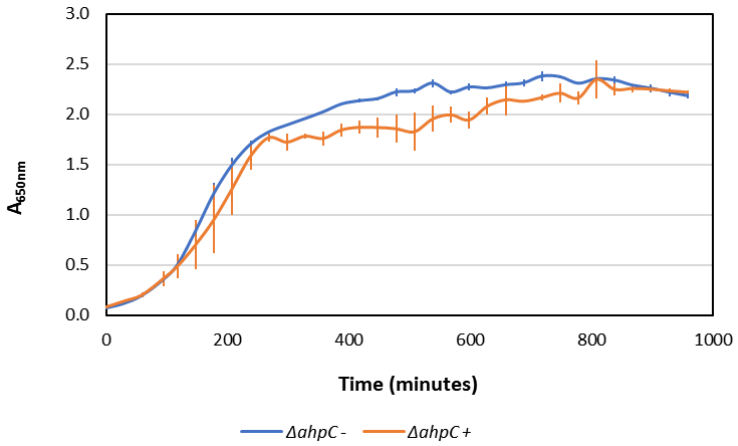

Control (-) and 0.01625 mM Octopirox (+) exposure at approx. 0.2 A_{650nm} of *ΔkatG E. coli* with monitoring every 30 minutes for 16 hours.

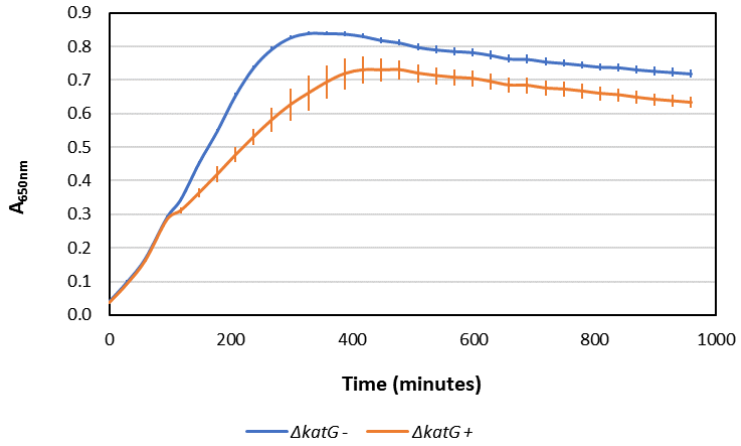

Control (-) and 0.01625 mM Octopirox (+) exposure at approx. 0.2 A_{650nm} of *ΔsodA E. coli* with monitoring every 30 minutes for 16 hours.

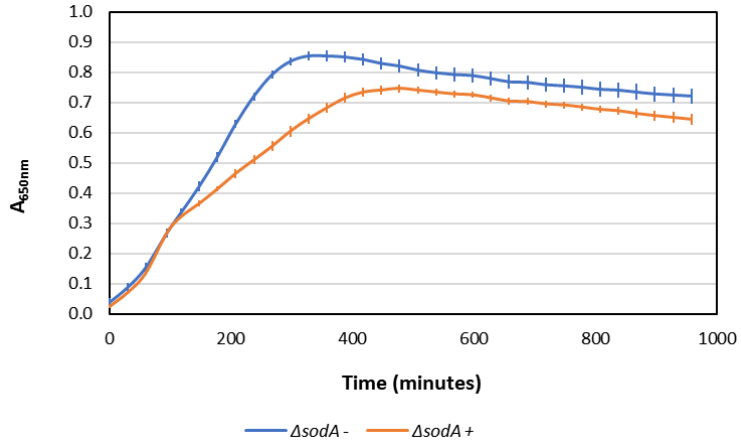

Control (-) and 0.01625 mM Octopirox (+) exposure at approx. 0.2 A_{650nm} of *ΔsodB E. coli* with monitoring every 30 minutes for 16 hours.

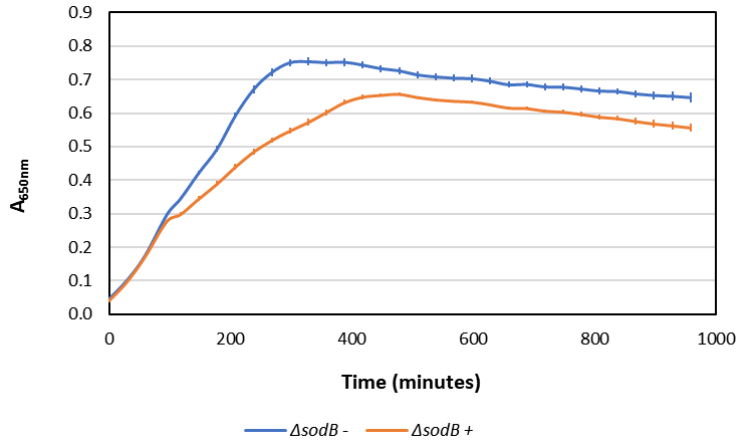

Control (-) and 0.01625 mM Octopirox (+) exposure at approx. 0.2 A_{650nm} of *ΔsodC E. coli* with monitoring every 30 minutes for 16 hours.

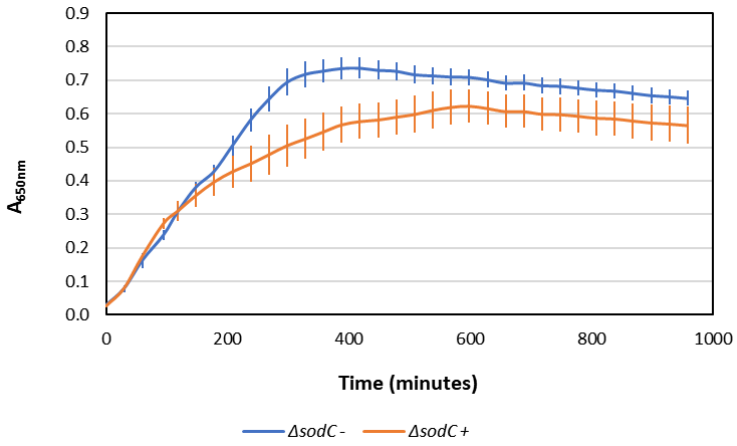

Control (-) and 0.01625 mM Octopirox (+) exposure at approx. 0.2 A_{650nm} of *ΔfepA E. coli* with monitoring every 30 minutes for 16 hours.

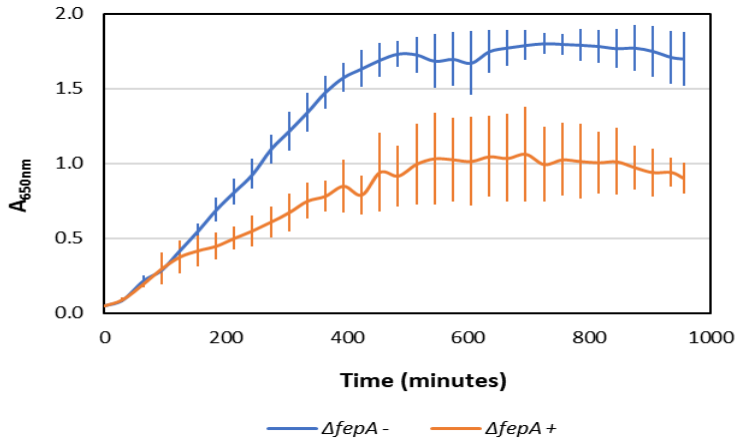

Control (-) and 0.01625 mM Octopirox (+) exposure at approx. 0.2 A_{650nm} of *ΔfeoB E. coli* with monitoring every 30 minutes for 16 hours.

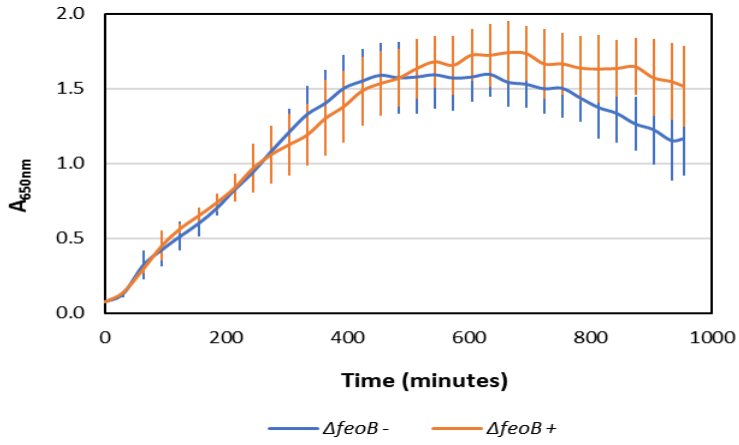

Control (-) and 0.01625 mM Octopirox (+) exposure at approx. 0.2 A_{650nm} of *Δftn E. coli* with monitoring every 30 minutes for 16 hours.

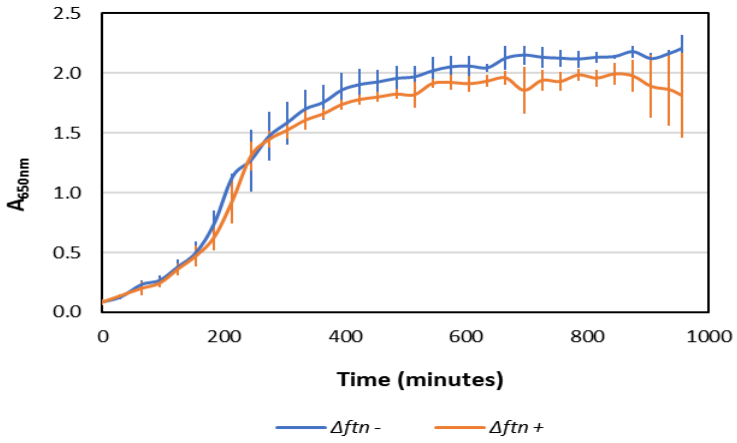

Control (-) and 0.01625 mM Octopirox (+) exposure at approx. 0.2 A_{650nm} of *Δfur E. coli* with monitoring every 30 minutes for 16 hours.

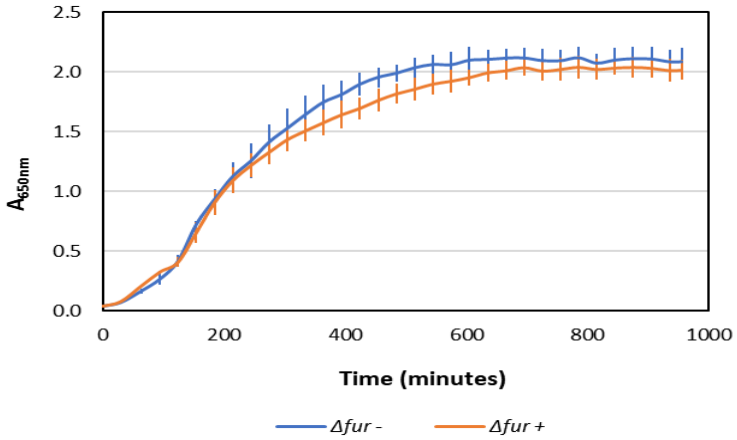

Control (-) and 0.01625 mM Octopirox (+) exposure at approx. 0.2 A_{650nm} of *ΔmntH E. coli* with monitoring every 30 minutes for 16 hours.

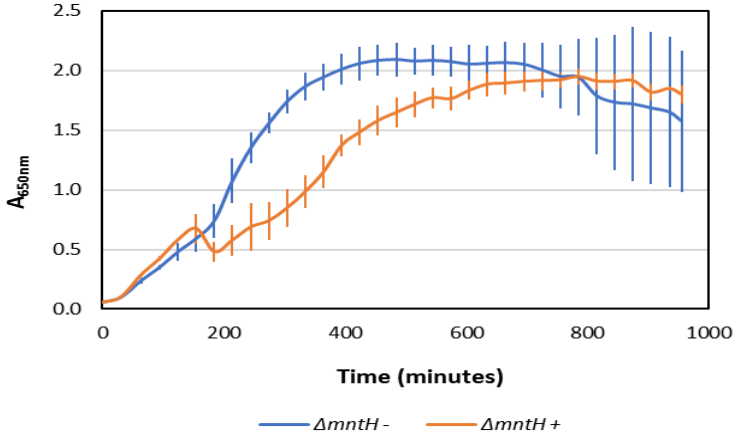

Control (-) and 0.01625 mM Octopirox (+) exposure at approx. 0.2 A_{650nm} of *ΔcopA E. coli* with monitoring every 30 minutes for 16 hours.

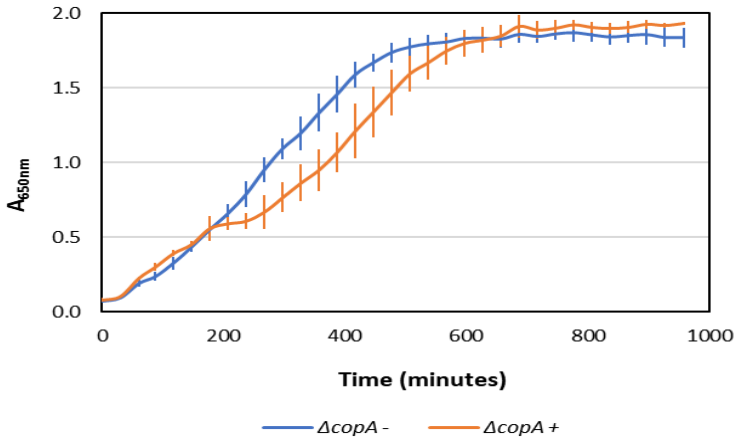

Control (-) and 0.01625 mM Octopirox (+) exposure at approx. 0.2 A_{650nm} of *ΔcueR E. coli* with monitoring every 30 minutes for 16 hours.

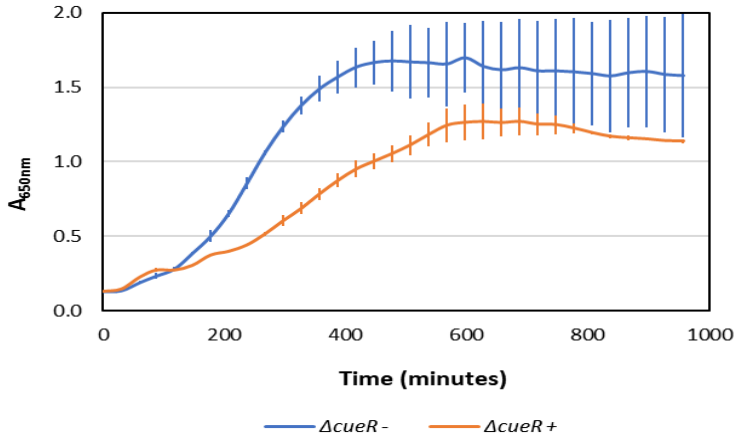

Control (-) and 0.01625 mM Octopirox (+) exposure at approx. 0.2 A_{650nm} of *ΔcueO E. coli* with monitoring every 30 minutes for 16 hours.

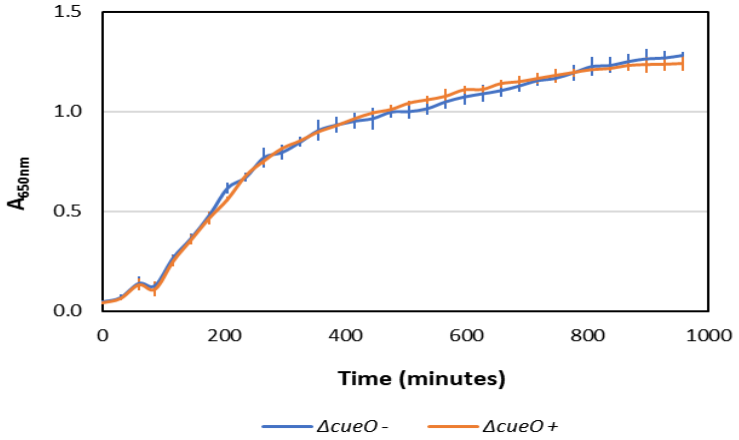

Control (-) and 0.01625 mM Octopirox (+) exposure at approx. 0.2 A_{650nm} of *ΔcusR E. coli* with monitoring every 30 minutes for 16 hours.

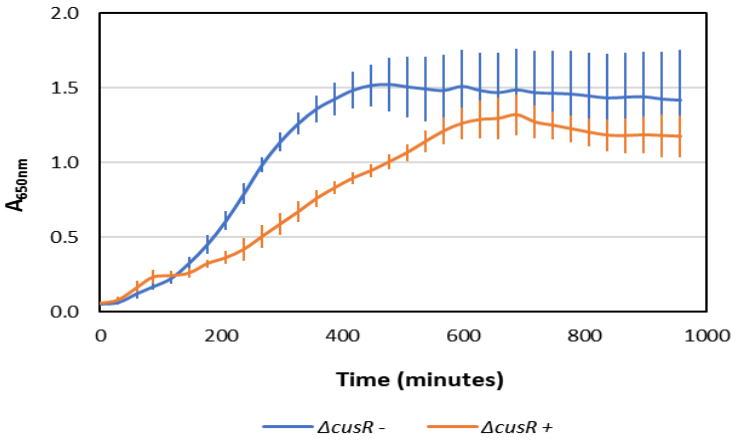

Control (-) and 0.01625 mM Octopirox (+) exposure at approx. 0.2 A_{650nm} of *ΔcorA E. coli* with monitoring every 30 minutes for 16 hours.

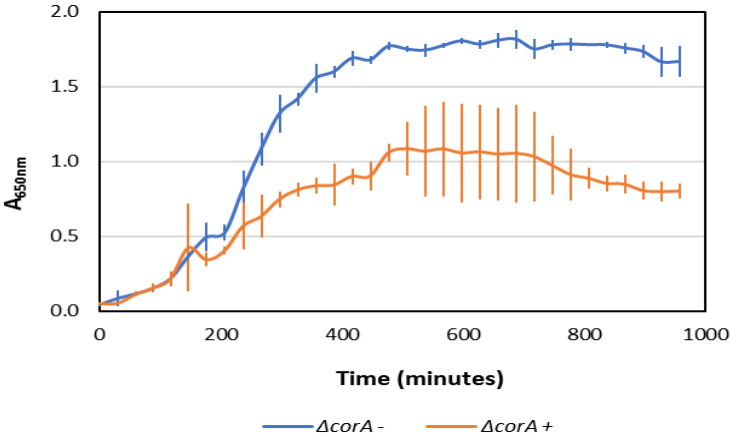

Control (-) and 0.01625 mM Octopirox (+) exposure at approx. 0.2 A_{650nm} of *ΔnikA E. coli* with monitoring every 30 minutes for 16 hours.

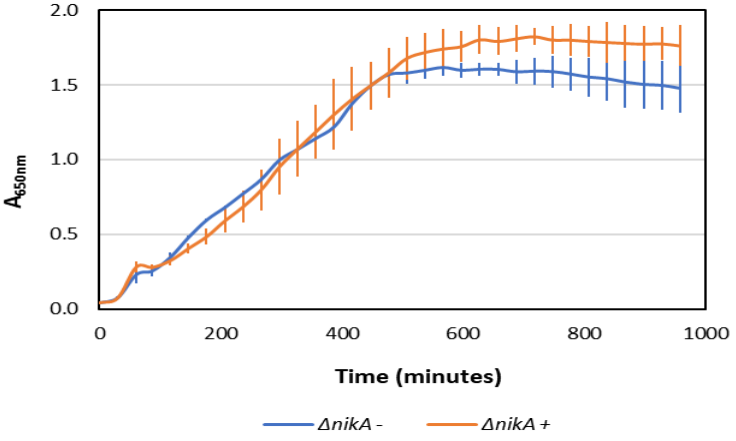

Control (-) and 0.01625 mM Octopirox (+) exposure at approx. 0.2 A_{650nm} of *ΔnikR E. coli* with monitoring every 30 minutes for 16 hours.

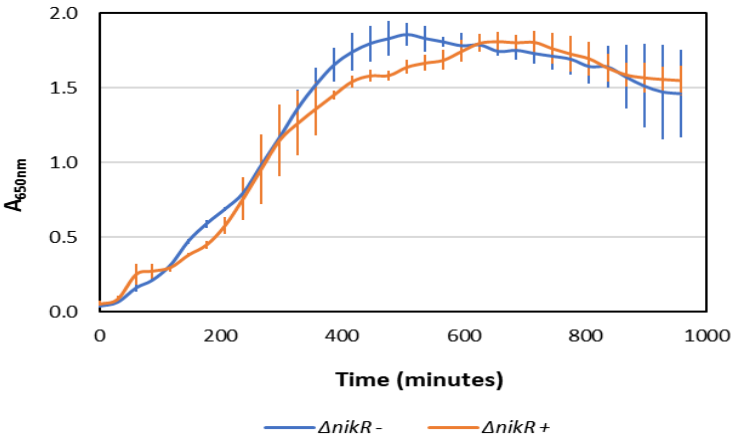

Control (-) and 0.01625 mM Octopirox (+) exposure at approx. 0.2 A_{650nm} of *ΔrcnB E. coli* with monitoring every 30 minutes for 16 hours.

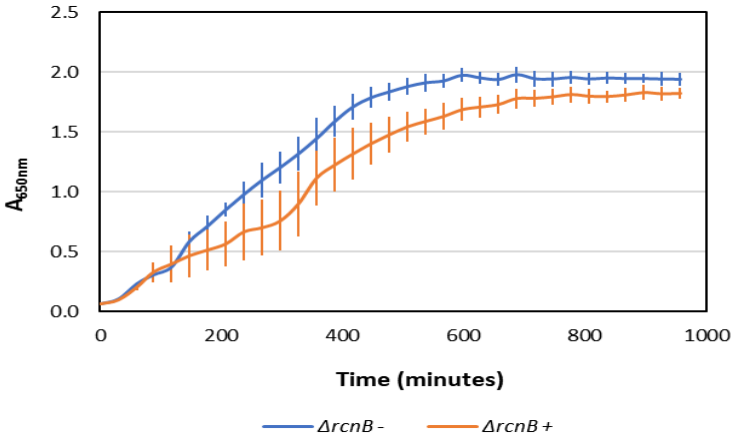

Control (-) and 0.01625 mM Octopirox (+) exposure at approx. 0.2 A_{650nm} of *ΔzntR E. coli* with monitoring every 30 minutes for 16 hours.

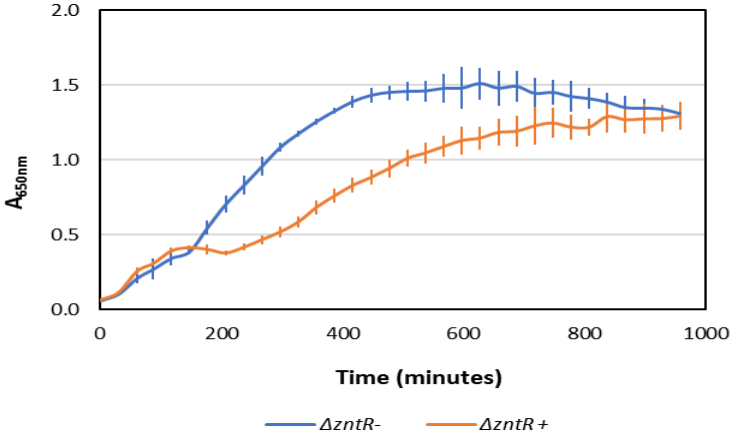

Control (-) and 0.01625 mM Octopirox (+) exposure at approx. 0.2 A_{650nm} of *ΔgshA E. coli* with monitoring every 30 minutes for 16 hours.

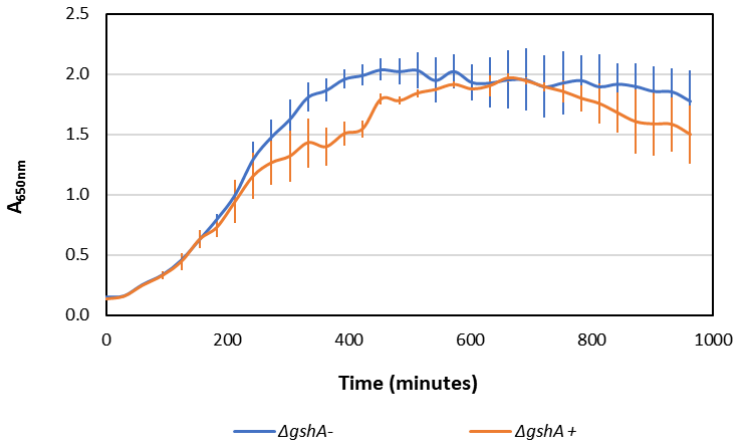

Control (-) and 0.01625 mM Octopirox (+) exposure at approx. 0.2 A_{650nm} of *ΔslyD E. coli* with monitoring every 30 minutes for 16 hours.

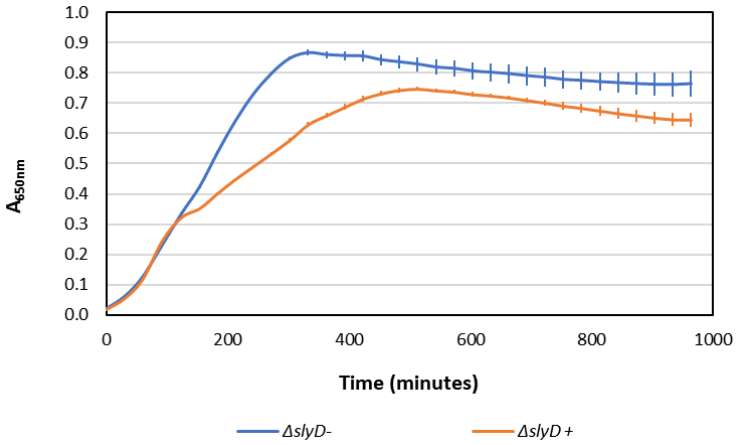

Control (-) and 0.01625 mM Octopirox (+) exposure at approx. 0.2 A_{650nm} of *ΔhybD E. coli* with monitoring every 30 minutes for 16 hours.

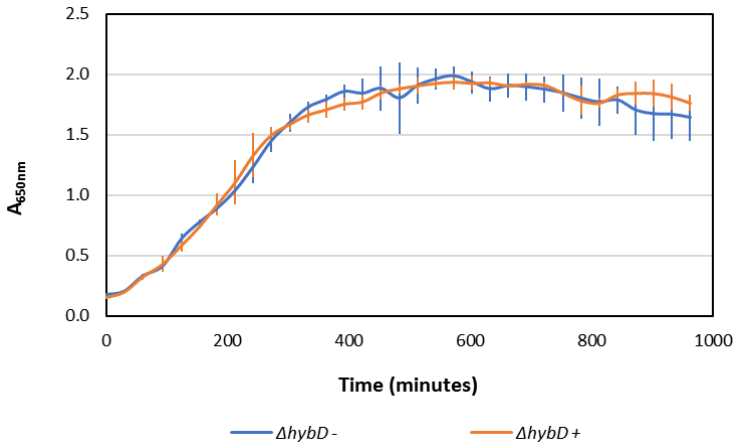

Control (-) and 0.01625 mM Octopirox (+) exposure at approx. 0.2 A_{650nm} of *ΔhybF E. coli* with monitoring every 30 minutes for 16 hours.

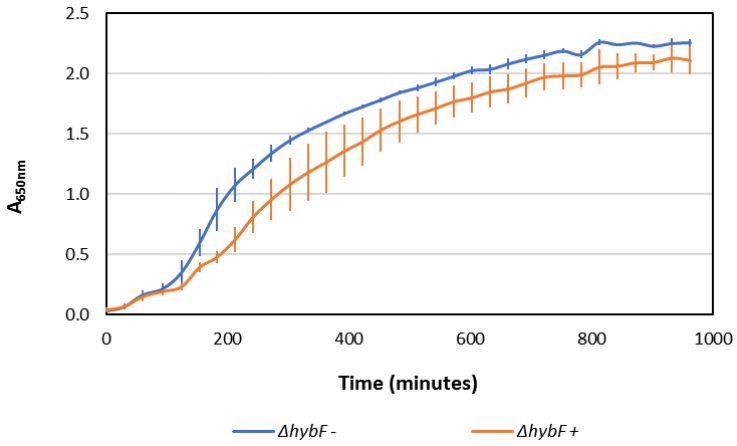

Control (-) and 0.01625 mM Octopirox (+) exposure at approx. 0.2 A_{650nm} of *ΔhycI E. coli* with monitoring every 30 minutes for 16 hours.

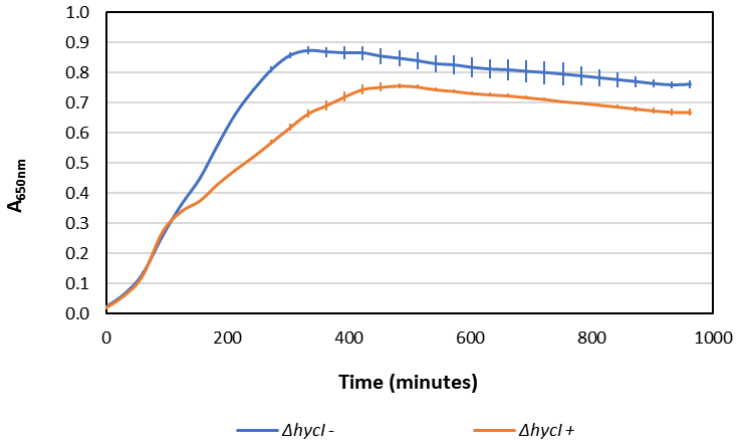

Control (-) and 0.01625 mM Octopirox (+) exposure at approx. 0.2 A_{650nm} of *ΔcpxA E. coli* with monitoring every 30 minutes for 16 hours.

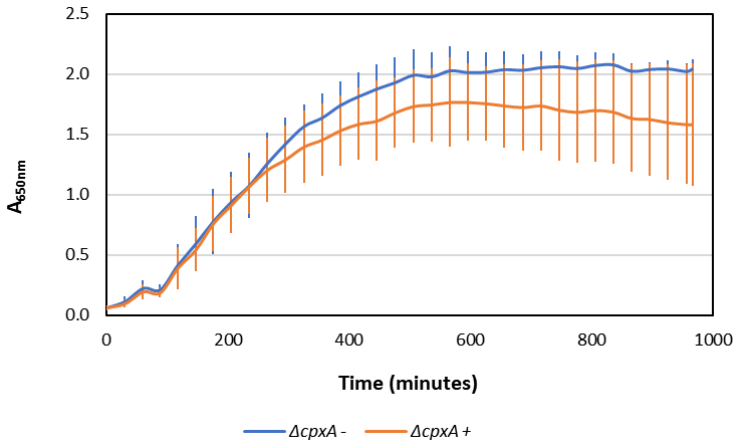

Control (-) and 0.01625 mM Octopirox (+) exposure at approx. 0.2 A_{650nm} of *ΔcpxR E. coli* with monitoring every 30 minutes for 16 hours.

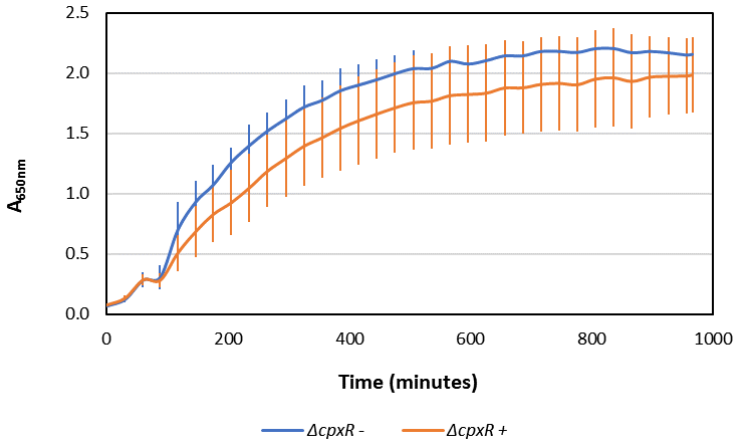

Control (-) and 0.01625 mM Octopirox (+) exposure at approx. 0.2 A_{650nm} of *ΔcpxP E. coli* with monitoring every 30 minutes for 16 hours.

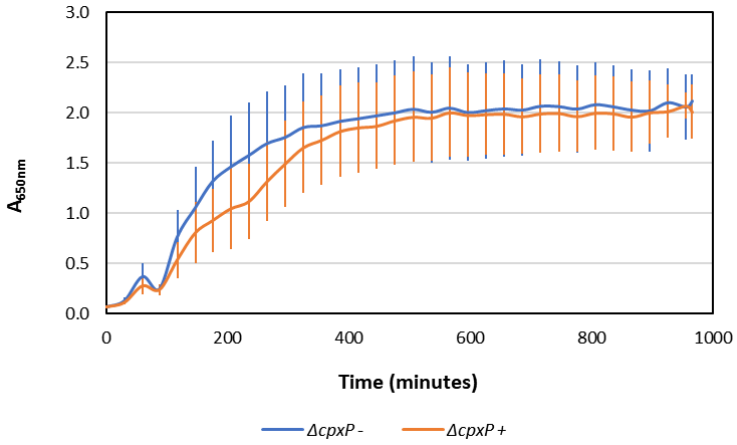

Control (-) and 0.01625 mM Octopirox (+) exposure at approx. 0.2 A_{650nm} of *ΔdsbA E. coli* with monitoring every 30 minutes for 16 hours.

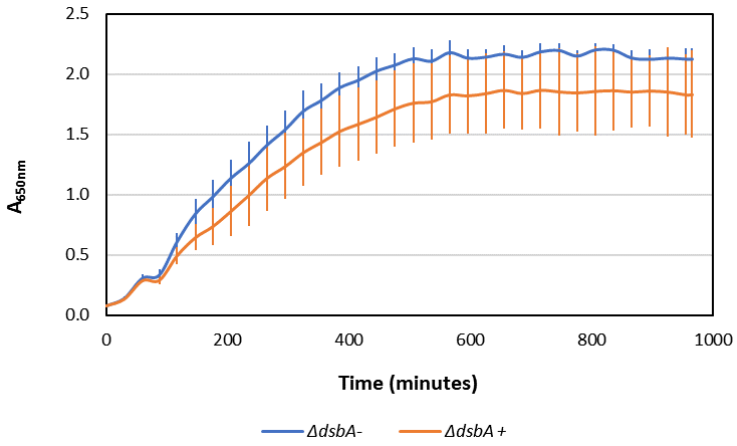

Appendix 3

TPEN & BCS

Representative data

[BCS]/μM	0	19.53	39.06	78.13	156.25	312.5	625	1250	[TPEN] /μM
0	100	113	115	100	80	3	- 0	0	
1562.50	113	113	105	91	65	1	- 0	0	
3125.00	117	115	103	99	76	11	- 0	0	
6250.00	105	116	104	88	81	11	- 0	0	
12500	108	119	89	82	81	43	1	0	
25000	105	104	77	71	49	26	6	1	
50000	83	88	71	68	60	38	14	1	
100000	59	65	72	57	53	42	15	1	

TPEN &GLDA

Representative data

[GLDA]/uM	0	19.53	39.06	78.13	156.25	312.5	625	[TPEN] /uM
0	115	121	113	76	30	- 0	0	
1953.13	130	129	120	89	53	16	- 0	
3906.25	125	131	128	105	66	19	6	
7812.50	124	127	131	103	74	19	- 0	
15625	112	115	112	100	68	13	- 0	
31250	111	114	97	41	1	- 0	- 0	
62500	47	9	1	- 0	1	0	- 0	
125000	- 0	0	0	- 0	1	0	- 0	

Bibliography

Abdul-Tehrani, H. *et al.* (1999) 'Ferritin mutants of *Escherichia coli* are iron deficient and growth impaired, and fur mutants are iron deficient.', *Journal of bacteriology*. American Society for Microbiology, 181(5), pp. 1415–28. Available at: http://www.ncbi.nlm.nih.gov/pubmed/10049371 (Accessed: 10 April 2018).

Adams, D. E. and West, S. C. (1995) 'Unwinding of Closed Circular DNA by the *Escherichia coli* RuvA and RuvB Recombination / Repair Proteins', *J. Mol. Biol*, 247, pp. 404–417. Available at: https://ac.els-cdn.com/S0022283685701490/1-s2.0-S0022283685701490-main.pdf?_tid=b21ccc11-3a19-4752-84dc-bcdcbadab1a4&acdnat=1526837620_f432ebdc96851dc74c704cd4789d29c4 (Accessed: 20 May 2018).

Akita, H., Nakashima, N. and Hoshino, T. (2016) 'Pyruvate production using engineered *Escherichia coli*.', *AMB Express*. Springer, 6(1), p. 94. doi: 10.1186/s13568-016-0259-z.

AkzoNobel (2014) 'Dissolvine ® GL technical brochure Dissolvine makes a difference'. Asterdam: Akzo Nobel N.V., pp. 1–16. Available at: https://chelates.akzonobel.com/siteassets/20170714-download-product-dissolvinegl-technicalbrochure.pdf (Accessed: 20 February 2018).

Alakomi, H.-L., Saarela, M. and Helander, I. M. (2003) 'Effect of EDTA on Salmonella enterica serovar Typhimurium involves a component not assignable to lipopolysaccharide release', *Microbiology*. Microbiology Society, 149(8), pp. 2015–2021. doi: 10.1099/mic.0.26312-0.

Alvarez-Añorve, L. I., Calcagno, M. L. and Plumbridge, J. (2005) 'Why does *Escherichia coli* grow more slowly on glucosamine than on N-acetylglucosamine? Effects of enzyme levels and allosteric activation of GlcN6P deaminase (NagB) on growth rates.', *Journal of Bacteriology*. American Society for Microbiology, 187(9), pp. 2974–82. doi: 10.1128/JB.187.9.2974-2982.2005.

Alvarez, M. *et al.* (1998) 'Triose-phosphate isomerase (TIM) of the psychrophilic bacterium Vibrio marinus. Kinetic and structural properties.', *The Journal of biological chemistry*. American Society for Biochemistry and Molecular Biology, 273(4), pp. 2199–206. doi: 10.1074/JBC.273.4.2199.

Anastassopoulou, J. and Theophanides, T. (1995) 'The Role of Metal Ions in Biological Systems and Medicine', in *Bioinorganic Chemistry*. Dordrecht: Springer Netherlands, pp. 209–218. doi: 10.1007/978-94-011-0255-1_17.

Andreini, C. *et al.* (2008) 'Metal ions in biological catalysis: From enzyme databases to general principles', *Journal of Biological Inorganic Chemistry*, 13(8), pp. 1205–1218.

Andreini, C., Bertini, I. and Rosato, A. (2004) 'A hint to search for metalloproteins in gene banks', *Bioinformatics*, 20(9), pp. 1373–1380. doi: 10.1093/bioinformatics/bth095.

Andrew, S. (2010) *Babraham Bioinformatics - FastQC A Quality Control tool for High Throughput Sequence Data*. Available at: https://www.bioinformatics.babraham.ac.uk/projects/fastqc/ (Accessed: 11 January 2018).

Andrews, J. M. (2001) ‘Determination of minimum inhibitory concentrations’, *Journal of Antimicrobial Chemotherapy*. Oxford University Press, 48(suppl_1), pp. 5–16. doi: 10.1093/jac/48.suppl_1.5.

Andrews, S. C. (1998) ‘Iron Storage in Bacteria’, *Advances in Microbial Physiology*. Academic Press, 40, pp. 281–351. doi: 10.1016/S0065-2911(08)60134-4.

Andrews, S. C., Robinson, A. K. and Rodríguez-Quiñones, F. (2003) ‘Bacterial iron homeostasis’, *FEMS Microbiology Letters*, 27(2–3), pp. 215–237. doi: 10.1016/S0168-6445(03)00055-X.

Anjem, A., Varghese, S. and Imlay, J. A. (2009) ‘Manganese import is a key element of the OxyR response to hydrogen peroxide in *Escherichia coli*’, *Molecular Microbiology*. Wiley/Blackwell (10.1111), 72(4), pp. 844–858. doi: 10.1111/j.1365-2958.2009.06699.x.

Apontoweil, P. and Berends, W. (1975) ‘Glutathione biosynthesis in *Escherichia coli* K 12. Properties of the enzymes and regulation.’, *Biochimica et biophysica acta*, 399(1), pp. 1–9. Available at: http://www.ncbi.nlm.nih.gov/pubmed/238647 (Accessed: 19 May 2018).

Arié, J. P., Sassoon, N. and Betton, J. M. (2001) ‘Chaperone function of FkpA, a heat shock prolyl isomerase, in the periplasm of *Escherichia coli*.’, *Molecular Microbiology*, 39(1), pp. 199–210. Available at: http://www.ncbi.nlm.nih.gov/pubmed/11123702 (Accessed: 21 March 2018).

Arif, M., Howard, J. and Tisa, L. S. (2014) ‘Calcium Homeostasis in *Escherichia coli*: Characterization of Mutants and Genome Expression of MG1655’, *Bangladesh Journal of Microbiology in Bangladesh J Microbiol*, 31(1), pp. 1–8. Available at: https://dx.doi.org/10.3329/bjm.v31i1.28457 (Accessed: 31 May 2018).

Aristarkhov, A. *et al.* (1996) ‘Translation of the adhE transcript to produce ethanol dehydrogenase requires RNase III cleavage in *Escherichia coli*.’, *Journal of bacteriology*, 178(14), pp. 4327–32. Available at: http://www.ncbi.nlm.nih.gov/pubmed/8763968 (Accessed: 8 April 2018).

Arslan, P. *et al.* (1985) ‘Cytosolic Ca2+ homeostasis in Ehrlich and Yoshida carcinomas. A new, membrane-permeant chelator of heavy metals reveals that these ascites tumor cell lines have normal cytosolic free Ca2+.’, *The Journal of Biological Chemistry*. American Society for Biochemistry and Molecular Biology, 260, pp. 2719–2727. Available at: http://www.jbc.org/content/260/5/2719.abstract (Accessed: 26 February 2018).

Ashburner, M. *et al.* (2000) ‘Gene Ontology: tool for the unification of biology’, *Nature Genetics*, 25(1), pp. 25–29. doi: 10.1038/75556.

Baba, T. *et al.* (2006) ‘Construction of *Escherichia coli* K-12 in-frame, single-gene knockout mutants: the Keio collection’, *Molecular Systems Biology*, 2, p. 2006.0008. doi: 10.1038/msb4100050.

Bae, W. *et al.* (2000) ‘*Escherichia coli* CspA-family RNA chaperones are transcription antiterminators.’, *Proceedings of the National Academy of Sciences of the United States of America*, 97(14), pp. 7784–9. Available at: http://www.ncbi.nlm.nih.gov/pubmed/10884409 (Accessed: 26

March 2018).

Bagg, A. and Neilands, J. B. (1987) ‘Ferric uptake regulation protein acts as a repressor, employing iron(II) as a cofactor to bind the operator of an iron transport operon in *Escherichia coli*’, *Biochemistry*. American Chemical Society, 26(17), pp. 5471–5477. doi: 10.1021/bi00391a039.

Ballantine, S. P. and Boxer, D. H. (1985) ‘Nickel-containing hydrogenase isoenzymes from anaerobically grown *Escherichia coli* K-12.’, *Journal of bacteriology*, 163(2), pp. 454–9. Available at: http://www.ncbi.nlm.nih.gov/pubmed/3894325 (Accessed: 19 April 2018).

Balouiri, M., Sadiki, M. and Ibnsouda, S. K. (2016) ‘Methods for in vitro evaluating antimicrobial activity: A review’, *Journal of Pharmaceutical Analysis*. Elsevier, 6(2), pp. 71–79. doi: 10.1016/J.JPHA.2015.11.005.

Balsalobre, C. *et al.* (1999) ‘Alterations in protein expression caused by the hha mutation in *Escherichia coli*: influence of growth medium osmolarity. - PubMed - NCBI’, *Journal of Bacteriology*, 181(10), pp. 3018–24. Available at: https://www.ncbi.nlm.nih.gov/pubmed/10322001 (Accessed: 30 March 2018).

Barak, R., Abouhamad, W. N. and Eisenbach, M. (1998) ‘Both acetate kinase and acetyl coenzyme A synthetase are involved in acetate-stimulated change in the direction of flagellar rotation in *Escherichia coli*.’, *Journal of bacteriology*, 180(4), pp. 985–8. Available at: http://www.ncbi.nlm.nih.gov/pubmed/9473056 (Accessed: 8 April 2018).

Bardey, V. *et al.* (2005) ‘Characterization of the molecular mechanisms involved in the differential production of erythrose-4-phosphate dehydrogenase, 3-phosphoglycerate kinase and class II fructose-1,6-bisphosphate aldolase in *Escherichia coli*’, *Molecular Microbiology*, 57(5), pp. 1265–1287. doi: 10.1111/j.1365-2958.2005.04762.x.

Barry, M. *et al.* (1974) ‘Long-term Chelation Therapy in Thalassaemia Major: Effect on Liver Iron Concentration, Liver Histology, and Clinical Progress’, *British Medical Journal*, 2, pp. 16–20. Available at: https://www.ncbi.nlm.nih.gov/pmc/articles/PMC1610120/pdf/brmedj01971-0028.pdf (Accessed: 31 May 2018).

Batchelor, E. *et al.* (2005) ‘The *Escherichia coli* CpxA-CpxR envelope stress response system regulates expression of the porins ompF and ompC.’, *Journal of bacteriology*. American Society for Microbiology, 187(16), pp. 5723–31. doi: 10.1128/JB.187.16.5723-5731.2005.

Bateman, A. *et al.* (2017) ‘UniProt: the universal protein knowledgebase’, *Nucleic Acids Research*. Oxford University Press, 45(D1), pp. D158–D169. doi: 10.1093/nar/gkw1099.

Beinert, H., Holm, R. H. and Münck, E. (1997) ‘Iron-Sulfur Clusters: Nature’s Modular, Multipurpose Structures’, *Science*, 277(5326), pp. 653–659. doi: 10.1126/science.270.5233.59.

Benovs, L. T. and Fridovichg, I. (1994) ‘*Escherichia coli* Expresses a Copper-and Zinc-containing Superoxide Dismutase*’, *The Journal of Biological Chemistry*, 269(41), pp. 25310–25314. Available

at: http://www.jbc.org/content/269/41/25310.full.pdf (Accessed: 23 April 2018).

Benz, R., Schmid, A. and Vos-Scheperkeuter, G. H. (1987) 'Mechanism of sugar transport through the sugar-specific LamB channel of*Escherichia coli* outer membrane', *The Journal of Membrane Biology*. Springer-Verlag, 100(1), pp. 21–29. doi: 10.1007/bf02209137.

Berenbaum, M. C. (1984) 'Synergy assessment with growth curves', *Journal of Infectious Diseases*, 150, p. 304.

Berg, B. L. *et al.* (1991) 'Nitrate-inducible formate dehydrogenase in *Escherichia coli* K-12. I. Nucleotide sequence of the fdnGHI operon and evidence that opal (UGA) encodes selenocysteine.', *The Journal of Biological Chemistry*, 266(33), pp. 22380–5. Available at: http://www.ncbi.nlm.nih.gov/pubmed/1834669 (Accessed: 8 April 2018).

Bergeron, R. J., Wiegand, J. and Brittenham, G. M. (1998) 'HBED: A potential alternative to deferoxamine for iron-chelating therapy.', *Blood*, 91(4), pp. 1446–52. Available at: http://www.ncbi.nlm.nih.gov/pubmed/9454776 (Accessed: 21 February 2018).

Bertin, P. *et al.* (1994) 'The H-NS protein is involved in the biogenesis of flagella in *Escherichia coli*.', *Journal of bacteriology*, 176(17), pp. 5537–40. Available at: http://www.ncbi.nlm.nih.gov/pubmed/8071234 (Accessed: 30 March 2018).

Bertini, I. and Cavallaro, G. (2007) 'Metals in the "omics" world: copper homeostasis and cytochrome c oxidase assembly in a new light', *Journal of Biological Inorganic Chemistry*, 13(1), pp. 3–14. doi: 10.1007/s00775-007-0316-9.

De Biase, D. *et al.* (1999) 'The response to stationary-phase stress conditions in *Escherichia coli*: role and regulation of the glutamic acid decarboxylase system.', *Molecular Microbiology*, 32(6), pp. 1198–211. Available at: http://www.ncbi.nlm.nih.gov/pubmed/10383761 (Accessed: 30 March 2018).

Bindereif, A. and Neilands, J. B. (1985) 'Promoter mapping and transcriptional regulation of the iron assimilation system of plasmid ColV-K30 in *Escherichia coli* K-12.', *Journal of Bacteriology*. American Society for Microbiology, 162(3), pp. 1039–1046. Available at: http://jb.asm.org/content/162/3/1039.abstract?ijkey=3d3e2326280432fbb06a38a72ef22f2b6a284681&keytype2=tf_ipsecsha (Accessed: 29 May 2018).

Binns, D. *et al.* (2009) 'QuickGO: a web-based tool for Gene Ontology searching', *Bioinformatics Applications Note*, 25(22), pp. 3045–304610. doi: 10.1093/bioinformatics/btp536.

Bleriot, C. *et al.* (2011) 'RcnB Is a Periplasmic Protein Essential for Maintaining Intracellular Ni and Co Concentrations in *Escherichia coli*', *Journal of Bacteriology*, 193(15), pp. 3785–3793. doi: 10.1128/JB.05032-11.

van Bokhorst-van de Veen, H. *et al.* (2011) 'Short- and long-term adaptation to ethanol stress and its cross-protective consequences in Lactobacillus plantarum.', *Applied and Environmental Microbiology*. American Society for Microbiology, 77(15), pp. 5247–56. doi: 10.1128/AEM.00515-

11.

Bonnefoy, E. and Rouviere-Yaniv, J. (1991) ‘HU and IHF, two homologous histone-like proteins of Escherichia coil, form different protein -DNA complexes with short DNA fragments’, *The EMBO Journal*, 10(3), pp. 687–696. Available at: https://www.ncbi.nlm.nih.gov/pmc/articles/PMC452703/pdf/emboj00101-0183.pdf (Accessed: 30 March 2018).

Böttger, E. C. (1989) ‘Rapid determination of bacterial ribosomal RNA sequences by direct sequencing of enzymatically amplified DNA’, *FEMS Microbiology Letters*. No longer published by Elsevier, 65(1), pp. 171–176. Available at: http://www.sciencedirect.com/science/article/pii/0378109789903868 (Accessed: 17 January 2018).

Bouvier, J. *et al.* (1998) ‘Interplay between global regulators of *Escherichia coli*: effect of RpoS, Lrp and H-NS on transcription of the gene osmC.’, *Molecular Microbiology*, 28(5), pp. 971–80. Available at: http://www.ncbi.nlm.nih.gov/pubmed/9663683 (Accessed: 30 March 2018).

Boyer, P. D. (1976) ‘Oxidation-Reduction, Part C’, in *The enzymes*. 3rd edn. New york: Academic Press, p. vol. XIII.

Bradford, M. M. (1976) ‘A rapid and sensitive method for the quantitation of microgram quantities of protein utilizing the principle of protein-dye binding.’, *Analytical biochemistry*, 72, pp. 248–54. Available at: http://www.ncbi.nlm.nih.gov/pubmed/942051 (Accessed: 15 January 2018).

Brandi, A. and Pon, C. L. (2012) ‘Expression of *Escherichia coli* cspA during early exponential growth at 37°C’, *Gene*, 492(2), pp. 382–388. doi: 10.1016/j.gene.2011.10.047.

Braun, V. and Braun, M. (2002) ‘Iron transport and signaling in *Escherichia coli*’, *FEBS Letters*. No longer published by Elsevier, 529(1), pp. 78–85. doi: 10.1016/S0014-5793(02)03185-X.

Brocklehurst, K. R. *et al.* (1999) ‘ZntR is a Zn(II)-responsive MerR-like transcriptional regulator of zntA in *Escherichia coli*.’, *Molecular Microbiology*, 31(3), pp. 893–902. Available at: http://www.ncbi.nlm.nih.gov/pubmed/10048032 (Accessed: 18 May 2018).

Brown, L. *et al.* (2002) ‘DksA affects ppGpp induction of RpoS at a translational level.’, *Journal of bacteriology*, 184(16), pp. 4455–65. Available at: http://www.ncbi.nlm.nih.gov/pubmed/12142416 (Accessed: 26 March 2018).

Cameron, J. C. *et al.* (2013) ‘Biogenesis of a Bacterial Organelle: The Carboxysome Assembly Pathway’, *Cell*, 155(5), pp. 1131–1140. doi: 10.1016/j.cell.2013.10.044.

Cassat, J. E. and Skaar, E. P. (2013) ‘Iron in infection and immunity.’, *Cell host & microbe*. Elsevier, 13(5), pp. 509–519. doi: 10.1016/j.chom.2013.04.010.

Chadani, Y. *et al.* (2017) ‘Intrinsic Ribosome Destabilization Underlies Translation and Provides an Organism with a Strategy of Environmental Sensing’, *Molecular Cell*, 68(3), p. 528–539.e5. doi: 10.1016/j.molcel.2017.10.020.

Chaturvedi, K. S. and Henderson, J. P. (2014) 'Pathogenic adaptations to host-derived antibacterial copper', *Frontiers in Cellular and Infection Microbiology*. Frontiers, 4, p. 3. doi: 10.3389/fcimb.2014.00003.

Chaves, S. *et al.* (2010) 'New Tris(hydroxypyridinones) as Iron and Aluminium Sequestering Agents: Synthesis, Complexation and In Vivo Studies', *Chemistry - A European Journal*, 16(34), pp. 10535–10545. doi: 10.1002/chem.201001335.

ChEBI (2016) *N,N,N',N'-tetrakis(2-pyridylmethyl)ethylenediamine (CHEBI:88217)*, *EMBL-EBI*. Available at: http://www.ebi.ac.uk/chebi/searchId.do?chebiId=CHEBI:88217 (Accessed: 21 February 2018).

Chen, D. *et al.* (2016) 'An improved Bathocuproine assay for accurate valence identification and quantification of copper bound by biomolecules', *Analytical Biochemistry*, 497, pp. 27–35. doi: 10.1016/j.ab.2015.12.014.

Chen, E. A. *et al.* (2014) 'Effect of RNA integrity on uniquely mapped reads in RNA-Seq', *BMC Research Notes*. BioMed Central, 7(1), p. 753. doi: 10.1186/1756-0500-7-753.

Chiancone, E. *et al.* (2000) 'The dodecameric ferritin from *Listeria innocua* contains a novel intersubunit iron-binding site', *Nature Structural Biology*. Nature Publishing Group, 7(1), pp. 38–43. doi: 10.1038/71236.

Chimienti, F. *et al.* (2001) 'Role of cellular zinc in programmed cell death: temporal relationship between zinc depletion, activation of caspases, and cleavage of Sp family transcription factors', *Biochemical Pharmacology*. Elsevier, 62(1), pp. 51–62. doi: 10.1016/S0006-2952(01)00624-4.

Cho, E. *et al.* (2010) 'Endogenous Zinc Mediates Apoptotic Programmed Cell Death in the Developing Brain', *Neurotoxicity Research*. Springer-Verlag, 17(2), pp. 156–166. doi: 10.1007/s12640-009-9085-2.

Cho, Y.-E. *et al.* (2007) 'Cellular Zn depletion by metal ion chelators (TPEN, DTPA and chelex resin) and its application to osteoblastic MC3T3-E1 cells', *Nutrition Research and Practice*, 1(1), p. 29. doi: 10.4162/nrp.2007.1.1.29.

Choi, S.-H. *et al.* (2017) 'Zinc-dependent regulation of zinc import and export genes by Zur.', *Nature communications*. Nature Publishing Group, 8, p. 15812. doi: 10.1038/ncomms15812.

Christman, M. F., Storz, G. and Ames, B. N. (1989) 'OxyR, a positive regulator of hydrogen peroxide-inducible genes in *Escherichia coli* and Salmonella typhimurium, is homologous to a family of bacterial regulatory proteins.', *Proceedings of the National Academy of Sciences of the United States of America*, 86(10), pp. 3484–8. Available at: http://www.ncbi.nlm.nih.gov/pubmed/2471187 (Accessed: 5 July 2018).

Clark, H. L. *et al.* (2016) 'Zinc and Manganese Chelation by Neutrophil S100A8/A9 (Calprotectin) Limits Extracellular *Aspergillus fumigatus* Hyphal Growth and Corneal Infection', *The Journal of*

Immunology, 196(1), pp. 336–344. doi: 10.4049/jimmunol.1502037.

Cloonan, N. *et al.* (2008) 'Stem cell transcriptome profiling via massive-scale mRNA sequencing', *Nature Methods*, 5(7), pp. 613–619. doi: 10.1038/NMETH.1223.

Clugston, S. L. *et al.* (1998) 'Overproduction and Characterization of a Dimeric Non-Zinc Glyoxalase I from *Escherichia coli* : Evidence for Optimal Activation by Nickel Ions † , ‡', *Biochemistry*, 37(24), pp. 8754–8763. doi: 10.1021/bi972791w.

Coloso, R. M., Drake, M. R. and Stipanuk, M. H. (1990) 'Effect of bathocuproine disulfonate, a copper chelator, on cyst(e)ine metabolism by freshly isolated rat hepatocytes.', *The American journal of physiology*. American Physiological Society Bethesda, MD , 259(3 Pt 1), pp. E443-50. doi: 10.1152/ajpendo.1990.259.3.E443.

Connell, I. *et al.* (1996) 'Type 1 fimbrial expression enhances *Escherichia coli* virulence for the urinary tract.', *Proceedings of the National Academy of Sciences of the United States of America*. National Academy of Sciences, 93(18), pp. 9827–32. doi: 10.1073/PNAS.93.18.9827.

Connolly, B. *et al.* (1991) 'Resolution of Holliday junctions in vitro requires the *Escherichia coli* ruvC gene product.', *Proceedings of the National Academy of Sciences of the United States of America*. National Academy of Sciences, 88(14), pp. 6063–7. doi: 10.1073/PNAS.88.14.6063.

Conter, A., Menchon, C. and Gutierrez, C. (1997) 'Role of DNA supercoiling and RpoS sigma factor in the osmotic and growth phase-dependent induction of the Gene osmE of *Escherichia coli* K12', *Journal of Molecular Biology*, 273(1), pp. 75–83. doi: 10.1006/jmbi.1997.1308.

Cotruvo, J. A. and Stubbe, J. (2012) 'Metallation and mismetallation of iron and manganese proteins in vitro and in vivo: the class I ribonucleotide reductases as a case study.', *Metallomics*. NIH Public Access, 4(10), pp. 1020–36. doi: 10.1039/c2mt20142a.

Courcelle, J. and Hanawalt, P. C. (2003) 'RecA-Dependent Recovery of Arrested DNA Replication Forks', *Annual Review of Genetics*, 37(1), pp. 611–646. doi: 10.1146/annurev.genet.37.110801.142616.

Cowart, R. E. (2002) 'Reduction of iron by extracellular iron reductases: implications for microbial iron acquisition', *Archives of Biochemistry and Biophysics*. Academic Press, 400(2), pp. 273–281. doi: 10.1016/S0003-9861(02)00012-7.

Cozi, E., Yost, F. J. and Fridovich, I. (1973) 'An Iron-contaiming Superoxide Dismutase', *THE JOURNAL OF BIOLOGICAL CHEMISTRY*, 248(14), pp. 4905–4908. Available at: http://www.jbc.org/content/248/14/4905.full.pdf (Accessed: 23 April 2018).

Croucher, N. J. and Thomson, N. R. (2010) 'Studying bacterial transcriptomes using RNA-seq', *Current Opinion in Microbiology*. Elsevier Current Trends, 13(5), pp. 619–624. doi: 10.1016/J.MIB.2010.09.009.

Crumbliss, A. L. (1990) 'Iron Bioavailability And The Coordination Chemistry Of Hydroxamic

Acids', *Coordination Chemistry Reviews*, 105, pp. 155–179. Available at: https://ac.els-cdn.com/001085459080021K/1-s2.0-001085459080021K-main.pdf?_tid=spdf-b817e433-0c44-4cd7-889f-37ea3edd183c&acdnat=1519665049_79e96f37400def53c7fe27beda77ef52 (Accessed: 26 February 2018).

Culotta, V. C., Yang, M. and O'Halloran, T. V. (2006) 'Activation of superoxide dismutases: Putting the metal to the pedal', *Biochimica et Biophysica Acta - Molecular Cell Research*, 1763(7), pp. 747–758. doi: 10.1016/j.bbamcr.2006.05.003.

Cusnir, R. *et al.* (2017) 'Hydroxypyridinone Chelators: From Iron Scavenging to Radiopharmaceuticals for PET Imaging with Gallium-68.', *International journal of molecular sciences*. Multidisciplinary Digital Publishing Institute (MDPI), 18(1). doi: 10.3390/ijms18010116.

D'Amato, R. F. *et al.* (1975) 'Effect of Calcium and Magnesium Ions on the Susceptibility of Pseudomonas Species to Tetracycline, Gentamicin Polymyxin B, and Carbenicillin', *Antimicrobial Agents and Chemotherapy*, 7(5), pp. 596–600. Available at: http://aac.asm.org/content/7/5/596.full.pdf (Accessed: 13 February 2018).

Dahl, J.-U. *et al.* (2011) 'The Identification of a Novel Protein Involved in Molybdenum Cofactor Biosynthesis in *Escherichia coli*', *Journal of Biological Chemistry*, 286(41), pp. 35801–35812. doi: 10.1074/jbc.M111.282368.

Dai, L. *et al.* (2018) 'Chiral DOTA chelators as an improved platform for biomedical imaging and therapy applications', *Nature Communications*. Nature Publishing Group, 9(1), p. 857. doi: 10.1038/s41467-018-03315-8.

Dai, X. *et al.* (2018) 'Slowdown of Translational Elongation in *Escherichia coli* under Hyperosmotic Stress.', *mBio*. American Society for Microbiology, 9(1), pp. e02375-17. doi: 10.1128/mBio.02375-17.

Dailey, H. A. *et al.* (2011) 'The *Escherichia coli* Protein YfeX Functions as a Porphyrinogen Oxidase, Not a Heme Dechelatase', *mBio*, 2(6), pp. e00248-11-e00248-11. doi: 10.1128/mBio.00248-11.

Dame, R. T. (2005) 'The role of nucleoid-associated proteins in the organization and compaction of bacterial chromatin', *Molecular Microbiology*, 56(4), pp. 858–870. doi: 10.1111/j.1365-2958.2005.04598.x.

Dame, R. T., Wyman, C. and Goosen, N. (2000) 'H-NS mediated compaction of DNA visualised by atomic force microscopy.', *Nucleic acids research*, 28(18), pp. 3504–10. Available at: http://www.ncbi.nlm.nih.gov/pubmed/10982869 (Accessed: 29 March 2018).

Damo, S. M. *et al.* (2013) 'Molecular basis for manganese sequestration by calprotectin and roles in the innate immune response to invading bacterial pathogens.', *Proceedings of the National Academy of Sciences of the United States of America*. National Academy of Sciences, 110(10), pp. 3841–6. doi: 10.1073/pnas.1220341110.

Darwin, K. H. (2015) '*Mycobacterium tuberculosis* and Copper: A Newly Appreciated Defense against an Old Foe?', *Journal of Biological Chemistry*, 290(31), pp. 18962–18966. doi: 10.1074/jbc.R115.640193.

Darwish, N. M. (1963) *The Action of Ethylenediaminetetraacetic Acid (EDTA) in Increasing Zinc Utilization in Poultry. itle*. University of California, Davis.

Datsenko, K. A. and Wanner, B. L. (2000) 'One-step inactivation of chromosomal genes in *Escherichia coli* K-12 using PCR products.', *Proceedings of the National Academy of Sciences of the United States of America*. National Academy of Sciences, 97(12), pp. 6640–5. doi: 10.1073/pnas.120163297.

Delcour, A. H. (2009) 'Outer membrane permeability and antibiotic resistance.', *Biochimica et biophysica acta*. NIH Public Access, 1794(5), pp. 808–16. doi: 10.1016/j.bbapap.2008.11.005.

Dip, P. V., Kamariah, N., Nartey, W., *et al.* (2014) 'Key roles of the *Escherichia coli* AhpC C-terminus in assembly and catalysis of alkylhydroperoxide reductase, an enzyme essential for the alleviation of oxidative stress', *Biochimica et Biophysica Acta (BBA) - Bioenergetics*, 1837(12), pp. 1932–1943. doi: 10.1016/j.bbabio.2014.08.007.

Dip, P. V., Kamariah, N., Subramanian Manimekalai, M. S., *et al.* (2014) 'Structure, mechanism and ensemble formation of the alkylhydroperoxide reductase subunits AhpC and AhpF from *Escherichia coli*', *Acta Crystallographica Section D Biological Crystallography*, 70(11), pp. 2848–2862. doi: 10.1107/S1399004714019233.

Djoko, K. Y. *et al.* (2014) 'Antimicrobial effects of copper(ii) bis(thiosemicarbazonato) complexes provide new insight into their biochemical mode of action', *Metallomics*. The Royal Society of Chemistry, 6(4), pp. 854–863. doi: 10.1039/C3MT00348E.

Djoko, K. Y. *et al.* (2015) 'Copper(II)-Bis(Thiosemicarbazonato) Complexes as Antibacterial Agents: Insights into Their Mode of Action and Potential as Therapeutics.', *Antimicrobial agents and chemotherapy*. American Society for Microbiology, 59(10), pp. 6444–53. doi: 10.1128/AAC.01289-15.

Djoko, K. Y., Donnelly, P. S. and McEwan, A. G. (2014) 'Inhibition of respiratory Complex I by copper(ii)-bis(thiosemicarbazonato) complexes', *Metallomics*. The Royal Society of Chemistry, 6(12), pp. 2250–2259. doi: 10.1039/C4MT00226A.

Donato, G. M. and Kawula, T. H. (1999) 'Phenotypic analysis of random hns mutations differentiate DNA-binding activity from properties of fimA promoter inversion modulation and bacterial motility.', *Journal of bacteriology*, 181(3), pp. 941–8. Available at: http://www.ncbi.nlm.nih.gov/pubmed/9922259 (Accessed: 30 March 2018).

Donato, R. (1999) 'Functional roles of S100 proteins, calcium-binding proteins of the EF-hand type', *Biochimica et Biophysica Acta (BBA) - Molecular Cell Research*. Elsevier, 1450(3), pp. 191–231. doi: 10.1016/S0167-4889(99)00058-0.

Doolittle, W. F. *et al.* (1975) 'Sequence studies on 16S ribosomal RNA from a blue-green alga', *Journal of Molecular Evolution*. Springer-Verlag, 4(4), pp. 307–315. doi: 10.1007/BF01732533.

Dorman, C. J. (2004) 'H-NS: a universal regulator for a dynamic genome', *Nature Reviews Microbiology*, 2(5), pp. 391–400. doi: 10.1038/nrmicro883.

Drzyzga, D. *et al.* (2017) 'Biodegradation of the aminopolyphosphonate DTPMP by the cyanobacterium *A nabaena variabilis* proceeds via a C-P lyase-independent pathway', *Environmental Microbiology*, 19(3), pp. 1065–1076. doi: 10.1111/1462-2920.13616.

Dubini, F. *et al.* (2011) 'In vitro Antimycotic Activity and Nail Permeation Models of a Piroctone Olamine (Octopirox) Containing Transungual Water Soluble Technology', *Arzneimittelforschung*. Editio Cantor Verlag, 55(08), pp. 478–483. doi: 10.1055/s-0031-1296892.

Dubrac, S. and Touati, D. (2000) 'Fur positive regulation of iron superoxide dismutase in *Escherichia coli*: functional analysis of the sodB promoter.', *Journal of bacteriology*. American Society for Microbiology, 182(13), pp. 3802–8. doi: 10.1128/JB.182.13.3802-3808.2000.

Dunderdale, H. J. *et al.* (1991) 'Formation and resolution of recombination intermediates by *E. coli*RecA and RuvC proteins', *Nature*, 354(6354), pp. 506–510. doi: 10.1038/354506a0.

Dupont, C. L. *et al.* (2006) 'Modern proteomes contain putative imprints of ancient shifts in trace metal geochemistry.', *Proceedings of the National Academy of Sciences of the United States of America*. National Academy of Sciences, 103(47), pp. 17822–7. doi: 10.1073/pnas.0605798103.

Edwards, A. N. *et al.* (2011) 'Circuitry linking the Csr and stringent response global regulatory systems', *Molecular Microbiology*, 80(6), pp. 1561–1580. doi: 10.1111/j.1365-2958.2011.07663.x.

Eggleston, A. K., Mitchell, A. H. and West, S. C. (1997) 'In Vitro Reconstitution of the Late Steps of Genetic Recombination in *E. coli*', *Cell*. Cell Press, 89(4), pp. 607–617. doi: 10.1016/S0092-8674(00)80242-1.

Ehresmann, C. *et al.* (1975) 'Primary sequence of the 16S ribosomal RNA of *Escherichia coli*', *Nucleic Acids Research*. Oxford University Press, 2(2), pp. 265–278. doi: 10.1093/nar/2.2.265.

van Eijkeren, J. C. H. *et al.* (2017) 'Modeling the effect of succimer (DMSA; dimercaptosuccinic acid) chelation therapy in patients poisoned by lead', *Clinical Toxicology*. Taylor & Francis, 55(2), pp. 133–141. doi: 10.1080/15563650.2016.1263855.

Eitinger, T. and Mandrand-Berthelot, M.-A. (2000) 'Nickel transport systems in microorganisms', *Archives of Microbiology*. Springer-Verlag, 173(1), pp. 1–9. doi: 10.1007/s002030050001.

Erni, B., Zanolari, B. and Kochers, H. P. (1987) 'The Mannose Permease of *Escherichia coli* Consists of Three Different Proteins Amino Acid Sequence and Function in Sugar transport, Sugar phosphorylation, and penetration of Phage X DNA', *The Journal of Biological Chemistry*, 262(11), pp. 5238–5247. Available at: http://www.jbc.org/content/262/11/5238.full.pdf (Accessed: 7 February 2018).

Escolar, L., Pérez-Martín, J. and de Lorenzo, V. (1999) 'Opening the iron box: transcriptional metalloregulation by the Fur protein.', *Journal of bacteriology*. American Society for Microbiology, 181(20), pp. 6223–9. Available at: http://www.ncbi.nlm.nih.gov/pubmed/10515908 (Accessed: 17 May 2018).

Falconi, M. *et al.* (1993) 'Expression of the gene encoding the major bacterial nucleotide protein H-NS is subject to transcriptional auto-repression.', *Molecular Microbiology*, 10(2), pp. 273–82. Available at: http://www.ncbi.nlm.nih.gov/pubmed/7934818 (Accessed: 30 March 2018).

Farr, S. B. and Kogoma, T. (1991) 'Oxidative Stress Responses in *Escherichia coli* and Salmonella typhimurium', *Microbiological Reviews*, 55(4), pp. 561–585. Available at: http://mmbr.asm.org/content/55/4/561.full.pdf (Accessed: 23 April 2018).

Faulkner, K. M., Liochev, S. I. and Fridovich, I. (1994) 'Stable Mn(III) porphyrins mimic superoxide dismutase in vitro and substitute for it in vivo.', *The Journal of biological chemistry*. American Society for Biochemistry and Molecular Biology, 269, pp. 23471–23476. Available at: http://www.jbc.org/content/269/38/23471.short (Accessed: 10 April 2018).

Fayet, O., Ziegelhoffer, T. and Georgopoulos, C. (1989) 'The groES and groEL Heat Shock Gene Products of *Escherichia coli* Are Essential for Bacterial Growth at All Temperatures', *Journal of Bacteriology*, 171(3), pp. 1379–1385. Available at: http://jb.asm.org/content/171/3/1379.full.pdf (Accessed: 21 March 2018).

Ferguson, G. P. and Booth, I. R. (1998) 'Importance of glutathione for growth and survival of *Escherichia coli* cells: detoxification of methylglyoxal and maintenance of intracellular K+.', *Journal of bacteriology*. American Society for Microbiology, 180(16), pp. 4314–8. Available at: http://www.ncbi.nlm.nih.gov/pubmed/9696786 (Accessed: 10 June 2018).

Finkelstein, J. (2009) 'Metalloproteins', *Nature*, 460(7257), p. 813.

Finnegan, S. and Percival, S. L. (2015) 'EDTA: An Antimicrobial and Antibiofilm Agent for Use in Wound Care', *Advances in Wound Care*. Mary Ann Liebert, Inc. 140 Huguenot Street, 3rd Floor New Rochelle, NY 10801 USA , 4(7), pp. 415–421. doi: 10.1089/wound.2014.0577.

Folorunso, O. S., Amisu, K. O. and Ogungbe, B. F. (2015) 'EDTA-Treated Cell Membrane and Multiple Subculturing Affect the Virulence of Enteropathogenic Bacteria', *Research Journal of Microbiology*, 10(4), pp. 158–169. doi: 10.3923/jm.2015.158.169.

Fox, G. *et al.* (1980) 'The phylogeny of prokaryotes', *Science*, 209(4455), pp. 457–463. doi: 10.1126/science.6771870.

Francetic, O. *et al.* (2000) 'Expression of the endogenous type II secretion pathway in *Escherichia coli* leads to chitinase secretion', *The EMBO Journal*, 19(24), pp. 6697–6703. doi: 10.1093/emboj/19.24.6697.

Freedman, J. C. (2012) 'Ionophores in Planar Lipid Bilayers', in *Cell Physiology Source Book*.

Elsevier, pp. 61–66. doi: 10.1016/B978-0-12-387738-3.00004-4.

Fujii, R. (1979) *The complexing and adsorption of cadmium in soils in the presence of EDTA and NTA.*

Futai, M., Noumi, T. and Maeda, M. (1989) 'ATP SYNTHASE (H+ -ATPase): Results by Combined Biochemical and Molecular Biological Approaches', *Annual Review of Biochemistry*, 58, pp. 111–136.

Gallego Romero, I. *et al.* (2014) 'RNA-seq: impact of RNA degradation on transcript quantification', *BMC Biology*. BioMed Central, 12(1), p. 42. doi: 10.1186/1741-7007-12-42.

García-Sáez, I. *et al.* (2003) 'The 1.5-Å Structure of *Chryseobacterium meningosepticum* Zinc β-Lactamase in Complex with the Inhibitor, D-Captopril', *Journal of Biological Chemistry*, 278(26), pp. 23868–23873. doi: 10.1074/jbc.M301062200.

Giangrossi, M. *et al.* (2005) 'Antagonistic Role of H-NS and GadX in the Regulation of the Glutamate Decarboxylase-dependent Acid Resistance System in *Escherichia coli*', *Journal of Biological Chemistry*, 280(22), pp. 21498–21505. doi: 10.1074/jbc.M413255200.

Giangrossi, M., Gualerzi, C. O. and Pon, C. L. (2001) 'Mutagenesis of the downstream region of the *Escherichia coli* hns promoter.', *Biochimie*, 83(2), pp. 251–9. Available at: http://www.ncbi.nlm.nih.gov/pubmed/11278076 (Accessed: 26 March 2018).

Gläser, R. *et al.* (2005) 'Antimicrobial psoriasin (S100A7) protects human skin from *Escherichia coli* infection', *Nature Immunology*. Nature Publishing Group, 6(1), pp. 57–64. doi: 10.1038/ni1142.

Goldberg, S. S. *et al.* (1983) 'Release of lipopolysaccharide (LPS) from cell surface of Trypanosoma cruzi by EDTA', *International Journal for Parasitology*, 13(1), pp. 11–18.

van Gool, A. J. *et al.* (1999) 'Assembly of the *Escherichia coli* RuvABC resolvasome directs the orientation of holliday junction resolution.', *Genes & development*. Cold Spring Harbor Laboratory Press, 13(14), pp. 1861–70. Available at: http://www.ncbi.nlm.nih.gov/pubmed/10421637 (Accessed: 17 June 2018).

Górna, M. W. *et al.* (2010) 'The regulatory protein RraA modulates RNA-binding and helicase activities of the *E. coli* RNA degradosome.', *RNA (New York, N.Y.)*. Cold Spring Harbor Laboratory Press, 16(3), pp. 553–62. doi: 10.1261/rna.1858010.

Gort, A. S., Ferber, D. M. and Imlay, J. A. (1999) 'The regulation and role of the periplasmic copper, zinc superoxide dismutase of *Escherichia coli*.', *Molecular Microbiology*, 32(1), pp. 179–91. Available at: http://www.ncbi.nlm.nih.gov/pubmed/10216871 (Accessed: 20 May 2018).

Gragerov, A. *et al.* (1992) 'Cooperation of GroEL/GroES and DnaK/DnaJ heat shock proteins in preventing protein misfolding in *Escherichia coli*.', *Proceedings of the National Academy of Sciences of the United States of America*, 89(21), pp. 10341–4.

Grass, G., Otto, M., *et al.* (2005) 'FieF (YiiP) from *Escherichia coli* mediates decreased cellular accumulation of iron and relieves iron stress', *Archives of Microbiology*, 183(1), pp. 9–18. doi: 10.1007/s00203-004-0739-4.

Grass, G., Franke, S., *et al.* (2005) 'The metal permease ZupT from *Escherichia coli* is a transporter with a broad substrate spectrum.', *Journal of bacteriology*. American Society for Microbiology, 187(5), pp. 1604–11. doi: 10.1128/JB.187.5.1604-1611.2005.

Grass, G. and Rensing, C. (2001) 'Genes involved in copper homeostasis in *Escherichia coli*.', *Journal of bacteriology*. American Society for Microbiology (ASM), 183(6), pp. 2145–7. doi: 10.1128/JB.183.6.2145-2147.2001.

Grey, B. and Steck, T. R. (2001) 'Concentrations of copper thought to be toxic to *Escherichia coli* can induce the viable but nonculturable condition.', *Applied and environmental Microbiology*. American Society for Microbiology (ASM), 67(11), pp. 5325–7. doi: 10.1128/AEM.67.11.5325-5327.2001.

Griffiths, A. *et al.* (2000) 'Discovery of the lac system: negative control', in *An introduction to Genetic Analysis*. 7th edn. New York: W.H.Freeman & Co Ltd, pp. 400–412. Available at: https://www.ncbi.nlm.nih.gov/books/NBK21954/#_A1999_.

Grover, H. S., Yadav, A. and Nanda, P. (2011) 'A comparative evaluation of the efficacy of Citric Acid, Ethylene Diamine Tetra Acetic Acid (EDTA) and Tetracycline Hydrochloride as root biomodification agents: An in vitro SEM study', *International Journal of Contemporary Dentistry*, 2(3). Available at: https://search.proquest.com/openview/b4eb1dc2cc92f9dca2a67925f12597ee/1?pq-origsite=gscholar&cbl=686353 (Accessed: 9 June 2018).

Grunberg-Manago, M. (1999) 'Messenger RNA Stability and Its Role in Control of Gene Expression in Bacteria and Phages', *Annual Review of Genetics*, 33(1), pp. 193–227. doi: 10.1146/annurev.genet.33.1.193.

Guedon, E. and Helmann, J. D. (2003) 'Origins of metal ion selectivity in the DtxR/MntR family of metalloregulators', *Molecular Microbiology*. Wiley/Blackwell (10.1111), 48(2), pp. 495–506. doi: 10.1046/j.1365-2958.2003.03445.x.

Guo, X. *et al.* (2013) 'Treatment of *Escherichia coli* BW25113 with Subinhibitory Levels of Kanamycin Results in Antibiotic Cross-Resistance and TolC Upregulation', *Journal of Experimental Microbiology and Immunology (JEMI)*, 17, pp. 19–23. Available at: https://microbiology.ubc.ca/sites/default/files/roles/drupal_ungrad/JEMI/17/04.3E.pdf (Accessed: 15 February 2018).

Gustavsson, N., Diez, A. and Nyström, T. (2002) 'The universal stress protein paralogues of *Escherichia coli* are co-ordinately regulated and co-operate in the defence against DNA damage.', *Molecular Microbiology*, 43(1), pp. 107–17. Available at: http://www.ncbi.nlm.nih.gov/pubmed/11849540 (Accessed: 11 April 2018).

Gutierrez, C., Gordia, S. and Bonnassie, S. (1995) 'Characterization of the osmotically inducible gene

osmE of *Escherichia coli* K-12.', *Molecular Microbiology*, 16(3), pp. 553–63. Available at: http://www.ncbi.nlm.nih.gov/pubmed/7565114 (Accessed: 9 April 2018).

Haase, H. and Rink, L. (2014) 'Multiple impacts of zinc on immune function', *Metallomics*. The Royal Society of Chemistry, 6(7), p. 1175. doi: 10.1039/c3mt00353a.

Hall, M. J., Middleton, R. F. and Westmacott, D. (1983) 'The fractional inhibitory concentration (FIC) index as a measure of synergy', *Journal of Antimicrobial Chemotherapy*, 11, pp. 427–433. Available at: https://watermark.silverchair.com/11-5-427.pdf?token=AQECAHi208BE49Ooan9kkhW_Ercy7Dm3ZL_9Cf3qfKAc485ysgAAAbUwggGxBgkqhkiG9w0BBwagggGiMIIBngIBADCCAZcGCSqGSIb3DQEHATAeBglghkgBZQMEAS4wEQQMQE8xZbwItb-k0NoRAgEQgIIBaD5YpfM7ktdKGb_pIV-4s3TQlgXXeJOR7eIXT1NSx7KKCv (Accessed: 13 February 2018).

Hamilton-Miller, J. M. T. (1985) 'Rationalization of terminology and methodology in the study of antibiotic interaction', *Journal of Antimicrobial Chemotherapy*. Oxford University Press, 15(6), pp. 655–657. doi: 10.1093/jac/15.6.655.

Hansen, S., Lewis, K. and Vulić, M. (2008) 'Role of global regulators and nucleotide metabolism in antibiotic tolerance in *Escherichia coli*.', *Antimicrobial agents and chemotherapy*. American Society for Microbiology, 52(8), pp. 2718–26. doi: 10.1128/AAC.00144-08.

Hantash, F. M. and Earhart, C. F. (2000) 'Membrane association of the *Escherichia coli* enterobactin synthase proteins EntB/G, EntE, and EntF.', *Journal of bacteriology*. American Society for Microbiology, 182(6), pp. 1768–73. doi: 10.1128/JB.182.6.1768-1773.2000.

Hantke, K. (1976) 'Phage T6--colicin K receptor and nucleoside transport in *Escherichia coli*.', *FEBS letters*, 70(1), pp. 109–12. Available at: http://www.ncbi.nlm.nih.gov/pubmed/791677 (Accessed: 9 April 2018).

Hantke, K. (1981) 'Regulation of ferric iron transport in *Escherichia coli* K12: Isolation of a constitutive mutant', *Molecular & General Genetics MGG* . Springer-Verlag, 182(2), pp. 288–292. doi: 10.1007/BF00269672.

Hantke, K. (2001) 'Iron and metal regulation in bacteria', *Current Opinion in Microbiology*, 4(2), pp. 172–177. doi: 10.1016/S1369-5274(00)00184-3.

Hassan, H. and Fridovich, I. (1977) 'Regulation of the Synthesis of Superoxide Dismutase Escherichia', *Survival*, (8), pp. 7667–7672.

Hassan, H. and Fridovich, I. (1977) 'Regulation of the Synthesis of Superoxide Dismutase in *Escherichia coli*. Induction by methyl viologen', *The Journal of Biological Chemistry*, 252(21), pp. 7667–7672. Available at: https://www.researchgate.net/profile/Hosni_Hassan/publication/22803285_Regulation_of_the_synthesis_of_superoxide_dismutase_in_Escherichia_coli_Induction_by_methyl_viologen/links/0046351406c7feb482000000/Regulation-of-the-synthesis-of-superoxide-dismutase- (Accessed: 5 March 2018).

Hassan, H. M. *et al.* (1977) 'Regulation of the synthesis of superoxide dismutase in *Escherichia coli*. Induction by methyl viologen', *Article in Journal of Biological Chemistry*.

Hassan, H. M. and Sun, H.-C. C. (1992) 'Regulatory roles of Fnr, Fur, and Arc in expression of manganese-containing superoxide dismutase in *Escherichia coli*.', *Proceedings of the National Academy of Sciences of the United States of America*, 89(8), pp. 3217–21. Available at: http://www.pubmedcentral.nih.gov/articlerender.fcgi?artid=48837&tool=pmcentrez&rendertype=abstract.

Heine, H. G., Kyngdon, J. and Ferenci, T. (1987) 'Sequence determinants in the lamB gene of *Escherichia coli* influencing the binding and pore selectivity of maltoporin.', *Gene*, 53(2–3), pp. 287–92. Available at: http://www.ncbi.nlm.nih.gov/pubmed/3301537 (Accessed: 9 April 2018).

Hensley, M. P. (2012) *Zinc Homeostasis in E. coli*. Miami University. Available at: https://etd.ohiolink.edu/pg_10?0::NO:10:P10_ACCESSION_NUM:miami1333655875 (Accessed: 30 May 2018).

Hesslinger, C., Fairhurst, S. A. and Sawers, G. (1998) 'Novel keto acid formate-lyase and propionate kinase enzymes are components of an anaerobic pathway in *Escherichia coli* that degrades L-threonine to propionate.', *Molecular Microbiology*, 27(2), pp. 477–92. Available at: http://www.ncbi.nlm.nih.gov/pubmed/9484901 (Accessed: 8 April 2018).

Hetrick, E. M. and Schoenfisch, M. H. (2006) 'Reducing implant-related infections: active release strategies', *Chemical Society Reviews*, 35(9), pp. 780–789. doi: 10.1039/b515219b.

Hickson, I. D. *et al.* (1985) 'Reconstitution of RecBC DNase activity from purified *Escherichia coli* RecB and RecC proteins.', *The Journal of biological chemistry*, 260(2), pp. 1224–9. Available at: http://www.ncbi.nlm.nih.gov/pubmed/3155726 (Accessed: 20 May 2018).

Higashi, K. *et al.* (2016) 'H-NS Facilitates Sequence Diversification of Horizontally Transferred DNAs during Their Integration in Host Chromosomes', *PLOS Genetics*. Edited by M. El Karoui, 12(1), p. e1005796. doi: 10.1371/journal.pgen.1005796.

Hillar, A. *et al.* (2000) 'Modulation of the activities of catalase-peroxidase HPI of *Escherichia coli* by site-directed mutagenesis.', *Biochemistry*, 39(19), pp. 5868–75. Available at: http://www.ncbi.nlm.nih.gov/pubmed/10801338 (Accessed: 20 May 2018).

Hille, R. (2002) 'Molybdenum and tungsten in biology', *Trends in Biochemical Sciences*. Elsevier Current Trends, 27(7), pp. 360–367. doi: 10.1016/S0968-0004(02)02107-2.

Hirakawa, H. *et al.* (2003) 'Beta-Lactam resistance modulated by the overexpression of response regulators of two-component signal transduction systems in *Escherichia coli*', *Journal of Antimicrobial Chemotherapy*, 52(4), pp. 576–582. doi: 10.1093/jac/dkg406.

Hoeser, J. *et al.* (2014) 'Subunit CydX of *Escherichia coli* cytochrome bd ubiquinol oxidase is essential for assembly and stability of the di-heme active site', *FEBS Letters*. No longer published by

Elsevier, 588(9), pp. 1537–1541. doi: 10.1016/J.FEBSLET.2014.03.036.

Hogan, D. J. *et al.* (2008) 'Diverse RNA-Binding Proteins Interact with Functionally Related Sets of RNAs, Suggesting an Extensive Regulatory System', *PLoS Biology*. Edited by Sean R. Eddy. Public Library of Science, 6(10), p. e255. doi: 10.1371/journal.pbio.0060255.

Hommais, F. *et al.* (2001) 'Large-scale monitoring of pleiotropic regulation of gene expression by the prokaryotic nucleoid-associated protein, H-NS.', *Molecular Microbiology*, 40(1), pp. 20–36. Available at: http://www.ncbi.nlm.nih.gov/pubmed/11298273 (Accessed: 29 March 2018).

Hood, M. I. and Skaar, E. P. (2012) 'Nutritional immunity: transition metals at the pathogen-host interface.', *Nature reviews. Microbiology*. NIH Public Access, 10(8), pp. 525–37. doi: 10.1038/nrmicro2836.

Hopkin, K. A., Papazian, M. A. and Steinman, H. M. (1992) 'Functional Differences between Manganese and Iron Superoxide Dismutases in *Escherichia coli* K-12', *The Journal of biological chemistry*, 267(34), pp. 24253–24258. Available at: http://www.jbc.org/content/267/34/24253.full.pdf (Accessed: 11 July 2018).

Hu, K. H. *et al.* (1996) 'Overproduction of three genes leads to camphor resistance and chromosome condensation in *Escherichia coli*.', *Genetics*, 143(4), pp. 1521–32. Available at: http://www.ncbi.nlm.nih.gov/pubmed/8844142 (Accessed: 26 March 2018).

Huang, H.-T. *et al.* (2018) 'Co(II) and Ni(II) binding of the *Escherichia coli* transcriptional repressor RcnR orders its N terminus, alters helix dynamics, and reduces DNA affinity.', *The Journal of biological chemistry*. American Society for Biochemistry and Molecular Biology, 293(1), pp. 324–332. doi: 10.1074/jbc.RA117.000398.

Hube, M., Blokesch, M. and Böck, A. (2002) 'Network of hydrogenase maturation in *Escherichia coli*: role of accessory proteins HypA and HybF.', *Journal of bacteriology*. American Society for Microbiology, 184(14), pp. 3879–85. doi: 10.1128/JB.184.14.3879-3885.2002.

Hudson, A. J. *et al.* (1993) 'Overproduction, purification and characterization of the *Escherichia coli* ferritin.', *European journal of biochemistry*, 218(3), pp. 985–95. Available at: http://www.ncbi.nlm.nih.gov/pubmed/8281950 (Accessed: 17 May 2018).

Hyun, H. J. *et al.* (2001) 'Depletion of intracellular zinc and copper with TPEN results in apoptosis of cultured human retinal pigment epithelial cells.', *Investigative ophthalmology & visual science*, 42(2), pp. 460–5. Available at: http://www.ncbi.nlm.nih.gov/pubmed/11157883 (Accessed: 5 June 2018).

Imlay, K. R. and Imlay, J. A. (1996) 'Cloning and analysis of sodC, encoding the copper-zinc superoxide dismutase of *Escherichia coli*.', *Journal of bacteriology*, 178(9), pp. 2564–71. Available at: http://www.ncbi.nlm.nih.gov/pubmed/8626323 (Accessed: 14 June 2018).

Inoue, T. *et al.* (2007) 'Genome-Wide Screening of Genes Required for Swarming Motility in *Escherichia coli* K-12', *Journal of Bacteriology*, 189(3), pp. 950–957. doi: 10.1128/JB.01294-06.

Iobbi-Nivol, C. and Leimkühler, S. (2013) ‘Molybdenum enzymes, their maturation and molybdenum cofactor biosynthesis in *Escherichia coli*’, *Biochimica et Biophysica Acta (BBA) - Bioenergetics*. Elsevier, 1827(8–9), pp. 1086–1101. doi: 10.1016/J.BBABIO.2012.11.007.

Irving, H. and Williams, R. J. P. (1953) ‘637. The stability of transition-metal complexes’, *Journal of the Chemical Society (Resumed)*. The Royal Society of Chemistry, pp. 3192–3210. doi: 10.1039/jr9530003192.

Iwig, J. S., Rowe, J. L. and Chivers, P. T. (2006) ‘Nickel homeostasis in *Escherichia coli* the rcnR-rcnA efflux pathway and its linkage to NikR function’, *Molecular Microbiology*, 62(1), pp. 252–262. doi: 10.1111/j.1365-2958.2006.05369.x.

Jachula, J., Kolodyńska, D. and Hubicki, Z. (2011) ‘Sorption of Cu(II) and Ni(II) ions in the presence of the methylglycinediacetic acid by microporous ion exchangers and sorbents from aqueos solutions’, *Central European Journal of Chemistry*, 9(1), pp. 52–85. doi: 10.2478/s11532-010-0115-y.

Jacob, F. and Monod, J. (1961) ‘Genetic regulatory mechanisms in the synthesis of proteins’, *Journal of Molecular Biology*. Academic Press, 3(3), pp. 318–356. doi: 10.1016/S0022-2836(61)80072-7.

Jakubovics, N. S. and Jenkinson, H. F. (2001) ‘Out of the iron age: new insights into the critical role of manganese homeostasis in bacteria’, *Microbiology*. Microbiology Society, 147(7), pp. 1709–1718. doi: 10.1099/00221287-147-7-1709.

Jawetz, E. *et al.* (1955) ‘A Laboratory Test for Bacterial Sensitivity to Combinations of Antibiotics.’, *American Journal of Clinical Pathology*. Williams & Wilkins Co, 25(9), pp. 1016–1031. Available at: https://www.cabdirect.org/cabdirect/abstract/19562700514 (Accessed: 13 February 2018).

Jennings, M. P. and Beacham, I. R. (1990) ‘Analysis of the *Escherichia coli* gene encoding L-asparaginase II, ansB, and its regulation by cyclic AMP receptor and FNR proteins.’, *Journal of bacteriology*, 172(3), pp. 1491–8. Available at: http://www.ncbi.nlm.nih.gov/pubmed/2407723 (Accessed: 3 April 2018).

Jerlström, P. G., Liu, J. and Beacham, I. R. (1987) ‘Regulation of *Escherichia coli*-asparaginase II and l-aspartase by the fnr gene-product’, *FEMS Microbiology Letters*. No longer published by Elsevier, 41(2), pp. 127–130. Available at: https://www.sciencedirect.com/science/article/pii/0378109787902242 (Accessed: 3 April 2018).

Jiang, W., Fang, L. and Inouye, M. (1996) ‘The role of the 5’-end untranslated region of the mRNA for CspA, the major cold-shock protein of *Escherichia coli*, in cold-shock adaptation.’, *Journal of bacteriology*, 178(16), pp. 4919–25. Available at: http://www.ncbi.nlm.nih.gov/pubmed/8759856 (Accessed: 26 March 2018).

Jiang, W., Hou, Y. and Inouye, M. (1997) ‘CspA, the major cold-shock protein of *Escherichia coli*, is an RNA chaperone.’, *The Journal of biological chemistry*, 272(1), pp. 196–202. Available at: http://www.ncbi.nlm.nih.gov/pubmed/8995247 (Accessed: 26 March 2018).

Johnston, D. *et al.* (2006) ‘Specificity of DNA Binding and Dimerization by CspE from *Escherichia coli*’, *Journal of Biological Chemistry*, 281(52), pp. 40208–40215. doi: 10.1074/jbc.M606414200.

Jones, H. M. and Gunsalus, R. P. (1987) ‘Regulation of *Escherichia coli* fumarate reductase (frdABCD) operon expression by respiratory electron acceptors and the fnr gene product.’, *Journal of bacteriology*. American Society for Microbiology (ASM), 169(7), pp. 3340–9. Available at: http://www.ncbi.nlm.nih.gov/pubmed/3298218 (Accessed: 5 April 2018).

Jones, P. G. *et al.* (1992) ‘DNA gyrase, CS7.4, and the cold shock response in *Escherichia coli*.’, *Journal of bacteriology*, 174(18), pp. 5798–802. Available at: http://www.ncbi.nlm.nih.gov/pubmed/1325964 (Accessed: 26 March 2018).

Jormakka, M. *et al.* (2002) ‘Molecular Basis of Proton Motive Force Generation: Structure of Formate Dehydrogenase-N’, *Science*, 295(5561), pp. 1863–1868. doi: 10.1126/science.1068186.

Jörnvall, H. (1977) ‘Differences between alcohol dehydrogenases. Structural properties and evolutionary aspects.’, *European journal of biochemistry*, 72(3), pp. 443–52. Available at: http://www.ncbi.nlm.nih.gov/pubmed/320001 (Accessed: 8 April 2018).

Juárez, A. *et al.* (2000) ‘Interaction of the nucleoid-associated proteins Hha and H-NS to modulate expression of the hemolysin operon in *Escherichia coli*.’, *Advances in experimental medicine and biology*, 485, pp. 127–31. Available at: http://www.ncbi.nlm.nih.gov/pubmed/11109097 (Accessed: 30 March 2018).

Juttukonda, L. J. and Skaar, E. P. (2015) ‘Manganese homeostasis and utilization in pathogenic bacteria.’, *Molecular Bcrobiology*. NIH Public Access, 97(2), pp. 216–28. doi: 10.1111/mmi.13034.

Kaga, N. *et al.* (2002) ‘RNase G-Dependent Degradation of the eno mRNA Encoding a Glycolysis Enzyme Enolase in *Escherichia coli*’, *Biosci. Biotechnol. Biochem*, 66(10), pp. 2216–2220. Available at: https://www.tandfonline.com/doi/pdf/10.1271/bbb.66.2216 (Accessed: 7 April 2018).

Kakuda, H. *et al.* (1994) ‘Construction of Pta-Ack pathway deletion mutants of *Escherichia coli* and characteristic growth profiles of the mutants in a rich medium.’, *Bioscience, biotechnology, and biochemistry*, 58(12), pp. 2232–5. Available at: http://www.ncbi.nlm.nih.gov/pubmed/7765717 (Accessed: 8 April 2018).

Kaluarachchi, H., Zhang, J. W. and Zamble, D. B. (2011) ‘*Escherichia coli* SlyD, More Than a Ni(II) Reservoir’, *Biochemistry*, 50(50), pp. 10761–10763. doi: 10.1021/bi201590d.

Kammler, M., Schon, C. and Hantke, K. (1993) ‘Characterization of the Ferrous Iron Uptake System of *Escherichia coli*’, *Journal of Bacteriology*, 175(19), pp. 6212–6219. Available at: http://jb.asm.org/content/175/19/6212.full.pdf?ref=herseybedava.info (Accessed: 17 May 2018).

Kane, M. D. *et al.* (2000) ‘Assessment of the sensitivity and specificity of oligonucleotide (50mer) microarrays.’, *Nucleic acids research*. Oxford University Press, 28(22), pp. 4552–7. Available at: http://www.ncbi.nlm.nih.gov/pubmed/11071945 (Accessed: 18 January 2018).

Kanehisa Laboratories (2017) *Fructose and mannose metabolism - Reference pathway, Kegg*. Available at: http://www.genome.jp/kegg-bin/show_pathway?scale=1.0&query=N-acetylglucosamine&map=map00051&scale=&auto_image=&show_description=hide&multi_query= (Accessed: 29 March 2018).

Kanehisa, M. *et al.* (2016) 'KEGG as a reference resource for gene and protein annotation', *Nucleic Acids Research*, 44(D1), pp. D457–D462. doi: 10.1093/nar/gkv1070.

Kanehisa, M. *et al.* (2017) 'KEGG: new perspectives on genomes, pathways, diseases and drugs', *Nucleic Acids Research*, 45(D1), pp. D353–D361. doi: 10.1093/nar/gkw1092.

Kanehisa, M. and Goto, S. (2000) 'KEGG: kyoto encyclopedia of genes and genomes.', *Nucleic acids research*, 28(1), pp. 27–30. Available at: http://www.ncbi.nlm.nih.gov/pubmed/10592173 (Accessed: 7 February 2018).

Karp, P. D. *et al.* (2014) 'The EcoCyc Database', *EcoSal Plus*, 6(1). doi: 10.1128/ecosalplus.ESP-0009-2013.

Katayama, A. *et al.* (2002) 'Systematic search for zinc-binding proteins in *Escherichia coli*.', *European journal of biochemistry*, 269, pp. 2403–2413.

Kato, A., Tanabe, H. and Utsumi, R. (1999) 'Molecular characterization of the PhoP-PhoQ two-component system in *Escherichia coli* K-12: identification of extracellular Mg2+-responsive promoters.', *Journal of bacteriology*, 181(17), pp. 5516–20. Available at: http://www.ncbi.nlm.nih.gov/pubmed/10464230 (Accessed: 31 May 2018).

Keele, B. B., Mccord, J. M. and Fridovich, I. (1970) 'Superoxide Dismutase from *Escherichia coli* B A NEW MANGANESE-CONTAINING ENZYME*', *THE JOURNAL OP BIOLOCWAL CHEMISTRY*, 245(22), pp. 6175–6181. Available at: http://www.jbc.org/content/245/22/6176.full.pdf (Accessed: 23 April 2018).

Kehl-Fie, T. E. *et al.* (2011) 'Nutrient Metal Sequestration by Calprotectin Inhibits Bacterial Superoxide Defense, Enhancing Neutrophil Killing of Staphylococcus aureus', *Cell Host & Microbe*. Cell Press, 10(2), pp. 158–164. doi: 10.1016/J.CHOM.2011.07.004.

Kehl-Fie, T. E. and Skaar, E. P. (2010) 'Nutritional immunity beyond iron: a role for manganese and zinc.', *Current opinion in chemical biology*. NIH Public Access, 14(2), pp. 218–24. doi: 10.1016/j.cbpa.2009.11.008.

Kehres, D. G. *et al.* (2000) 'The NRAMP proteins of Salmonella typhimurium and *Escherichia coli* are selective manganese transporters involved in the response to reactive oxygen', *Molecular Microbiology*. Wiley/Blackwell (10.1111), 36(5), pp. 1085–1100. doi: 10.1046/j.1365-2958.2000.01922.x.

Kehres, D. G. and Maguire, M. E. (2003) 'Emerging themes in manganese transport, biochemistry and pathogenesis in bacteria', *FEMS Microbiology Reviews*. Oxford University Press, 27(2–3), pp.

263–290. doi: 10.1016/S0168-6445(03)00052-4.

Kern, R. *et al.* (2007) '*Escherichia coli* HdeB is an acid stress chaperone.', *Journal of bacteriology*. American Society for Microbiology, 189(2), pp. 603–10. doi: 10.1128/JB.01522-06.

Keseler, I. M. *et al.* (2013) 'EcoCyc: fusing model organism databases with systems biology', *Nucleic Acids Research*. Oxford University Press, 41(D1), pp. D605–D612. doi: 10.1093/nar/gks1027.

Khorasani-Motlagh, M., Lacasse, M. J. and Zamble, D. B. (2017) 'High-affinity metal binding by the *Escherichia coli* [NiFe]-hydrogenase accessory protein HypB is selectively modulated by SlyD', *Metallomics*. The Royal Society of Chemistry, 9(5), pp. 482–493. doi: 10.1039/C7MT00037E.

Kim, C. *et al.* (2001) 'Oxidation of Phenolate Siderophores by the Multicopper Oxidase Encoded by the *Escherichia coli* yacK Gene', *Journal of Bacteriology*, 183(16), pp. 4866–4875. doi: 10.1128/JB.183.16.4866-4875.2001.

Kim, D., Langmead, B. and Salzberg, S. L. (2015) 'HISAT: a fast spliced aligner with low memory requirements', *Nature Methods*, 12(4), pp. 357–360. doi: 10.1038/nmeth.3317.

Kim, E. H. *et al.* (2011) 'Switch or funnel: How RND-type transport systems control periplasmic metal homeostasis', *Journal of Bacteriology*, 193(10), pp. 2381–2387. doi: 10.1128/JB.01323-10.

Kim, S. *et al.* (2016) 'PubChem Substance and Compound databases.', *Nucleic Acids Research*, 44(D1), pp. D1202-13.

Kim, Y. *et al.* (2009) 'Toxin-Antitoxin Systems in *Escherichia coli* Influence Biofilm Formation through YjgK (TabA) and Fimbriae', *Journal of Bacteriology*, 191(4), pp. 1258–1267. doi: 10.1128/JB.01465-08.

Kim, Y. *et al.* (2011) 'Increased in vivo efficacy of lenalidomide by addition of piroctone olamine.', *In vivo (Athens, Greece)*. International Institute of Anticancer Research, 25(1), pp. 99–103. Available at: http://www.ncbi.nlm.nih.gov/pubmed/21282741 (Accessed: 26 February 2018).

Kishigami, S. and Ito, K. (1996) 'Roles of cysteine residues of DsbB in its activity to reoxidize DsbA, the protein disulphide bond catalyst of *Escherichia coli*', *Genes to Cells*, 1, pp. 201–208. Available at: https://onlinelibrary.wiley.com/doi/pdf/10.1046/j.1365-2443.1996.d01-233.x (Accessed: 21 May 2018).

Koch, D., Nies, D. H. and Grass, G. (2007) 'The RcnRA (YohLM) system of *Escherichia coli*: A connection between nickel, cobalt and iron homeostasis', *BioMetals*, 20, pp. 759–771. doi: 10.1007/s10534-006-9039-6.

Koh, E.-I. *et al.* (2017) 'Copper import in *Escherichia coli* by the yersiniabactin metallophore system', *Nature Chemical Biology*, 13(9), pp. 1016–1021. doi: 10.1038/nchembio.2441.

Kolodynska, D. (2011) 'Chelating agents of a new generation as an alternative to conventional chelators for heavy metal ions removal from different waste waters', *Maria Curie Sklodowska*

University, Poland, pp. 339–370. doi: 10.5772/826.

Kolodyńska, D., Jachula, J. and Hubicki, Z. (2009) 'MGDA as a new biodegradable complexing agent for sorption of heavy metal ions on anion exchanger Lewatit Monoplus M 600', in *Proceedings of the 24 International Symposium on Physico-Chemical Methods of Separation*, p. 275. Available at: http://www.iaea.org/inis/collection/NCLCollectionStore/_Public/40/108/40108108.pdf (Accessed: 20 February 2018).

Kozlowski, H. *et al.* (2009) 'Copper, iron, and zinc ions homeostasis and their role in neurodegenerative disorders (metal uptake, transport, distribution and regulation)', *Coordination Chemistry Reviews*. Elsevier, 253(21–22), pp. 2665–2685. doi: 10.1016/J.CCR.2009.05.011.

Krapp, A. R., Humbert, M. V. and Carrillo, N. (2011) 'The soxRS response of *Escherichia coli* can be induced in the absence of oxidative stress and oxygen by modulation of NADPH content', *Microbiology*, 157(4), pp. 957–965. doi: 10.1099/mic.0.039461-0.

Kumar, J. K., Tabor, S. and Richardson, C. C. (2004) 'Proteomic analysis of thioredoxin-targeted proteins in *Escherichia coli*', *Proceedings of the National Academy of Sciences*, 101(11), pp. 3759–3764. doi: 10.1073/pnas.0308701101.

Kuzminov, A. (1999) 'Recombinational repair of DNA damage in *Escherichia coli* and bacteriophage lambda.', *Microbiology and molecular biology reviews : MMBR*, 63(4), p. 751–813, table of contents. Available at: http://www.ncbi.nlm.nih.gov/pubmed/10585965 (Accessed: 17 June 2018).

Lacasse, M. J., Douglas, C. D. and Zamble, D. B. (2016) 'Mechanism of Selective Nickel Transfer from HypB to HypA, *Escherichia coli* [NiFe]-Hydrogenase Accessory Proteins', *Biochemistry*, 55(49), pp. 6821–6831. doi: 10.1021/acs.biochem.6b00706.

Ladomersky, E. *et al.* (2017) 'Host and Pathogen Copper-Transporting P-Type ATPases Function Antagonistically during Salmonella Infection.', *Infection and immunity*. American Society for Microbiology, 85(9), pp. e00351-17. doi: 10.1128/IAI.00351-17.

Lahti, R. *et al.* (1990) 'A site-directed mutagenesis study on *Escherichia coli* inorganic pyrophosphatase. Glutamic acid-98 and lysine-104 are important for structural integrity, whereas aspartic acids-97 and -102 are essential for catalytic activity.', *Biochemistry*, 29(24), pp. 5761–6. Available at: http://www.ncbi.nlm.nih.gov/pubmed/1974462 (Accessed: 9 April 2018).

Laminet, A. A. *et al.* (1990) 'The *Escherichia coli* heat shock proteins GroEL and GroES modulate the folding of the beta-lactamase precursor.', *The EMBO journal*. European Molecular Biology Organization, 9(7), pp. 2315–9. Available at: http://www.ncbi.nlm.nih.gov/pubmed/2192863 (Accessed: 9 June 2018).

Landini, P. (2009) 'Cross-talk mechanisms in biofilm formation and responses to environmental and physiological stress in *Escherichia coli*', *Research in Microbiology*. Elsevier Masson, 160(4), pp. 259–266. doi: 10.1016/J.RESMIC.2009.03.001.

LaPorte, D. C., Walsh, K. and Koshland, D. E. (1984) ‘The branch point effect. Ultrasensitivity and subsensitivity to metabolic control.’, *The Journal of biological chemistry*, 259(22), pp. 14068–75. Available at: http://www.ncbi.nlm.nih.gov/pubmed/6389540 (Accessed: 8 April 2018).

Lau, C. K. Y., Krewulak, K. D. and Vogel, H. J. (2016) ‘Bacterial ferrous iron transport: the Feo system’, *FEMS Microbiology Reviews*. Edited by W. Bitter. Oxford University Press, 40(2), pp. 273–298. doi: 10.1093/femsre/fuv049.

Lee, K. *et al.* (2003) ‘RraA. a protein inhibitor of RNase E activity that globally modulates RNA abundance in *E. coli*.’, *Cell*, 114(5), pp. 623–34. Available at: http://www.ncbi.nlm.nih.gov/pubmed/13678585 (Accessed: 26 March 2018).

Lee, S. J. *et al.* (1994) ‘Family of the major cold-shock protein, CspA (CS7.4), of *Escherichia coli*, whose members show a high sequence similarity with the eukaryotic Y-box binding proteins.’, *Molecular Microbiology*, 11(5), pp. 833–9. Available at: http://www.ncbi.nlm.nih.gov/pubmed/8022261 (Accessed: 26 March 2018).

Leer, J. C., Hammer-Jespersen, K. and Schwartz, M. (1977) ‘Uridine phosphorylase from *Escherichia coli*. Physical and chemical characterization.’, *European journal of biochemistry*, 75(1), pp. 217–24. Available at: http://www.ncbi.nlm.nih.gov/pubmed/16751 (Accessed: 5 April 2018).

Leimkühler, S. (2014) ‘The Biosynthesis of the Molybdenum Cofactor in *Escherichia coli* and Its Connection to FeS Cluster Assembly and the Thiolation of tRNA’, *Advances in Biology*. Hindawi, 2014, pp. 1–21. doi: 10.1155/2014/808569.

Leitch, H. A. *et al.* (2017) ‘Overall survival in lower IPSS risk MDS by receipt of iron chelation therapy, adjusting for patient-related factors and measuring from time of first red blood cell transfusion dependence: an MDS-CAN analysis’, *British Journal of Haematology*. Wiley/Blackwell (10.1111), 179(1), pp. 83–97. doi: 10.1111/bjh.14825.

Leive, L. (1965) ‘A Nonspecific Increase in Permeability in *Escherichia coli* Produced by EDTA’, *Proceedings of the National Academy of Sciences of the United States of America*, 53, pp. 745–750. Available at: https://www.ncbi.nlm.nih.gov/pmc/articles/PMC221061/pdf/pnas00156-0045.pdf (Accessed: 5 March 2018).

Leive, L., Shovlin, V. K. and Mergenhagen, S. E. (1968) ‘Physical, chemical, and immunological properties of lipopolysaccharide released from *Escherichia coli* by ethylenediaminetetraacetate.’, *The Journal of biological chemistry*, 243(24), pp. 6384–91. Available at: http://www.ncbi.nlm.nih.gov/pubmed/4973230 (Accessed: 7 February 2018).

Lemire, J. A., Harrison, J. J. and Turner, R. J. (2013) ‘Antimicrobial activity of metals: mechanisms, molecular targets and applications’, *Nature Reviews Microbiology*, 11, pp. 371–384.

Levchenko, I. *et al.* (2000) ‘A specificity-enhancing factor for the ClpXP degradation machine.’, *Science (New York, N.Y.)*, 289(5488), pp. 2354–6. Available at: http://www.ncbi.nlm.nih.gov/pubmed/11009422 (Accessed: 22 March 2018).

Li, H. *et al.* (2009) 'The Sequence Alignment/Map format and SAMtools', *Bioinformatics*, 25(16), pp. 2078–2079. doi: 10.1093/bioinformatics/btp352.

Li, M. *et al.* (2006) 'Effect of lpdA gene knockout on the metabolism in *Escherichia coli* based on enzyme activities, intracellular metabolite concentrations and metabolic flux analysis by 13C-labeling experiments', *Journal of Biotechnology*, 122(2), pp. 254–266. doi: 10.1016/j.jbiotec.2005.09.016.

Lister, R. *et al.* (2008) 'Highly Integrated Single-Base Resolution Maps of the Epigenome in Arabidopsis', *Cell*. Cell Press, 133(3), pp. 523–536. doi: 10.1016/J.CELL.2008.03.029.

Liu, A. *et al.* (2010) 'Antibiotic sensitivity profiles determined with an *Escherichia coli* gene knockout collection: generating an antibiotic bar code.', *Antimicrobial agents and chemotherapy*. American Society for Microbiology, 54(4), pp. 1393–403. doi: 10.1128/AAC.00906-09.

Lo, J. *et al.* (2015) 'The bifunctional alcohol and aldehyde dehydrogenase gene, adhE, is necessary for ethanol production in Clostridium thermocellum and Thermoanaerobacterium saccharolyticum.', *Journal of bacteriology*. American Society for Microbiology, 197(8), pp. 1386–93. doi: 10.1128/JB.02450-14.

Loewen, P. C. and Switala, J. (1986) 'Purification and characterization of catalase HPII from *Escherichia coli* K12.', *Biochemistry and cell biology = Biochimie et biologie cellulaire*, 64(7), pp. 638–46. Available at: http://www.ncbi.nlm.nih.gov/pubmed/3019370 (Accessed: 20 May 2018).

López-Rayo, S., Hernández, D. and Lucena, J. J. (2009) 'Chemical Evaluation of HBED/Fe (3+) and the Novel HJB/Fe (3+) Chelates as Fertilizers to Alleviate Iron Chlorosis', *Journal of Agricultural and Food Chemistry*, 57(18), pp. 8504–8513. doi: 10.1021/jf9019147.

Love, M. I., Huber, W. and Anders, S. (2014) 'Moderated estimation of fold change and dispersion for RNA-seq data with DESeq2', *Genome Biology*. BioMed Central, 15(12), p. 550. doi: 10.1186/s13059-014-0550-8.

Lucht, J. M. *et al.* (1994) 'Interactions of the nucleoid-associated DNA-binding protein H-NS with the regulatory region of the osmotically controlled proU operon of *Escherichia coli*.', *The Journal of biological chemistry*, 269(9), pp. 6578–8. Available at: http://www.ncbi.nlm.nih.gov/pubmed/8120010 (Accessed: 30 March 2018).

Ludwig, A. *et al.* (1995) 'SlyA, a regulatory protein from Salmonella typhimurium, induces a haemolytic and pore-forming protein in *Escherichia coli*.', *Molecular & general genetics : MGG*, 249(5), pp. 474–86. Available at: http://www.ncbi.nlm.nih.gov/pubmed/8544813 (Accessed: 19 April 2018).

Lugtenberg, B. and Van Alphen, L. (1983) 'Molecular architecture and functioning of the outer membrane of *Escherichia coli* and other gram-negative bacteria.', *Biochimica et biophysica acta*, 737(1), pp. 51–115. Available at: http://www.ncbi.nlm.nih.gov/pubmed/6337630 (Accessed: 5 June 2018).

Lukong, K. E. *et al.* (2008) 'RNA-binding proteins in human genetic disease', *Trends in Genetics*. Elsevier Current Trends, 24(8), pp. 416–425. doi: 10.1016/J.TIG.2008.05.004.

Luo, C., Shen, Z. and Li, X. (2005) 'Enhanced phytoextraction of Cu, Pb, Zn and Cd with EDTA and EDDS', *Chemosphere*. Pergamon, 59(1), pp. 1–11. doi: 10.1016/J.CHEMOSPHERE.2004.09.100.

Macomber, L. and Imlay, J. A. (2009) 'The iron-sulfur clusters of dehydratases are primary intracellular targets of copper toxicity.', *Proceedings of the National Academy of Sciences of the United States of America*. National Academy of Sciences, 106(20), pp. 8344–9. doi: 10.1073/pnas.0812808106.

MacRitchie, D. M. *et al.* (2008) 'Two-Component Signaling and Gram Negative Envelope Stress Response Systems', in *Bacterial Signal Transduction: Networks and Drug Targets*. New York, NY: Springer New York, pp. 80–110. doi: 10.1007/978-0-387-78885-2_6.

Magnuson, K. *et al.* (1993) 'Regulation of Fatty Acid Biosynthesis in *Escherichia coli*', *MICROBIOLOGICAL REVIEWS*, 57(3), pp. 522–542. Available at: http://mmbr.asm.org/content/57/3/522.full.pdf (Accessed: 8 April 2018).

Mahmoud, M. A. *et al.* (2011) 'Evalution of a New Environmentally Friendly CHelating Agent for High-Temperature Applications', *SPE Journal*, pp. 559–574. Available at: https://www.researchgate.net/profile/Hisham_Nasr-El-Din/publication/241794364_Evaluation_of_a_New_Environmentally_Friendly_Chelating_Agent_for_High-Temperature_Applications/links/570ff39808aefb6cadaaa31e/Evaluation-of-a-New-Environmentally-Friendly-Chelat (Accessed: 20 February 2018).

Maier, C. *et al.* (1988) 'Pore-forming activity of the Tsx protein from the outer membrane of *Escherichia coli*. Demonstration of a nucleoside-specific binding site.', *The Journal of biological chemistry*, 263(5), pp. 2493–9. Available at: http://www.ncbi.nlm.nih.gov/pubmed/3276691 (Accessed: 9 April 2018).

Maki, H. and Sekiguchi, M. (1992) 'MutT protein specifically hydrolyses a potent mutagenic substrate for DNA synthesis', *Nature*. Nature Publishing Group, 355(6357), pp. 273–275. doi: 10.1038/355273a0.

Makui, H. *et al.* (2000) 'Identification of the *Escherichia coli* K-12 Nramp orthologue (MntH) as a selective divalent metal ion transporter.', *Molecular Microbiology*, 35(5), pp. 1065–78. Available at: http://www.ncbi.nlm.nih.gov/pubmed/10712688 (Accessed: 11 December 2018).

Malcovati, M., Valentini, G. and Kornberg, H. L. (1973) 'Two forms of pyruvate kinase in *E. coli*: their properties and regulation.', *Acta vitaminologica et enzymologica*, 27(1), pp. 96–111. Available at: http://www.ncbi.nlm.nih.gov/pubmed/4584473 (Accessed: 7 April 2018).

Malgieri, G. *et al.* (2015) 'The prokaryotic zinc-finger: structure, function and comparison with the eukaryotic counterpart', *FEBS Journal*. Wiley/Blackwell (10.1111), 282(23), pp. 4480–4496. doi: 10.1111/febs.13503.

Al Mamun, A. A. M. *et al.* (2012) 'Identity and function of a large gene network underlying mutagenic repair of DNA breaks.', *Science (New York, N.Y.)*. NIH Public Access, 338(6112), pp. 1344–8. doi: 10.1126/science.1226683.

Maret, W. (2016) *Metallomics A primer of Integrated Biometal Sciences*. London: Imperial College Press.

Marguerat, S., Wilhelm, B. T. and Bähler, J. (2008) 'Next-generation sequencing: applications beyond genomes.', *Biochemical Society transactions*. Portland Press Limited, 36(5), pp. 1091–1096. doi: 10.1042/BST0361091.

Martin, J. E. *et al.* (2015) 'The *Escherichia coli* Small Protein MntS and Exporter MntP Optimize the Intracellular Concentration of Manganese', *PLOS Genetics*. Edited by W. F. Burkholder. Public Library of Science, 11(3), p. e1004977. doi: 10.1371/journal.pgen.1004977.

Martin, J. E. and Imlay, J. A. (2011) 'The alternative aerobic ribonucleotide reductase of *Escherichia coli*, NrdEF, is a manganese-dependent enzyme that enables cell replication during periods of iron starvation', *Molecular Microbiology*. Wiley/Blackwell (10.1111), 80(2), pp. 319–334. doi: 10.1111/j.1365-2958.2011.07593.x.

Martinez, A. and Kolter, R. (1997) 'Protection of DNA during oxidative stress by the nonspecific DNA-binding protein Dps.', *Journal of bacteriology*, 179(16), pp. 5188–94. Available at: http://www.ncbi.nlm.nih.gov/pubmed/9260963 (Accessed: 30 March 2018).

Marvin, H. J. P., Ter Beest, M. B. A. and Witholt, B. (1989) 'Release of Outer Membrane Fragments from Wild-Type *Escherichia coli* and from Several *E. coli* Lipopolysaccharide Mutants by EDTA and Heat Shock Treatments', *Journal of Bacteriology*, 171(10), pp. 5262–5267. Available at: http://jb.asm.org/content/171/10/5262.full.pdf (Accessed: 5 June 2018).

Massé, E., Escorcia, F. E. and Gottesman, S. (2003) 'Coupled degradation of a small regulatory RNA and its mRNA targets in *Escherichia coli*.', *Genes & development*. Cold Spring Harbor Laboratory Press, 17(19), pp. 2374–83. doi: 10.1101/gad.1127103.

Massé, E. and Gottesman, S. (2002) 'A small RNA regulates the expression of genes involved in iron metabolism in *Escherichia coli*.', *Proceedings of the National Academy of Sciences of the United States of America*. National Academy of Sciences, 99(7), pp. 4620–5. doi: 10.1073/pnas.032066599.

Mattevi, A. *et al.* (1995) 'Crystal structure of *Escherichia coli* pyruvate kinase type I: molecular basis of the allosteric transition.', *Structure (London, England : 1993)*, 3(7), pp. 729–41. Available at: http://www.ncbi.nlm.nih.gov/pubmed/8591049 (Accessed: 7 April 2018).

Mayer, C. and Boos, W. (2005) 'Hexose/Pentose and Hexitol/Pentitol Metabolism.', *EcoSal Plus*, 1(2). doi: 10.1128/ecosalplus.3.4.1.

McCabe, M. J., Jiang, S. and Orrenius, S. (1993) 'Chelation of intracellular zinc triggers apoptosis in mature thymocytes.', *Laboratory Investigation: a Journal of Technical Methods and Pathology*,

69(1), pp. 101–110.

McClure, R. *et al.* (2013) 'Computational analysis of bacterial RNA-Seq data.', *Nucleic acids research*. Oxford University Press, 41(14), p. e140. doi: 10.1093/nar/gkt444.

McKee, J. S. and Nimmo, H. G. (1989) 'Evidence for an arginine residue at the coenzyme-binding site of *Escherichia coli* isocitrate dehydrogenase.', *The Biochemical journal*, 261(1), pp. 301–4. Available at: http://www.ncbi.nlm.nih.gov/pubmed/2673216 (Accessed: 8 April 2018).

Meddows, T. R. *et al.* (2005) 'RecN protein and transcription factor DksA combine to promote faithful recombinational repair of DNA double-strand breaks', *Molecular Microbiology*, 57(1), pp. 97–110. doi: 10.1111/j.1365-2958.2005.04677.x.

Mehta, A. P. *et al.* (2013) 'Catalysis of a New Ribose Carbon-Insertion Reaction by the Molybdenum Cofactor Biosynthetic Enzyme MoaA', *Biochemistry*, 52(7), pp. 1134–1136. doi: 10.1021/bi3016026.

Mélèse, T. and Xue, Z. (1995) 'The nucleolus: an organelle formed by the act of building a ribosome', *Current Opinion in Cell Biology*. Elsevier Current Trends, 7(3), pp. 319–324. doi: 10.1016/0955-0674(95)80085-9.

Meletiadis, J. *et al.* (2010) 'Defining fractional inhibitory concentration index cutoffs for additive interactions based on self-drug additive combinations, Monte Carlo simulation analysis, and in vitro-in vivo correlation data for antifungal drug combinations against Aspergillus fumi', *Antimicrobial agents and chemotherapy*. American Society for Microbiology (ASM), 54(2), pp. 602–9. doi: 10.1128/AAC.00999-09.

Membrillo-Hernández, J. *et al.* (2000) 'Evolution of the *adhE* Gene Product of *Escherichia coli* from a Functional Reductase to a Dehydrogenase', *Journal of Biological Chemistry*, 275(43), pp. 33869–33875. doi: 10.1074/jbc.M005464200.

Mendes, R. E. *et al.* (2006) 'Metalo-beta-lactamases', *Jornal Brasileiro de Patologia e Medicina Laboratorial*. SBPC, SBP, SBC, 42(2), pp. 103–113. doi: 10.1590/S1676-24442006000200007.

Menon, N. K. *et al.* (1991) 'Mutational analysis and characterization of the *Escherichia coli* hya operon, which encodes [NiFe] hydrogenase 1.', *Journal of bacteriology*, 173(15), pp. 4851–61. Available at: http://www.ncbi.nlm.nih.gov/pubmed/1856178 (Accessed: 19 May 2018).

Michaels, M. L. *et al.* (1992) 'A repair system for 8-oxo-7,8-dihydrodeoxyguanine.', *Biochemistry*, 31(45), pp. 10964–8. Available at: http://www.ncbi.nlm.nih.gov/pubmed/1445834 (Accessed: 17 June 2018).

Michel, B. (2005) 'After 30 years of study, the bacterial SOS response still surprises us.', *PLoS biology*. Public Library of Science, 3(7), p. e255. doi: 10.1371/journal.pbio.0030255.

Minagawa, S. *et al.* (2003) 'Identification and molecular characterization of the Mg2+ stimulon of *Escherichia coli*.', *Journal of bacteriology*, 185(13), pp. 3696–702. Available at: http://www.ncbi.nlm.nih.gov/pubmed/12813061 (Accessed: 9 April 2018).

Missiakas, D. and Raina, S. (1997) ‘Signal transduction pathways in response to protein misfolding in the extracytoplasmic compartments of E.coli : role of two new phosphoprotein phosphatases PrpA and PrpB’, *The EMBO Journal*, 16(7), pp. 1670–1685. doi: 10.1093/emboj/16.7.1670.

Mohindru, A., Fisher, J. M. and Rabinovitz, M. (1983) ‘Bathocuproine sulphonate: a tissue culture-compatible indicator of copper-mediated toxicity’, *Nature*. Nature Publishing Group, 303(5912), pp. 64–65. doi: 10.1038/303064a0.

Mortazavi, A. *et al.* (2008) ‘Mapping and quantifying mammalian transcriptomes by RNA-Seq’, *Nature Methods*, 5(7), pp. 621–628. doi: 10.1038/nmeth.1226.

Mou, J. *et al.* (1996) ‘High resolution surface structure of *E. coli* GroES oligomer by atomic force microscopy’, *FEBS Letters*, 381, pp. 161–164. Available at: https://ac.els-cdn.com/0014579396001123/1-s2.0-0014579396001123-main.pdf?_tid=b8f24347-7958-44b0-97c7-a873f6bf5cc7&acdnat=1521657475_521edf4564bc13b9d6e474b6125c3134 (Accessed: 21 March 2018).

Mulla, R. S. *et al.* (2018) ‘On the Antibacterial Activity of Azacarboxylate Ligands: Lowered Metal Ion Affinities for Bis-amide Derivatives of EDTA do not mean Reduced Activity’, *Chemistry - A European Journal*. Wiley-Blackwell, 24(28), pp. 7137–7148. doi: 10.1002/chem.201800026.

Munson, G. P. *et al.* (2000) ‘Identification of a copper-responsive two-component system on the chromosome of *Escherichia coli* K-12.’, *Journal of bacteriology*, 182(20), pp. 5864–71. Available at: http://www.ncbi.nlm.nih.gov/pubmed/11004187 (Accessed: 10 May 2018).

Nachin, L., Nannmark, U. and Nystrom, T. (2005) ‘Differential Roles of the Universal Stress Proteins of *Escherichia coli* in Oxidative Stress Resistance, Adhesion, and Motility’, *Journal of Bacteriology*, 187(18), pp. 6265–6272. doi: 10.1128/JB.187.18.6265-6272.2005.

Nakashima, K., Horikoshi, K. and Mizuno, T. (1995) ‘Effect of Hydrostatic Pressure on the Synthesis of Outer Membrane Proteins in *Escherichia coli*’, *Bioscience, Biotechnology, and Biochemistry*, 59(1), pp. 130–132. doi: 10.1271/bbb.59.130.

Nakatani, T. *et al.* (2000) ‘Apoptosis induced by chelation of intracellular zinc is associated with depletion of cellular reduced glutathione level in rat hepatocytes’, *Chemico-Biological Interactions*. Elsevier, 125(3), pp. 151–163. doi: 10.1016/S0009-2797(99)00166-0.

Nandal, A. *et al.* (2010) ‘Induction of the ferritin gene (*ftnA*) of *Escherichia coli* by Fe^{2+} -Fur is mediated by reversal of H-NS silencing and is RyhB independent’, *Molecular Microbiology*, 75(3), pp. 637–657. doi: 10.1111/j.1365-2958.2009.06977.x.

Neilands, J. B. (1995) ‘Siderophores: structure and function of microbial iron transport compounds.’, *The Journal of biological chemistry*. American Society for Biochemistry and Molecular Biology, 270(45), pp. 26723–6. doi: 10.1074/JBC.270.45.26723.

Nenortiene, P., Sapragoniene, M. and Stankevicius, A. (2002) ‘[Synthesis of hydroxamic acids and

study of their complexes with iron (II) and (III) ions].', *Medicina (Kaunas, Lithuania)*, 38(7), pp. 744–51. Available at: http://www.ncbi.nlm.nih.gov/pubmed/12474660 (Accessed: 13 June 2018).

Niederhoffer, E. C. *et al.* (1990) 'Control of *Escherichia coli* Superoxide Dismutase (sodA and sodB) Genes by the Ferric Uptake Regulation (fur) Locus', *Journal of Bacteriology*, 172(4), pp. 1930–1938. Available at: http://jb.asm.org/content/172/4/1930.full.pdf (Accessed: 23 April 2018).

Nieto, J. M. *et al.* (1997) 'Construction of a double hha hns mutant of *Escherichia coli*: effect on DNA supercoiling and alpha-haemolysin production.', *FEMS Microbiology Letters*, 155(1), pp. 39–44. Available at: http://www.ncbi.nlm.nih.gov/pubmed/9345762 (Accessed: 30 March 2018).

Nieto, J. M. *et al.* (2000) 'Expression of the hemolysin operon in *Escherichia coli* is modulated by a nucleoid-protein complex that includes the proteins Hha and H-NS.', *Molecular & general genetics : MGG*, 263(2), pp. 349–58. Available at: http://www.ncbi.nlm.nih.gov/pubmed/10778755 (Accessed: 30 March 2018).

Nobelmann, B. and Lengeler, J. W. (1996) 'Molecular Analysis of the gat Genes from *Escherichia coli* and of Their Roles in Galactitol Transport and Metabolism', *Journal Of Bacteriology*, 178(23), pp. 6790–6795. Available at: http://jb.asm.org/content/178/23/6790.full.pdf (Accessed: 3 April 2018).

Nomura, M. *et al.* (1980) 'Feedback regulation of ribosomal protein gene expression in *Escherichia coli*: Structural homology of ribosomal RNA and ribosomal protein mRNA (translational repressor/ribosome assembly/RNA-protein interaction/RNA secondary structure)', *Biochemistry*, 77(12), pp. 7084–7088. Available at: http://www.pnas.org/content/pnas/77/12/7084.full.pdf (Accessed: 5 February 2018).

Nörtemann, B. (1999) 'Biodegradation of EDTA', *Applied Microbiology and Biotechnology*, 51(6), pp. 751–759. doi: 10.1007/s002530051458.

Nose, Y. *et al.* (2010) 'Ctr1 is an apical copper transporter in mammalian intestinal epithelial cells in vivo that is controlled at the level of protein stability'. doi: 10.1074/jbc.M110.143826.

Oehler, S. (2009) 'Feedback regulation of Lac repressor expression in *Escherichia coli*.', *Journal of bacteriology*. American Society for Microbiology, 191(16), pp. 5301–3. doi: 10.1128/JB.00427-09.

Okamura-Ikeda, K. *et al.* (1993) 'Cloning and nucleotide sequence of the gcv operon encoding the *Escherichia coli* glycine-cleavage system.', *European journal of biochemistry*, 216(2), pp. 539–48. Available at: http://www.ncbi.nlm.nih.gov/pubmed/8375392 (Accessed: 3 April 2018).

Okochi, M. *et al.* (2007) 'Increase of organic solvent tolerance by overexpression of manXYZ in *Escherichia coli*', *Applied Microbiology and Biotechnology*. Springer-Verlag, 73(6), pp. 1394–1399. doi: 10.1007/s00253-006-0624-y.

Oliver, H. F. *et al.* (2009) 'Deep RNA sequencing of L. monocytogenes reveals overlapping and extensive stationary phase and sigma B-dependent transcriptomes, including multiple highly transcribed noncoding RNAs', *BMC Genomics*. BioMed Central, 10(1), p. 641. doi: 10.1186/1471-

2164-10-641.

Orndorff, P. E. and Falkow, S. (1985) ‘Nucleotide sequence of pilA, the gene encoding the structural component of type 1 pili in *Escherichia coli*.’, *Journal of bacteriology*, 162(1), pp. 454–7. Available at: http://www.ncbi.nlm.nih.gov/pubmed/2858471 (Accessed: 10 April 2018).

Osano, E. *et al.* (1994) ‘Molecular Characterization of an Enterobacterial Metallo 1-Lactamase Found in a Clinical Isolate of Serratia marcescens That Shows Imipenem Resistance’, *Antimicrobial agents and chemotherapy*, 38(1), pp. 71–78. Available at: http://aac.asm.org/content/38/1/71.full.pdf (Accessed: 5 June 2018).

Osman, D. *et al.* (2013) ‘The copper supply pathway to a Salmonella Cu,Zn-superoxide dismutase (SodCII) involves P1B-type ATPase copper efflux and periplasmic CueP’, *Molecular Microbiology*, 87(3), pp. 466–477. doi: 10.1111/mmi.12107.

Otto, K. *et al.* (2001) ‘Adhesion of Type 1-Fimbriated *Escherichia coli* to Abiotic Surfaces Leads to Altered Composition of Outer Membrane Proteins’, *Journal of Bacteriology*, 183(8), pp. 2445–2453. doi: 10.1128/JB.183.8.2445-2453.2001.

Outten, C. E. and O’Halloran, T. V. (2001) ‘Femtomolar Sensitivity of Metalloregulatory Proteins Controlling Zinc Homeostasis’, *Science*, 292, pp. 2488–2492.

Outten, F. W. *et al.* (2000) ‘Transcriptional Activation of an *Escherichia coli* Copper Efflux Regulon by the Chromosomal MerR Homologue, CueR’, *Journal of Biological Chemistry*, 275(40), pp. 31024–31029. doi: 10.1074/jbc.M006508200.

Outten, F. W. *et al.* (2001) ‘The Independent *cue* and *cus* Systems Confer Copper Tolerance during Aerobic and Anaerobic Growth in *Escherichia coli*’, *Journal of Biological Chemistry*, 276(33), pp. 30670–30677. doi: 10.1074/jbc.M104122200.

Oviedo, C. and Rodríguez, J. (2003) ‘EDTA: the chelating agent under environmental scrutiny’, *Química Nova*. SBQ, 26(6), pp. 901–905. doi: 10.1590/S0100-40422003000600020.

Ozbudak, E. M. *et al.* (2004) ‘Multistability in the lactose utilization network of *Escherichia coli*’, *Nature*, 427, pp. 737–740. doi: 10.1038/nature02298.

Palma, P., Sapragoniene, M. and Stankevicius, A. (2003) ‘[Octanhydroxamate of iron: synthesis, analysis and investigation of stability].’, *Medicina (Kaunas, Lithuania)*, 39 Suppl 2, pp. 55–9. Available at: http://www.ncbi.nlm.nih.gov/pubmed/14617860 (Accessed: 15 February 2018).

Papp-Wallace, K. M. and Maguire, M. E. (2006) ‘Manganese Transport and the Role of Manganese in Virulence’, *Annual Review of Microbiology*, 60(1), pp. 187–209. doi: 10.1146/annurev.micro.60.080805.142149.

Parat, M.-O. *et al.* (1997) ‘Zinc and DNA fragmentation in keratinocyte apoptosis: its inhibitory effect in UVB irradiated cells’, *Journal of Photochemistry and Photobiology B: Biology*. Elsevier, 37(1–2), pp. 101–106. doi: 10.1016/S1011-1344(96)07334-4.

Park, M. H., Wong, B. B. and Lusk, J. E. (1976) ‘Mutants in three genes affecting transport of magnesium in *Escherichia coli*: genetics and physiology.’, *Journal of bacteriology*, 126(3), pp. 1096–103. Available at: http://www.ncbi.nlm.nih.gov/pubmed/780341 (Accessed: 31 May 2018).

Parker, M. W. and Blake, C. C. F. (1988) ‘Iron-and manganese-containing superoxide dismutases can be distinguished by analysis of their primary structures’, 229(2), pp. 377–382. Available at: https://febs.onlinelibrary.wiley.com/doi/pdf/10.1016/0014-5793%2888%2981160-8 (Accessed: 20 May 2018).

Parrow, N. L., Fleming, R. E. and Minnick, M. F. (2013) ‘Sequestration and scavenging of iron in infection.’, *Infection and immunity*. American Society for Microbiology (ASM), 81(10), pp. 3503–14. doi: 10.1128/IAI.00602-13.

Partridge, J. D. *et al.* (2008) ‘Characterization of the *Escherichia coli* K-12 ydhYVWXUT operon: regulation by FNR, NarL and NarP’, *Microbiology*. Microbiology Society, 154(2), pp. 608–618. doi: 10.1099/mic.0.2007/012146-0.

Passalacqua, K. D. *et al.* (2009) ‘Structure and complexity of a bacterial transcriptome.’, *Journal of bacteriology*. American Society for Microbiology, 191(10), pp. 3203–3211. doi: 10.1128/JB.00122-09.

Patrzykat, A. *et al.* (2002) ‘Sublethal concentrations of pleurocidin-derived antimicrobial peptides inhibit macromolecular synthesis in *Escherichia coli*.’, *Antimicrobial agents and chemotherapy*. American Society for Microbiology, 46(3), pp. 605–14. doi: 10.1128/AAC.46.3.605-614.2002.

Patzer, S. I. and Hantke, K. (1998) ‘The ZnuABC high-affinity zinc uptake system and its regulator Zur in *Escherichia coli*’, *Molecular Microbiology*. Blackwell Science Ltd, 28(6), pp. 1199–1210. doi: 10.1046/j.1365-2958.1998.00883.x.

Patzer, S. I. and Hantke, K. (2000) ‘The zinc-responsive regulator Zur and its control of the znu gene cluster encoding the ZnuABC zinc uptake system in *Escherichia coli*.’, *The Journal of biological chemistry*. American Society for Biochemistry and Molecular Biology, 275(32), pp. 24321–32. doi: 10.1074/jbc.M001775200.

Patzer, S. I. and Hantke, K. (2001) ‘Dual repression by Fe(2+)-Fur and Mn(2+)-MntR of the mntH gene, encoding an NRAMP-like Mn(2+) transporter in *Escherichia coli*.’, *Journal of bacteriology*. American Society for Microbiology (ASM), 183(16), pp. 4806–13. doi: 10.1128/JB.183.16.4806-4813.2001.

Paul, B. J. *et al.* (2004) ‘DksA: a critical component of the transcription initiation machinery that potentiates the regulation of rRNA promoters by ppGpp and the initiating NTP.’, *Cell*, 118(3), pp. 311–322. doi: 10.1016/j.cell.2004.07.009.

Payankaulam, S., Li, L. M. and Arnosti, D. N. (2010) ‘Transcriptional Repression: Conserved and Evolved Features’, *Current Biology*. Cell Press, 20(17), pp. R764–R771. doi: 10.1016/J.CUB.2010.06.037.

Pelletier, C., Bourlioux, P. and Van Heijenoort, J. (1994) 'Effects of sub-minimal inhibitory concentrations of EDTA on growth of *Escherichia coli* and the release of lipopolysaccharide', *FEMS Microbiology Letters*, 117, pp. 203–206. doi: 10.1111/j.1574-6968.1994.tb06765.x.

Perederina, A. *et al.* (2004) 'Regulation through the Secondary Channel—Structural Framework for ppGpp-DksA Synergism during Transcription', *Cell*. Cell Press, 118(3), pp. 297–309. doi: 10.1016/J.CELL.2004.06.030.

Perera, C., McNeil, H. P. and Geczy, C. L. (2010) 'S100 Calgranulins in inflammatory arthritis', *Immunology and Cell Biology*, 88, pp. 41–49.

Perkins, T. T. *et al.* (2009) 'A Strand-Specific RNA–Seq Analysis of the Transcriptome of the Typhoid Bacillus Salmonella Typhi', *PLoS Genetics*. Edited by J. Casadesús. Public Library of Science, 5(7), p. e1000569. doi: 10.1371/journal.pgen.1000569.

Pettit, L. D. (2006) 'The IUPAC Stability Constants Database', *Chemistry International*. De Gruyter, 28(5), pp. 14–15. doi: 10.1515/ci.2006.28.5.14.

Phadtare, S. and Inouye, M. (2001) 'Role of CspC and CspE in Regulation of Expression of RpoS and UspA, the Stress Response Proteins in *Escherichia coli*', *Journal of Bacteriology*, 183(4), pp. 1205–1214. doi: 10.1128/JB.183.4.1205-1214.2001.

Piérard, G. *et al.* (1996) 'Improvement in the inflammatory aspect of androgenetic alopecia. A pilot study with an antimicrobial lotion', *Journal of Dermatological Treatment*. Taylor & Francis, 7(3), pp. 153–157. doi: 10.3109/09546639609086877.

Pinske, C., Sargent, F. and Sawers, R. G. (2015) 'SlyD-dependent nickel delivery limits maturation of [NiFe]-hydrogenases in late-stationary phase *Escherichia coli* cells.', *Metallomics : integrated biometal science*, 7(4), pp. 683–90. doi: 10.1039/c5mt00019j.

Pinto, I. S. S., Neto, I. F. F. and Soares, H. M. V. M. (2014) 'Biodegradable chelating agents for industrial, domestic, and agricultural applications—a review', *Environmental Science and Pollution Research*. Springer Berlin Heidelberg, 21(20), pp. 11893–11906. doi: 10.1007/s11356-014-2592-6.

Plamann, M. D., Rapp, W. D. and Stauffer, G. V (1983) '*Escherichia coli* K12 Mutants Defective in the Glycine Cleavage Enzyme System', *Mol Gen Genet*, 192, pp. 15–20. Available at: https://link.springer.com/content/pdf/10.1007/BF00327641.pdf (Accessed: 3 April 2018).

Plesa, M. *et al.* (2006) 'The SlyB outer membrane lipoprotein of Burkholderia multivorans contributes to membrane integrity', *Research in Microbiology*. Elsevier Masson, 157(6), pp. 582–592. doi: 10.1016/J.RESMIC.2005.11.015.

Plumbridge, J. (1998) 'Control of the expression of the manXYZ operon in *Escherichia coli*: Mlc is a negative regulator of the mannose PTS', *Molecular Microbiology*. Wiley/Blackwell (10.1111), 27(2), pp. 369–380. doi: 10.1046/j.1365-2958.1998.00685.x.

Ponka, P., Grady Ania Wilczynska, R. W. and Schulman, H. M. (1984) 'The Effect of Various

Chelating Agents on yhe Mobilization of Iron From Reticulocytes in the Presence and Absence of Pyridoxal Isonicotinoyl Hydrazone', *Biochimica et Biophysica Acta*, 802, pp. 477–489. Available at: https://ac.els-cdn.com/0304416584903672/1-s2.0-0304416584903672-main.pdf?_tid=3807a8b9-6ca5-4ec6-a91f-8b9b394bffb4&acdnat=1530174415_5a6c279960ae58316e20c713490d5b4b (Accessed: 28 June 2018).

Posey, J. E. and Gherardini, F. C. (2000) 'Lack of a Role for Iron in the Lyme Disease Pathogen', *Science*, 288(5471), pp. 1651–1653.

Powell, L. W. and Thomas, M. J. (1967) 'Use of diethylenetriamine penta-acetic acid (D.T.P.A.) in the clinical assessment of total body iron stores', *Journal of Clinical Pathology*, 20, pp. 896–904. Available at: https://www.ncbi.nlm.nih.gov/pmc/articles/PMC473636/pdf/jclinpath00371-0102.pdf (Accessed: 18 February 2018).

PREMIER Biosoft (2005) *Microarray Technology: An introduction to DNA Microarray*. Available at: http://www.premierbiosoft.com/tech_notes/microarray.html (Accessed: 18 January 2018).

Prichard, M. N. and Shipman, C. (1990) 'A three-dimensional model to analyze drug-drug interactions', *Antiviral Research*, 14, pp. 181–206. Available at: https://deepblue.lib.umich.edu/bitstream/handle/2027.42/28365/0000130.pdf?sequence=1&isAllowed=y (Accessed: 13 February 2018).

Qiu, Y. *et al.* (2008) 'The 1.38 A crystal structure of DmsD protein from Salmonella typhimurium, a proofreading chaperone on the Tat pathway.', *Proteins*. NIH Public Access, 71(2), pp. 525–33. doi: 10.1002/prot.21828.

QuickGo (2001a) *GO:0006412 : translation*, *EMBL-EBI*.

QuickGo (2001b) *GO:0006996 : organelle organization*, *EMBL-EBI*.

QuickGo (2001c) *GO:0008645 : hexose transmembrane transport*, *EMBL-EBI*.

QuickGo (2001d) *GO:0009059 : macromolecule biosynthetic process*, *EMBL-EBI*.

QuickGo (2001e) *GO:0015761 : mannose transmembrane transport*, *EMBL-EBI*.

QuickGo (2001f) *GO:0015764 : N-acetylglucosamine transport*, *EMBL-EBI*.

QuickGo (2001g) *GO:0016043 : cellular component organization*, *EMBL-EBI*.

QuickGo (2001h) *GO:0019538 : protein metabolic process*, *EMBL-EBI*.

QuickGo (2002) *GO:0042273 : ribosomal large subunit biogenesis*, *EMBL-EBI*.

QuickGo (2004a) *GO:0043170 : macromolecule metabolic process*, *EMBL-EBI*.

QuickGo (2004b) *GO:0044260 : cellular macromolecule metabolic process*, *EMBL-EBI*.

QuickGo (2004c) *GO:0044271 : cellular nitrogen compound biosynthetic process*, *EMBL-EBI*.

QuickGo (2006) *GO:0043603 : cellular amide metabolic process*, *EMBL-EBI*.

QuickGo (2007a) *GO:0010467 : Gene expression*, *EMBL-EBI*.

QuickGo (2007b) *GO:0022613 : ribonucleoprotein complex biogenesis*, *EMBL-EBI*.

QuickGo (2008a) *GO:0010608 : posttranscriptional regulation of gene expression*, *EMBL-EBI*.

QuickGo (2008b) *GO:0034641 : cellular nitrogen compound metabolic process*, *EMBL-EBI*.

QuickGo (2008c) *GO:0034645 : cellular macromolecule biosynthetic process*, *EMBL-EBI*.

QuickGo (2008d) *GO:0043933 : protein-containing complex subunit organization*, *EMBL-EBI*.

QuickGo (2009) *GO:0043933 : protein-containing complex subunit organization*, *EMBL-EBI*.

QuickGo (2012a) *GO:1901564 : organonitrogen compound metabolic process*, *EMBL-EBI*.

QuickGo (2012b) *GO:1901566 : organonitrogen compound biosynthetic process*, *EMBL-EBI*.

QuickGo (2013) *GO:1990145 : maintenance of translational fidelity*, *EMBL-EBI*.

QuickGO (2015) *GO:1904659 : glucose transmembrane transport*, *EMBL-EBI*.

Raivio, T. L. (2005) 'MicroReview: Envelope stress responses and Gram-negative bacterial pathogenesis', *Molecular Microbiology*, 56(5), pp. 1119–1128. doi: 10.1111/j.1365-2958.2005.04625.x.

Raivio, T. L., Leblanc, S. K. D. and Price, N. L. (2013) 'The *Escherichia coli* Cpx envelope stress response regulates genes of diverse function that impact antibiotic resistance and membrane integrity.', *Journal of bacteriology*. American Society for Microbiology, 195(12), pp. 2755–67. doi: 10.1128/JB.00105-13.

Rajagopalan, K. V, Johnson, J. L. and Hainline, B. E. (1982) 'The pterin of the molybdenum cofactor.', *Federation proceedings*, 41(9), pp. 2608–12. Available at: http://www.ncbi.nlm.nih.gov/pubmed/6953016 (Accessed: 19 April 2018).

Rangarajan, S., Woodgate, R. and Goodman, M. F. (2002) 'Replication restart in UV-irradiated *Escherichia coli* involving pols II, III, V, PriA, RecA and RecFOR proteins', *Molecular Microbiology*. Wiley/Blackwell (10.1111), 43(3), pp. 617–628. doi: 10.1046/j.1365-2958.2002.02747.x.

Rawlings, M. and Cronan, J. E. (1992) 'The gene encoding *Escherichia coli* acyl carrier protein lies within a cluster of fatty acid biosynthetic genes.', *The Journal of biological chemistry*, 267(9), pp. 5751–4. Available at: http://www.ncbi.nlm.nih.gov/pubmed/1556094 (Accessed: 8 April 2018).

Raymond, K. N., Dertz, E. A. and Kim, S. S. (2003) 'Enterobactin: an archetype for microbial iron transport.', *Proceedings of the National Academy of Sciences of the United States of America*. National Academy of Sciences, 100(7), pp. 3584–8. doi: 10.1073/pnas.0630018100.

Reaves, M. L. *et al.* (2013) 'Pyrimidine homeostasis is accomplished by directed overflow metabolism', *Nature*, 500(7461), pp. 237–241. doi: 10.1038/nature12445.

Redelberger, D. *et al.* (2011) 'YcdY protein of *Escherichia coli*, an atypical member of the TorD chaperone family.', *Journal of bacteriology*. American Society for Microbiology (ASM), 193(23), pp. 6512–6. doi: 10.1128/JB.05927-11.

Reed, J. L. *et al.* (2003) 'An expanded genome-scale model of *Escherichia coli* K-12 (iJR904 GSM/GPR).', *Genome Biology*, 4(9), p. R54. doi: 10.1186/gb-2003-4-9-r54.

Reisner, A. *et al.* (2003) 'Development and maturation of *Escherichia coli* K-12 biofilms', *Molecular Microbiology*. Wiley/Blackwell (10.1111), 48(4), pp. 933–946. doi: 10.1046/j.1365-2958.2003.03490.x.

Relogio, A. *et al.* (2002) 'Optimization of oligonucleotide-based DNA microarrays', *Nucleic Acids Research*. Oxford University Press, 30(11), p. 51e–51. doi: 10.1093/nar/30.11.e51.

Rensing, C. and Grass, G. (2003) '*Escherichia coli* mechanisms of copper homeostasis in a changing environment', *FEMS Microbiology Reviews*, 27(2–3), pp. 197–213. doi: 10.1016/S0168-6445(03)00049-4.

De Reuse, H. and Danchin, A. (1988) 'The ptsH, ptsI, and crr genes of the *Escherichia coli* phosphoenolpyruvate-dependent phosphotransferase system: a complex operon with several modes of transcription.', *Journal of bacteriology*, 170(9), pp. 3827–37. Available at: http://www.ncbi.nlm.nih.gov/pubmed/2457575 (Accessed: 3 April 2018).

Rimsky, S. and Spassky, A. (1990) 'Sequence determinants for H1 binding on *Escherichia coli* lac and gal promoters.', *Biochemistry*, 29(15), pp. 3765–71. Available at: http://www.ncbi.nlm.nih.gov/pubmed/2160266 (Accessed: 30 March 2018).

Risuleo, G., Gualerzi, C. and Pon, C. (1976) 'Specificity and properties of the destabilization, induced by initiation factor IF-3, of ternary complexes of the 30-S ribosomal subunit, aminoacyl-tRNA and polynucleotides.', *European journal of biochemistry*, 67(2), pp. 603–13. Available at: http://www.ncbi.nlm.nih.gov/pubmed/9282 (Accessed: 21 March 2018).

Rogan, W. J. *et al.* (2001) 'The Effect of Chelation Therapy with Succimer on Neuropsychological Development in Children Exposed to Lead', *New England Journal of Medicine*. Massachusetts Medical Society , 344(19), pp. 1421–1426. doi: 10.1056/NEJM200105103441902.

Rogers, H. J. (1973) 'Iron-Binding Catechols and Virulence in *Escherichia coli*.', *Infection and immunity*. American Society for Microbiology, 7(3), pp. 445–56. Available at: http://www.ncbi.nlm.nih.gov/pubmed/16558077 (Accessed: 13 June 2018).

Ross, W. *et al.* (2016) 'ppGpp Binding to a Site at the RNAP-DksA Interface Accounts for Its Dramatic Effects on Transcription Initiation during the Stringent Response', *Molecular Cell*, 62(6), pp. 811–823. doi: 10.1016/j.molcel.2016.04.029.

Rossmann, R. *et al.* (1995) 'Characterisation of a protease from *Escherichia coli* involved in hydrogenase maturation.', *European journal of biochemistry*, 227(1–2), pp. 545–50. Available at: http://www.ncbi.nlm.nih.gov/pubmed/7851435 (Accessed: 19 May 2018).

Rouillard, A. D. *et al.* (2016) 'The harmonizome: a collection of processed datasets gathered to serve and mine knowledge about genes and proteins', *Database*. Oxford University Press, 2016, p. baw100. doi: 10.1093/database/baw100.

Rowe, J. L., Starnes, G. L. and Chivers, P. T. (2005) 'Complex transcriptional control links NikABCDE-dependent nickel transport with hydrogenase expression in *Escherichia coli*.', *Journal of bacteriology*. American Society for Microbiology, 187(18), pp. 6317–23. doi: 10.1128/JB.187.18.6317-6323.2005.

RStudio Team (2015) *RStudio: Integrated Development for R*. Available at: http://www.rstudio.com/ (Accessed: 11 January 2018).

Ruiz, N. and Silhavy, T. J. (2005) 'Sensing external stress: watchdogs of the *Escherichia coli* cell envelope', *Current Opinion in Microbiology*. Elsevier Current Trends, 8(2), pp. 122–126. doi: 10.1016/J.MIB.2005.02.013.

Sambasivarao, D. *et al.* (1990) 'Organization of dimethyl sulfoxide reductase in the plasma membrane of *Escherichia coli*.', *Journal of bacteriology*, 172(10), pp. 5938–48. Available at: http://www.ncbi.nlm.nih.gov/pubmed/2170332 (Accessed: 5 April 2018).

Sancar, A. and Sancar, G. B. (1988) 'DNA Repair Enzymes', *Annual Review of Biochemistry*, 57(1), pp. 29–67. doi: 10.1146/annurev.bi.57.070188.000333.

Sand, O. *et al.* (2003) 'Phenotypic characterization of overexpression or deletion of the *Escherichia coli* crcA, cspE and crcB genes', *Microbiology*, 149(8), pp. 2107–2117. doi: 10.1099/mic.0.26363-0.

Saul, F. A. *et al.* (2004) 'Structural and functional studies of FkpA from *Escherichia coli*, a cis/trans peptidyl-prolyl isomerase with chaperone activity.', *Journal of molecular biology*, 335(2), pp. 595–608. Available at: http://www.ncbi.nlm.nih.gov/pubmed/14672666 (Accessed: 21 March 2018).

Sawers, G. (2004) 'A novel mechanism controls anaerobic and catabolite regulation of the *Escherichia coli* tdc operon', *Molecular Microbiology*. Wiley/Blackwell (10.1111), 39(5), pp. 1285–1298. doi: 10.1111/j.1365-2958.2001.02316.x.

Scholz, C. *et al.* (2006) 'SlyD Proteins from Different Species Exhibit High Prolyl Isomerase and Chaperone Activities †', *Biochemistry*, 45(1), pp. 20–33. doi: 10.1021/bi051922n.

Schreiter, E. R. *et al.* (2006) 'NikR-operator complex structure and the mechanism of repressor activation by metal ions.', *Proceedings of the National Academy of Sciences of the United States of America*. National Academy of Sciences, 103(37), pp. 13676–81. doi: 10.1073/pnas.0606247103.

Seeberg, E., Eide, L. and Bjørås, M. (1995) 'The base excision repair pathway', *Trends in Biochemical Sciences*. Elsevier Current Trends, 20(10), pp. 391–397. doi: 10.1016/S0968-

0004(00)89086-6.

Sekiguchi, T. *et al.* (2013) 'Elimination and utilization of oxidized guanine nucleotides in the synthesis of RNA and its precursors.', *The Journal of biological chemistry*. American Society for Biochemistry and Molecular Biology, 288(12), pp. 8128–35. doi: 10.1074/jbc.M112.418723.

Selinger, D. W. *et al.* (2003) 'Global RNA half-life analysis in *Escherichia coli* reveals positional patterns of transcript degradation.', *Genome research*. Cold Spring Harbor Laboratory Press, 13(2), pp. 216–23. doi: 10.1101/gr.912603.

Senda, K., Arakawa, Y., Nakashima, K., *et al.* (1996) 'Multifocal Outbreaks of Metallo-□-Lactamase-Producing Pseudomonas aeruginosa Resistant to Broad-Spectrum □-Lactams, including Carbapenems', *Antimicrobial agents and chemotherapy*, 402526(21), pp. 349–353. Available at: http://aac.asm.org/content/40/2/349.full.pdf (Accessed: 5 June 2018).

Senda, K., Arakawa, Y., Ichiyama, S., *et al.* (1996) 'PCR Detection of Metallo-□-Lactamase Gene (bla IMP) in Gram-Negative Rods Resistant to Broad-Spectrum □-Lactams', *Journal of Clinical Microbiology*, 34(12), pp. 2909–2913. Available at: http://jcm.asm.org/content/34/12/2909.full.pdf (Accessed: 5 June 2018).

Senior, A. E. (1988) 'ATP synthesis by oxidative phosphorylation', *Physiological Reviews*, 68(1), pp. 177–231. doi: 10.1152/physrev.1988.68.1.177.

Seo, S. W. *et al.* (2014) 'Deciphering Fur transcriptional regulatory network highlights its complex role beyond iron metabolism in *Escherichia coli*', *Nature Communications*. Nature Publishing Group, 5, p. 4910. doi: 10.1038/ncomms5910.

Sepehri, Z. *et al.* (2017) 'Essential and toxic metals in serum of individuals with active pulmonary tuberculosis in an endemic region', *Journal of Clinical Tuberculosis and Other Mycobacterial Diseases*. Elsevier, 6, pp. 8–13. doi: 10.1016/J.JCTUBE.2017.01.001.

Shakibaie, M. *et al.* (2014) 'Preparation and evaluation of the effect of Fe 3 O 4 @piroctone olamine magnetic nanoparticles on matrix metalloproteinase-2: A preliminary in vitro study', *Biotechnology and Applied Biochemistry*, 61(6), pp. 676–682. doi: 10.1002/bab.1231.

Sharma, C. M. and Vogel, J. (2009) 'Experimental approaches for the discovery and characterization of regulatory small RNA', *Current Opinion in Microbiology*. Elsevier Current Trends, 12(5), pp. 536–546. doi: 10.1016/J.MIB.2009.07.006.

Shi, I. Y., Stansbury, J. and Kuzminov, A. (2005) 'A Defect in the Acetyl Coenzyme A Acetate Pathway Poisons Recombinational Repair-Deficient Mutants of *Escherichia coli*', *Journal of Bacteriology*, 187(4), pp. 1266–1275. doi: 10.1128/JB.187.4.1266-1275.2005.

Shin, M. *et al.* (2005) 'DNA looping-mediated repression by histone-like protein H-NS: specific requirement of E 70 as a cofactor for looping', *Genes & Development*, 19(19), pp. 2388–2398. doi: 10.1101/gad.1316305.

Shine, J. and Dalgarno, L. (1975) ‘Terminal-Sequence Analysis of Bacterial Ribosomal RNA. Correlation between the 3’-Terminal-Polypyrimidine Sequence of 16-S RNA and Translational Specificity of the Ribosome’, *European Journal of Biochemistry*. Blackwell Publishing Ltd, 57(1), pp. 221–230. doi: 10.1111/j.1432-1033.1975.tb02294.x.

Sigdel, T. K., Easton, J. A. and Crowder, M. W. (2006) ‘Transcriptional response of *Escherichia coli* to TPEN’, *Journal of Bacteriology*, 188(18), pp. 6709–6713. doi: 10.1128/JB.00680-06.

Sigle, H. C. *et al.* (2006) ‘In vitro investigations on the mode of action of the hydroxypyridone antimycotics rilopirox and piroctone on Candida albicans’, *Mycoses*. Wiley/Blackwell (10.1111), 49(3), pp. 159–168. doi: 10.1111/j.1439-0507.2006.01228.x.

Singh, N. S. *et al.* (2005) ‘Evidence for a role of initiation factor 3 in recycling of ribosomal complexes stalled on mRNAs in *Escherichia coli*’, *Nucleic Acids Research*, 33(17), pp. 5591–5601. doi: 10.1093/nar/gki864.

Singh, N. S. *et al.* (2008) ‘Recycling of Ribosomal Complexes Stalled at the Step of Elongation in *Escherichia coli*’, *Journal of Molecular Biology*, 380(3), pp. 451–464. doi: 10.1016/j.jmb.2008.05.033.

Skoâ Rko-Glonek, J. *et al.* (1999) ‘The *Escherichia coli* heat shock protease HtrA participates in defense against oxidative stress’, *Molecular Genetics and Genomics*, 262, pp. 342–350. Available at: https://link.springer.com/content/pdf/10.1007/s004380051092.pdf (Accessed: 5 March 2018).

Smith, R. L. *et al.* (1993) ‘Sequence and topology of the CorA magnesium transport systems of Salmonella typhimurium and *Escherichia coli*. Identification of a new class of transport protein.’, *The Journal of biological chemistry*, 268(19), pp. 14071–80. Available at: http://www.ncbi.nlm.nih.gov/pubmed/8314774 (Accessed: 18 May 2018).

Smith, R. L. and Maguire, M. E. (1998) ‘Microbial magnesium transport: unusual transporters searching for identity’, *Molecular Microbiology*. Wiley/Blackwell (10.1111), 28(2), pp. 217–226. doi: 10.1046/j.1365-2958.1998.00810.x.

Smith, S. W. (2013) ‘The role of chelation in the treatment of other metal poisonings.’, *Journal of medical toxicology : official journal of the American College of Medical Toxicology*. Springer, 9(4), pp. 355–69. doi: 10.1007/s13181-013-0343-6.

Sopirala, M. M. *et al.* (2010) ‘Synergy testing by Etest, microdilution checkerboard, and time-kill methods for pan-drug-resistant Acinetobacter baumannii.’, *Antimicrobial agents and chemotherapy*. American Society for Microbiology, 54(11), pp. 4678–83. doi: 10.1128/AAC.00497-10.

Sprenger, G. A. *et al.* (1995) ‘Transaldolase B of *Escherichia coli* K-12: cloning of its gene, talB, and characterization of the enzyme from recombinant strains.’, *Journal of bacteriology*. American Society for Microbiology, 177(20), pp. 5930–6. doi: 10.1128/JB.177.20.5930-5936.1995.

Spring, K. J. *et al.* (1986) ‘L-asparaginase genes in *Escherichia coli*: isolation of mutants and

characterization of the ansA gene and its protein product.', *Journal of bacteriology*, 166(1), pp. 135–42. Available at: http://www.ncbi.nlm.nih.gov/pubmed/3514575 (Accessed: 3 April 2018).

Stachowski, E. K. and Schwarcz, R. (2012) 'Regulation of quinolinic acid neosynthesis in mouse, rat and human brain by iron and iron chelators in vitro', *Journal of Neural Transmission*, 119(2), pp. 123–131. doi: 10.1007/s00702-011-0694-6.

Stafford, S. L. *et al.* (2013) 'Metal ions in macrophage antimicrobial pathways: emerging roles for zinc and copper.', *Bioscience reports*. Portland Press Ltd, 33(4). doi: 10.1042/BSR20130014.

Stancik, L. M. *et al.* (2002) 'pH-dependent expression of periplasmic proteins and amino acid catabolism in *Escherichia coli*.', *Journal of bacteriology*, 184(15), pp. 4246–58. Available at: http://www.ncbi.nlm.nih.gov/pubmed/12107143 (Accessed: 9 April 2018).

Stillman, T. . *et al.* (2001) 'The high-resolution X-ray crystallographic structure of the ferritin (EcFtnA) of *Escherichia coli*; comparison with human H ferritin (HuHF) and the structures of the Fe3+ and Zn2+ derivatives11Edited by R. Huber', *Journal of Molecular Biology*, 307(2), pp. 587–603. doi: 10.1006/jmbi.2001.4475.

Storz, G. and Imlay, J. A. (1999) 'Oxidative Stress', *Current Opinion in Microbiology*, 2, pp. 188–194. Available at: https://ac.els-cdn.com/S1369527499800332/1-s2.0-S1369527499800332-main.pdf?_tid=83191ace-04b4-43b1-89ef-70fc14b4baea&acdnat=1530778298_84d1a6a28cf3543beed88c45efb4e7ff (Accessed: 5 July 2018).

Stoyanov, J. V and Brown, N. L. (2003) 'The *Escherichia coli* copper-responsive copA promoter is activated by gold.', *The Journal of biological chemistry*. American Society for Biochemistry and Molecular Biology, 278(3), pp. 1407–10. doi: 10.1074/jbc.C200580200.

Stoyanov, J. V, Hobman, J. L. and Brown, N. L. (2001) 'CueR (YbbI) of *Escherichia coli* is a MerR family regulator controlling expression of the copper exporter CopA.', *Molecular Microbiology*, 39(2), pp. 502–11. Available at: http://www.ncbi.nlm.nih.gov/pubmed/11136469 (Accessed: 10 May 2018).

Stracy, M. *et al.* (2016) 'Single-molecule imaging of UvrA and UvrB recruitment to DNA lesions in living *Escherichia coli*', *Nature Communications*, 7, p. 12568. doi: 10.1038/ncomms12568.

Strom, A. R. and Kaasen, I. (1993) 'Trehalose metabolism in *Escherichia coli*: stress protection and stress regulation of gene expression', *Molecular Microbiology*. Wiley/Blackwell (10.1111), 8(2), pp. 205–210. doi: 10.1111/j.1365-2958.1993.tb01564.x.

Sugano, Y. *et al.* (2017) 'SecY-SecA fusion protein retains the ability to mediate protein transport', *PLOS ONE*. Edited by S. M. Theg, 12(8), p. e0183434. doi: 10.1371/journal.pone.0183434.

Supek, F. *et al.* (2011) 'REVIGO Summarizes and Visualizes Long Lists of Gene Ontology Terms', *PLoS ONE*. Edited by C. Gibas. Public Library of Science, 6(7), p. e21800. doi: 10.1371/journal.pone.0021800.

Tajiri, T., Maki, H. and Sekiguchi, M. (1995) 'Functional cooperation of MutT, MutM and MutY proteins in preventing mutations caused by spontaneous oxidation of guanine nucleotide in *Escherichia coli*', *Mutation Research*, 336, pp. 257--267.

Takahashi, H. *et al.* (2015) 'The dynamic balance of import and export of zinc in *Escherichia coli* suggests a heterogeneous population response to stress.', *Journal of the Royal Society, Interface*. The Royal Society, 12(106), p. 20150069. doi: 10.1098/rsif.2015.0069.

Tao, T. *et al.* (1995) 'Magnesium transport in Salmonella typhimurium: mgtA encodes a P-type ATPase and is regulated by Mg2+ in a manner similar to that of the mgtB P-type ATPase.', *Journal of bacteriology*, 177(10), pp. 2654–62. Available at: http://www.ncbi.nlm.nih.gov/pubmed/7751273 (Accessed: 31 May 2018).

The Gene Ontology Consortium (2017) 'Expansion of the Gene Ontology knowledgebase and resources', *Nucleic Acids Research*, 45(D1), pp. D331–D338. doi: 10.1093/nar/gkw1108.

Thomson, J. *et al.* (1979) 'ColE1 Hybrid Plasmids for *Escherichia coli* Genes of Glycolysis and the Hexose Monophosphate Shunt', *JOURNAL OF BACTERIOLOGY*, 137(1), pp. 502–506. Available at: http://jb.asm.org/content/137/1/502.full.pdf (Accessed: 7 April 2018).

Touati, D. (1988) 'Transcriptional and Posttranscriptional Regulation of Manganese Superoxide Dismutase Biosynthesis in *Escherichia coli*, Studied with Operon and Protein Fusion', *Journal of Bacteriology Bacteriol*, 170(6), pp. 2511–2520. Available at: http://jb.asm.org/content/170/6/2511.short.

Touati, D. (2000) 'Iron and Oxidative Stress in Bacteria', *Archives of Biochemistry and Biophysics*. Academic Press, 373(1), pp. 1–6. doi: 10.1006/ABBI.1999.1518.

Trapnell, C. *et al.* (2012) 'Differential gene and transcript expression analysis of RNA-seq experiments with TopHat and Cufflinks', *Nature Protocols*. Nature Publishing Group, 7(3), pp. 562–578. doi: 10.1038/nprot.2012.016.

Trchounian, A. (2004) '*Escherichia coli* proton-translocating F0F1-ATP synthase and its association with solute secondary transporters and/or enzymes of anaerobic oxidation–reduction under fermentation', *Biochemical and Biophysical Research Communications*, 315(4), pp. 1051–1057. doi: 10.1016/j.bbrc.2004.02.005.

Truglio, J. J. *et al.* (2006) 'Prokaryotic Nucleotide Excision Repair: The UvrABC System', *Chemical Reviews*, 106(2), pp. 233–252. doi: 10.1021/cr040471u.

Trumpower, B. L. and Gennis, R. B. (1994) 'Energy Transduction by Cytochrome Complexes in Mitochondrial and Bacterial Respiration: The Enzymology of Coupling Electron Transfer Reactions to Transmembrane Proton Translocation', *Annual Review of Biochemistry*. Annual Reviews 4139 El Camino Way, P.O. Box 10139, Palo Alto, CA 94303-0139, USA , 63(1), pp. 675–716. doi: 10.1146/annurev.bi.63.070194.003331.

Tsang, D. C. W. and Hartley, N. R. (2014) ‘Metal distribution and spectroscopic analysis after soil washing with chelating agents and humic substances’, *Environmental Science and Pollution Research*. Springer Berlin Heidelberg, 21(5), pp. 3987–3995. doi: 10.1007/s11356-013-2300-y.

Tschauner, K. *et al.* (2014) ‘Dynamic Interaction between the CpxA Sensor Kinase and the Periplasmic Accessory Protein CpxP Mediates Signal Recognition in *E. coli*’, *PLoS ONE*. Edited by E. Cascales, 9(9), p. e107383. doi: 10.1371/journal.pone.0107383.

Turowski-Wanke, A. and Simsch, W. (2003) ‘Hair Treatments Comprising Zinc Salts of Proctone Olamine’. Germany. Available at: https://patents.google.com/patent/US20030049292A1/en.

Uehara, T. and Park, J. T. (2004) ‘The N-acetyl-D-glucosamine kinase of *Escherichia coli* and its role in murein recycling.’, *Journal of Bacteriology*. American Society for Microbiology, 186(21), pp. 7273–9. doi: 10.1128/JB.186.21.7273-7279.2004.

Ulvatne, H. *et al.* (2004) ‘Lactoferricin B inhibits bacterial macromolecular synthesis in *Escherichia coli* and Bacillus subtilis’, *FEMS Microbiology Letters*. Oxford University Press, 237(2), pp. 377–384. doi: 10.1111/j.1574-6968.2004.tb09720.x.

Uniprot (2005) *UniProtKB - P0ABS1 (DKSA_ECOLI) Title*, *Uniprot*. Available at: http://www.uniprot.org/uniprot/P0ABS1 (Accessed: 26 March 2018).

Uppal, S., Akkipeddi, V. S. N. and Jawali, N. (2008) ‘Posttranscriptional regulation of cspE in *Escherichia coli* : involvement of the short 5â€^{2}-untranslated region’, *FEMS Microbiology Letters*, 279(1), pp. 83–91. doi: 10.1111/j.1574-6968.2007.01009.x.

Urano, H. *et al.* (2015) ‘Cooperative regulation of the common target genes between H2O2-sensing YedVW and Cu2+-sensing CusSR in *Escherichia coli*’, *Microbiology*, 161(4), pp. 729–738. doi: 10.1099/mic.0.000026.

Urano, H. *et al.* (2017) ‘Cross-regulation between two common ancestral response regulators, HprR and CusR, in *Escherichia coli*’, *Microbiology*, 163(2), pp. 243–252. doi: 10.1099/mic.0.000410.

Vaara, M. (1992) ‘Agents That Increase the Permeability of the Outer Membrane’, *Microbiological Reviews*, 56(3), pp. 395–411. Available at: https://www.ncbi.nlm.nih.gov/pmc/articles/PMC372877/pdf/microrev00030-0033.pdf (Accessed: 5 March 2018).

Valentini, G. *et al.* (2000) ‘The Allosteric Regulation of Pyruvate Kinase’, *Journal of Biological Chemistry*, 275(24), pp. 18145–18152. doi: 10.1074/jbc.M001870200.

Vallee, B. L. and Auld, D. S. (1993) ‘Zinc: Biological Functions and Coordination Motifs’, *Accounts of Chemical Research*, 26, pp. 543–551. Available at: https://pubs.acs.org/doi/pdf/10.1021/ar00034a005 (Accessed: 5 July 2018).

Vanbogelen, R. A., Kelley, P. M. and Neidhardt, F. C. (1987) ‘Differential Induction of Heat Shock, SOS, and Oxidation Stress Regulons and Accumulation of Nucleotides in *Escherichia coli*’, *Journal*

of Bacteriology, 169(1), pp. 26–32. Available at: http://jb.asm.org/content/169/1/26.full.pdf (Accessed: 23 April 2018).

Verhoeven, E. E. *et al.* (2000) 'Catalytic sites for 3' and 5' incision of *Escherichia coli* nucleotide excision repair are both located in UvrC.', *The Journal of biological chemistry*, 275(7), pp. 5120–3. Available at: http://www.ncbi.nlm.nih.gov/pubmed/10671556 (Accessed: 20 May 2018).

Vignais, P. M. and Colbeau, A. (2004) 'Molecular Biology of Microbial Hydrogenases 159', *Current Issues in Molecular Biology*, 6(2), pp. 159–188. Available at: http://www.caister.com/cimb/v/v6/159.pdf (Accessed: 8 April 2018).

Waldron, K. J. *et al.* (2009) 'Metalloproteins and metal sensing', *Nature*, 460(7257), pp. 823–830. doi: 10.1038/nature08300.

Waldron, K. J. and Robinson, N. J. (2009) 'How do bacterial cells ensure that metalloproteins get the correct metal?', *Nature Reviews*, 6, pp. 25–35. Available at: https://www.researchgate.net/profile/Kevin_Waldron/publication/23660181_How_Do_Bacterial_Cells_Ensure_that_Metalloproteins_Get_the_Correct_Metal/links/02e7e51d5404225b08000000/How-Do-Bacterial-Cells-Ensure-that-Metalloproteins-Get-the-Correct-Metal.pdf (Accessed: 5 March 2018).

Walkup, G. K. *et al.* (2000) 'A New Cell-Permeable Fluorescent Probe for Zn2+', *Journal of American Chemistry Society*. American Chemical Society, 122(23), pp. 5644–5645. doi: 10.1021/JA000868P.

Walsh, K. and Koshland, D. E. (1985) 'Branch point control by the phosphorylation state of isocitrate dehydrogenase. A quantitative examination of fluxes during a regulatory transition.', *The Journal of biological chemistry*, 260(14), pp. 8430–7. Available at: http://www.ncbi.nlm.nih.gov/pubmed/2861202 (Accessed: 8 April 2018).

Wambaugh, M. A. *et al.* (2017) 'High-throughput identification and rational design of synergistic small-molecule pairs for combating and bypassing antibiotic resistance', *PLOS Biology*. Edited by A. Read. Public Library of Science, 15(6), p. e2001644. doi: 10.1371/journal.pbio.2001644.

Wang, D. and Fierke, C. A. (2013) 'The BaeSR regulon is involved in defense against zinc toxicity in *E. coli*.', *Metallomics : integrated biometal science*. NIH Public Access, 5(4), pp. 372–83. doi: 10.1039/c3mt20217h.

Wang, D., Hosteen, O. and Fierke, C. A. (2012) 'ZntR-mediated transcription of zntA responds to nanomolar intracellular free zinc', *Journal of Inorganic Biochemistry*, 111, pp. 173–181. doi: 10.1016/j.jinorgbio.2012.02.008.

Wang, H. *et al.* (2017) 'Increasing intracellular magnesium levels with the 31-amino acid MgtS protein', *Proceedings of the National Academy of Sciences*, 114(22), pp. 5689–5694. doi: 10.1073/pnas.1703415114.

Wang, Z., Gerstein, M. and Snyder, M. (2009) 'RNA-Seq: a revolutionary tool for transcriptomics', *Nature Reviews Genetics*. Nature Publishing Group, 10(1), pp. 57–63. doi: 10.1038/nrg2484.

Waters, L. S., Sandoval, M. and Storz, G. (2011) 'The *Escherichia coli* MntR miniregulon includes genes encoding a small protein and an efflux pump required for manganese homeostasis', *Journal of Bacteriology*, 193(21), pp. 5887–5897. doi: 10.1128/JB.05872-11.

Weatherspoon-Griffin, N. *et al.* (2014) 'The CpxR/CpxA two-component regulatory system up-regulates the multidrug resistance cascade to facilitate *Escherichia coli* resistance to a model antimicrobial peptide.', *The Journal of biological chemistry*. American Society for Biochemistry and Molecular Biology, 289(47), pp. 32571–82. doi: 10.1074/jbc.M114.565762.

Weiner, J. H. *et al.* (1988) 'Purification and Properties of *Escherichia coli* Dimethyl Sulfoxide Reductase, an Iron-Sulfur Molybdoenzyme with Broad Substrate Specificity', *JOURNAL OF BACTERIOLOGY*, 170(4), pp. 1505–1510. Available at: http://jb.asm.org/content/170/4/1505.full.pdf (Accessed: 5 April 2018).

Weisburg, W. G. *et al.* (1991) '16S Ribosomal DNA Amplification for Phylogenetic Study', *JOURNAL OF BACTERIOLOGY*, 173(2), pp. 697–703. Available at: http://jb.asm.org/content/173/2/697.full.pdf (Accessed: 17 January 2018).

White, C. *et al.* (2009) 'Copper transport into the secretory pathway is regulated by oxygen in macrophages.', *Journal of cell science*. Company of Biologists, 122(Pt 9), pp. 1315–21. doi: 10.1242/jcs.043216.

White, R. L. *et al.* (1996) 'Comparison of Three Different In Vitro Methods of Detecting Synergy: Time-Kill, Checkerboard, and E test', *ANTIMICROBIAL AGENTS AND CHEMOTHERAPY*, 40(8), pp. 1914–1918. Available at: http://aac.asm.org/content/40/8/1914.full.pdf (Accessed: 19 March 2018).

Widdel, F. (2010) *Theory and Measurement of Bacterial Growth A. Basic and practical aspects*. Available at: https://www.mpi-bremen.de/Binaries/Binary307/Wachstumsversuch.pdf (Accessed: 9 January 2018).

Wiegand, I., Hilpert, K. and Hancock, R. E. W. (2008) 'Agar and broth dilution methods to determine the minimal inhibitory concentration (MIC) of antimicrobial substances', *Nature Protocols*, 3(2), pp. 163–175.

Wooley, R. E., Jones, M. S. and Shotts, E. B. (1984) 'Uptake of antibiotics in gram-negative bacteria exposed to EDTA-Tris', *Veterinary Microbiology*. Elsevier, 10(1), pp. 57–70. doi: 10.1016/0378-1135(84)90056-7.

De Wulf, P. and Lin, E. C. (2000) 'Cpx two-component signal transduction in *Escherichia coli*: excessive CpxR-P levels underlie CpxA* phenotypes.', *Journal of bacteriology*, 182(5), pp. 1423–6. Available at: http://www.ncbi.nlm.nih.gov/pubmed/10671468 (Accessed: 21 May 2018).

Wülfing, C., Lombardero, J. and Plückthun, A. (1994) ‘An *Escherichia coli* protein consisting of a domain homologous to FK506-binding proteins (FKBP) and a new metal binding motif.’, *The Journal of biological chemistry*, 269(4), pp. 2895–901. Available at: http://www.ncbi.nlm.nih.gov/pubmed/8300624 (Accessed: 19 May 2018).

Yamada, H., Muramatsu, S. and Mizuno, T. (1990) ‘An *Escherichia coli* protein that preferentially binds to sharply curved DNA.’, *Journal of biochemistry*, 108(3), pp. 420–5. Available at: http://www.ncbi.nlm.nih.gov/pubmed/2126011 (Accessed: 30 March 2018).

Yamada, K., Ariyoshi, M. and Morikawa, K. (2004) ‘Three-dimensional structural views of branch migration and resolution in DNA homologous recombination’, *Current Opinion in Structural Biology*, 14(2), pp. 130–137. doi: 10.1016/j.sbi.2004.03.005.

Yamamoto, K. and Ishihama, A. (2005) ‘Transcriptional response of *Escherichia coli* to external copper’, *Molecular Microbiology*. Wiley/Blackwell (10.1111), 56(1), pp. 215–227. doi: 10.1111/j.1365-2958.2005.04532.x.

Yamamoto, N. *et al.* (2009) ‘Update on the Keio collection of *Escherichia coli* single-gene deletion mutants.’, *Molecular systems biology*. European Molecular Biology Organization, 5, p. 335. doi: 10.1038/msb.2009.92.

Yeom, J.-H. and Lee, K. (2006) ‘RraA rescues *Escherichia coli* cells over-producing RNase E from growth arrest by modulating the ribonucleolytic activity’, *Biochemical and Biophysical Research Communications*, 345(4), pp. 1372–1376. doi: 10.1016/j.bbrc.2006.05.018.

Yocum, C. F. and Pecoraro, V. L. (1999) ‘Recent advances in the understanding of the biological chemistry of manganese’, *Current Opinion in Chemical Biology*. Elsevier Current Trends, 3(2), pp. 182–187. doi: 10.1016/S1367-5931(99)80031-3.

Yoon, S.-H. *et al.* (2003) ‘MutY is down-regulated by oxidative stress in *E. coli*.’, *Free radical research*, 37(8), pp. 873–9. Available at: http://www.ncbi.nlm.nih.gov/pubmed/14567447 (Accessed: 12 December 2018).

Zablen, L. B. *et al.* (1975) ‘Phylogenetic Origin of the Chloroplast and Prokaryotic Nature of Its Ribosomal RNA (Euglena/16S rRNA/evolution)’, *Proceedings of the National Academy of Sciences of the United States of America*, 72(6), pp. 2418–2422. Available at: http://www.pnas.org/content/72/6/2418.full.pdf (Accessed: 17 January 2018).

Zakataeva, N. P. *et al.* (1999) ‘The novel transmembrane *Escherichia coli* proteins involved in the amino acid efflux.’, *FEBS letters*, 452(3), pp. 228–32. Available at: http://www.ncbi.nlm.nih.gov/pubmed/10386596 (Accessed: 3 April 2018).

Zeppenfeld, T. *et al.* (2000) ‘Glucose transporter mutants of *Escherichia coli* K-12 with changes in substrate recognition of IICB(Glc) and induction behavior of the ptsG gene.’, *Journal of bacteriology*. American Society for Microbiology (ASM), 182(16), pp. 4443–52. Available at: http://www.ncbi.nlm.nih.gov/pubmed/10913077 (Accessed: 3 April 2018).

Zhang, Q.-M. *et al.* (1998) '*Escherichia coli* MutY protein has a guanine-DNA glycosylase that acts on 7,8-dihydro-8-oxoguanine:guanine mispair to prevent spontaneous G:C->C:G transversions', *Nucleic Acids Research*. Oxford University Press, 26(20), pp. 4669–4675. doi: 10.1093/nar/26.20.4669.

Zhao, M. *et al.* (2006) 'Regulation of RraA, a Protein Inhibitor of RNase E-Mediated RNA Decay', *Journal of Bacteriology*, 188(9), pp. 3257–3263. doi: 10.1128/JB.188.9.3257-3263.2006.

Zhao, S. *et al.* (2014) 'Comparison of RNA-Seq and Microarray in Transcriptome Profiling of Activated T Cells', *PLoS ONE*. Edited by S.-D. Zhang. Public Library of Science, 9(1), p. e78644. doi: 10.1371/journal.pone.0078644.

Zhou, S. *et al.* (2010) 'Comparative Evaluation of Disodium Edetate and Diethylenetriaminepentaacetic Acid as Iron Chelators to Prevent Metal -Catalyzed Destabilization of a Therapeutic Monoclonal Antibody', *Journal of Pharmaceutical Sciences*, 90(10), pp. 4239–50.

Zientz, E., Six, S. and Unden, G. (1996) 'Identification of a third secondary carrier (DcuC) for anaerobic C4-dicarboxylate transport in *Escherichia coli*: roles of the three Dcu carriers in uptake and exchange.', *Journal of bacteriology*, 178(24), pp. 7241–7. Available at: http://www.ncbi.nlm.nih.gov/pubmed/8955408 (Accessed: 8 April 2018).

Zschimmer & Schwarz (2018) *DTPMP Diethylenetriamine-penta(methylene phosphonic acid), Zschimmer & Schwarz*. Available at: https://www.zschimmer-schwarz.com/phosphonate/grundstrukturen/dtpmp/ (Accessed: 19 February 2018).